THE SYNTHESIS OF COMBINED HEAT AND MASS EXCHANGE NETWORKS (CHAMENs) WITH RENEWABLES CONSIDERING ENVIRONMENTAL IMPACT

So-mang Kim

A Thesis presented for the degree of

Master of Science in Engineering

In Chemical Engineering

Environmental and Process System Engineering

Department of Chemical Engineering

University of Cape Town

Cape Town, South Africa

Supervisor: Assoc. Prof. AJ Isafiade

2019

Acknowledgements

I would like to express my very great appreciation to God Almighty for giving me the strength, knowledge, and opportunity to undertake this research. My utmost love goes to Him.

Psalm 59:16

But I will sing of your strength,

In the morning I will sing of your love;

For you are my fortress,

My refuge in times of trouble.

Firstly, my deepest gratitude goes to my supervisor, Assoc. Prof. AJ Isafiade. He provided insight, expertise and motivation that greatly helped me during my journey towards this degree. Without all the support from him, this research would never have been possible.

I would also like to thank Dr M. Short who has always found the time to provide feedback and ideas despite his overloaded schedule. My appreciation also be extended to Ms T. Y. Chitaka and Dr V. Russo for helping me with SimaPro. Special thanks to Jafaru Egieya and Ben Abikoye and the environmental and process systems research group in the chemical engineering department, UCT, for good friendship and support during my study at UCT.

Finally, I must express my very profound gratitude to my parents for providing me with unfailing love and continuous encouragement throughout my years of study. I say a big thank you to my twin brother Sowon Kim and my dearest friend Chris Cho, Brenda Mehlo, Lindi Mthimunye, Marion Yi, MK Lee, GH Lee, SH Park, Ian Lee and my 'old' friend Alan Rynhoud, for giving me the necessary distractions from my research and providing good life advice during my hard times. Thank you for always being there for me.

Declaration

I know the meaning of plagiarism and declare that all the work in the document, save for that which is properly acknowledged, is my own. This thesis/dissertation has been submitted to the Turnitin module (or equivalent similarity and originality checking software) and I confirm that my supervisor has seen my report and any concerns revealed by such have been resolved with my supervisor

So-mang Kim

Abstract

Process synthesis is used to evaluate different potential designs to select the most suitable that fulfils some process goals. There is ever-increasing pressure to reduce operating cost and emission of pollutants as energy prices continue to increase and more regulations are set by government. To address these concerns, optimisation methods based on heuristics, pinch technology and mathematical programming can be adopted. Since the early 90s, mathematical programming has gained significant attention to solve large and complex problems.

Extensive studies have been conducted for heat exchange network synthesis (HENS), which was first used to optimise utility usage and operating costs. Many existing mass exchange network synthesis (MENS) methods are derived from HENS techniques since analogies exist between the two networks. Integrating the synthesis of mass and heat exchange networks in what is known as combined heat and mass exchange network synthesis (CHAMENS) can be beneficial because mass transfer is affected by operating temperature. However, very little research has been done in this area of process synthesis due to their complex nature. It is even more challenging to find literature involving the regeneration of multiple recyclable MSAs in a network synthesis context. Furthermore, the few studies that have considered CHAMENS have done the optimisation considering economic performance alone, whereas the consideration of environmental impact as an additional objective can help attain a more sustainable process.

This thesis builds on current knowledge of CHAMENs synthesis methods by considering CHAMENs with detailed regeneration networks (RENs) involving multiple recyclable MSAs, multiple regenerating streams, and solar thermal as an alternative energy source, using a multi-period synthesis approach. Simultaneously optimising a combination of these networks is not a trivial task due to the resulting large model size having many binary and non-linear terms and the interactions among them. Stage-wise superstructure (SWS)

synthesis approaches for heat and mass exchanger networks are adopted in this thesis for the synthesis of CHAMENs. A new superstructure for RENs, which is equivalent to that of a MEN, is presented in this thesis. The combined superstructure, which involves multiple MSAs, multiple regenerants, and multiple hot and cold process streams, is integrated with solar thermal energy as a renewable energy option. The availability of solar thermal energy is simplified by discretizing into two time periods of daytime and nighttime operations. The proposed CHAMEN model is also extended to handle multi-objective optimisation (MOO) of environmental impact and economic objectives to identify the optimal network configuration. Two examples were solved, and the results obtained showed that the implementation of integrated solar panels and thermal storage tanks could reduce the environmental impact of the combined networks by 76% and 26% for case studies 1 and 2 respectively. However, such eco-friendly infrastructure resulted in increased total annual cost (TAC) values of 36% and 15% respectively for the two case studies. These results indicate that by using the methodologies developed in this thesis, trade-offs can be established between economics and environmental impact as objectives.

Contents

Acknowledgements i
Abstract iii
LIST OF FIGURES viii
LIST OF TABLES x
NOMENCLATURE xi
Chapter 1 Introduction 2
1.1 Background on Process Synthesis 2
1.2 Motivation 5
1.3 Scope and Limitations 6
1.4 Overall Objectives and methodology 7
1.5 Thesis Structure 8
Chapter 2 8
Chapter 3 8
Chapter 4 8
Chapter 5 8
Chapter 2 Literature Review 10
2.1 Introduction 10
2.2 Heat Exchange Networks (HENs) 10
2.2.1 Insight-based Strategies 11
2.2.2 Framework Strategies (Mathematical Programming) 17
2.3 Mass Exchange Networks (MENs) 27
2.3.1 Pinch Technology for MENS 29
2.3.1.1 The minimum cost of MSAs target 30
2.3.1.2 The Minimum Number of Mass Exchanger Units Targeting 31
2.3.1.3 Capital Cost targeting for MENs 32
2.3.2 Mathematical Programming Applied to MENS 44
2.3.2.1 Sequential Mathematical Programming Methods 44
2.3.2.2 Simultaneous Mathematical Programming Methods 45

2.3.2.3 Stagewise Superstructure of Szitkai et al. (2006) 47
2.3.2.4 Multi-period MEN Synthesis 50
2.3.2.5 Initialisation of MENS model 50
2.4 Synthesis of Regeneration Network 51
2.4.1 The analogy of MENs and RENs 52
2.4.2 The Interconnection of MENs and RENs 53
2.4.3 Regeneration Methods 54
2.5 Synthesis of Combined and Heat and Mass Exchange Networks (CHAMENs) 60
2.5.1 Bibliography of CHAMENs Synthesis Methods 61
2.5.2 CHAMENs Model of Isafiade and Fraser (2009) 62
2.5.3 Incorporation of Utilities Generated from Renewable Energies 64
2.6 Environmental Impact in Process Synthesis 65
2.7 Multi-objective Optimization (MOO) 69
2.7.1 Pareto optimality 69
2.7.2 Multi-objective methodologies 70
2.8 Conclusions and Thesis contributions 72
Chapter 3 Combined Networks Synthesis Method 75
3.1 Synthesis Approach 75
3.2 Problem statement 79
3.3 Assumptions 80
3.4 MINLP model formulation 81
3.4.1 HENS model equations 81
3.4.2 MENS model equations 86
3.4.3 Regeneration network model equations 90
3.4.4 The combined economic objective function 94
3.4.5 Environmental impact objective function 97
3.4.6 Multi-objective function 98
3.4.7 Initialisations and Convergence 98
Chapter 4 Case Study 101

4.1 Ammonia removal (Case study 1) 101
4.1.1 Simultaneous synthesis of MEN (The first step) 105
4.1.2 Synthesis of combined MEN and REN (The second step) 106
4.1.3 Simultaneous synthesis of CHAMENs with REN (The third step) 108
4.2 H2S removal (Case Study 2) 117
4.2.1 Synthesis of MEN (The first step) 120
4.2.2 Simultaneous synthesis of MEN and REN (The second step) 121
4.2.3 Simultaneous synthesis of MEN, REN and HEN (The third step) 123
4.2.4 Sub-stream temperature optimisation 126
4.2.5 The synthesis of the combined model with MOO 133
Chapter 5 Conclusions and Future works 139
REFERENCES 141
Appendix A 147
A1: LEL to target composition conversion 147
A2: Henry's constants for case studies 147
Case Study 1 147
Case study 2 148
A3: Capital and costing data 150
A4: costs calculations 153
Steam costs 153
Liquid nitrogen cost 153
A5: K_w Calculation 154
Lumped *Kw* Calculation equation was obtained from Hallale (1998). 154
Appendix B 154
Sample code for the case study 1 (MEN with REG) 154
Sample code for the case study 2 with MOO 175

LIST OF FIGURES

Figure 1.1: The onion model of process design (Smith, 2005) 3
Figure 2.1: Construction of hot and cold composite curves 12
Figure 2.2: Division of the composite curve into vertical enthalpy intervals 14
Figure 2.3: The graphical representation of vertical (a) and non-vertical heat transfer (b) 15
Figure 2.4: A summary diagram of different synthesis methods for HENS (Furman and Sahinidis, 2002) 19
Figure 2.5: The Stage-wise superstructure developed by Yee and Grossmann (1990) 22
Figure 2.6: Schematic representation of MEN (El-Halwagi and Manousiouthakis, 1989) 28
Figure 2.7: The composite curves of the rich and lean streams on the same axes 31
Figure 2.8: Construction of the y-y* composite curve plot (b) from the mass transfer composite curve plot (a) (Hallale, 1998) 34
Figure 2.9: A diagram of the stagewise exchanger 35
Figure 2.10: Different types of continuous-contact columns: Packed columns (a), spray towers (b) and mechanically agitated exchanger (c) (El-Halwagi, 2017). 38
Figure 2.11: The Superstructure of MEN developed by Szitkai et al. (2006) with two rich streams and two lean streams. 48
Figure 2.12: A mass exchanger and regeneration column 53
Figure 2.13: A schematic diagram of MENs and RENs (El-Halwagi and Manousioutaki, 1990) 54
Figure 2.14: The solvent extraction principle: Removal of solute C (Müller et al., 2000) 55
Figure 2.15: General representation of steam stripping (a) and air stripping (b) 56
Figure 2.16: schematic diagram of coupled MEN and HEN (Isafiade and Fraser, 2009) 62
Figure 2.17: The stages involved in life cycle assessment (Fedkin, 2018) 66
Figure 2.18: Considered categories in Midpoint and endpoint of the ReCiPe approach 68
Figure 2.19: Pareto curve comparing environmental impact and costs (Miettinen and Mäkelä, 1999) 70
Figure 3.1: General proposed approach of the combined networks synthesis 76

Figure 3.2: A schematic of combined heat, mass and regeneration networks involving multiple streams..... 78
Figure 4.1: The MEN configuration of case study 1 (values above streams are composition in mass fractions; while values in boxes indicate mass load transferred in mass exchangers [kg/s])..... 105
Figure 4.2: The MEN with REN configuration of case study 1 (values above streams are composition in mass fractions; while values in boxes indicate mass load transferred in mass exchangers [kg/s]) 106
Figure 4.3: The multi-period CHAMENs configuration for case study 1 (values above streams are composition in mass fractions; while values in boxes indicate mass load transferred in mass exchangers [kg/s])..... 110
Figure 4.4: The multi-period CHAMENs configuration with solar panels and heat storage vessels. 112
Figure 4.5: The HEN and solar network configurations of the CHAMEN for periods 1 and 2 113
Figure 4.6:Detailed TAC for CHAMEN without solar panels for case study 1 114
Figure 4.7: Detailed TAC for CHAMEN with solar panels for case study 1 115
Figure 4.8: A schematic representation of Case study 2 118
Figure 4.9: The MEN configuration of H_2S removal process (values above streams are composition in mass fractions; while values in boxes indicate mass load transferred in mass exchangers [kg/s]) 121
Figure 4.10 The MEN and REN configuration (values above streams are composition in mass fractions; while values in boxes indicate mass load transferred in mass exchangers [kg/s])..... 122
Figure 4.11: The CHAMENs configuration without solar panels for case study 2 (values above streams are composition in mass fractions; while values in boxes indicate mass load transferred in mass exchangers [kg/s])..... 124
Figure 4.12: Variation of S_3 absorption temperature and the resulting TAC 126
Figure 4.13: Variation of S_3 stripping temperature and the resulting TAC..... 127

Figure 4.14: Variation of S2 absorption temperature and the resulting TAC 128
Figure 4.15: Variation of S_2 stripping temperature and the resulting TAC 129
Figure 4.16: The economically optimised CHAMENs configuration (values above streams are composition in mass fractions; while values in boxes indicate mass load transferred in mass exchangers [kg/s]) 130
Figure 4.17: The CHAMENs with solar panels detailed TAC 131
Figure 4.18: The CHAMENs without solar panels detailed TAC 132
Figure 4.19: The Pareto optimal of the combined networks with NMP as S_3 solvent 134
Figure 4.20: The combined networks with a moderate level of both TAC and EI (values above streams are composition in mass fractions; while values in boxes indicate mass load transferred in mass exchangers [kg/s]) 136
Figure 4.21: The CHAMENs with NMP detailed TAC 137

LIST OF TABLES

Table 2.1: The analogy of MENS and HENS (Szitkai et al., 2006) 29
Table 2.2: A summary of the advantages and disadvantages of different types of solvents (Kidnay et al., 2011) 59
Table 4.1: The MENs stream data for case study 1 (concentrations given in mas fractions; Data from Hallale, 1998) 102
Table 4.2: The RENs stream data for case study 1 (compositions given in mass fractions) 103
Table 4.3: The environmental impact of lean and regenerating streams 104
Table 4.4: The HENs stream data and costs for case study 1 109
Table 4.5: The total heat balance of HEN over the periods 113
Table 4.6: Mass exchanger sizes of solar thermal integrated CHAMEN 116
Table 4.7: The MEN stream data (compositions given in mass fractions; El-Halwagi and Manousiouthakis, 1989) 118
Table 4.8: The REN stream data (compositions given in mass fractions) 119

Table 4.9: The environmental impact of lean and regenerating streams for Case Study 2 120
Table 4.10: The HEN stream data for case study 2 123
Table 4.11: NMP lean stream data (compositions given in mass fractions; Srinivas and El-Halwagi, 1994) 133
Table 4.12: The regenerating stream data (compositions given in mass fractions) 133

NOMENCLATURE

Abbreviations

AOC	Annual operating cost
CHAMEN	Combined Heat and Mass Exchange Network
COG	Coke oven gas
CW	Cooling Water
DOP	Duration of Period
EI	Environmental Impact
EMAC	Exchange Minimum Approach Composition
EMAT	Exchange Minimum Approach Temperature
GAMS	General Algebraic Modelling System
HEN	Heat Exchange Network
HPS	High Pressure Steam
HTU	Height of Theoretical Units
HU	Hot utility
HUC	Hot utility Costs
IBMS	Interval-Based MINLP Synthesis
LCA	Life Cycle Assessment
LCIA	Life Cycle Impact Assessment
LMCD	Logarithmic Mean Concentration Differences
LMTD	Logarithmic Mean Temperature Differences

LP	Linear Programming
MEN	Mass Exchange Network
MILP	Mixed Integer Linear Programming
MINLP	Mixed Integer Non-Linear Programming
MSAs	Mass Separating Agents
NOP	Number of periods
NTU	Number of theoretical units
REMAC	Regeneration network Exchange Minimum Approach Composition
REN	Regenerating Network
SWS	Stage-wise superstructure
TAC	Total Annualized Cost

Symbols

$\Delta T_{\min}$	Minimum temperature difference
ΔT_{lm}	The logarithmic mean temperature difference
Δy	Rich streams composition difference
Δy_{lm}	Logarithmic mean composition difference
$	The conditional operator used in GAMS
$K_y a$	Overall mass transfer coefficient

HENS notations

Sets

H	Hot process and utility streams
C	Cold process and utility streams
Kh	Temperature locations in superstructure

P	Operation periods

Indices

Ih	Indices for hot process or utility stream
Jc	Indices for cold process or utility stream
Kh	Indices for temperature location (kh = 1,⋯ NOKh)
P	Index for operation period

Parameters

AC	Area cost coefficient
AE	Area cost index
CF	Fixed charge for exchangers
CUC_{jc}	Cost per unit of cold utility
HUC_{ih}	Cost per unit of hot utility
h_c	Stream heat transfer coefficient
$T_{kh,p}$	The temperature at location kh for period p
$T^s_{ih,p}$	Supply temperature of hot stream ih for period p
$T^t_{ih,p}$	Target temperature of hot stream ih for period p
$T^s_{jc,p}$	Supply temperature of cold stream jc for period p
$T^t_{jc,p}$	Target temperature of cold stream jc for period p
$U_{ih,jc}$	Overall heat transfer coefficient
$\Omega_{p,\mathrm{HEN}}$	Upper bound for heat exchanged in match ih, jc in period p
Γ_h	Upper bound for driving force in match ih, jc in period p

Binary variables

$zhn_{ih,jc,kh}$	Binary variable indicating the existence of match *ih*, *jc* in location *kh* in the optimal network

Positive variable

$dt_{ih,jc,kh,p}$	Driving force for match *ih, jc* in location *kh* and period *p*
$F_{ih,p}$	Flow rate of hot stream *ih* in period *p*
$F_{jc,p}$	Flow rate of cold stream *jc* in period *p*
$q_{ih,jc,kh,p}$	Heat exchanged between stream *ih, jc* in temperature location *kh* and period *p*
$t_{ih,kh,p}$	Temperature of hot stream *ih* at hot end of location *kh* and period *p*
$t_{jc,kh,p}$	Temperature of cold stream *jc* at hot end of location *kh* and period *p*

MENS notations

Sets

R	Rich process streams
S	Process and external lean streams
K	Composition location in the superstructure
P	Operation periods

Indices

R	Indices for rich process stream
L	Indices for process and external lean streams
K	Indices for composition location ($k = 1, \cdots$ NOK)
P	Index for operation period

Parameters

AC_l	Annual operating cost per unit of lean stream *l*
ACT_{rl}	Annual cost per stage for staged columns involving rich stream *r* and lean stream *l*
ACH_{rl}	Annual cost per height for continuous contact columns involving rich stream *r* and lean stream *l*
CB_{rl}	Fixed charge (or installation cost) for columns involving rich stream *r* and lean stream *l*
D^{rl}	Cost exponent for columns involving rich stream *r* and lean stream *l*
M	Equilibrium relation constant
B	Intercept of the linear equilibrium line
K_w	Lumped mass transfer coefficient
W	Weighting function
$X_{l,p}^{s}$	Supply composition of lean stream *l* in period *p*
$X_{l,p}^{t}$	Target composition of lean stream *l* in period *p*
$Y_{r,p}^{s}$	Supply composition of rich stream *r* in period *p*
$Y_{r,p}^{t}$	Target composition of rich stream *r* in period *p*
$Y_{l,p}^{*s}$	Equilibrium supply composition of lean stream *l* in period *p*
$Y_{l,p}^{*t}$	Equilibrium target composition of lean stream *l* in period *p*
$\Omega_{p,\mathrm{MEN}}$	Upper bound for mass exchanged in match *r, l* in period *p*
Γ_{mn}	Upper bound for driving force in match *r, l* in period *p*
$\varepsilon_{\min}$	Minimum composition difference

Binary variables

$zmn_{r,l,k}$	Binary variable indicating the existence of match *r, l* in location *k* in the optimal network

Positive variable

$dy_{r,l,k,p}$	Driving force for match *r, l* in location *k* and period *p*
$G_{r,p}$	Flow rate of rich stream *r* for period *p*
$L_{l,p}$	Flow rate of lean stream *l* for period *p*
$M_{r,l,k,p}$	Mass exchanged between rich stream *r* and lean stream *l* in location *k* and period *p*
N_{stages}	Number of stages in staged column
$x_{l,k,p}$	Composition of lean stream *r* in composition location *k* and period *p*
$y_{r,k,p}$	Composition of rich stream r in composition location *k* and period *p*
$y^*_{l,k,p}$	Equilibrium composition of lean stream *l* in composition location *k* and period *p*

RENS notations

Sets

S	Exhausted (rich) external MSAs
V	regenerants
Kr	Composition location in the regeneration superstructure
P	Operation periods

Indices

L	Indices for exhausted (rich) external MSAs
V	Indices for regenerants
Kr	Indices for composition location ($kr = 1, \cdots$ NOKr)

Parameters

AC_v	Annual operating cost per unit of regenerating stream v
ACT_{lv}	Annual cost per stage for staged columns involving exhausted external MSAs streams l and regenerating streams v
ACH_{lv}	Annual cost per height for continuous contact columns involving exhausted external MSAs streams l and regenerating stream v
CB_{lv}	Fixed charge (or installation cost) for columns involving exhausted external MSAs streams l and regenerating streams v
D^{lv}	Cost exponent for columns involving exhausted external MSAs streams l and regenerating streams v
m_v	Equilibrium relation constant for regenerants
B	Intercept of the linear equilibrium line
W	Weighting function
$X_{l,p}^{s}$	Supply composition of exhausted lean stream l in period p
$X_{l,p}^{t}$	Target composition of exhausted lean stream l in period p
$Z_{v,p}^{*s}$	Equilibrium supply composition of regenerating stream v in period p

$Z_{v,p}^{*t}$	Equilibrium target composition of regenerating stream *v* in period *p*
$\Omega_{p,\mathrm{REN}}$	Upper bound for mass exchanged in match *l, v* in period *p*
Γ_{rn}	Upper bound for driving force in match *l, v* in location *kr*
$\varepsilon_{\min}$	Minimum composition difference

Binary variables

$zrn_{l,v,kr}$	Binary variable indicating the existence of match *l, v* in location *kr* in the optimal network

Positive variable

$drn_{l,v,kr,p}$	Driving force for match *l, v* in location *kr* and period *p*
$L_{l,p}$	Flow rate of exhausted lean streams *l* for period *p*
$QR_{v,p}$	Flow rate of regenerating streams *v* for period *p*
$M_{l,v,kr,p}$	Mass exchanged between exhausted lean streams *l* and regenerating streams *r* in location *kr* and period *p*
$x_{l,kr,p}$	Composition of exhausted lean streams *l* in composition location *kr* and period *p*
$z_{v,kr,p}$	Composition of regenerating streams *v* in composition location *kr* and period *p*
$z_{v,kr,p}^{*}$	Equilibrium composition of regenerating streams *v* in composition location *kr* and period *p*

Chapter 1

Introduction

Chapter 1 Introduction

1.1 Background on Process Synthesis

Chemical processes involve converting raw materials into finished products. The main aim of process synthesis is to establish the best complete design to achieve a chemical-manufacturing goal. The term 'synthesis' in process design was first introduced in the paper by Rudd (1968), as well as in the first textbook for process synthesis (Rudd et al., 1973). The first review article in this field was published in the 1970s (Farkas, 2006). Process synthesis is thus a developing field and many previous works studied search algorithms for the optimal network and these synthesis methods are applied to various areas of chemical engineering.

Westerberg (1987) defined process synthesis as: "*the discrete decision-making activities of conjecturing (1) which of the many available component parts one should use, and (2) how they should be interconnected to structure the optimal solution to a given design problem*". Therefore, process synthesis may involve the integration of various sub-systems. These sub-systems may further involve stages such as chemical reactions, separations, and physical and thermal mixing (Smith, 2005). The stages need to be well-integrated to achieve the production goal. El-Halwagi (1998) stated that integration is a holistic approach to process design with emphasis on the unity of the process. Process integration provides a framework through a systemic approach which allows observation of fundamental understanding of the processes. The inter-connected stages of process synthesis are presented in the onion diagram shown in Figure 1.1.

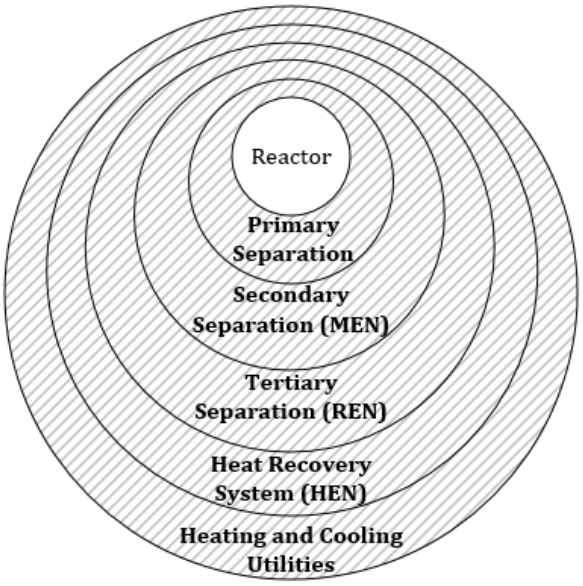

Figure 1.1: The onion model of process design (Hallale and Fraser, 2000b)

Manufacturing technologies and infrastructures are used to transform feedstocks (raw materials) by both physical and chemical means to final products. The value-added products mixed with by-products and impurities require further purification. Therefore, the reactor design stage shown in Figure 1.1 defines the separation system requirements. Hallale and Fraser (2000b) classified the separation system into three subdivisions. The first system is called the primary separation system which is determined by the reactor design stage while the next is the secondary separation, which involves the MEN. The second subdivision's specifications are affected by the reactor design and/or the primary separation system. An example can include a series of absorbers forming a MEN to purify one or more gaseous reactor feed/effluent streams. The last subdivision is the tertiary separation which is shaped by the MEN. A typical example is the regeneration of exhausted MSAs. In this thesis, the last subdivision is named as a regeneration network (REN) which allows multiple MSAs to be recycled back to the MEN. These stages involving both the reactor design and the separation systems then determine the energy requirements for heating and cooling systems and the amount of recoverable heat within the process. In this thesis, the last five layers (highlighted with the hatch symbol) of the six stages in Figure 1.1 are considered. Through heat integration, which is the fifth and the sixth layers of the onion diagram, heating and cooling

requirements are designed to have the minimum values which result in optimised operating cost. However, there has been a fast-growing awareness of the environmental impact of chemical processes since many industrial processes exploit great portions of resources and leave significant footprints on the ecosystem. Since there have been more governmental regulations it is not only the cost associated with chemical processes that is important, but also reducing the environmental impact of such operations. Note that implementing simple end-of-pipe treatments alone cannot adequately mitigate the impacts of the processes, and therefore, the incorporation of pollution prevention in the process synthesis step is necessary (Szitkai, 2004). The excess energy within the exchanger networks can be integrated with the separation systems to enhance mass transfer which allows optimal utilisation of energy and can thus reduce the emissions of pollutants to lower the impacts of chemical processes on the environment.

Over the past three decades, there exists extensive literature on the heat exchanger network synthesis (HENS) problem, where significant progress has been made within the process synthesis field. One of the essential operations in the process industries is that of mass exchange. This has motivated many recent studies to explore different synthesis methods on MENs. Pollutants are selectively removed from waste streams (rich streams) through absorption into mass separating agents (MSAs) which are then regenerated or disposed of, depending on its economic and environmental consequences. The study of both HENs and MENs is aimed at developing more sustainable chemical processes through optimised usage of utilities in each network. When these networks are integrated, HENs can be used to enhance the mass transfer in MENs since mass transfer is a function of temperature (Seader et al., 1998) and therefore, the interaction between the networks can be studied. The implementation of such integrated networks can significantly improve the sustainability of processes, but to adequately account for all processing design parameters within the synthesis, the regeneration of MSAs should be included. The few existing works in CHAMENS in the literature have studied the regeneration of single MSA flowing through just one unit, however, to explore the more complex scenarios involving multiple regenerable MSAs, the

methodology of this thesis is extended to the development of RENs. The model formulation and the synthesis method are discussed in Chapter 3.

There are two types of process synthesis strategies. The first is insight-based which depends on the designer to use sets of physical and thermodynamic knowledge to design a process. In this strategy, targets can be set which are independent of the physical structure of the process. The insight-based strategy can provide valuable understanding of a system performance and characteristics such as costs and configurations of equipment without the final system configurations. The second strategy involves a framework that embeds all possible configurations of the process (El-Halwagi and Foo, 2014). The development of such a structure is typically achieved using the mathematical representation and can produce more robust results, but its success strongly depends on the ability of the structure to embed as many configurations as possible. A summary of these strategies will be discussed in Chapter 2.

1.2 Motivation

There are various synthesis methods available for individual HENs and MENs to find optimal network configurations. These methods are limited in their study of the interactions between the networks. Even though mass exchange operations are influenced by heating and cooling, there is a paucity of literature on combined heat and mass exchange network synthesis (CHAMENS). This is due to the combinatorial nature of competing variables associated with the combined problem resulting in challenges in the synthesis of such combined networks.

It is also worth stating that MENS methods involving regeneration are not well developed. However, pollution minimisation through regeneration in a chemical industry has become an essential aspect of reducing both cost and environmental impact associated with effluent streams. Of the existing methods involving regeneration, only a few papers have studied the regeneration in a simplified regeneration network with a single regeneration unit. Such

simplification was done so as to avoid the complexity involved in solving MENs and RENs simultaneously as both networks consist of highly non-linear equations with various competing variables. Nonetheless, the MENs and RENs have an interrelationship with one another through the external MSAs and investigating the integration of multiple lean streams and regenerants in a detailed network can enhance the optmisation of the combined network.

To the best knowledge of the current author, no literature has considered a detailed REN superstructure involving multiple regenerable external MSAs with multiple regenerants. Furthermore, no study has investigated the effect on the total annual cost of the combined network of MEN and REN with heat integration, when absorption/stripping temperature are varied through a HEN.

Lastly, many studies optimised a process in terms of costs without considering its environmental impacts. Considering economics as a sole objective function may not be enough and it is desirable to perform multi-objective optimisation (MOO) to ensure the synthesised network satisfies both costs and environmental constraints. Despite the importance of the study of environmental impacts in the synthesis step, there is limited literature available. To further optimise a process, there are some studies on the implementation of renewable energies in process synthesis. In general, these energies are fluctuating in supply, and it is essential to extend existing MENS methods to handle such fluctuations as multi-period operations. It was also observed that, MENS methods involving multi-period operation are still in its infancy, unlike its multi-period HENS counterpart. Therefore, this thesis will address these concerns in an effort to bridge the knowledge gap in multi-period CHAMENs literature and extend the existing simplified regeneration approach to RENs.

1.3 Scope and Limitations

This thesis will extend existing CHAMENs superstructure to include multiple external MSAs and detailed REN. Note that regenerating external MSAs can be beneficial in both economic

and environmental aspects. Finding feasible flow rates for these MSAs and regenerating streams is therefore crucial in a process synthesis task. However, to the best knowledge of the current author of this thesis, no literature has considered the synthesis of RENs in CHAMENs. New synthesis methods will not be developed in this thesis, but various existing synthesis approaches will be combined to study the interactions between the different networks.

The general algebraic modelling systems (GAMS) will be used as the environment for the optimization of such networks. The DICOPT algorithm will be used to solve the mixed integer non-linear programming (MINLP) problem since this solver provides solutions quickly and has been shown to be effective for large-scale MINLP formulations.

The environmental impact is obtained by using an environmental impact simulation tool, SimaPro. To produce more realistic solutions, more detailed SimaPro simulations are required. However, such a level of detail is not considered in this thesis. The results involving the environmental impacts obtained in this thesis, however, can be used as a preliminary design.

1.4 Overall Objectives and methodology

This thesis presents a synthesis method for CHAMENs that includes a regeneration exchange network (REN) superstructure with multiple recyclable mass separating agents (MSAs) and multiple regenerating streams. The method involves the SWS approach published by Yee and Grossmann (1990) and Szitkai et al. (2006) for heat and mass exchange network synthesis respectively. The work of Isafiade and Fraser (2009) on CHAMENs involving a single regeneration unit forms the basis of this study where the single unit is extended in a REN in the current thesis. Also, the CHAMENs superstructure with RENs is integrated with utilities generated from both fossil-based and renewable energy sources where the method provided by Isafiade (2017) is adapted to incorporate solar panels and heat storage tanks into the CHAMENs superstructure, and the environmental impact of such networks is determined.

The synthesis method is further formulated as a multi-objective optimisation (MOO) problem to simultaneously optimise CHAMENs in terms of both economics and environmental aspects.

1.5 Thesis Structure

Chapter 2

In this chapter, the review of the relevant literature to this study is provided. pinch technology and mathematical programming for HENS, MENS, and CHAMENs are presented. The SWS of Yee and Grossmann (1990), the SWS of Szitkai et al. (2006), and the CHAMENs model of Isafiade and Fraser (2009) are reviewed in detail due to their applicability to this study.

Chapter 3

The model equations of CHAMENs model including the REN synthesis (RENS) method are presented in this chapter. The complexities and challenges in the combined synthesis method of HENs, MENs and RENs, are also discussed.

Chapter 4

The developed combined model is applied to two case studies. The problem data was adapted and modified to study multiple utility and multiple regenerants scenario in CHAMENs.

Chapter 5

This chapter includes conclusions of this thesis and proposed future works.

Chapter 2

Literature Review

Chapter 2 Literature Review

2.1 Introduction

This chapter provides a review of relevant literature for this study. The first section discusses the synthesis methods for HENs and presents a bibliography on the synthesis methods. The analogy between HENs and MENs provided a platform for synthesis methods to be developed from HENS for MENS. These methods, which are chiefly pinch technology and mathematical programming based, are reviewed. Also, synthesis methods for CHAMNEN is reviewed in this chapter. The last part of the review entails synthesis methods in general that involve environmental impacts and MOO strategies.

2.2 Heat Exchange Networks (HENs)

Heating and cooling are essential in the process industries. An enormous amount of external heating/cooling utilities are implemented to drive chemical reaction, separation and to maintain favourable operating conditions (El-Halwagi, 2017). The energy crisis in the 1970s triggered considerable attention to develop methods to synthesise HENs since the large amount of energy requirements of the industries resulted in significant economical burdens. The heavy exploitation of natural resources has resulted in a scarcity of energy sources such as fossil fuels, and this has also triggered the study of HENS (Vaskan et al., 2012). In HENs, heat integration of hot process streams with cold process streams takes place first, and then the remaining energy requirements are achieved by implementing external utilities to minimize operating cost. The HENS problem is defined by the following problem statement provided in the work of El-Halwagi (1998):

> *There are a number of hot and cold process streams to be cooled and heated respectively. It is aimed to synthesise a heat exchanger network (HEN) which can transfer heat from the hot streams to the cold streams to achieve a minimum total annual cost (TAC) network. Given also are the heat capacity flowrates, heat transfer coefficients, and supply and target temperatures of*

each process stream. Also, information associated with the cooling and heating utility costs, heat transfer coefficients, supply and target temperatures as well as annual operating time, heat exchanger costs and the annual capital cost factor are provided.

There are many synthesis strategies available, which can be classified into two categories. One category is called insight-based methods which are based on fundamental thermodynamics. The other category is based on a framework represented as a mathematical programming model. These synthesis strategies are reviewed in the following sections.

2.2.1 Insight-based Strategies

In this approach, certain variables are targeted to achieve a good, near optimal design solutions. One of the most extensively studied insight-based strategies is pinch technology developed by Linnhoff and Hindmarsh (1983) which can be used to synthesise HENs based on fundamental thermodynamics. pinch technology first targets the minimum hot and cold utilities required by a network at a specific pinch temperature and then this information is used to design network configurations. pinch technology has two main divisions which are energy and cost targeting. These divisions are discussed next.

2.2.1.1 Energy Targeting

In the energy target, pinch technology can be further classified into the graphical approach and the algebraic approach. In each approach, the composite curve plot and problem table are used respectively to find the pinch point. In the composite curve plot, the overall energy available in the hot streams and the overall energy demand of the cold streams are presented along with temperature versus cumulative enthalpy axes as shown in Figure 2.1.

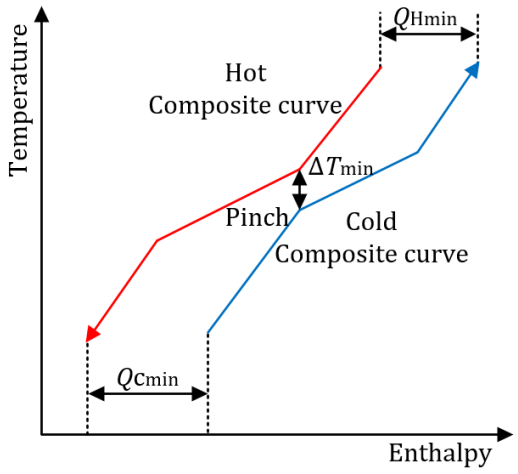

Figure 2.1: Construction of hot and cold composite curves

The hot stream is represented by the line with the arrowhead pointing to the left while the cold stream arrowhead is pointing to the right. The region of vertical overlap between the hot and cold stream composites is denoted as the heat recovery region while the other two regions adjacent to the heat recovery region represent the minimum heating (Q_{Hmin}) and cooling ($\mathrm{Q_{Cmin}}$) duty of a design. The pinch point indicated in Figure 2.1 is the closest approach between the lines and occurs at the point of ΔT_{min}. The pinch point can be used to classify two distinct regions. The first region involves streams with a higher temperature than the pinch temperature which is denoted as the region above the pinch. In this region, hot streams transfer heat to the cold streams, and then external heating is required if the target temperature is not achieved from the heat transfer between the streams. The second region is situated below the pinch and contains streams colder than the pinch temperature. In contrast to the first region, the second region involves heat transfer between the process streams and cold utility duties to satisfy heat deficit. These thermodynamically independent regions can be treated separately without any heat transfer across the pinch. Note that the hot stream composite can be shifted towards the cold stream composite for higher heat recovery while shifting away from the cold stream results in lower heat recovery. The distances between the hot and cold composite affect the heating and cooling duties of a design. The degree of shifting is denoted by the minimum temperature difference, ΔT_{min} which can be specified before the design. Higher values of ΔT_{min} cause higher utility

requirements while lower values result in larger heat exchangers which can be expensive and therefore, reasonable ΔT_{min} values should be selected based on past experiences. Note that typically, ΔT_{min} value of 10 °C or 20 °C is widely used for many industries.

In the algebraic approach, the imprecise nature of the graphical approach can be overcome by implementing the problem table. The pinch point and the minimum energy target can be calculated in the table (Kemp, 2011). pinch technology is not the primary consideration in this thesis and therefore the algebraic method will not be discussed further. pinch technology was primarily developed to achieve the optimal energy networks; however, it is possible to adapt its use for achieving the optimal cost networks.

2.2.1.2 Capital Cost Targeting

In the case of the cost target, it depends on two fundamental thermodynamic factors. The first one is the driving force and the second is the effect of heat loads. There are also various factors such as number of heat exchangers, total heat exchange area, the materials of construction and pressure ratings, etc., which influence the cost targets.

Number of units Targeting

The number of units dominates the capital cost of a process, and therefore, it is beneficial to minimise the number of heat exchangers used in the process. Using a low number of units also allows a practical and straightforward network design. Linnhoff and Hindmarsh (1983) stated that a target for the minimum number of units is one less than the total number of streams which includes the number of utilities. The number of units targeting can be performed in the two regions divided by the pinch and then added to give the overall target. However, it was found that the minimum number of units target does not always give the minimum TAC and may result in a reduction of the solution space (Fraser and Hallale, 2000). As much as the number of units affects the capital cost, the heat exchange area also influences the cost significantly.

The total area targeting

The total heat exchange area requirement for heat exchanger units can be determined before the network design. Linnhoff and Hindmarsh (1983) defined the minimum area as the overall area calculated by assuming ideal counter-current heat exchange between the hot and cold streams. The following equation is used to calculate the ideal area, A, for a counter-current heat exchanger:

$$A = \frac{Q}{U \cdot LMTD} \tag{2.1}$$

In Equation 2.1, Q is the enthalpy change, U and $LMTD$ are the overall heat transfer coefficient, and the log mean temperature differences respectively. The composite curves can be divided into vertical enthalpy intervals as shown in Figure 2.2.

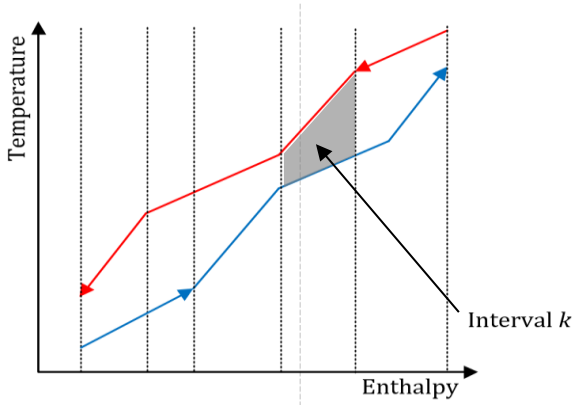

Figure 2.2: Division of the composite curve into vertical enthalpy intervals

These enthalpy intervals are divided at the inflection points of the hot and cold curves. Each interval represents an imaginary heat exchanger. Assuming vertical heat transfer and constant overall heat transfer coefficient, the theoretical heat exchange area can be calculated at each segment using the following equation:

$$A = \frac{1}{U} \sum_{k}^{\text{Intervals}} \frac{Q_k}{\Delta T_{lm,k}} \tag{2.2}$$

The area calculated using the above equation is approximately equal to the total heat exchange area calculated using the composite curves presented in Figure 2.2 (Hohmann, 1971). The meaning of the vertical transfer is that the heat transfer between the hot and cold streams must be matched in exact proportion throughout the interval *k* as shown in Figure 2.3a. Note that the shortcoming of assuming vertical heat transfer in each interval results in substantial stream splitting which causes complex networks and can become impractical and expensive to install pipelines. In the case of non-uniform heat transfer coefficient, there may exist significant variations in heat transfer coefficients, and non-vertical heat transfer (criss-crossing) may need to occur to obtain minimum heat exchange area. The graphic representation of criss-crossing is shown in Figure 2.3b.

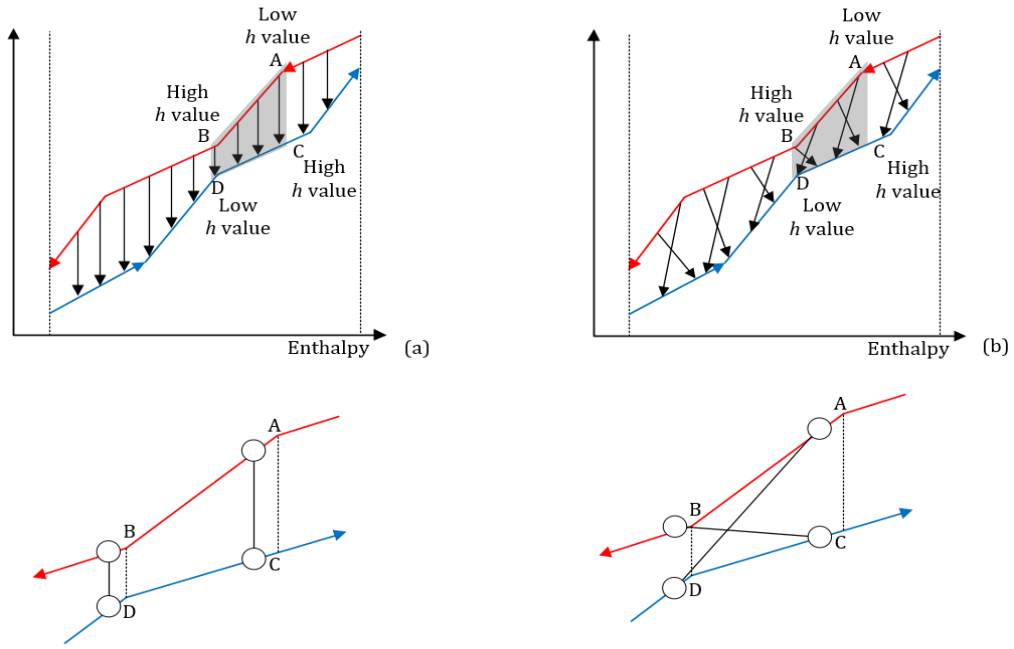

Figure 2.3: The graphical representation of vertical (a) and non-vertical heat transfer (b)

Note that the overall heat transfer coefficient is not a constant but rather dependent on stream characteristics. The coefficient can be calculated using the stream film heat transfer coefficients of hot and cold streams due to the additive nature of the heat transfer coefficients:

$$\frac{1}{U} = \frac{1}{h_{ih}} + \frac{1}{h_{jc}} \tag{2.3}$$

Where h_{ih} and h_{jc} are the stream film heat transfer coefficients for hot and cold streams respectively. In the vertical heat transfer match between A-C and B-D (as shown in Figure 2.3a) which involves significantly different values of film heat transfer coefficients, the design can result in a higher heat exchange area while the non-vertical heat transfer match between A-D and B-C (as presented in Figure 2.3b) which involves the similar values of film heat transfer coefficients can end up using the driving forces more efficiently and result in a smaller heat exchange area. However, the equation involved with the vertical heat transfer is relatively simple and the results obtained from the equation can be used to provide a guideline to a preliminary design to estimate the capital cost of the network.

Townsend and Linnhoff (1984) combined Equation 2.2 and 2.3 to calculate the total minimum heat exchange area and this combined equation is called the Bath formula:

$$A_{\min} = \sum_{k}^{\text{Interval},K} \frac{1}{\Delta T_{lm,k}} \left[\sum_{ih}^{\text{Hot streams}} \frac{q_{ih}}{h_{ih}} + \sum_{jc}^{\text{Cold streams}} \frac{q_{jc}}{h_{jc}} \right] \tag{2.4}$$

In Equation 2.4, q_{ih} and q_{jc} are the enthalpy changes in each stream. When the stream film heat transfer coefficient variations are significant, Kemp (2011) suggested that a linear programming algorithm can be used to calculate the minimum area. However, Equation 2.4 can provide a solution with a deviation within 10 percent when the magnitudes of film heat transfer coefficients are different by less than an order of magnitude. Note that knowledge on stream film heat transfer coefficients is scarce in general. These coefficients can be estimated from different sources such as existing heat exchangers, sizing calculations and stream pressure drop information. The results obtained from the total area target can be used to estimate the capital costs of the exchangers in HENs. The following equation can be implemented (Smith, 2005):

$$\text{Total Network Capital Cost} = N \left[a + b \left(\frac{A_{\min}}{N} \right)^{c} \right] \tag{2.5}$$

Where N is the minimum number of units. The constants a, b and c are the cost law constants describing materials of construction, pressure rating and type of exchangers respectively. The total minimum area is divided by the minimum number of units. Smith (2005) stated that this might seem like a primitive assumption but, this provides exceptionally good estimation since the equally divided heat transfer areas tend to overestimate the capital cost while the minimum area target usually underestimates the areas compared to the final design of practical networks in general. Therefore, these negative and positive factors partially cancel each other and provide reasonable estimations of the capital cost given that the magnitude of the heat transfer coefficients is within one order of magnitude. In summary, the main advantage of using insight-based methods is that the methods can provide useful guidelines without any complex synthesis and it can produce feasible network designs. However, the insight-based methods can become tedious when involving a large number of streams, and the steps are dependent on each other which prevents the simultaneous trading-off of variables (Furman and Sahinidis, 2002).

2.2.2 Framework Strategies (Mathematical Programming)

In framework strategies, often denoted as simultaneous synthesis methods, mathematical programming is used to formulate the entire synthesis task as a mathematical optimisation problem. This technique garnered much attention in the last decades due to the fast development of computers and the rapid increase in computational capacity. The solutions obtained from mathematical programming can provide a desired optimal network structure and a network's TAC simultaneously which is the main improvement compared to the previously discussed insight-based strategies. It is worth mentioning that obtaining a solution to complex optimisation problems is difficult in general and therefore, the development of new optimisation algorithms and the optimisation model formulations are extensively studied, remaining a continuously developing research area.

The framework strategies first involve generation of a framework which is claimed to contain all the possible configurations. Secondly, a mathematical representation of the

framework is formulated. Lastly, the objective function is evaluated to optimise the mathematical model. One of the most widely used mathematical models is the MINLP model (Vaskan et al., 2012). Note that the solution time of the MINLP model increases exponentially with an increase in number of binary variables and therefore, Grossmann (1996) suggested that to achieve a good MINLP model, the model equations should be linear if possible. The author also mentioned that if the problem allows, reformulating the model as a convex problem can help in achieving a globally optimal solution. In the case of a convex problem, the mathematical programming methods can guarantee a global optimum solution, but for a non-convex problem, this method can be trapped in local optima (Furman and Sahinidis, 2002). Nevertheless, many newly developed synthesis methods tend towards mathematical programming to avoid the tedious nature of the insight-based strategies and to simultaneously optimise a network configuration.

2.2.2.1 Bibliography of Mathematical Programming

In the review provided by Furman and Sahinidis (2002) a summarised bibliography for HENs synthesis methods in the 20th century is divided into two categories namely, the insight-based (sequential) and the framework-based (simultaneous) approaches. The details of each branch are summarised in Figure 2.4.

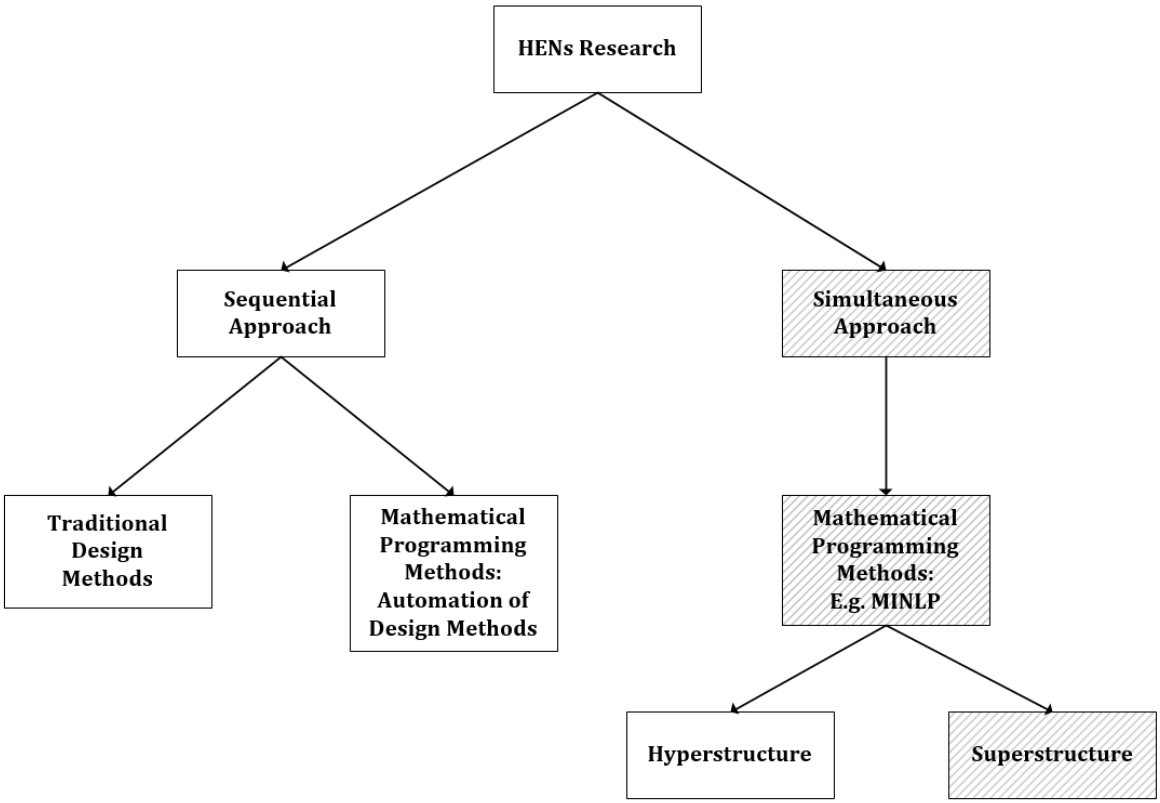

Figure 2.4: A summary diagram of different synthesis methods for HENS (Furman and Sahinidis, 2002)

In the sequential approach, a process is divided into a series of sub-systems to simplify the problem in obtaining a network design. It can further be classified into the traditional design methods such as pinch technology and the mathematical programming technique. The mathematical programming techniques under the sequential approaches, however, do not involve any frameworks but solely based on the automation of pinch technology and/or heuristics. These methods are therefore still sequential. The transhipment model of Papoulias and Grossmann (1983) and the transportation model of Cerda and Westerburg (1983) fall under this category. The main disadvantage of the sequential method is that the trade-offs between the different costs involved in the TAC cannot be obtained simultaneously and therefore, a network generated from such approach cannot guarantee the global optimum (Furman and Sahinidis, 2002).

The simultaneous approach can be further classified into hyperstructure and superstructure depending on the framework used in the approach. Floudas and Ciric (1989) developed a HENS hyperstructure model using a MINLP where the target and design steps involved in pinch technology are combined as a single step. Papalexandri et al. (1994) also developed a HENS hyperstructure model. However, the nature of the hyperstructure is highly non-linear and therefore, the initialisation of the structure can be a challenging task when considering a problem involving many streams. Also, the global optimum solution cannot be guaranteed in the hyperstructure methods (Floudas, 1995).

In an attempt to develop a structure with fairly linear nature, superstructure approach was developed by Yee and Grossmann (1990). The superstructure is based on the key variables such as temperature to simplify a problem. This model is the first method to consider all the costs contributing to the TAC of the HENS problem. Some works of literature (Aaltola, 2002; Björk and Westerlund, 2002; Verheyen and Zhang, 2006) have adopted the superstructure of Yee and Grossmann (1990). Also, the HENS model of Yee and Grossmann (1990) was extended to MENS in the work of Szitkai et al. (2006). The works of Yee and Grossmann (1990) and Szitkai et al., (2006) are revised in detail later in this chapter as these approaches serve as the basis of the CHAMENs model developed this thesis.

There are some attempts in process synthesis to combine insight and framework-based strategies which can involve past engineering experiences or the rules of thumb. The work provided by Kravanja and Grossmann (1997) combined hierarchical decomposition heuristic methods with mathematical programming methods. In the published work of Isafiade and Fraser (2007), the mathematical programming approach was combined with pinch technology to synthesise a network superstructure. These methods can be regarded as the third general strategy in process synthesis (Szitkai, 2004); however, the main scope of this thesis is mathematical programming methods based on the superstructure. Thus, those knowledge-based methods are not discussed further.

In concluding remarks, the design approach based on mathematical programming is exceptionally beneficial when common sense engineering is not enough to predict the best

design options. Also, the mathematical programming approaches have been the leading choice for synthesis methods from the late 1980s. The next section reviews the superstructure model of Yee and Grossmann (1990) as mentioned above.

2.2.2.2 Stage-wise Superstructure of Yee and Grossmann (1990)

The MINLP model of Yee and Grossmann (1990) focuses on searching for both optimal operating costs and capital costs simultaneously. The result of the model defines a network by providing utility requirements, stream matches, energy requirements and operating temperature of each exchanger, a network configuration with stream flows and lastly, an area of each exchanger. A general formulation of the MINLP model is presented in Equation 2.6 (Grossmann, 1996):

$$\begin{aligned} &\min Z = f(\bar{x}, \bar{y}) \\ &\text{s.t.} \\ &h(\bar{x}, \bar{y}) = 0 \\ &g(\bar{x}, \bar{y}) \leq 0 \\ &\bar{x} \in X, \bar{y} \in \{0, 1\} \end{aligned} \tag{2.6}$$

Where $f(\bar{x}, \bar{y})$ is the objective function which minimises TAC of a network and $h(\bar{x}, \bar{y})$ refers to the equations describing the physical properties such energy balances of a problem and lastly, the inequalities are presented as $g(\bar{x}, \bar{y}) \leq 0$ which constrains solution space to obtain feasible networks. The variable $\bar{x}$ denotes design variables such as flowrates, compositions and temperatures etc. while $\bar{y}$ denotes the binary variables. When all the functions involved in the model formulation are linear, the problem is called a mixed-integer linear program (MILP). If there are no binary variables in the formulation, then the problem is denoted as linear programming (LP) or non-linear programming (NLP) problem depending on the linearity of the functions involved.

In a stage-wise superstructure, a large number of potential network topologies are presented from which the optimum solution is selected. The establishment of boundaries in the superstructure is a crucial step which can improve the feasibility and promote the model to achieve the optimum. These boundaries also reduce solution search time. A superstructure with two hot and two cold streams is presented in Figure 2.5.

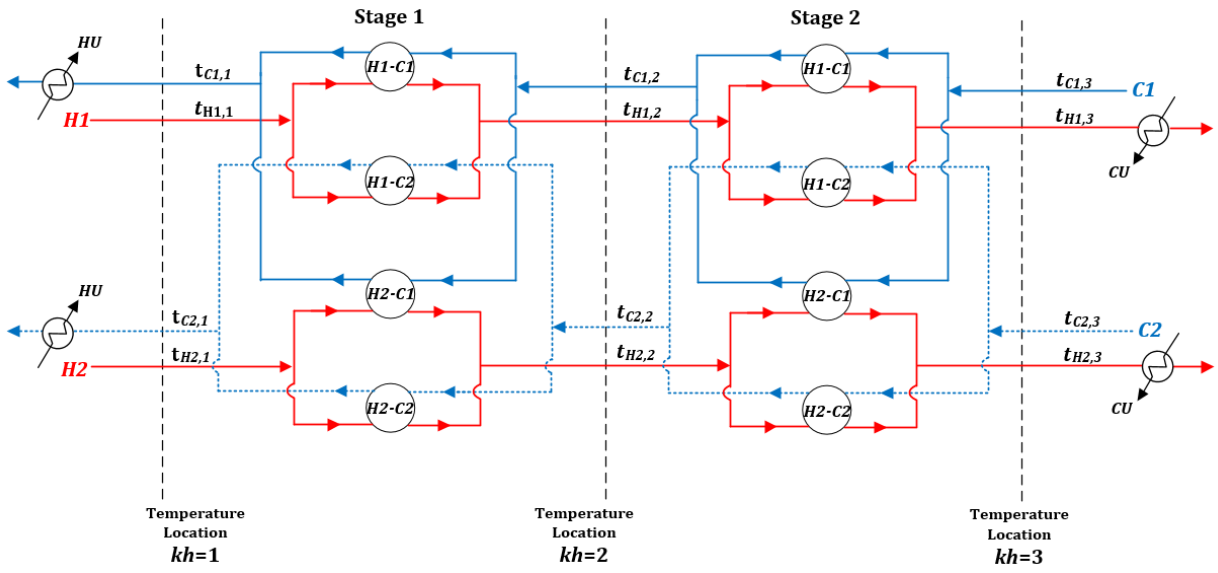

Figure 2.5: The Stage-wise superstructure developed by Yee and Grossmann (1990)

The superstructure shown in Figure 2.5 consists of temperature stages (*kh*). Yee and Grossmann (1990) suggested that the number of temperature stages can be equal to the maximum number of hot or cold streams in a system. To simplify the problem further, the hot and cold utility exchangers are placed outside of the superstructure boundaries as denoted with *HU* and *CU* respectively. The model also assumes isothermal mixing of streams.

The hot stream *H1* and *H2* are designated to enter the superstructure at the first temperature location of *kh* = 1 and exit the structure at the end of the boundary at the last temperature location of *kh* = 3. Any hot and cold streams can be matched once in each stage to exchange heat. Since there are two cold streams, *C1* and *C2* in Figure 2, the hot stream *H1* can split into two streams in which each split stream exchange heat with each cold stream. The split

matches are indicated with *H1-C1* and *H1-C2* circles in the figure. The exit streams from the matched exchangers are mixed at the same temperature for simplicity. The temperature of the mixed streams then becomes the hot inlet temperature in stage 2 which is indicated by the symbol $t_{H1,2}$ where this is selected as a variable to be optimized. The stream with temperature $t_{H1,2}$ will go through the same procedure as in stage 1. In each stage, *H2* is also optimized in the same manner as *H1*. To calculate the temperature of *H1* in each stage, various constraints were used to ensure only logical heat exchanges would take place in each stage.

To ensure a synthesised network produces thermodynamically logical solutions, various balances and constraints are used in the superstructure. In overall stream heat balance, the sum of exchanged heat in each stage is set equal to the heat loads of streams. Heat balances within each stage are also activated since temperatures of hot/cold streams in each stage are variables to be optimised. As explained earlier, the first and the last boundaries of a superstructure were defined using supply and target temperature of hot/cold streams.

Thermodynamic feasibility of heat exchanges in each stage is governed by introducing a set of constraints to achieve a monotonic decrease across the temperature stages from left to right. To represent the existence of heat exchangers in the superstructure, binary variables are used to indicate the existence of a match between a hot and a cold stream. The integer value of '0' indicates no match between a hot/cold stream while '1' indicates the existence of a match. Lastly, the objective function is presented to optimise the HEN. The heat exchange area calculations are included in the objective equation to calculate the capital cost of the heaters, coolers, located at the boundary of the network, and heat exchangers situated within the superstructure. *HU* and *CU* costs are also included in the objective equation, and then these expressions are summed to give a TAC. A general expression for the objective function is presented in Equation 2.7.

$$TAC = \min \left\{ \begin{array}{c} [(\text{Operating cost of HU}) + (\text{Capital cost of heater})] \\ +[(\text{Operating cost of CU}) + (\text{Capital cost of cooler})] \\ +[\text{Capital cost of process heat excahngers}] \end{array} \right\} \quad (2.7)$$

In summary, the aim of the MINLP model of Yee and Grossmann (1990) is to minimise the objective function in terms of the feasible solution space governed by energy balances and constraints. The variables to be optimised by the model are intermediate temperatures across the superstructure, heat duty and driving forces for each heat exchanger. The model is formulated to give non-negative values for the variables. Yee and Grossmann's (1990) model assumes constant operating conditions. However, fluctuations may occur in real operation. Some authors including Floudas and Grossmann (1986), Papalexandri et al. (1994), Aaltola (2002), Verheyen and Zhang (2006), Isafiade and Fraser (2010) and Ahmad et al. (2012) have considered multi-period scenarios in their model formulations.

2.2.2.3 Multi-period HEN Synthesis

Operating conditions and parameters in a process can vary with time. The variations may arise from scheduled changes in operations to enhance the performance of a plant or may be the result of unplanned events involving fluctuations in process stream parameters such as flowrates, supply/target temperature and changes in ambient temperature (Ahmad et al., 2012). The segmentation of these variations is called 'periods' in multi-period HEN synthesis and aims to establish networks that can achieve the required heating and cooling of all considered operating conditions while minimising TAC.

The synthesis of multi-period HENs can also further be classified into sequential and simultaneous methods. Floudas and Grossmann (1986) presented a sequential model to optimise multi-period HEN. The drawback of this model is that configurations with a high number of heat exchanger units with lower total annualised costs were ignored from the solution space. Papalexandri et al. (1994) developed a simultaneous hyperstructure model to handle multi-period scenarios, however, the model suffered from severe non-linearity.

In order to consider multi-period variations simultaneously, Aaltola (2002) modified the SWS model of Yee and Grossmann (1990). The author's approach used the average of the heat exchange areas as the representative period. However, selecting the average area may become a problem when the period of interest requires a higher heat exchange area than the selected average area. This motivated Verheyen and Zhang (2006) to improve the model of Aaltola (2002) further to select the maximum heat exchange area per period. Isafiade and Fraser (2010) adapted a variant of the stage-wise superstructure for multi-period HENS while also using the maximum area approach. However, the drawback of the stage-wise superstructure approach is that it can exclude some possible optimal solutions due to its simplified nature. In order to overcome such shortcomings, Ahmad et al. (2012) presented a simulated annealing synthesis method. This method involves a small random perturbation to a variable in a system. The objective function is then calculated. If the calculated value is less than the previous solution, the perturbation is accepted.

In the stage-wise superstructure approach in multi-period HENS, the index '*p*' was introduced to represent multiple operations in the model equations which include energy balances, constraints and objective function. The objective equation contains both capital and operating costs. Aaltola (2002) included weighed utility costs which allowed the most common operating conditions to dominate in the cost calculation while other operating conditions are also considered. The utility costs are weighed depending on the duration of each period over the entire operating periods. The same objective function is applied in the model of Verheyen and Zhang (2006). Isafiade and Fraser, (2010) observed that the weighting terms used in the previous work of Aaltola (2002) and Verheyen and Zhang (2006) can only provide an accurate annual operating cost per period when the same durations are used in each period, and therefore, the authors proposed more general weighting terms to calculate AOC in the objective function. The model equations and the weighting terms will be presented in Chapter 3.

As much as the single period superstructure approach may require special initialisation and boundary setting techniques for the variables in the model to obtain feasible solutions in a

short duration of time, the HENs problem involving multi-period operations can be an even more complex problem where more advanced initialisation schemes are necessary. In addition, there are some authors who considered problems involving multiple utilities in HENS. Many industrial cases involve more than one type of utility and therefore, studying multiple utilities can provide more reliable solutions. However, the degrees of freedom will increase and solving such problems can be challenging.

2.2.2.4 Multiple Utility Operations

The benefit of studying multiple utilities in process synthesis is the capability of selecting utilities considering economics. Many synthesis methods which are based on sequential and mathematical approaches have been developed. Shenoy et al. (1998) proposed a sequential method based on pinch technology involving single period operations with multiple utilities while some of the mathematical programming methods of Isafiade and Fraser (2008a) and Ponce-Ortega et al. (2010) are available in the literature. The MINLP models of Isafiade and Fraser (2008a) and Ponce-Ortega et al. (2010) allow utilities to be placed at any stages in the superstructure. In order to surmount inefficient superstructure geometry and reduce the large search area for an optimal solution in these models, Na et al. (2015) presented a method involving utility substages. The implementation of utility substages simplifies the solution space by fixing positions of utilities heuristically in the order of temperature. A reduced model size enhances solution quality and time compared to the previous methods.

Note that these aforementioned methods involve single-period operation, and therefore, Isafiade et al. (2015) extended the single-period model to handle both multi-period and multiple utility operations. The authors implemented the slightly modified superstructure model by Bogataj and Kravanja (2012), which adapted the Yee and Grossmann (1990)'s HENs model. The modification allows process streams to exchange heat with different types of utilities, unlike the original superstructure. In this model, utilities were restricted in the first and the last intervals. This was necessary to reduce the effect of non-convexities when the superstructure involves both multiple periods of operations and multiple utilities. The

same approach of Isafiade et al. (2015) will be followed in this thesis as the problem of interest is developed as a multi-period involving multiple utilities. As mentioned before, the CHAMENs also involves MENs. A summary of MENS is presented next.

2.3 Mass Exchange Networks (MENs)

Mass exchangers are essential operations for pollution prevention. Pollutants are selectively removed from waste streams (rich streams) by implementing MSAs which can be called lean streams. There are different domains of mass exchange operations such as absorption, adsorption, extraction, ion exchange, leaching and stripping (El-Halwagi 1998). The concept of reducing the environmental impact of a process through the use of MENS was originally proposed by El-Halwagi and Manousiouthakis (1989) where the methodology was based on the conventional heat transfer pinch technology. The MEN synthesis problem statement is presented as follows (El-Halwagi, 1998):

> *Given a number of waste (rich) streams (sources) and a number of MSAs (lean streams), it is desired to synthesise a cost-effective network of mass exchanger units that can preferentially transfer certain undesirable species from the waste streams to the MSAs. Given also are the flowrate of each rich streams, supply and target compositions of both rich and lean streams. The flowrate of each MSA is a variable to be optimised so as to minimise the network cost.*

The MENs synthesis methods were motivated by the need to develop a cost-effective network that can selectively remove undesirable species from the waste streams and to select appropriate MSAs as well as competing technologies while optimizing costs associated with the network based on the thermodynamic considerations. A schematic representation of a number of rich streams (N_R) with associated flowrates and a number of lean streams (N_S) is presented as follows:

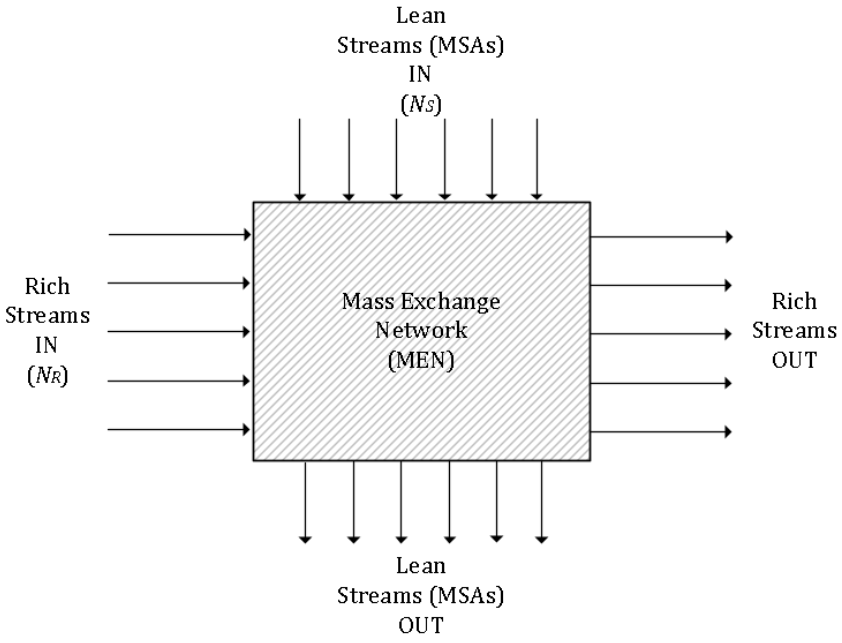

Figure 2.6: Schematic representation of MEN (El-Halwagi and Manousiouthakis, 1989)

The 'box' shown in Figure 2.6 is the mass exchange network, which is aimed at utilising the lean streams for waste minimisation. The supply and target compositions of rich and lean streams are satisfied through the network synthesis, and the flowrates of the lean streams are determined to minimise the network cost. The lean streams used in the MENs synthesis can be classified into once-through MSAs and regenerable MSAs. The once-through MSAs can be assumed to remove pollutants from the rich streams at a very low costs while the regenerable MSAs are sent to a regeneration unit for further purification and re-use (El-Halwagi and Manousiouthakis, 1990). The regeneration will be discussed later in this chapter.

Ever since the MENS concept was established, many studies on MENS have been published to explore different methods to obtain optimal networks. Some of the studies include the automated pinch technology synthesis methods (El-Halwagi and Manousiouthakis, 1990); hyper-structure approach (Papalexandri et al., 1994); synthesis with genetic algorithm (Garrard and Fraga, 1998); super-targeting method (Hallale and Fraser, 2000a; 2000b; 2000c; 2000d); stage-wise superstructure approach (Chen and Hung, 2005; Szitkai et al.,

2006); Interval based MINLP superstructure method (Isafiade and Fraser, 2008b); Supply and target based superstructure approach (Azeez et al., 2013; 2012). Lastly, detailed costing approach of Short et al. (2018) and generalized disjunctive programming (GDP) approach of Velázquez-Guevara et al. (2018).

As mentioned previously, the MENS methods are counter-parts of HENS methods, and therefore, the synthesis methods for MENs can also be classified into two main categories: insight-based and the mathematical programming methods. A summary of different MENS methods is presented in the following section.

2.3.1 Pinch Technology for MENS

Many existing methods for HENs are adapted to synthesise MENs due to the analogies that exist between the two systems. Like the HENs pinch technology, the graphical and the algebraic approaches are available for MENS. The similarities are summarised in Table 2.1.

Table 2.1: The analogy of MENS and HENS (Szitkai et al., 2006)

	MEN	**HEN**
Transported quantity	Mass	Heat
Driving force	Concentration differences	Temperature differences
Source	Rich process streams	Hot process streams
Sink	Lean process streams	Cold process streams

MENS and HENS are similar in that both networks utilise driving forces involving mass and heat. Also, there are sources and sinks in which the quantities can be transported. However, there are a few fundamental differences between the two systems. Equilibrium relations between streams drive mass exchange in MENS. The analogies between the systems can only be applied to single component MENS as no multiple components heat analogue exist. Besides, the physical application of MENs are very different from HENs and therefore,

defining new variables, and stream conditions in a MENS context is necessary. In 1989, El-Halwagi and Manousiouthakis first formulated the concept of MENS by adopting pinch technology of HENS which involves two synthesis steps: targeting and design. In the targeting step, the best achievable cost is targeted based on thermodynamic constraints. Then, in the design step, a network that meets the target is designed. The different targeting methods aim to minimise the cost of MSAs, number of units, capital costs and TAC respectively. These targeting methods are discussed next.

2.3.1.1 The minimum cost of MSAs target

The minimum cost of MSAs target, developed by El-Halwagi and Manousiouthakis (1989), is adapted from the minimum energy target of HENS. The cost data of MSAs are integrated with the thermodynamic feasibility to identify the minimum flow rate and cost of each MSA required to achieve the target. In the minimum cost of MSAs target, the use of the process MSAs is maximised prior to implementing external MSAs (El-Halwagi, 1998). El-Halwagi and Manousiouthakis (1989) introduced the concept of corresponding concentration scales since the driving force of mass transfer in the actual and equilibrium concentrations are different. Note that each MSA has different composition scale and therefore, to compare different MSAs together, the composition, x_l, of each MSA is mapped to its corresponding y_r compositions to allow all MSAs to be plotted on the same axis. Following the same way to construct the composite curves in HENS, the rich and lean composite curves are obtained by combining the compositions based on composition intervals. The rich and lean composite curves are plotted together to form the mass transfer composite curve for MENs. The MSA targets are performed at a specified minimum approach concentration (ε) to avoid infinitely large mass exchangers. The lean composite curves are shifted towards the rich composite curve and the point of contact is called the pinch point. The pinch divides the synthesis problem into two regions; above the pinch and the below the pinch. The mass transfer composite curve for MENs is presented in Figure 2.7.

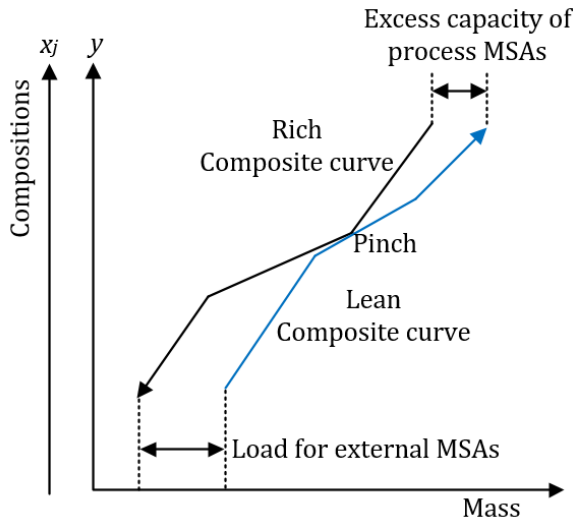

Figure 2.7: The composite curves of the rich and lean streams on the same axes

The overlap of the two composite curves represents the maximum amount of exchangeable mass between the rich streams and the process lean streams. The overshoot between the rich and lean composite curves above the pinch represents the excess process MSAs which cannot be used due to limitations based on thermodynamics. This excess can be reduced by lowering flowrate and/or outlet compositions of process MSAs. The distance located below the lower end of the lean composite curve denotes the amount of mass to be transferred by external MSAs. The information presented on the mass transfer composite curves can then be used to obtain the minimum cost of MSAs.

2.3.1.2 The Minimum Number of Mass Exchanger Units Targeting

El-Halwagi and Manousiouthakis (1989) also presented the minimum number of mass exchanger units target. In a practical context, minimising the number of mass exchange units to save the cost of installing pipes, foundations, equipment and maintenance, is logical to optimise a network. El-Halwagi and Manousiouthakis (1989) stated that the minimum number of units and the total number of streams have the relationship:

$$N_{\text{units,Pinch}} = \left(N_{R,\text{Above Pinch}} + N_{S,\text{Above Pinch}} - 1\right) + \left(N_{\text{R,Below Pinch}} + N_{S,\text{Below Pinch}} - 1\right) \quad (2.8)$$

Where $N_{\text{units,pinch}}$ is the minimum number of units, and this can be obtained by the sum of the total number of rich and lean streams above the pinch, denoted as $N_{R,\text{Above pinch}}$ and $N_{S,\text{Above pinch}}$ respectively, and the sum of the total number of rich and lean streams below the pinch written as $N_{\text{R,Below pinch}}$ and $N_{S,\text{Below pinch}}$respectively in Equation 2.8 above. The capital cost of the network is indirectly minimised as the capital cost, in general, is a concave function of the unit size. Besides the number of units, factors such as the number of stages and height associated with mass exchanger units affect the capital cost of the mass exchange network. Due to the lack of capital cost targeting methods in literature at that time, El-Halwagi and Manousiouthakis (1989) were not able to perform targeting for TAC which is called supertargeting. The capital cost targeting methods were published in a series of publications in the year 2000 by Hallale and Fraser.

2.3.1.3 Capital Cost targeting for MENs

The mass transfer composite curve of El-Halwagi and Manousiouthakis (1989) was a good adoption of the HENS pinch technology for MENS problems. However, the driving force of mass transfer was not depicted on the mass transfer composite curves. This implies that the sizing of mass exchanger units was not possible. The limitation in the sizing is the reason Hallale and Fraser (2000a, 2000b, 2000c, 2000d) developed methods for capital cost targets. Prior to this the synthesis steps involved minimum MSA cost target and design to meet the target as discussed in the previous section.

In order to overcome the knowledge gap, Hallale and Fraser (1998) introduced a new tool called the *y-x* composite curve plot where the rich stream composition (*y*) is plotted against the lean stream composition (*x*) instead of mass. The y-x composite curve plot consists of a composite operating line and the mass transfer equilibrium line. The modification allowed the driving force to be depicted and therefore, sizing of the equipment became possible. However, Hallale and Fraser (1998) noticed that the *y-x* composite curve plot could only be used in a problem involving non-overlapping MSAs. The non-overlapping MSAs implies that

each MSA usage is restricted to a specific region of the composite plot and the *y-x* composite curve plot can be used to display different MSAs which do not overlap on the same axis. However, when the MSAs overlap, this can cause a problem when the *y-x* composite curve plot is used as each MSA has different equilibrium relations and therefore, there are no common bases to compare different MSA compositions (x). To compare different types of MSAs on the same axis, Hallale and Fraser (2000a) developed the *y-y** composite curve plots to compare MSAs on the same scale. The authors expressed MSA composition (x) as the rich stream composition in equilibrium (y^*). The transformation is presented as follows:

$$y^* = m_l(x_l) + b_l \tag{2.9}$$

Prior to developing the *y-y** composite curve plot, the mass transfer composite curve of El-Halwagi and Manousiouthakis (1989) is updated in terms of y^*. The rich and lean composite curve is developed in the same way as before in the mass transfer composite curve presented in section 2.3.1.1. The "diagonal rule" is used to add up mass in the composition intervals where overlaps occur. In the case of the lean composite curve, it is plotted against y^* instead of x as shown in Figure 2.8a. Hallale and Fraser (2000a) modified the minimum composition difference in terms of the rich stream as follows:

$$\Delta y_{\min} = m_l \cdot \varepsilon \tag{2.10}$$

The rich and lean composite curves are plotted on the same axes and shifted until the minimum distance between the curves is the same as the $\Delta y_{\min}$. This plot is presented in Figure 2.8a.

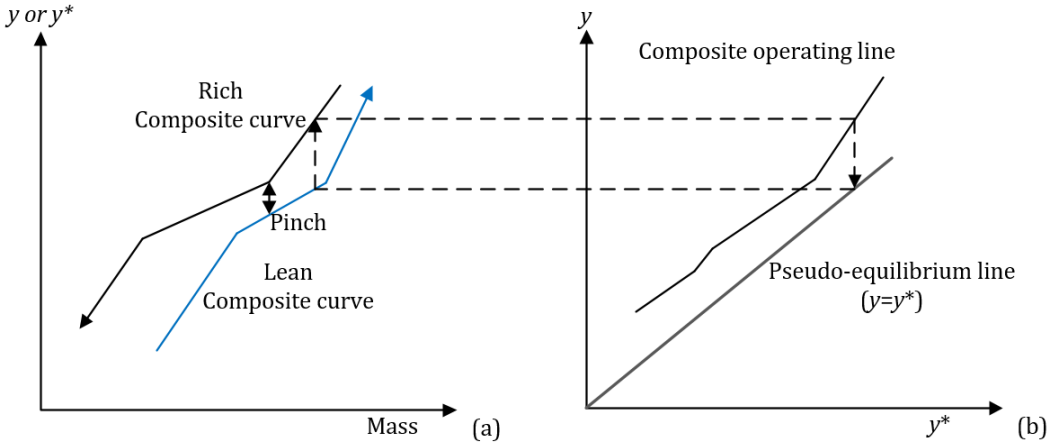

Figure 2.8: Construction of the y-y composite curve plot (b) from the mass transfer composite curve plot (a) (Hallale, 1998)*

The mass transfer composite curve presented in Figure 2.8a is converted into the y-y^* composite curve plot by plotting y values against the y^* values to obtain the composite operating line as shown in Figure 2.8b. The converted plot consists of the composite operating line and pseudo-equilibrium line which is the line with a slope of 1. The composite operating line represents how x (*or* y^*) and y varies throughout the entire network. The composition differences in the mass transfer composite plot are translated into the y-y^* composite curve plot as indicated with the dotted line.

The significant achievement of the y-y^* composite curve plot is that this can handle both non-overlapping and overlapping MSAs problems and therefore, this is a general approach to MENS problems. The y-y^* composite curve plot also can be divided into composition intervals at the inflection points on the composite operating line. Each interval can be treated as an imaginary mass exchanger. The plot also shows vertical transfer profile which is analogous to the HENS targeting approaches. In the case of stage-wise exchangers, a number of stages can be obtained graphically or by using the Kremser equation. The number of transfer units of continuous-contact columns can also be obtained from the plot since the driving forces composition differences are presented on the y-y^* composite curve plot. The plot allows capital cost targeting methods to be developed for MENS. Since this section focuses on the

capital cost targetings for MENS, the targeting methods defined in terms of the number of stages, exchanger height and exchanger mass are introduced next.

The minimum number of stages targeting

A stage-wise exchanger is a vertical, cylindrical pressure vessel where the primary design goal of the exchanger is to establish sufficient contact areas for the rich and lean streams (Seader et al., 1998). In a stage-wise exchanger, the rich and lean streams are allowed to transfer mass through intimate contact through different stages in the exchange in a countercurrent flow (El-Halwagi, 1998). A simplified diagram for a stagewise exchanger is shown in Figure 2.9.

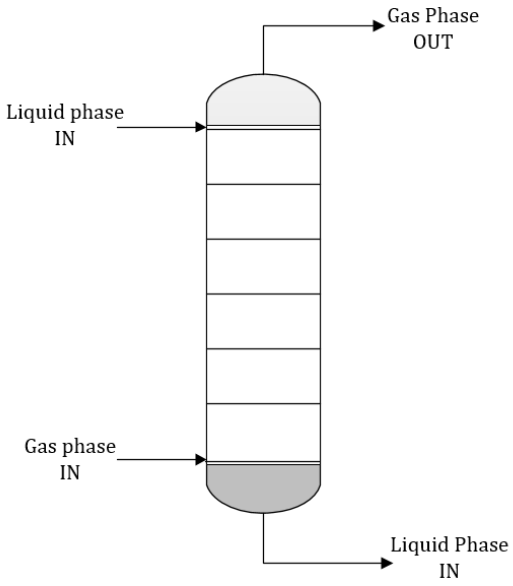

Figure 2.9: A diagram of the stagewise exchanger

Having enough contact time and mixing, the rich and lean phases will be in an equilibrium state with one another, and therefore each stage in the exchanger is denoted as an equilibrium stage. In the case of isothermal, dilute mass exchange systems, and when both the operating and equilibrium lines are linear, the Kremser equation (Treybal, 1980) can be used to determine the equilibrium stages:

$$N_{stages} = \frac{\ln\left[\left(1 - \frac{m_l G_r}{L_l}\right)\left(\frac{y_r^{in} - m_l x_l^{in} - b_l}{y_r^{out} - m_l x_l^{in} - b_l}\right) + \frac{m_l G_r}{L_l}\right]}{\ln\left(\frac{L_l}{m_l G_r}\right)} \tag{2.11}$$

The term $\left(\frac{L_l}{m_l G_r}\right)$ is defined as the removal factor and this is the ratio of the slope of the operating line and the equilibrium line. When the removal factor is equal to '1', the following expression can be used:

$$N_{stages} = \frac{y_r^{in} - y_r^{out}}{y_r^{in} - m_l x_l^{in} - b_l} \tag{2.12}$$

Hallale (1998) mentioned that the operating line in MENs will always be straight since the stream flowrates are kept constant. It was also stated that the equilibrium lines are often linear and therefore, the Kremser equations will be suitable in many cases. When non-linear equilibrium lines are required, the graphical approach must be followed since the number of equilibrium stages is not an additive property which means, breaking non-linear equilibrium lines into linear segments and then adding the number of equilibrium stages in each segment will result in errors. In the Kremser equation, the presence of singularities and its non-linearity result in numerical challenges in a mathematical programming environment. In order to overcome such challenges, Shenoy and Fraser (2003) developed a simpler formulation of the Kremser equation:

$$N_{stages} = \left(\frac{\Delta y^n + \Delta y^{*n}}{\Delta y_1^n + \Delta y_2^n}\right)^{\frac{1}{n}} \tag{2.13}$$

Where: Δy^n is the rich stream concentration difference,

Δy^{*n} is the lean stream equilibrium concentration difference,

Δy_1^n is the driving force at the rich end of the exchanger,

Δy_2^n is the driving force at the lean end of the exchanger and

n is the ratio of logarithmic mean terms.

The n value of 1/3 (Underwood, 1970) and 0.3275 (Chen, 1987) can be used when sizing the mass exchangers. In practice, enough time may not be allowed for each stage to reach equilibrium. The insufficient contact time can result in poor mass transfer, and eventually more stages will be required. The number of actual stages can be determined by incorporating the overall exchanger efficiency (η_o):

$$N_{actual} = \frac{N_{stages}}{\eta_o} \tag{2.14}$$

The past 70 years of extensive studies have shown that the overall exchanger efficiency is a complex function of geometry, design of the contacting trays, flowrates of vapour and liquid streams and composition of streams associated with a column (Seader et al., 1998). The overall exchanger efficiency can be obtained from past experiences of similar systems and determined from empirical equations and semi-theoretical models based on mass and heat transfer rates (Perry et al., 1997; Sinnott, 1999). For preliminary design, Coulson et al. (1993) stated that overall exchanger efficiency of 50 percent could be assumed where the efficiencies generally are between 30 percent and 70 percent.

Each interval in the *y*-*y** composite curve plot can be treated as a fictitious mass exchanger, and the total number of stages can be obtained by summing up the number of stages in each interval as follows:

$$N_{actual,total} = \sum_{r}^{\text{Rich streams}} \left[N_{actual,r}\right]_{\text{Above Pinch}} + \sum_{r}^{\text{Rich streams}} \left[N_{actual,r}\right]_{\text{Below Pinch}} \tag{2.15}$$

The number of actual stages which accounts for the overall exchanger efficiency is targeted for the regions above and below the pinch and rounded up to provide a logical number of

stages. The minimum number of stages target can then be further implemented in the capital cost target of stage-wise exchanger (Hallale and Fraser, 2000a):

$$\text{Capital cost target} = N\left[a + b\left(\frac{N_{stages,\min}}{N}\right)^{c}\right] \tag{2.16}$$

Where N is the minimum number of units and the symbol a, b, c are the constants in the cost law. $N_{stages,\min}$ is the minimum number of stages.

The minimum total exchanger height targeting

In a continues-contact exchanger, the gas and liquid phases are allowed to flow through the exchangers without intermediate phase separation and re-contacting. The continuous-contact exchangers include packed columns, spray towers and mechanically agitated exchanger. These exchange units are presented in Figure 2.10.

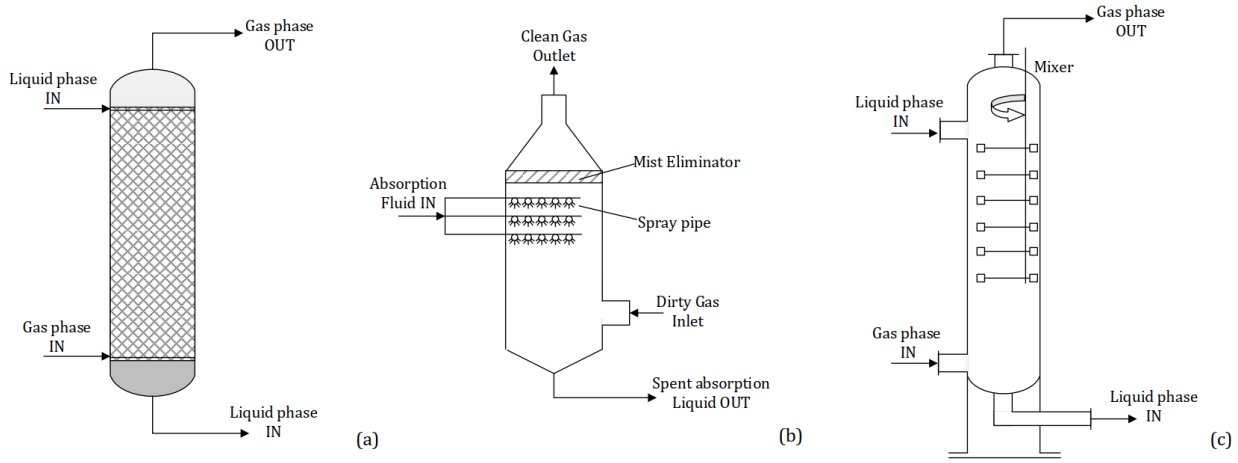

Figure 2.10: Different types of continuous-contact columns: Packed columns (a), spray towers (b) and mechanically agitated exchanger (c) (El-Halwagi, 2017).

The packed towers consist of small packing particles which promote mass transfer. Both counterflow and crossflows can be implemented, but counterflow packed towers are widely used due to higher efficiencies. In the spray towers, a series of nozzles located at the top of the column is used to spray the contaminated streams while hot air is blown to remove the pollutants (Obaid-ur-Rehman and Beg, 1990). The mechanically agitated exchanger uses an impeller to give enhanced rates of mixing and mass transfer (Scargiali, 2007). When sizing such exchangers, the height of the column is an important design consideration, and the equation to estimate the height is given by El-Halwagi (1998):

$$H = HTU_y \cdot NTU_y = HTU_x \cdot NTU_x \tag{2.17}$$

The *HTU* is the overall height of transfer units, and subscript *y* and *x* denote the *HTU* based on the rich phase and lean phase respectively. The *NTU* refers to the overall number of transfer units, and as mentioned before, *NTU* may be calculated based on the rich phase or lean phase denoted with the subscript *y* and *x* respectively. The *HTU* can be provided by the contact-column manufacturer, or correlations can be implemented for estimations. The overall transfer unit heights can be obtained using Equation 2.18 and 2.19:

$$HTU_y = \frac{G_r'}{K_y a} \tag{2.18}$$

$$HTU_x = \frac{L_l'}{K_x a} \tag{2.19}$$

Where G_r' and L_l' are superficial flowrates of the rich and lean streams respectively. The overall mass transfer coefficients for rich phases ($K_y a$) and lean phases ($K_x a$) are used in these equations respectively. The *NTU* can theoretically be calculated when isothermal, dilute mass exchange operations with linear equilibrium are considered:

$$NTU_y = \frac{y_r^{in} - y_r^{out}}{\Delta y_{lm}} \tag{2.20}$$

Where the logarithmic mean concentration difference based on rich phase (Δy_{lm}) can be obtained as follows:

$$\Delta y_{lm} = \frac{\left(y_r^{in} - m_l x_l^{out} - b_l\right) - \left(y_r^{out} - m_l x_l^{in} - b_l\right)}{\ln\left(\frac{\left(y_r^{in} - m_l x_l^{in} - b_l\right)}{\left(y_r^{out} - m_l x_l^{in} - b_l\right)}\right)} \tag{2.21}$$

and

$$NTU_x = \frac{x_l^{out} - x_l^{in}}{\Delta x_{lm}} \tag{2.22}$$

Where the logarithmic mean concentration difference based on the lean phase (Δx_{lm}) is expressed as follows:

$$\Delta x_{lm} = \frac{\left[x_l^{out} - \left(\frac{y_r^{in} - b_l}{m_l}\right)\right] - \left[x_j^{in} - \left(\frac{y_r^{out} - b_l}{m_l}\right)\right]}{\ln\left(\frac{\left[x_l^{out} - \left(\frac{y_r^{in} - b_l}{m_l}\right)\right]}{\left[x_l^{in} - \left(\frac{y_r^{out} - b_l}{m_l}\right)\right]}\right)} \tag{2.23}$$

Hallale (1998) stated that these equations for sizing continuous-contact exchangers could be used in the case involving non-linear equilibrium lines due to the differential nature of such exchanger. The differential nature implies that the curved equilibrium lines can be divided into linear segments and the heights in each segment can be added. There are many available correlations in the literature (Coulson et al., 1993) to estimate column diameters based on the flow rate ratio of different phases in an exchanger. However, the flowrates are unknown

during the targeting procedure, and therefore, many of the correlations cannot be used. Notice that Backhurst and Harker (1973), as cited in Hallale (1998) presented a preliminary estimation of gas-liquid packed column diameter which involves gas density and flowrates. Hallale (1998) modified the equation of Backhurst and Hacker (1973) as follows:

$$D = 1.09{\rho_v}^{-0.25} \cdot V_m \tag{2.24}$$

Where D is the column diameter, ρ_v is the gas density, V_m is the gas mass flow rate. These equations presented above can be used to estimate exchanger heights and diameters. The y-y^* composite curve plot can be divided into composition intervals as mentioned before, and the following targeting equation can be applied to each interval to obtain the minimum total exchanger height target:

$$H_{\min} = \sum_{k}^{\text{intervals}} NTU_{y,k} \left[\sum_{r}^{\text{Rich streams}} HTU_{y,r} \right] \tag{2.25}$$

The exchanger height can be obtained for above and below the pinch to allow the pinch division in the height target. This target gives good results assuming all the exchanger cross-sectional areas are the same and there is an identical overall mass transfer coefficient, $K_y a$ for each exchanger in a problem. If those factors do not vary by more than an order of magnitude, the errors associated with the assumptions are not significant. The capital cost target can then be defined in terms of the minimum total exchanger height ($H_{\min}$) of continuous-contact exchanger as follows:

$$\text{Capital cost target} = N \left[a + b \left(\frac{H_{\min}}{N} \right)^c \right] \tag{2.26}$$

Hallale (1998) further developed detailed costing methods based on exchanger mass to overcome the following limitations:

1. A true minimum may not always be obtained using the number of stages target.
2. The height target results may be affected due to the challenges in estimating exchanger diameters during targeting.

3. In the cases of targets based on stages and height discussed above, the targeting methods are developed assuming that rich streams will not split. However, rich streams can split when dealing with overlapping MSAs and therefore, the assumptions that rich streams will not be split in design may not always hold, and stages or height targets may be unachievable.

The capital cost targeting based on exchanger mass

Hallale (1998) adapted the concept of vertical heat transfer in HENS to develop a targeting method based on exchanger mass. The author observed that the minimum area target in HENS is not affected by stream splitting as heat loads also split. In MENS, the vertical transfer concept is used to minimise the mass transfer in each interval of the y-y^* composite curve plot. The transferred mass can be linked to the mass of an exchanger shell through Equation 2.27.

$$M = \frac{W}{K_w \cdot \Delta y_{lm}} \tag{2.27}$$

where M is the mass of an exchanger shell, and W is the transferred mass of a component. Δy_{lm} is the logarithmic composition differences, K_W is a lumped mass transfer coefficient which can be calculated in Equation 2.28.

$$K_w = \frac{K_y a(2 \cdot Jf - P_i)}{4 \cdot P_i \cdot \rho_m (1 + f_i)(1 + f_e)(1 + f_c)} \tag{2.28}$$

where: K_w is the lumped overall mass transfer coefficient,

$K_y a$ is the overall mass transfer coefficient based on rich stream,

J is the type of joint,

f is the design stress which depends on the construction material at the design temperature,

P_i is the internal design pressure,

ρ_m is the density of the construction material,

f_i is the fractional allowance for inactive height,

f_e is the fractional allowance for components such as skirts, nozzles, manholes, etc.,

f_c is the fractional allowance for corrosion.

Details of the K_w calculation can be found in Appendix A5. Note that K_w is analogous to overall heat transfer coefficient in HENS and therefore, assuming that the K_w is constant, the vertical transfer in MENS can be used to target the minimum total exchanger mass as follows:

$$M_{\min} = \frac{1}{K_w} \sum_{k}^{\text{intervals}} \frac{W_k}{\Delta y_{lm,k}} \tag{2.29}$$

Hallale (1998) shows that the K_W can be calculated before design and therefore, the above equation can be used to estimate the preliminary cost associated with a MENS problem. This target is not affected by stream splitting, and therefore, practically achievable targets are obtained. The exchanger mass target can be implemented with the minimum number of the unit targeting to provide capital cost target as presented in Equation 2.30.

$$\text{Capital cost target (shell)} = N\left[a + b\left(\frac{M_{\min}}{N}\right)^c\right] \tag{2.30}$$

The mass of the shell is used in Equation 2.30 since it is one of the dominant factors contributing to the capital cost of the exchanger. For a rough estimate, the internal column cost can be assumed to be 20 percent of the shell cost for stagewise exchangers while 10 per cent can be used for packed columns (Douglas, 1988). Note that those capital target equations presented above assume an even distribution of the stages, height and shell mass which can lead to some errors but Hallale (1998) stated that this inaccuracy results in insignificant effects in general. Performing these targets using graphical methods can result in inaccuracy, and the targeting process may become inconvenient when a problem involves

a large number of streams. These shortcomings resulted in the development of mathematical programming methods for MENS.

2.3.2 Mathematical Programming Applied to MENS

The synthesis of mass exchange network did not receive as much attention as its HENS counterpart in the past. As mentioned before, the analogy between the HENs and MENs allowed many advanced synthesis methods for MENS to be adapted from the existing HENS methods. The mathematical programming methods in MENS can also be classified as sequential and simultaneous methods.

2.3.2.1 Sequential Mathematical Programming Methods

El-Halwagi and Manousiouthakis (1989) first formulated the concept of MENS as discussed in section 2.3.1.1. The same authors adapted the HENS transhipment model of Papoulias and Grossmann (1983) to automate pinch technology for MENS (El-Halwagi and Manousiouthakis, 1990). The automated model was developed to handle problems involving many streams which can become inconvenient when the graphical or algebraic pinch technology tools are used. This automated model is referred to as a sequential mathematical programming method as the synthesis steps still comprise targeting and design steps in which simultaneous trade-off between the capital and the operating costs cannot be considered.

In the automated model of El-Halwagi and Manousiouthakis (1990), the minimum utility target is first formulated as an LP. In the second step, the minimum number of mass exchange units are determined as a MILP. The network synthesis procedure is performed at a set value of exchanger minimum approach composition (EMAC) and the capital costing is not considered. There are many works of literature which followed the sequential mathematical model of El-Halwagi and Manousiouthakis (1990). Some of the papers include the removal of phenol from refinery wastewater (El-Halwagi et al., 1992); multiple component removal

(Gupta and Manousiouthakis, 1994); reactive MENs (Srinivas and El-Halwagi, 1994); MENs involving regeneration (El-Halwagi et al., 1996; El-Halwagi and Manousiouthakis, 1990).

2.3.2.2 Simultaneous Mathematical Programming Methods

Grossmann (1996) stated that the decomposition of the sequential methods could result in suboptimal final solutions. In order to avoid the need of going through targeting and design steps and to have adequate trade-offs between the competing costs, Papalexandri et al., 1994) first developed a MINLP hyperstructure which does not involve any partitioning. Papalexandri et al. (1994) adapted the hyperstructure model of (Floudas and Ciric, 1989) for HENS. The hyperstructure included all the stream matches and bypasses in the absence of thermodynamic feasibility. The nonconvexity of the model resulted from the mass balance of the model and from the Kremser equation for calculating the theoretical number of stages. However, due to the level of complexity and non-linearity of the hyperstructure, intensive computation was required, and appropriate initialisations were necessary. Therefore, the hyperstructure model results in poor solution times and it was found to have difficulties in obtaining globally optimal solutions. In general, solving nonconvex mathematical problems are challenging, and therefore, some authors combined thermodynamic insights into simultaneous mathematical programming. In the work of Comeaux (2000), a superstructure involving thermodynamically feasible matches is constructed without binary variables to denote the existence of matches. These simplifications resulted in a smaller model which was formulated as a simple NLP problem which is still applied in many cases. However, this method entirely depends on the designer's insights on pinch technology, and it was found to produce suboptimal solutions.

Chen and Hung (2005) and Szitkai et al. (2006) both adapted a general and straightforward mathematical approach based on the SWS of Yee and Grossmann (1990) for MENS. The operating costs from external MSA usage, and the annualised capital cost for exchangers are simultaneously minimised. The method of Szitkai et al. (2006) attempted to construct a fairly linear model to allow feasible solutions to be obtained in shorter solving time while the

model of Chen and Hung (2005) implemented non-linear component mass balance. The exclusion of the non-linear mass balance simplifies the superstructure model which helps to obtain solutions more quickly; however, it may exclude some possible configurations in the optimisation. Nonetheless, the stage-wise superstructure is beneficial as there is no need to consider the Pinch point and it is not necessary to involve subnetworks. Isafiade and Fraser (2008b) developed an interval-based MINLP superstructure (IBMS) in which each interval is defined with the supply and target compositions of the rich and lean streams to solve MENS problems. The IBMS model for MEN enhanced the stage-wise superstructure of Szitkai et al. (2006) to improve the initialisation of such a superstructure and to reduce solution search time. Azeez et al. (2013; 2012) presented a new superstructure formulation called the supply and target-based superstructure. The authors applied the new superstructure to several benchmark examples available in the literature, and it was found that the new formulation of the superstructure can result in new solutions.

Short et al., (2018) presented a MENS method considering detailed cost functions and column performances. Most of the literature available in this field presented synthesis methods based on simplified cost function where the column diameter of 1m was assumed in many methods, and the capital cost of the packed column only depends on column height. The model is based on the superstructure formulation presented by Azeez et al. (2013).

Velázquez-Guevara et al. (2018) presented an alternative method to represent superstructures which included the use of generalised disjunctive programming (GDP). The method involves the use of disjunctions and logic propositions to model the superstructure. The GDP consists of three elements namely, states, task and equipment which can be grouped into two elements representing state-task-network (STN) and state-equipment-task (SET). The stage refers to the set of physical and chemical properties identifying the process streams. Some examples of the stages are composition, temperature and pressure etc. The task is associated with the chemical and physical transformations required between the next stages. Heat and mass transfers are the main examples of the tasks. This model of Velázquez-Guevara et al., (2018) solved the copper removal example previously reported in

El-Halwagi and Manousiouthakis (1990) and Chen and Hung (2005), and it was shown that the solution obtained from the new model is similar to the results of the other authors.

Over the past decade, there has been some development in MENS methods; however, there is still a limited number of papers presenting the simultaneous mathematical programming methods in MENS. There are some difficulties involved in this research field such as the challenges in the model formulation and the limitations associated with the current generation of MINLP solvers. Many of the published papers involve single external MSA, and in many cases, regeneration which is discussed later in this chapter is not included in the optimisation procedure. As mentioned before, a case involving many streams can be challenging to solve and, in this thesis, it is aimed to study the synthesis of HENs and MENs simultaneously while considering regeneration. This study will be highly likely to involve a large model size and therefore, to obtain feasible near-optimal solutions, the fairly linear superstructure approach of Szitkai et al. (2006) is adopted. More details of Szitkai et al. (2006) model are reviewed next.

2.3.2.3 Stagewise Superstructure of Szitkai et al. (2006)

Szitkai et al. (2006) adapted the model principle of the well-functioning HENS model of Yee and Grossmann (1990). This model keeps most of the features of the HENS model. Thermodynamic feasibility was combined with mathematical programming to synthesise MENs. The MENs superstructure is presented in Figure 2.11.

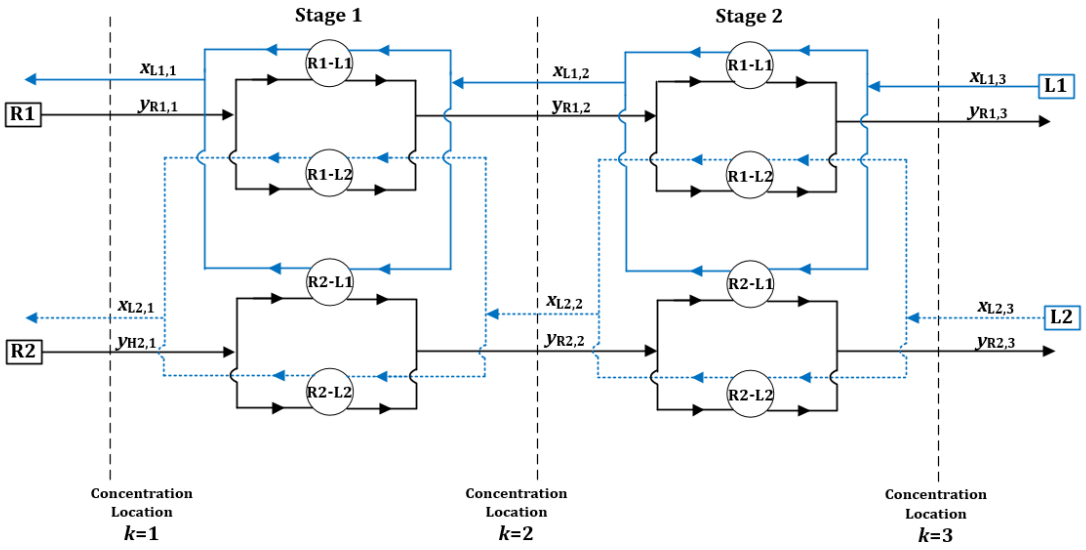

Figure 2.11: The Superstructure of MEN developed by Szitkai et al. (2006) with two rich streams and two lean streams.

The superstructure consists of stages (k) where lean and rich streams are contacted in counter-current as shown in Figure 2.11. The first and the last boundaries are defined by the supply, and the target concentration of rich/lean streams and the boundaries are presented in dotted lines. In each stage, any of rich and lean streams can be matched once, and each rich stream is allowed to exchange mass with other available lean streams and therefore, stream splits can take place in each stage. Those split streams are mixed, and the composition of the newly mixed streams are used to define adjacent composition boundary in the superstructure.

It can be noted that no distinction between process and external lean streams is made and therefore, both types of lean streams can exist in the superstructure stages. This is because external lean streams may not be the leanest and therefore, the external lean streams cannot be exclusively used outside of the superstructure, unlike heating and cooling utilities in HENs. To simplify the superstructure, equal concentration mixing was allowed. The mixed concentration is then used in the next stage to reach its target concentration through similar procedure followed in the HEN superstructure.

In the model formulation, a set of mathematical equations and logical constraints are introduced to obtain feasible mass transfers. Since the optimised variable is the amount of transferred mass, the mass balance for rich/lean streams are are established in each stage. Logical constraints are used to ensure that all mass transfers in each stage have positive values. Like Yee and Grossmann (1990)'s model, binary variables are used to indicate the existence of matches. Since the model of Szitkai et al. (2006) is formulated as a mathematical programming model, it does not require any concept of the pinch point, and engineering knowledge can be implemented into the model by forbidding matches and/or restricting model variables.

The model's objective is to optimise both capital cost of mass exchangers in a network and the operating costs incurred from usage of MSAs. Szitkai et al (2006) also included the integer-infeasible path MINLP (IIP-MINLP) model formulation developed by Soršak and Kravanja (2002) which provides stability and helps the solver to search for feasible solutions. A general expression of the objective function is shown in Equation 2.31.

$$TAC = \min \begin{Bmatrix} \text{(Operating cost of MSAs)} \\ +\text{(Capital cost)} \\ +\text{(numerical stability expression)} \end{Bmatrix} \tag{2.31}$$

The resulting MINLP model of Szitkai et al. (2006) aims to minimise the objective function where feasible solution space is constructed in terms of mass balances and constraints. The compositions at each stage (driving forces) and the MSA flowrates are the variables to be optimised.

It is worth mentioning that Szitkai et al. (2006) considered cases involving single external MSA and the initialisation approach was not discussed. Chen and Hung, (2005) managed to solve a case involving two external MSAs, but the initialisation was not discussed as well. The situation which involves multiple external MSAs is challenging to handle because of the multidimensional nature of the trade-offs (Isafiade and Fraser, 2008b) and therefore, a model involving multiple utilities require a good initialisation procedure to obtain a feasible solution in reasonable time.

Note that the synthesis methods discussed above are based on the single-period operation which involves constant operating conditions. In reality, these conditions can fluctuate with time, hence some authors attempted to study multi-period MEN synthesis methods.

2.3.2.4 Multi-period MEN Synthesis

There are few papers that have studied multi-period MENS problems. These are the hyperstructure model of Papalexandri et al. (1994), the MINLP superstructure model of Zhu et al. (1995), the SWS model of Chen and Hung (2007), the multi-period IBMS model of Isafiade and Fraser (2009) and the detailed costing MENS model of Isafiade and Short (2016).

The multi-period hyperstructure of Papalexandri et al. (1994) is complex and suffers from the same shortcomings as mentioned in the previous sections. The model of Zhu et al. (1995) first synthesises a minimum-cost network and then process parameters are varied to ensure the synthesised network can handle the possible range of variation. In the case of the SWS model of Chen and Hung (2007), the synthesis procedure is decomposed into three iterative steps. The first step involves synthesising a minimum-cost network given a finite number of operating conditions, while in the second step, the applicability of the synthesised network over the randomly generated operating condition values is tested while ignoring the size of the exchanger. In the last step, the size of the exchanger is considered to test the network qualified in the second step and increasing the exchanger sizes if necessary. The IBMS model of Isafiade and Fraser (2009) involves the index 'p' to consider a finite set of operating conditions within the specified range of variations. Isafiade and Short (2016) followed the method of Isafiade and Fraser (2009) to extend the single-period detailed costing MENS model to handle multi-period problems.

2.3.2.5 Initialisation of MENS model

An initialisation strategy is required in order to provide a good starting point for the MINLP solver to produce near-optimal solutions. There is no formalised initialisation strategy for

MINLP solvers available in the literature for MENs (Msiza and Fraser, 2003). The solutions from pinch analysis can be supplied as a good initialisation point. A flow sheet can be used to identify initial values for MENs. Zhu et al. (1995) provided an initialisation based on block decomposition. Nevertheless, initialization methods presented in the literature are problem specific and requires the designer's engineering judgment. In this thesis, an initialisation strategy is presented in Chapter 3 for each network involved in CHAMENs.

2.4 Synthesis of Regeneration Network

Waste minimisation in chemical industries is a significant concern, and the importance of extracting harmful pollutants from industrial effluents has resulted in the application of regeneration networks for waste minimisation. There are few papers which considered regeneration, including El-Halwagi and Manousiouthakis (1990), El-Halwagi et al. (1996), Garrard and Fraga (1998), Chen and Hung (2005).

The concept of regeneration of recyclable lean streams in MENS was first published by El-Halwagi and Manousiouthakis (1990). This model follows the same framework presented in El-Halwagi and Manousiouthakis (1989) which is based on pinch technology for MENS. In the paper of El-Halwagi and Manousiouthakis (1990), the MINLP model is first used to obtain the minimum cost, and then MILP is provided to solve the configuration by achieving the minimum number of mass exchange units. El-Halwagi et al. (1996) also presented a sequential mathematical MENS paper which includes regeneration. The example presented in El-Halwagi et al. (1996) involves one recyclable lean stream and two stripping nitrogen gas at different temperature. The model follows the sequential mathematical method in which simultaneous trade-offs cannot be studied, and the match between the lean stream and the regenerating streams is preselected. In an example presented by Garrard and Fraga (1998), their approach mixed a number of exhausted lean streams into a single stream before being regenerated in a single unit. In the SWS model developed by Chen and Hung (2005), the authors presented a set of regeneration network model equations in their work

but, the regeneration was not studied in a network context but rather as a single unit operation.

Isafiade and Fraser (2008b) implemented the IBMS MENS method including regeneration. However, like the model of Chen and Hung (2005), the regeneration takes place outside of the MEN superstructure in a one-unit operation. Isafiade and Fraser, (2009) extended the IBMS MENS model to CHAMENs model including regeneration. However, the same framework presented in Isafiade and Fraser (2008b) was followed for the regeneration part of the study.

The current author observed the knowledge gap in the simultaneous synthesis methods involving regeneration networks (RENs). A thorough search of the relevant literature showed that a study considering multiple regenerable external MSAs with multiple regenerant scenarios in RENS has not been published. Most papers including regeneration simplified the problem by using a single regeneration column with a single regenerant. However, it is noted that MENs and RENs are very similar in principle.

2.4.1 The analogy of MENs and RENs

The fundamental principle of MENs and RENs is very similar in that both networks involve 'rich' streams to be cleaned, while there exist 'lean' streams to remove the wastes selectively. Looking at an individual mass exchanger, the mass transfer takes place between the rich stream of given supply and the target compositions (y^s and y^t) and the lean stream with the supply and the target compositions (x^s and x^t). The same principle applies in a regeneration column where the exhausted lean streams are treated as 'rich' streams while the regenerating streams take the role of 'lean' streams. The lean stream is also given the supply and target compositions (z^s and z^t). The principles of the mass exchanger and regeneration column are presented in Figure 2.12.

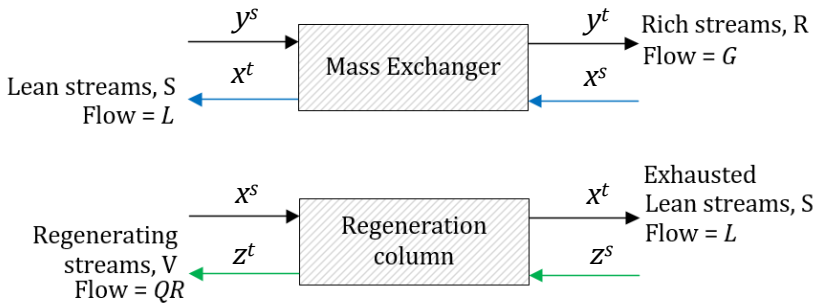

Figure 2.12: A mass exchanger and regeneration column

Given enough time for mixing, the composition of a rich stream (y) and the composition of a lean stream (x) reach equilibrium. The equilibrium relation is governed by Equation 2.9 presented in section 2.3.1.3. The equilibrium relations can be found in the literature or can be obtained experimentally. The same relation governs the composition of regenerating streams.

2.4.2 The Interconnection of MENs and RENs

The two networks have an interrelationship with one another through external MSAs and the choice of which regeneration technology to use can be an essential design consideration. Implementing a REN superstructure with the additional variables and mass balance equations to the MENS can allow multiple lean streams and regenerants to interact in a similar way to the rich and lean streams interaction in MENs and therefore, simultaneous synthesis method is pursued to study trade-offs between these networks.

In RENs, spent MSAs exiting from MENs are fed as rich streams. The MSAs can be classified as once-through MSAs and regenerable MSAs depending on the succeeding operations related to the MSAs. When there are no economic or environmental benefits to regenerate the lean stream leaving the MENs, such lean streams are denoted as once-through MSA. On the other hand, regenerable MSAs can have environmental and/or economic benefits. In terms of economics, regeneration can reduce the TAC of the networks significantly when the external MSAs prices are high. The regeneration also minimises waste into the environment

by controlling the amount of pollutants exiting the process boundaries. The MENs and RENs follow the same design principle and a schematic diagram of these networks are shown in Figure 2.13.

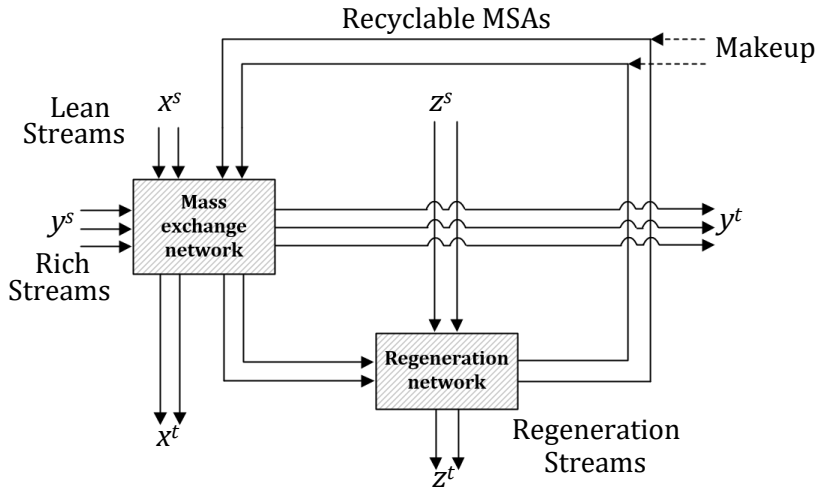

Figure 2.13: A schematic diagram of MENs and RENs (El-Halwagi and Manousioutaki, 1990)

After an external MSA has been fully burdened with the pollutants, regeneration streams such as steam and/or stripping air or energy utilities can be used to remove the loaded pollutants in the MSAs. In reality, there will be some solvent loss throughout the network, and therefore, makeup streams are placed to maintainthe constant flowrates of such streams.

2.4.3 Regeneration Methods

There are different regeneration methods available, and some widely used methods are solvent extraction, air and steam stripping methods, absorption, and removal of impurities through adsorption. These different regeneration methods are summarised in the following sections.

2.4.3.1 Solvent Extraction

Solvent extraction or liquid-liquid extraction is a separation process which uses the characteristics of the components to be differently distributed between two liquid phases. The amount of distribution depends on the mass transfer of the components to be separated from a first liquid phase to a second phase.

The feed to a solvent extraction contains the components to be separated (the solutes). The components are separated from the feed by introducing the solvent. The solvent may be pure but usually contains small quantities of the solutes and the feed liquid since the solvent is recycled in a regeneration network in general. The solvent leaving the mass exchanger is called extract and this contains high quantities of the solute (denoted with a letter '**C**') while the feed leaving the mass exchanger is denoted as raffinate which is virtually clean of the solute. The principle of solvent extraction is shown in figure 2.14.

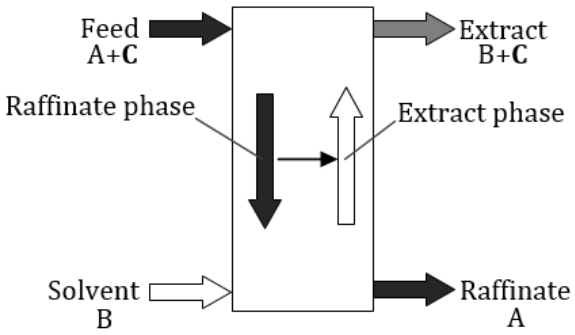

Figure 2.14: The solvent extraction principle: Removal of solute C (Müller et al., 2000)

In general, the extract is regenerated in a distillation column, and the solvent, free of the solutes, is recycled back into the mass exchanger. The solvent extraction is used when direct separation methods such as distillation and crystallisation cannot be implemented due to the nature of the process, or the separation methods are economically infeasible. In addition to that, the solvent extraction can be beneficial when the solute of interest is heat sensitive, such as antibiotics or non-volatile solutes like mineral salts (Müller et al., 2000).

2.4.3.2 Stripping methods

In chemical industries, there are many different physicochemical treatments to remove volatile compounds from process effluents. Some of the widely used methods are air stripping and steam stripping. During the stripping process, waste process effluents are contacted with gas to selectively remove the compounds from the liquid to gas phase (Seader et al., 1998). The stripping process can be either a batch or a continuous process, and packed column or tray columns can be used to remove the pollutants properly. In general, the process waste streams are fed at the top of the column while the gas phase is fed from the bottom. Overall process diagrams for steam stripping and air stripping are presented in Figure 2.15a and Figure 2.15b respectively. Since the higher temperature favours mass transfer in stripping columns, the treated effluent stream which is at a higher temperature than the feed wastes stream can be used to preheat the feed stream.

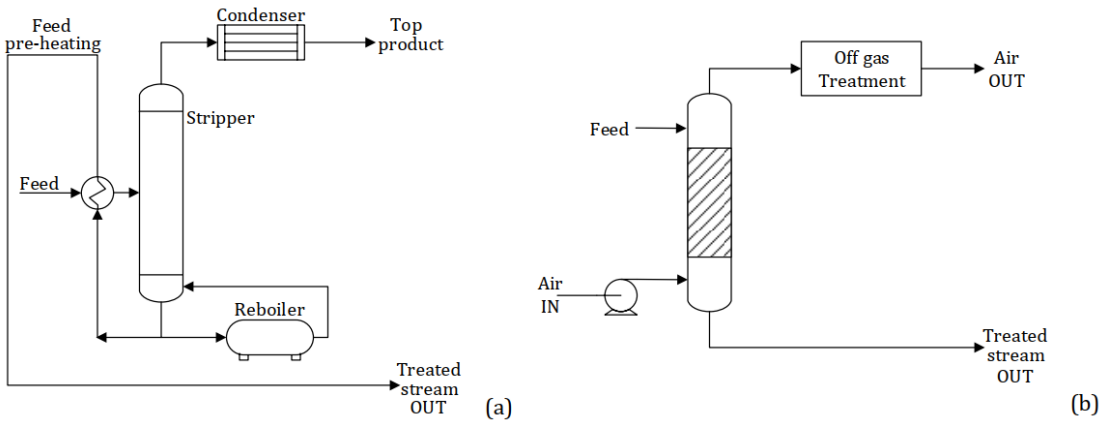

Figure 2.15: General representation of steam stripping (a) and air stripping (b)

The treated streams are removed at the bottom, and the gas phase containing the volatile compounds are found at the top of the column as shown in Figure 2.15. The stripping process can be applied to remove compounds such as hydrocarbons, ammonia, hydrogen sulphide and aromatic compounds (Toth and Mizsey, 2015).

In the case of air stripping, this is a process in which air and water are brought into contact in a packed tower to strip dissolved substances. The design principles for air stripping in

packed towers have been extensively developed in the chemical engineering literature over the past 30 to 40 years (Treybal, 1980; Warren et al., 1976).

In some applications, the gas phase rich in pollutants requires further treatment since a portion of the pollutants is just transferred from liquid to air. Further purification processes such as condensation, adsorption, absorption, chemisorption, thermal/catalytic oxidation and membrane separations are available. High temperature favours the mass transfer for the air stripping, and therefore, the inlet streams are heated up. The high operating temperature will also prevent organic growths within the stripping columns.

In the case of steam stripping, this process takes advantage of Henry's law; increases in temperature increase the Henry's law constant which in turn improves stripping efficiency. This also can remove low volatile compounds such as phenol from effluents. As similar to air stripping, the process uses a distillation column which may be a packed or a tray-column. The steam cost can be estimated through the following equation (Shah et al., 2013):

$$C_{steam} = 3.5 \times 10^{-3} \cdot M_{pollutant} \cdot t \cdot P_{steam} \tag{2.32}$$

Where C_{steam} is the annual steam cost, $M_{pollutant}$ is the volatile compound (pollutant) inlet loading into a stripping column, t is the operating hours per year and lastly, P_{steam} is the current price of steam in the market $\left(\frac{\$}{1000\ Kg}\right)$. A sample calculation can be found in Appendix A4.

Howe et al. (1986) stated that the solubility data for organic compounds in a solvent are important as the data is essential information to determine mass transfer and can be used to predict air or steam stripping behaviour. El-Halwagi (2017) presented an equation to approximate Henry's constants (H) for stripping process:

$$H = \frac{P_{total} \cdot y_i^{solubility}}{P^o_{solute}(T)} \tag{2.33}$$

Where P_{total} is the total pressure of the stripping gas, $y_i^{solubility}$ is the liquid phase solubility of the solute at a temperature T (in mole fraction of solute in the liquid effluent) and $P_{solute}^{o}(T)$ is the vapour pressure of the solute at a temperature T.

2.4.3.3 Absorption Process

Absorption involves removal of impurities, contaminants and pollutants from a gas. The substances transferred from the gas phase to the liquid absorbent are called solutes. Absorption process can be applied to purify gas streams containing low concentrations of solutes such as ammonia, water, cyanide and sulphur compounds. This process is also often used to remove catalyst poisons and to clean refinery gases for the effluents to meet the requirements provided by environmental regulations. In many gas treating processes, absorption is reversible and therefore, the solutes can be recovered without a change in its chemical properties (Ullmann et al., 1985).

There are two types of absorption namely, physical absorption and chemical absorption. This classification depends on whether the pollutants are dissolved physically or are chemically bonded to the solvent. When selecting a suitable solvent in the absorption process, economic consideration is the main concern. Physical solvents are easily regenerated through pressure reduction and mild re-boiling while chemical solvent regeneration can be an energy-intensive process. The advantages and disadvantages of chemical and physical solvents are summarised in Table 2.2 (Kidnay et al., 2011).

Table 2.2: A summary of the advantages and disadvantages of different types of solvents (Kidnay et al., 2011)

Type of solvent	Advantages	Disadvantages
Chemical solvent	Fairly insensitive to the partial pressure of solutes.	High energy requirements for the regeneration of the solvent
	Can provide good removal results.	In general, chemical solvents are not selective.
Physical solvent	Low regeneration requirements	Can results in a poor removal of solute.
	Can provide selective removal (e.g. in gas sweetening case, a physical solvent can selectively remove H_2S).	Highly sensitive to the partial pressure of the gas

2.4.1.4 Adsorption and Ion Exchange

In adsorption and ion exchange, a process called *sorption* is the fundamental foundation of such methods where solutes are selectively transferred to rigid insoluble particles in a suspended vessel or packed column. This process can be a physical or chemical process. In physical adsorption, pollutant species are attached on the solid phase through van der Waals forces while in chemical adsorption, the surface and the pollutants are held together through a strong chemical bonding (Kidnay et al., 2011).

There has been a rapid increase in research on adsorption of waste compounds using activated carbon in past decades. The activated carbon contains large surface areas and well-developed pore structure results in fast adsorption kinetics, and therefore, the activated

carbon has a wide range of applications in chemical industries (Ghasemzadeh et al., 2017). In the past, when the activated carbon reached its full saturation point, it was discarded and taken to a landfill. However, due to both environmental and economic reason, the activated carbon should be regenerated several cycles before being disposed of (Ghasemzadeh et al., 2017). Other widely used adsorbents are zeolites, silica gel and activated alumina.

The studies on ion exchanges were established in 1850 when the concept of ions was not discovered yet, and the commercial application of ion exchange came into practice over the last century (Dyer, 2000). In an ion exchange process, positively charged ions called cations or negatively charged ions called anions in a solution are replaced by displaceable ions. This displacement is reversible, and the structure of the ion exchanger remains the same and can be regenerated with sulfuric acid and sodium hydroxide to be used again.

In concluding remarks, various regeneration methods are reviewed in this section, and these methods can be implemented in RENs for waste minimisation. In this thesis, widely used regeneration options of air and steam stripping processes are emphasised. These two methods are implemented in the case studies presented in Chapter 3. To further develop a synthesis method involving combined MEN, REN and HEN, the integrated network synthesis methods are reviewed next.

2.5 Synthesis of Combined and Heat and Mass Exchange Networks (CHAMENs)

There are many individual HEN and individual MEN synthesis methods available in the literature. However, there are few attempts at developing CHAMENs synthesis methods due to their complex nature. Some of the works established in the literature include the approaches of Edgar and Huang (1993), Srinivas and El-Halwagi (1994), Papalexandri et al. (1994), Isafiade and Fraser (2007, 2009), Liu et al. (2013, 2015). A summary of these CHAMENs synthesis methods is discussed next.

2.5.1 Bibliography of CHAMENs Synthesis Methods

Edgar and Huang (1993) presented a sequential approach to study CHAMENs where the problem is divided into two subproblems to simplify the combined networks problem. In the first step, the operating temperature of the MEN is fixed to synthesise the corresponding MEN, and then in the second step, a HEN satisfying the thermal requirements of the previous step is synthesised. This is a good approach when the optimal MEN temperature is known before the synthesis; however, any design procedure involving preselection can result in sub-optimal results. Srinivas and El-Halwagi (1994) studied the combined networks through a sequential mathematical approach which is based on pinch technology to obtain the minimum annual operating costs (AOCs). The lean streams are divided into sub-streams to identify the optimal mass exchange temperatures. The primary shortcomings of the pinch technology-based approach are that the simultaneous trade-offs between competing variables cannot be studied and the solution procedure can become tedious.

Papalexandri et al. (1994) applied a hyperstructure to the CHAMENs problem. The model suffers from high non-linearity, and therefore a special initialisation technique is required. Isafiade and Fraser (2007) followed the pinch technology approach to study CHAMENs where the minimum total annual cost (TAC) is targeted. Due to the shortcomings of the sequential model, the same authors developed a simultaneous mathematical model. In their study, the authors followed the lean sub-stream approach of Srinivas and El-Halwagi (1994) to identify optimal MEN operating temperatures in a sequential manner (Isafiade and Fraser, 2009). This was done to simplify the highly combinatorial nature of CHAMENs. The recent CHAMENs studies were published by Liu et al. (2013, 2015) where the authors' paper in 2013 identified potential streams which would exchange heat prior to the network synthesis but, the method is based on the pinch technology. The same authors in 2015, developed the NLP mathematical model to solve the CHAMENs through a genetic algorithm-simulated annealing algorithm (GA-SA). It was noted that the model includes many non-linear model equations and therefore, obtaining a feasible solution can be difficult.

To conclude, there have been few attempts at synthesising CHAMENs over the past 30 years. Despite the significant improvement in computing power, the synthesis of CHAMENs has received little attention in process synthesis field due to the difficulties in the model formulations as well as the limitations on the current generation of mathematical solvers. Also, to the best knowledge of the current author, no literature has considered the regeneration in CHAMENs other than the work of Isafiade and Fraser (2009). Therefore, the literature on the regeneration in CHAMENs is even scarcer and requires more research. The CHAMENs model of Isafiade and Fraser (2009) is discussed next.

2.5.2 CHAMENs Model of Isafiade and Fraser (2009)

It is beneficial to study CHAMENs, including the interactions within the systems, because absorption is improved at lower temperatures while stripping is enhanced at higher temperatures. The combined system is illustrated in Figure 2.16.

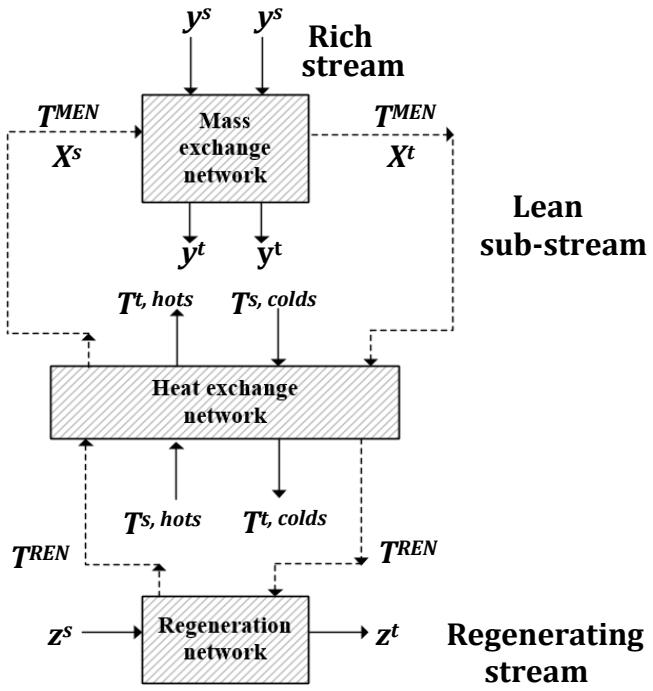

Figure 2.16: schematic diagram of coupled MEN and HEN (Isafiade and Fraser, 2009)

In this CHAMENs model, HENs and MENs are designed to interact with each other through the lean streams of the MENs. The linkage is presented with the dotted line in Figure 2.16 above. The coupling method of Srinivas and El-Halwagi (1994) was adapted to establish the optimal mass exchange temperature for lean streams where each lean stream is split into lean substreams whose temperature can vary between a supply (T_l^s) and a target (T_l^t) value. The optimisation task involves finding the optimal temperatures (T^{REN} and T^{MEN}). The network can be evaluated using larger number of sub-streams if more accurate results are desired. Each lean sub-stream is cooled down in the HEN and then sent to the MEN. The lean sub-streams, which are now rich in pollutants, are sent back to the HEN where they are again heated before being sent to the regeneration (stripping process) where the pollutants are being transferred to the regenerating streams.

The authors adopted the interval based MINLP superstructure approach of their previous works (Isafiade and Fraser, 2008a, 2008b) to synthesise separate heat exchange network and mass exchange network. The MINLP model of Isafiade and Fraser (2009) contains the following equations:

- Overall heat balance on hot and cold streams
- Interval heat balance
- Assignment of inlet temperature and compositions
- Feasibility of temperature and compositions along the superstructure
- Logical constraints
- Driving forces for temperature and compositions
- LMTD and LMCD
- Overall objective function

The overall objective function presented in Isafiade and Fraser (2009) comprises the cost of HEN, MEN and a regeneration column. The annualised operating costs include costs of hot/cold utilities of the HEN, costs of external MSAs used in the MEN and costs of regenerating stream in the regeneration column. The capital costs consist of the heat exchanger costs, mass exchangers and regenerating columns and these are presented in the

objective function. A general expression of the overall objective function is presented in Equation 2.34.

$$TAC = \min \left\{ \begin{array}{c} [(\text{Operating cost of HEN}) + (\text{Capital cost of HEN})] \\ +[(\text{Operating cost of MEN}) + (\text{Capital cost of MEN})] \\ +[(\text{Operating cost of a regenerant}) + (\text{Capital cost of a regenerating column})] \end{array} \right\} \quad (2.34)$$

The model assumes the effect of mass exchange temperature on the rich streams are negligible and therefore, the heat exchange network interacts with the mass exchange network through the lean streams and their temperatures.

2.5.3 Incorporation of Utilities Generated from Renewable Energies

The interactions between HENs and MENs shows that combining such networks can be beneficial and a host of studies involving the combined networks are discussed in the previous sections. Implementing renewable energies into process network synthesis can add additional advantages, but very few studies investigated this. Nemet et al. (2012) studied HENS in a batch operation context in which implementation of fluctuating renewable energies such as solar and wind are investigated. Isafiade et al. (2017) studied HENS method with utilities generated from various sources including fossil, wind, solar and biomass. The most relevant paper related to this thesis is the paper of Isafiade (2017) in which the author presented a CHAMENs model with utility generated from solar thermal energy.

The availabilities of renewable energy sources are usually uncertain. To study such pattern in process integration, the availability was discretised into fixed time periods '*p*' of daytime operation and nighttime operation in the work of Isafiade (2017). The combined superstructure is then formulated as a multi-period model involving solar panels. The implementation of solar thermal panels is usually perceived to exert less environmental

impact. There are different methods to measure environmental impact. These methods and the synthesis methods involving environmental impact are reviewed next.

2.6 Environmental Impact in Process Synthesis

HENs and MENs can reduce both economic and environmental burdens of a process. However, most of the earlier publications focused on optimising economic performance of the process. In recent years, there are some attempts that considered both economic and environmental performances. Some of the relevant works include the paper of López-Maldonado et al. (2011), Vaskan et al. (2012) and Isafiade et al. (2017).

In the work of López-Maldonado et al. (2011) and Vaskan et al. (2012), the authors aimed at synthesising HENs to minimise TAC and environmental impact simultaneously through MOO. The environmental impact was calculated through life cycle assessment (LCA) principles. The shortcomings of these studies are that the models are based on single-period HENs and no renewables were considered in their study.

Isafiade et al. (2017) studied a simultaneous interaction between TAC and environmental impact in HENs in which utilities generated from both fossil-based and renewable energy sources were considered. Environmental impact was calculated in SimaPro with the use of ReCiPe 2008 as LCA method. SimaPro is a simulation tool based on LCA to quantify the environmental impact of a process. The next section discusses LCA.

2.6.1 Life Cycle Assessment (LCA)

LCA involves the factual analysis of a product system through all stages of its life cycle in terms of sustainability (Jensen et al., 1997). During decision making (on a product, process or technology), LCA can provide information on the impacts to the environment and therefore, LCA prevents environmental problems from one place to another (EPA, 2006). The main stages considered in an LCA study are presented in Figure 2.17.

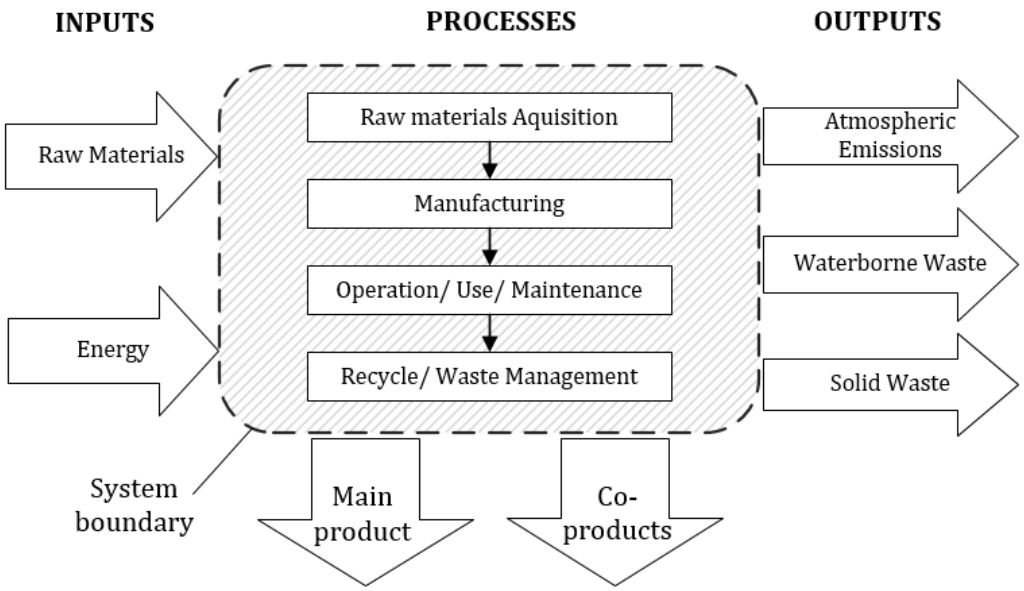

Figure 2.17: The stages involved in life cycle assessment (Fedkin, 2018)

LCA allows the estimation of the cumulative environmental impacts throughout the manufacturing process including the gathering of raw materials, usage of the product and lastly its disposal. The LCA involves four stages (International Organization for Standardization, 2006a):

1. goal and scope
2. inventory analysis
3. impact assessment
4. and interpretation.

The first step ensures that the assessment is performed consistently. The assessment is an approximation of reality. In order to minimise distortions, the assessment's goal and scopes are carefully defined. The definition involves the intended purpose, the audience of the study, the functional units of the study, which is a measure of the function of the investigated systems that are used to relate the inputs and outputs, and its system boundaries. It also defines all the key assumptions, the impact assessment methods, and its interpretation methods. In the second step, all the environmental inputs and outputs related to a product system are collected and quantified. The inputs involve raw materials and energy flows while

the output involves the emission of pollutants and waste streams. The next step involves the life cycle impact assessment (LCIA) where the environmental impacts are classified and evaluated so that the conclusions are drawn for better decisions. In the last step, the conclusions are validated through the ISO 14044 standard where the results of inventory analysis and impact assessments associated with the goal and scope of the study are interpreted. In general, an LCA goes through an iterative process as more data or more understandings of the investigated system are provided (International Organization for Standardization, 2006b).

LCIA is the most crucial phase of any steps in LCA where the inputs and outputs are interpreted in terms of environmental burdens, human health and resources. According to ISO 14044, LCIA requires four steps. (Institute for Environment and Sustainability, 2010):

1. Selection of impact categories and classification
2. Characterisation
3. Normalisation
4. Weighting

There are various methods available to handle an intensive amount of data and transform it into understandable information, which simplifies the LCA process. The LCIA methods can be classified further into two, i.e. midpoint and endpoint approaches. The earlier involves the quantification of impact using an indicator located somewhere along the impact pathways such as climate change, acidification and ecotoxicity. The endpoint approach quantifies all the way through the endpoint categories which includes human health, natural environment and natural resources. As mentioned above, the HENS model of López-Maldonado et al. (2011) and Vaskan et al. (2012) selected the Eco-indicator 99 (Guinée, 2002) which is the endpoint approach. On the other hand, the model of Isafiade et al. (2017) selected the ReCiPe 2008 method in SimaPro (Goedkoop et al., 2008) to quantify environmental impacts associated with hot and cold utility generations. Note that the ReCiPe methods combine the midpoint and endpoint approaches. The ReCiPe 2008 (Goedkoop et al., 2008) method was updated, and ReCiPe 2016 (Huijbregts et al., 2016) was

published recently where it includes both midpoint and endpoint impact categories as the previous version. The characterisation factors were representing the European scale in the previous version while the global scale characterisation factors are representative for ReCiPe 2016. The categories associated with midpoint and endpoint are presented in Figure 2.18.

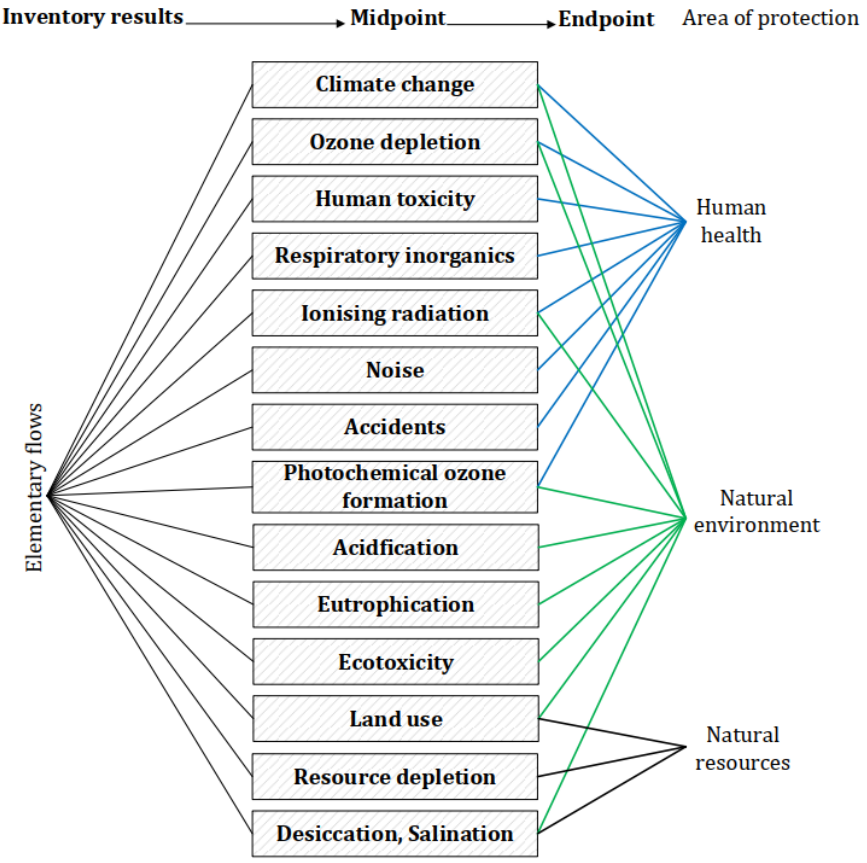

Figure 2.18: Considered categories in Midpoint and endpoint of the ReCiPe approach

In the case of normalisation and weighting steps in LCIA, they are optional due to the potential biases, unlike the first two steps mentioned above. According to the ISO 14044 standard, normalisation allows different impact category results to have the same unit while weighting provides a single score that combines the impacts of resources, ecosystem and human health. A weighting step provides easy comparisons between different processes' environmental impacts. Therefore, normalisation and weighting steps allow a designer to

identify important impact categories and can assist in understanding the meaning of results. In this thesis, ReCiPe Endpoint (Egalitarian) V1.06m normalisation/weighting set in SimaPro was used. Under this option, the Europe ReCiPe E/A was further selected.

2.7 Multi-objective Optimization (MOO)

The field of multi-objective optimisation has developed rapidly over the past two decades. Miettinen and Mäkelä (1999) defined multi-objective optimisation as:

$$\text{Minimise/Maximise } \{f_1(x), f_2(x), \cdots, f_n(x)\} \tag{2.35}$$

$$\text{Subject to } x \in S$$

Where n is the number of objective functions, x is solution and S is a feasible solution space. In this optimisation, all the objective functions are minimised simultaneously. If there are no conflicts between the objective functions, a solution can be found without incorporating special methods. However, it is assumed that objective functions interact with each other and therefore, there exists more than one optimal solution with respect to every objective function. In order to extract some of the information about each objective function and to examine the data, Pareto optimality can be used.

2.7.1 Pareto optimality

To compare trade-offs between the objective functions, Pareto optimality was developed by French-Italian economist Vilfredo Pareto in 1896 where one of the objective function vectors are kept independent during optimisation. Pareto optimality occurs when one of the objective functions cannot increase without weakening of the other objective functions. A general Pareto curve comparing cost and environmental impact is presented in Figure 2.19.

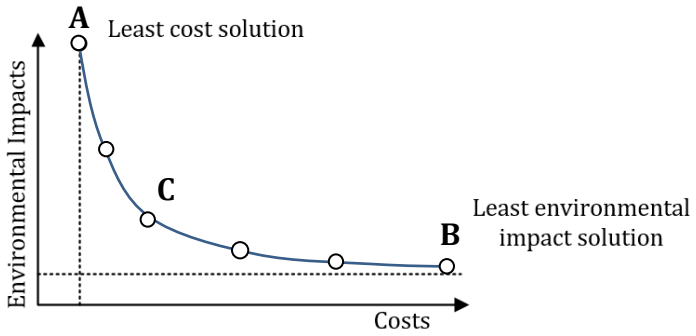

Figure 2.19: Pareto curve comparing environmental impact and costs (Miettinen and Mäkelä, 1999)

There can be a set of infinite numbers of Pareto optimal solutions. According to the definition of Pareto optimality, moving from one Pareto optimal solution to another requires trading-off. Note that every point in the Pareto optimal set is an equally acceptable solution of the multi-objective optimisation. In general, it makes sense to obtain an optimal solution in optimisation problem and therefore, selecting one out of the set of Pareto optimal solutions requires insights of an engineer (or a decision maker) and experience. The regions above the Pareto curve contain sub-optimal solutions while the regions below the Pareto curve is defined as infeasible space (Miettinen and Mäkelä, 1999).

2.7.2 Multi-objective methodologies

There are many methods available in the literature to perform MOO. These methods can assist in generating Pareto optimal solutions. It was observed that ε-constraint method and goal programming method are previously applied in network synthesis field and therefore, these methods will be discussed next.

2.7.2.1 *ε*-constraint method

This optimisation method was developed by Haimes (1971) where one of the objective functions is used as a constraint by setting an upper bound. When the ε-constraint method is applied to network synthesis context, this can be written mathematically as follows:

$$\text{minimise } Z_{multi} = TAC$$

s.t.

$$\text{minimise } EI \leq \varepsilon \tag{2.36}$$

The TAC of a network is minimised where environmental impact objective is constrained by a parameter (ε). Therefore, different values of ε will result in different values of the minimum TAC. When the value of the parameter is too small, finding a feasible solution can become a challenging task and therefore, the minimum value of the parameter can be found by examining the problem that minimises EI without considering TAC and this data point is denoted as 'B' in Figure 2.19. In contrast to that, when the problem is investigated by minimising TAC without including EI into the objectives, then it can be considered as an extreme point denoted as 'A' on the Pareto curve presented in Figure 2.19. It is an engineer's insight to decide which solution lies on the set of Pareto optimal solutions. In this study, the problem with the reasonable values of TAC and EI are desired. This point is presented as 'C' on the Pareto curve.

2.7.2.2 Goal programming method

Goal programming method is the most widely used solution method in practical applications. Charnes and Cooper (1957) first produced concepts of goal programming, and it is one of the first methods developed for multi-objective optimisation. This method involves the decision maker specifying an optimistic level for the objective function, and the method aims to reduce any deviations from the level. A goal consists of the optimistic level specified by the decision maker and the objective functions. López-Maldonado et al. (2011) defined goal programming in the context of network synthesis as follows:

$$\text{minimise } Z_{goal} = \delta_{TAC}^{+} + \delta_{TAC}^{-} + \delta_{EI}^{+} + \delta_{EI}^{-}$$

s.t.

$$Z_{TAC} - TAC_{min} = \delta_{TAC}^{+} + \delta_{TAC}^{-}$$

$$Z_{EI} - EI_{min} = \delta_{EI}^{+} + \delta_{EI}^{-}$$

$$\delta_i^{+} \geq 0;\ \delta_i^{-} \geq 0 \qquad (2.37)$$

Where δ_{TAC}^{+}, δ_{TAC}^{-}, δ_{EI}^{+} and δ_{EI}^{-} are positive and negative deviations to the aspiration level of TAC and EI. Note that the goals have the same format as the constraints in the problem formulation, and therefore, the constraints can be regarded as a subset of the goals. Once the optimistic levels have been set, the objective functions are minimised with reference to the optimistic levels. However, notice that selecting a good optimistic level for the goal programming can be difficult if the decision maker is not aware of the feasible region.

2.8 Conclusions and Thesis contributions

Throughout the literature reviews presented in this chapter, it was observed that many recently published methods shifted from the sequential-based pinch technology approach and the mathematical programming methods have gained the majority of attention in process synthesis field. The significant improvement of the mathematical programming method is its ability to simultaneously optimise both costs and network configurations and theoretically achieve the global optimality. There are many recent HENS and MENS papers which fall under the mathematical programming synthesis methods. However, despite the substantial development in computing powers in the last decades, these methods often result in sub-optimal solutions.

It was also noticed that there is a limitation in CHAMENs synthesis methods where many existing methods suffer from the large model size which makes obtaining a feasible solution very challenging. There are also few studies in the literature which included regeneration in the process synthesis step and there is no literature which studied a detailed regeneration network with heat integration. Also, finding data associated with regenerating streams, e.g. stream flowrates/compositions, equilibrium constants and solubility data, is not trivial, unlike general MENs stream data. Additionally, most of the synthesis methods available in the literature have optimised the networks in terms of economics rather than including the

environmental impact of such networks. Considering both economics and the environmental impact would result in MOO and there are few published papers that have studied MOO in process synthesis recently. This thesis implements superstructure-based mathematical programming methods to synthesise HENs, MENs and RENs, which are the individual networks in the CHAMEN. The proposed synthesis method of the integrated network is extended to handle multi-period operation, in order to incorporate renewable energies. The proposed method is then further extended to handle MOO.

Chapter 3

Combined Networks Synthesis Method

Chapter 3 Combined Networks Synthesis Method

This chapter presents the combined networks synthesis method considering utilities generated from both renewable and non-renewable energy sources. Most synthesis methods involving regeneration have simplified the problem by using a single lean stream through a single regeneration unit, and in some cases, no consideration was given to enhancing the regeneration through heating/cooling. However, synthesising a regeneration network allows the regeneration and recycle of multiple MSAs to the MEN in a simultaneous manner. This allows the analysis of the interactions between MENs and RENs.

The main challenge in synthesising the combined network of HENs, MENs and RENs is obtaining feasible solutions to the MINLP optimisation problem. There have been significant challenges in obtaining globally optimal solutions in the process synthesis field, and many available methodologies require special initialisation strategies to find feasible solutions. It is apparent that many existing modern synthesis models involving large numbers of streams result in local optima or fail to find feasible solutions. These shortcomings imply that keeping the low complexity of a model can assist in finding the feasible solutions. Note that introducing RENs into the CHAMENs results in the expansion of the existing MINLP formulation size which in turn increases the degrees of freedom and thus, the optimisation task becomes more difficult. In order to keep the model as simple as possible, the existing, simplified superstructure models are implemented. The results from the developed approach can be used as a preliminary design to make further engineering decisions.

3.1 Synthesis Approach

Of the many existing MINLP formulations for, the HENS model of Yee and Grossmann, (1990) and MENS model of Szitkai et al. (2006) are selected, as these formulations are relatively simple and can be adapted for further modifications. The HEN and MEN models use the supply and the target key factors such as temperature and composition of streams to define the boundaries of the superstructures. It is challenging to handle the multi-dimensional

nature of the combined heat and mass exchange problem involving multiple utilities as well as multi-period operation. Therefore, an initialisation technique is introduced in the synthesis approach of this chapter. A general overview of the methodology for this study is presented in Figure 3.1.

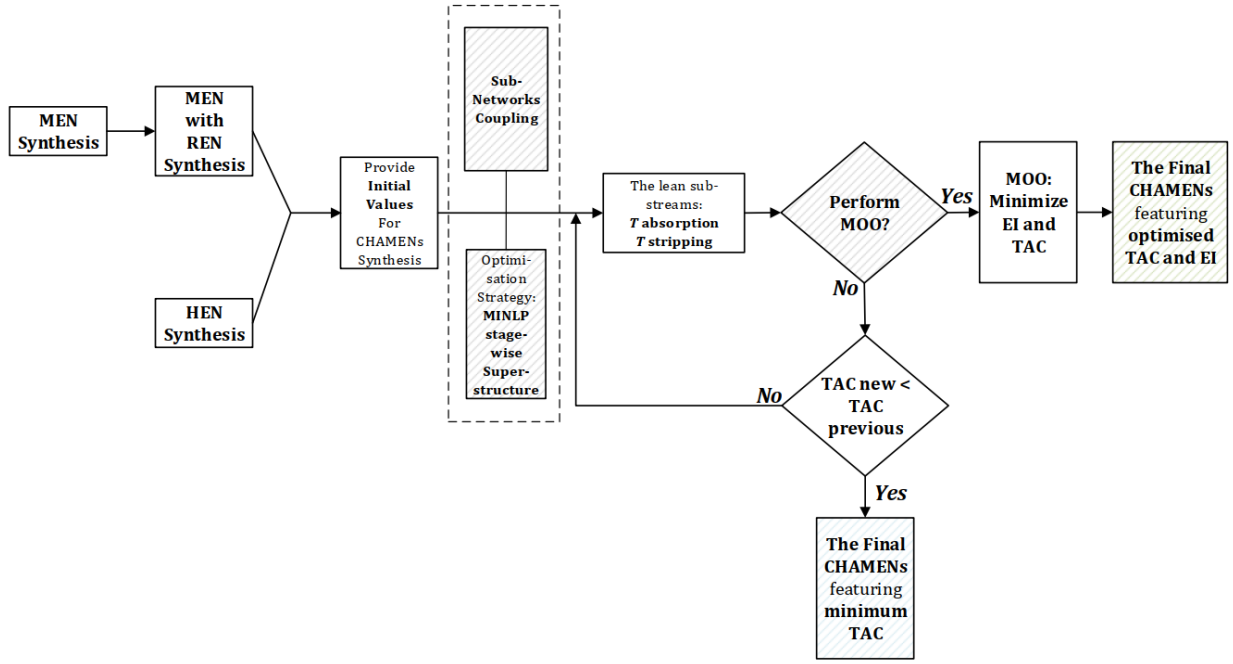

Figure 3.1: General proposed approach of the combined networks synthesis

Given a scenario, the first step of the proposed method involves a gathering of relevant data such as heat capacity flowrates of streams, availability of process and external MSAs, types of utilities, operating hours/periods, and the supply and target temperature/composition of streams. The synthesis of the CHAMEN requires good initialisation values to reduce challenges in obtaining feasible solutions. Therefore, relevant data for HEN, MEN and REN are used to first synthesise the networks separately in three steps. In the first step, MEN is synthesised to provide initialisation values for the second step; the latter involves MEN with REN synthesis. Once a feasible MEN with REN solution is obtained, HEN is synthesised separately to provide initialization values for the HEN aspect of CHAMEN. In the last step, the set of initial values that gave feasible solutions in the first two steps are used to initialise the CHAMEN model in the third step. These individual network syntheses of the first two

steps ensure that data associated with each network is rational and able to generate feasible solutions before being used in the combined network synthesis.

To the best of the knowledge of the current author, there are no literature considering detailed REN in CHAMENs. In order to include regeneration in CHAMENS, an analogue of the MEN stage-wise superstructure of Szitkai et al. (2006) was applied. In MEN, the MSAs serve as the lean streams which receive the pollutants in waste streams (the rich streams). The REN follows the same logic as the MEN but the role of the MSAs change; the spent MSAs leaving the MEN are fed into the REN as the rich streams which contain high compositions of the pollutants, and the regenerating streams serve as the lean streams. To link the MSA flowrates in MENs and RENs, the same index '*l*' is used in the model formulation. Besides, the optimal temperatures in MEN and REN are identified through the coupling methods presented by Srinivas and El-Halwagi (1994). In this method, each lean stream is divided into lean sub-streams. The number of lean sub-streams depends on the accuracy required for the problem. Each lean sub-stream is given a different temperature within a supply and a target value of the lean stream. The lean sub-streams do not exchange heat with each other, but each sub-stream temperature is used individually in the network synthesis to obtain a corresponding feasible solution. In this way, the optimal lean stream temperature which results in the minimum TAC of the combined network can be identified.

Beyond the individual HENs, MENs and RENs of the CHAMENs, additional model equations to handle multi-period operations are included. This is achieved by including the index '*p*' which accounts for different periods of solar irradiation availability. The extension of the model to handle multi-period operations allows incorporation of renewables, whose availability is time dependent. The incorporation of renewable introduces extra equations into the model formulations. These equations account for the optimal size of solar panels to capture heat for both direct and indirect heat integration (Isafiade, 2017). The equations also include an expression to determine the volume of heat storage vessel. The vessel is included to make provision for indirect heat integration in the network. These equations are presented in the model formulation section.

The method was also further extended to perform MOO using the goal method (Miettinen and Mäkelä, 1999) to simultaneously optimise combined networks in terms of both TAC and environmental impact. Using the MOO method, the current author wishes to find the solution that optimally trades off the economic benefits and environmental impact of a chosen design. In order to measure the environmental impact associated with different types of utilities in each network, the ReCiPe 2016 method (Huijbregts et al., 2016) was used. Overall, this method aims to extend the state of the art of CHAMENs synthesis methods by including REN involving multiple MSAs and multiple regenerating streams, as well as providing multiple options of utility sources while considering both economic and environmental impact of the combined network.

Figure 3.2 shows a schematic of how the MEN involving multiple MSAs is linked to the REN involving multiple regeneration streams through the HEN. The MSA flows passing through the MENs are represented with blue lines as these streams are cooled in HENs to enhance the absorption processes. The same MSA flows passing through the RENs are represented as red lines to indicate that these streams are heated in HENs to favour stripping processes in RENs. A solar panel is presented next to the hot streams entering the HENs to indicate the availability of such renewable energy in this combined model.

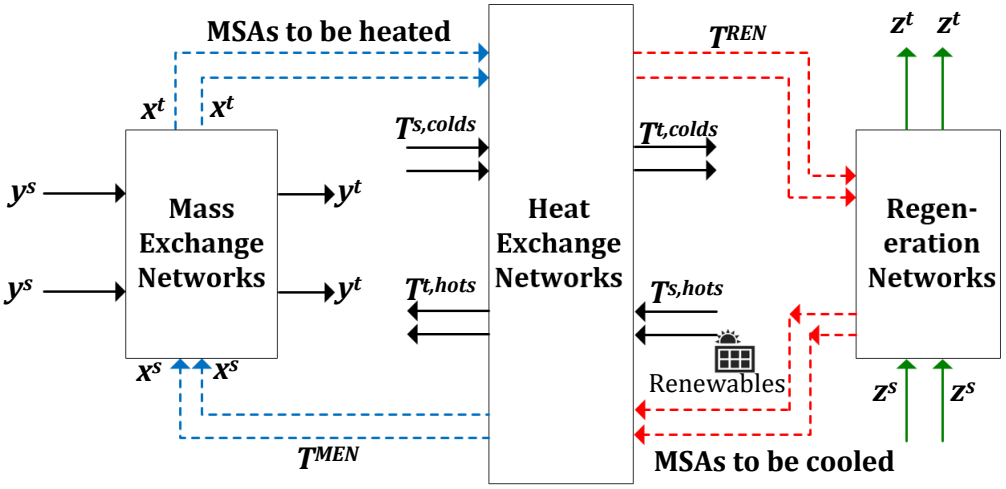

Figure 3.2: A schematic of combined heat, mass and regeneration networks involving multiple streams

The lean stream flowrates in MEN and REN are treated as variables to be optimised, and therefore, the flow rates are obtained simultaneously. The thermal flowrates of the lean streams used in the HEN are provided as a constant value. This was done to overcome the challenges involved in obtaining feasible solutions when thermal flowrates are simultaneously optimized with the lean stream flowrates, as this increases the degrees of freedom.

3.2 Problem statement

Given a set of rich streams (R) with flowrates (G) from which species such as SO_2, CO_2, NH_3 etc., are to be absorbed from their supply composition y^s to target composition y^t. There are a set of lean streams (S) available for the removal process where the lean streams consist of process and external lean streams. The process lean streams have maximum available onsite flowrates (L^U) with supply (y^{*s}) and target compositions (y^{*t}) expressed as the equivalent equilibrium rich stream phase. The external lean streams are equivalent to MSAs, and they have supply and target compositions as x^s and x^t respectively. Due to the high cost and environmental concerns associated with the external MSAs, it is beneficial to regenerate such streams and therefore, there are a set of regenerants available in the problem such as steam, stripping air etc.

The regenerants are provided with supply and target compositions z^s and z^t, and they can be used to strip the absorbed species from the external lean streams leaving the MEN. Note that the supply and target composition of the lean streams and their flowrates (L), as well as the supply and target compositions of regenerants and their respective flowrates (QR), are all variables to be optimised. Introducing HENs can enhance mass transfers in both MENs and RENs where hot utilities (HU) and cold utilities (CU) can be generated from both fossil-based energies such as coal, crude oil, etc., and renewable energy sources such as solar thermal and are available to heat and cool the external lean streams to corresponding optimal operating temperatures in REN (T^{REN}) and MEN (T^{MEN}) respectively. Also given are the costs of external

lean streams, regenerants and hot/cold utilities, heat and mass exchange units, as well as data associated with solar panels over specified different operation periods (p). Lastly, the environmental impacts associated with different types of utilities, MSAs and regenerating streams are obtained through the ReCiPe 2016 method in an attempt to synthesise multi-period networks of heat, mass and regeneration considering both economic and environmental impact.

3.3 Assumptions

A network involving heat and mass exchange is a complex system. The following simplifying assumptions are applied in the proposed CHAMENs synthesis model of this chapter:

1. For all material balance purposes, the flow rate of any stream remains constant throughout the networks during each period.
2. The exchangers in the networks operate isothermally and in an isobaric manner. These assumptions ensure that the equilibrium functions used in the synthesis remain constant.
3. The split streams are mixed at the same composition and temperature in the stage-wise superstructures. In HENs, this allows intermediate temperatures of streams to be characterised by the temperature at the superstructure stage boundaries. The streams going through stage-wise MEN superstructure are also defined in terms of composition at the stage boundaries.
4. The exchanger units are counter-current.
5. No mass exchange occur among the rich streams.
6. The solubility of lean streams in rich streams is negligible
7. Regeneration is perfect, and therefore, no solvent makeup is required.
8. The renewable energy source for solar panels, i.e. solar irradiation, is available at fixed periods per day which comprises day and night.

3.4 MINLP model formulation

This section focuses on the formulation of the proposed synthesis approach. The formulation is similar to that of Isafiade (2017) in which the models of Szitkai et al. (2006) and Yee and Grossmann (1990) are used to formulate the MEN and HEN respectively. The model consists of the equations for HENs and MENs in which equations are presented with inclusion of index '*p*' to extend the model to handle multi-period operations specifically to account for solar irradiation. The model equations of RENs are presented to simulate a CHAMEN with regeneration network. The model equations of HEN are presented first followed by MEN and REN.

3.4.1 HENS model equations

The HENS model consists of index *ih* which denotes the hot streams given in set *H,* and *jc* represents cold streams given in set *C*. Index *kh* shows the superstructure stages given in set *Kh*, and *p* represents the operation period given in set *P*. The superstructure is defined with the three indices: *ih, jc* and *kh*. In each stage (*kh*) of the superstructure, a hot (*ih*) and a cold (*jc*) stream can exchange heat once. The model consists of the following mathematical equations and inequalities:

Overall stream heat balance

$$\left(T^{s}_{ih,p} - T^{t}_{ih,p}\right) \cdot F_{ih,p} = \sum_{jc \in C} \sum_{kh \in Kh} q_{ih,jc,p,kh} \qquad ih \in H, p \in P \tag{3.1}$$

$$\left(T^{t}_{jc,p} - T^{s}_{jc,p}\right) \cdot F_{jc,p} = \sum_{ih \in H} \sum_{kh \in Kh} q_{ih,jc,p,kh} \qquad jc \in C, p \in P \tag{3.2}$$

Note that $T^{s}_{ih,p}$ and $T^{t}_{ih,p}$ are supply and target temperatures of hot stream *ih* for period *p* respectively. $T^{t}_{jc,p}$ and $T^{s}_{jc,p}$ are target and supply temperatures of cold stream *jc* for period *p*. $F_{ih,p}$ and $F_{jc,p}$ are the heat capacity flow rates of hot and cold streams in period *p* respectively.

$q_{ih,jc,p,kh}$ is the amount of heat exchanged between hot stream *ih* and cold stream *jc* in temperature location *kh* and period *p*, and is treated as a continuous variable.

Stage heat balance

$$\left(t_{ih,p,kh} - t_{ih,p,kh+1}\right) \cdot F_{ih,p} = \sum_{jc \in C} q_{ih,jc,p,kh} \qquad ih \in H, kh \in Kh, p \in P \tag{3.3}$$

$$\left(t_{jc,p,kh} - t_{jc,p,kh+1}\right) \cdot F_{jc,p} = \sum_{ih \in H} q_{ih,jc,p,kh} \qquad jc \in C, kh \in Kh, p \in P \tag{3.4}$$

In Equation 3.3 and 3.4, $t_{ih,p,kh}$ and $t_{ih,p,kh+1}$ are the temperatures of hot stream *ih* in temperature location *kh* for period *p* and the temperature of the same type of stream in the next temperature location *kh*+1 for period *p*. The same logic applies to $t_{jc,p,kh}$ and $t_{jc,p,kh+1}$ where these variables involve cold stream *jc* in temperature location *kh* and *kh*+1 for period *p* respectively.

Superstructure Inlet temperature assignment

The first temperature location, *kh* = 1, is assigned with the supply temperatures of hot streams in each period while the last temperature location, *kh = NOKh* + 1, is the location where the supply temperatures of each cold streams in each period are assigned. The following equations are used to assign the supply temperatures:

$$T^{S}_{ih,p} = t_{ih,1,p} \qquad ih \in H, p \in P \tag{3.5}$$

$$T^{S}_{jc,p} = t_{jc,NOKh+1,p} \qquad jc \in C, p \in P \tag{3.6}$$

Temperature feasibility

In the superstructure, temperatures of hot streams are designed to monotonically decrease from left to right while cold stream temperatures increase from right to left as described in Equation 3.7 and 3.8.

$$t_{ih,kh,p} \geq t_{ih,kh+1,p} \qquad kh \in Kh, ih \in H, p \in P \tag{3.7}$$

$$t_{jc,kh,p} \geq t_{jh,kh+1,p} \qquad kh \in Kh, jc \in C, p \in P \tag{3.8}$$

Logical constraints

When a hot stream exchanges heat with a cold stream in a temperature stage, a match exists in the temperature stage. The match is described by logical constraints and binary variables, $zhn_{ih,jc,kh}$. The logical constraint contains a parameter which bounds the amount of exchangeable heat ($\Omega_{p,\mathrm{HEN}}$). The upper bound can take the smaller value of the overall heat loads available in each of the streams involved in the match. The binary variable consists of '1' and '0' where the value of '1' indicates the existence of a match in a stage while the value of '0' indicates no match. The logical constraints are shown in Equation 3.9:

$$q_{ih,jc,kh,p} - \Omega_{p,\mathrm{HEN}} \cdot zhn_{ih,jc,kh} \leq 0 \qquad ih \in H, jc \in C, kh \in Kh, p \in P \tag{3.9}$$

When a match exists in a stage, the binary variable $zhn_{ih,jc,kh}$ has a value of '1' and the bounding variable ($\Omega_{p,\mathrm{HEN}}$) becomes active. Equation 3.9 prevents abnormal heat exchange between the streams in each period *p*.

Calculation of driving forces

The heat exchange area requirement of each heat exchanger is included in the objective function equation of the SWS model. The driving forces are determined as shown in Equations 3.10 and 3.11 to calculate the exchanger areas. These constraints ensure feasible

driving forces for exchangers selected in the optimisation and activation of such equations is determined by the binary variables in the equations.

$$dt_{ih,jc,kh,p} \leq t_{ih,kh,p} - t_{jc,kh,p} + \Gamma_h\left(1 - zhn_{ih,jc,kh}\right) \quad ih \in H, jc \in C, kh \in Kh, p \in P \quad (3.10)$$

$$dt_{ih,jc,kh+1,p} \leq t_{ih,kh+1,p} - t_{jc,kh+1,p} + \Gamma_h\left(1 - zhn_{ih,jc,kh}\right) \quad ih \in H, jc \in C, kh \in Kh, p \in P \quad (3.11)$$

The upper bound (Γ_h) with the binary variables ($zhn_{ih,jc,kh}$) in Equation 3.10 and 3.11, deactivate the constraints if the value of the binary variable is zero which implies that there is no match in temperature location *kh*. This deactivation ensures that no negative driving forces exist in the optimised network. In order to avoid infinite heat exchanger areas in the optimal network, an exchanger minimum approach temperature (*EMAT*) constraint is used:

$$dt_{ih,jc,kh,p} > EMAT \quad (3.12)$$

The temperature driving forces can be implemented in the logarithmic mean temperature difference (*LMTD*) expression which will be used to calculate the heat exchanger area in the objective equation. The $LMTD$ is calculated by:

$$LMTD_{ih,jc,kh,p} = \left[\frac{\left(dt_{ih,jc,kh,p}\right) \cdot \left(dt_{ih,jc,kh+1,p}\right) \cdot \left(dt_{ih,jc,kh,p} + dt_{ih,jc,kh+1,p}\right)}{2}\right]^{\frac{1}{3}} \quad (3.13)$$

The *LMTD* equation is approximated by using Chen's first approximation (Chen, 1987). Verheyen and Zhang (2006) introduced a constraint to select the maximum area over each period as presented in Equation 3.14:

$$A_{ih,jc,kh} \geq \frac{q_{ih,jc,kh,p}}{LMTD_{ih,jc,kh,p} \cdot U_{ih,jc}} \quad (3.14)$$

Note that the maximum area ($A_{ih,jc,kh}$) do not have index '*p*' since the maximum area over entire periods is selected in the optimisation procedure while other parts of the equation

contain the index 'p' including heat requirements $q_{ih,jc,kh,p}$ and the $LMTD$ expression. $U_{ih,jc}$ is the overall heat transfer coefficient of the streams involved in a match. Equations 3.1 to 3.14 form the equations for the HEN part of the CHAMEN model. The next section introduces solar panel and heat storage design equations.

Solar panels and heat storage vessels design equation

Isafiade (2017) used utilities generated from solar thermal energy considering solar panel sizing in an attempt to reduce the environmental impact of a process. To allow a solar panel to be effective across the periods, the maximum solar panel area ($ASC_{ih,jc,kh}$) is presented as follows:

$$ASC_{ih,jc,kh} \geq \frac{q_{ih,jc,p,kh}}{\eta_o(GHI_p) - a_1(T_c - Ta_p) - a_2(T_c - Ta_p)^2} \tag{3.15}$$

where $\eta_o$is the efficiency factor of the solar panel, $GHI_p$is the global horizontal irradiation for the period p in the location where the chemical plant is situated, a_1 and $a_2$are the thermal loss coefficients which can be obtained experimentally, T_c is the average of the inlet and outlet temperatures of the solar panel capture fluid and Ta_p is the ambient temperature at the plant location through period p. Isafiade (2017) also implemented heat storage vessels with the solar panel to preserve heat when solar irradiation is available and to use the heat from the vessels during the night-time operation. The model equation to calculate the volume is described in Equation 3.16.

$$VTS_{ih,jc,kh} \geq \frac{q_{ih,jc,p,kh}}{C \cdot \rho(T_{ih}^s - T_{ih}^t)} \tag{3.16}$$

where C and ρ are the heat capacity and density of the thermal storage fluid respectively. T_{ih}^s and T_{ih}^t are the supply and target temperatures of the thermal storage fluid in the vessel. The implementations of such infrastructures are usually perceived to exert less environmental impact.

3.4.2 MENS model equations

The MENs model equations consist of mass balances and constraints to govern the mass transfer across the MEN superstructure. Index *r* refers to rich process streams given in set *R* while the lean streams (including both process and external MSAs) are denoted by index *l* given in set *S*. The superstructure stages are denoted with the index *k*. Since the superstructure of MEN is adapted from the stage-wise superstructure of HEN, the superstructure is defined with the three indices, *r, l* and *k*, as done by Yee and Grossmann (1990). The model equations of MENS are comprised of the following expressions:

Overall mass balance for the rich and lean streams

The total amount of exchangeable mass is calculated by multiplying rich stream flow rates with the difference of the supply and target compositions of the rich streams in the process synthesis. The same logic is applied to the lean streams. These equations are described in Equations 3.17 and 3.18.

$$\left(Y_{r,p}^{s} - Y_{r,p}^{t}\right) \cdot G_{r,p} = \sum_{k \in K} \sum_{l \in S} M_{r,l,k,p} \qquad r \in R, p \in P \tag{3.17}$$

$$\left(Y_{l,p}^{*t} - Y_{l,p}^{*s}\right) \cdot L_{l,p} = \sum_{k \in K} \sum_{r \in R} M_{r,l,k,p} \qquad l \in S, p \in P \tag{3.18}$$

In Equation 3.17, $Y_{r,p}^{s}$ and $Y_{r,p}^{t}$are supply and target composition of rich streams in period *p* respectively. For lean streams, $Y_{l,p}^{*s}$ and $Y_{l,p}^{*t}$ are the supply and target equilibrium composition of lean stream *l* in the rich phase in period *p*; these parameters can be found in Equation 3.18. The composition differences are multiplied with the flowrates where $G_{r,p}$ and $L_{l,p}$ refers to rich and lean stream flow rates in period *p* respectively. The mass exchanged between rich stream *r* and lean stream *l* in composition location *k* and period *p* is represented as $M_{r,l,k,p}$ in both equations.

Mass balances for the rich and lean streams in each stage

The compositions of streams at each stage boundary are determined in the following equations:

$$\left(y_{r,k,p} - y_{r,k+1,p}\right) \cdot G_{r,p} = \sum_{l \in S} M_{r,l,k,p} \qquad r \in R, k \in K, p \in P \tag{3.19}$$

$$\left(y^*_{l,k,p} - y^*_{l,k+1,p}\right) \cdot L_{l,p} = \sum_{r \in R} M_{r,l,k,p} \qquad l \in S, k \in K, p \in P \tag{3.20}$$

Where $y_{r,k,p}$ and $y^*_{l,k,p}$ are the composition of rich and lean streams in composition location k and period p. The index 'k+1' implies the composition of streams in the next stage boundary location.

Assignment of target and supply concentrations

The first composition location, k = 1, and the last composition location, k = NOK +1 are the given supply composition of the rich streams in period p and the supply composition of the lean streams in period p respectively. These are described as following:

$$Y^s_{r,p} = y_{r,1,p} \qquad r \in R, p \in P \tag{3.21}$$

$$Y^{*s}_{l,p} = y_{l,NOK+1,p} \qquad l \in S, p \in P \tag{3.22}$$

The target compositions of rich and lean streams are described using inequality constraints. The last composition location, k = NOK +1 is assigned the target composition of the rich streams in period p while the first composition location, k = 1 is assigned the target composition of the lean streams in period p.

$$Y^t_{r,p} = y_{r,NOK+1,p} \qquad r \in R, p \in P \tag{3.23}$$

$$Y^{*t}_{l,p} = y_{l,1,p} \qquad l \in S, p \in P \tag{3.24}$$

Feasibility of the rich and lean stream concentrations

To ensure the rich streams become cleaner as they go through the superstructure, a constraint controlling the monotonic decrease through stages is implemented as shown in Equation 3.25.

$$y_{r,k,p} \geq y_{r,k+1,p} \qquad k \in K, r \in R, p \in P \tag{3.25}$$

Along the same line, the lean streams become richer in contaminants as the streams run through the superstructure. This is governed by the following constraint:

$$y^{*}_{l,k,p} \geq y^{*}_{l,k+1,p} \qquad k \in K, l \in S, p \in P \tag{3.26}$$

Relaxed binary variable

To improve the numerical stability of the solution, the integer-infeasible path MINLP (IIP-MINLP) formulation of Soršak and Kravanja (2002) is adapted in the model equations of Szitkai et al. (2006). This formulation involves relaxing the binary variables in the following way:

$$zmn_{r,l,k} = bzmn_{r,l,k} + pzmn_{r,l,k} - srmn_{r,l,k} \qquad r \in R, l \in S, k \in K \tag{3.27}$$

Equation 3.27 provides numerical stability of the optimisation procedure by converting the actual binary variable ($bzmn_{r,l,k}$) into the relaxed version ($zmn_{r,l,k}$). The motivation of this approach was to allow solvers to search for feasible solutions in both feasible and infeasible solution spaces and this can improve the search speed. The relaxed binary variable is calculated by including a positive tolerance ($pzmn_{r,l,k}$) and a negative tolerance ($srmn_{r,l,k}$) into the actual binary variable.

Logical constraints

When there is no match in a stage of the superstructure, the binary variable ($zmn_{r,l,k}$) has a value of zero. This is used to set the exchanged mass of an exchanger ($M_{r,l,k,p}$) to zero hence, the mass is exchanged only when there is a match. This is described in Equation 3.28.

$$M_{r,l,k,p} - \Omega_{p,\mathrm{MEN}} \cdot zmn_{r,l,k} \qquad r \in R, l \in S, k \in K \qquad (3.28)$$

The logical constraint presented in Equation 3.28 also includes an upper bound ($\Omega_{p,\mathrm{MEN}}$) on the exchangeable mass. The minimum mass load of any of the rich and lean streams involved in the match can be used as the upper bound.

Driving force for mass exchange

The driving forces at both ends of the mass exchangers are calculated when the matches exist. The rich end driving force is described as follows.

$$dy_{r,l,k,p} \leq y_{r,k,p} - y^{*}_{l,k,p} + \Gamma_m\left(1 - zmn_{r,l,k}\right) \qquad k \in K, r \in R, p \in P \qquad (3.29)$$

$$dy_{r,l,k,p} \geq y_{r,k,p} - y^{*}_{l,k,p} - \Gamma_m\left(1 - zmn_{r,l,k}\right) \qquad k \in K, r \in R, p \in P \qquad (3.30)$$

The lean end driving force of the mass exchangers are calculated as follows:

$$dy_{r,l,k+1,p} \leq y_{r,k+1,p} - y^{*}_{l,k+1,p} + \Gamma_m\left(1 - zmn_{r,l,k}\right) \qquad k \in K/last, r \in R, p \in P \quad (3.31)$$

$$dy_{r,l,k+1,p} \geq y_{r,k+1,p} - y^{*}_{l,k+1,p} - \Gamma_m\left(1 - zmn_{r,l,k}\right) \qquad k \in K/last, r \in R, p \in P \quad (3.32)$$

In these equations, the binary variable ($zmn_{r,l,k}$) activates the constraints when its value equals one. In this way, the upper bound (Γ_m) is cancelled out in the constraints, and the driving forces are calculated by comparing differences between rich and lean stream compositions of a particular match. As it was done in HENS model formulation, an exchanger minimum approach composition ($EMAC$) can be used as a lower bound to the driving forces.

The $EMAC$ helps avoid infinite height/stages in the network configurations. This is represented as:

$$dy_{r,l,k,p} \geq EMAC \tag{3.33}$$

With the driving forces, Chen's approximation for the Logarithmic Mean Concentration Differences ($LMCD$) can be used to size mass exchangers (Chen, 1987):

$$LMCD_{r,l,k,p} = \left[\frac{(dy_{r,l,k,p}) \cdot (dy_{r,l,k+1,p}) \cdot (dy_{r,l,k,p} + dy_{r,l,k+1,p})}{2}\right]^{\frac{1}{3}} \quad r \in R, l \in S, k \in K, p \in P \tag{3.34}$$

Szitkai et al. (2006) implemented the capital costing estimation of Hallale (1998) where the exchanger mass-based costing equations are used. The exchanged mass in an exchanger ($M_{r,l,k,p}$) is converted to the mass of the equipment ($mass_{r,l,k,p}$, in kg) in the following equation:

$$mass_{r,l,k,p} \cdot K_w \cdot LMCD_{r,l,k,p} = M_{r,l,k,p} \qquad r \in R, l \in S, k \in K, p \in P \tag{3.35}$$

where K_w is the lumped mass transfer coefficient. The next section presents the model equations of regeneration network.

3.4.3 Regeneration network model equations

The detailed regeneration network formulation, which is newly developed in this thesis, is adapted from analogies drawn from the MENS model of Szitkai et al. (2006). The MEN model also involves 'rich' streams, which are the exhausted lean streams, and the regenerating streams, which can be considered as the 'lean' streams. In the work of Chen and Hung (2005), which also considered regeneration of MSAs a simplified regeneration network where the regenerating unit is only appended to the end of the MEN superstructure was used. In this thesis, REN model equations are presented to study regeneration in a network synthesis

context involving multiple regenerating units. Note that the flow rate of the regenerable lean streams are assumed to be constant throughout the networks and therefore, the same index *l* is used to link the MEN and REN. Index *v* represents regenerating streams given in set *V*. The regeneration superstructure stages, *kr*, is used in the model formulation given in set *Kr*. The regeneration network model contains the following equations and inequalities:

Overall mass balance for the exhausted lean streams and regenerating streams

The supply and target compositions of the exhausted lean stream is multiplied by the lean stream flow rate to obtain the total amount of exchangeable mass for each stream. The same logic is applied to the regenerating streams. The overall stream mass balances for the regeneration network are as follows:

$$\left(X_{l,p}^{s} - X_{l,p}^{t}\right) \cdot L_{l,p} = \sum_{kr \in Kr} \sum_{v \in V} RM_{l,v,kr,p} \qquad l \in S, p \in P \tag{3.36}$$

$$\left(Z_{v,p}^{*t} - Z_{v,p}^{*s}\right) \cdot QR_{v,p} = \sum_{k \in K} \sum_{l \in S} RM_{l,v,kr,p} \qquad v \in V, p \in P \tag{3.37}$$

In Equation 3.36, $X_{l,p}^{s}$ and $X_{l,p}^{t}$ are supply and target composition of the exhausted lean streams in period *p* respectively. In Equation 3.37 which is for the regenerating streams, $Z_{v,p}^{*s}$ and $Z_{v,p}^{*t}$ are supply and target equilibrium compositions of the regenerating streams *v* in the rich phase. The composition differences are multiplied with the flowrates where $L_{l,p}$ and $QR_{v,p}$ refer to the lean and regenerating stream flowrates in period *p* respectively. The mass exchanged between the exhausted lean stream *l* and regenerating stream *v* in composition location *kr* and period *p* is represented as $RM_{l,v,kr,p}$ in both equations.

Mass balances for the exhausted lean streams and regenerants in each stage

The compositions of streams involved in the regeneration network at each stage boundary are calculated using the following equations:

$$\left(x_{l,kr,p} - x_{l,kr+1,p}\right) \cdot L_{l,p} = \sum_{v \in V} RM_{l,v,kr,p} \qquad l \in S, kr \in Kr, p \in P \tag{3.38}$$

$$\left(z^*_{v,kr,p} - z^*_{v,kr+1,p}\right) \cdot QR_{v,p} = \sum_{l \in S} RM_{l,v,kr,p} \qquad v \in V, kr \in Kr, p \in P \tag{3.39}$$

Where $x_{l,kr,p}$and $z^*_{v,kr,p}$are the compositions of the exhausted lean stream and regenerating stream in composition location *kr* and period *p*.

Assignment of target and supply concentrations

The first composition location, *kr* = 1, and the last composition location, *kr* = *NOKr* +1 are assigned the supply composition of the exhausted lean streams and the supply composition of the regenerating streams respectively. These are described as follows:

$$X^s_{l,p} = x_{l,1,p} \qquad l \in S, p \in P \tag{3.40}$$

$$Z^{*s}_{v,p} = z_{v,NOKr+1,p} \qquad v \in V, p \in P \tag{3.41}$$

The target compositions of the exhausted lean stream and regenerating stream are presented using inequality constraints. The last composition location, *kr* = *NOKr* +1 is assigned the target composition of the exhausted lean stream while the first composition location, *kr* = 1 is assigned the target composition of the regenerating streams.

$$X^t_{l,p} = x_{l,NOKr+1,p} \qquad l \in S, p \in P \tag{3.42}$$

$$Z^{*t}_{v,p} = z_{v,1,p} \qquad v \in V, p \in P \tag{3.43}$$

Feasibility of the exhausted lean stream and regenerating stream concentrations

The monotonicity of the exhausted lean stream compositions across the regeneration network is achieved with the following inequality:

$$x_{l,kr,p} \geq x_{l,kr+1,p} \qquad kr \in Kr, l \in S, p \in P \tag{3.44}$$

In the same way, the regenerating streams become richer as the streams run from left to right in the regeneration superstructure. This is governed by the following constraint:

$$z^*_{v,kr,p} \geq z^*_{v,kr+1,p} \qquad kr \in Kr, v \in V, p \in P \tag{3.45}$$

The relaxed binary variable of regeneration network

The formulation of Soršak and Kravanja (2002) is again applied to improve the numerical stability of the solution. Equation 3.46 relaxes the actual binary variables:

$$zrn_{l,v,kr} = bzrn_{l,v,kr} + pzrn_{l,v,kr} - srrn_{l,v,kr} \qquad l \in S, v \in V, kr \in Kr \tag{3.46}$$

Equation 3.46 is implemented to provide numerical stability by converting the actual binary variable ($bzrn_{l,v,kr}$) into the relaxed version ($zrn_{l,v,kr}$). The positive tolerance ($pzrn_{l,v,kr}$) and negative tolerance ($srrn_{l,v,kr}$) for regeneration network is included as done in the MENS model formulation.

Logical constraints in regeneration network

In order to allow mass to be exchanged only when there is a match between the exhausted lean streams and the regenerating streams, the logical constraint is applied as follows:

$$RM_{l,v,kr,p} - \Omega_{p,\mathrm{REN}} \cdot zrn_{l,v,kr} \qquad l \in S, v \in V, kr \in Kr \tag{3.47}$$

When there is no match in a stage of the REN superstructure, the binary variable ($zrn_{l,v,kr}$) has a value of zero. The binary variable is used to set the exchanged mass of regeneration columns ($RM_{l,v,kr,p}$) to zero. Equation 3.47 is constrained by an upper bound ($\Omega_{p,\mathrm{REN}}$) on the exchanged mass between the exhausted lean stream *l* and regenerating stream *v.* The minimum of the mass load between the exhausted lean stream and the regenerant involved in the match can be used as the upper bound.

Driving forces for regeneration network

The driving forces at both ends of the regeneration columns are calculated only when the matches exist. The driving forces on of the rich side can be described as follows:

$$drn_{l,v,kr,p} \leq x_{l,kr,p} - z^{*}_{v,kr,p} + \Gamma_{rn}\left(1 - zrn_{l,v,kr}\right) \qquad kr \in Kr, l \in S, p \in P \qquad (3.48)$$

$$drn_{l,v,kr,p} \geq x_{l,kr,p} - z^{*}_{v,kr,p} - \Gamma_{rn}\left(1 - zrn_{k,v,kr}\right) \qquad kr \in Kr, l \in S, p \in P \qquad (3.49)$$

The driving forces on the lean side of the regenerating exchanger are represented in Equation 3.50 and 3.51:

$$drn_{l,v,kr+1,p} \leq x_{l,kr+1,p} - z^{*}_{v,kr+1,p} + \Gamma_{rn}\left(1 - zrn_{l,v,kr}\right) \qquad kr \in Kr/last, l \in S, p \in P \qquad (3.50)$$

$$drn_{l,v,kr+1,p} \geq x_{l,kr+1,p} - z^{*}_{v,kr+1,p} - \Gamma_{rn}\left(1 - zrn_{l,v,kr}\right) \qquad kr \in Kr/last, l \in S, p \in P \qquad (3.51)$$

The binary variable is used as a switch to activate the above constraints when the value of the binary variable is one. This will cancel out the last term in these constraints, and the driving forces are calculated by comparing the differences between the compositions of the associated streams. In order to avoid infinite heights/stages in the optimal network, a regeneration exchanger minimum approach composition (*REMAC*) can be used as follows:

$$drn_{l,v,kr,p} \geq REMAC \qquad (3.52)$$

3.4.4 The combined economic objective function

The economic objective function of Isafiade (2017) is used to minimise the TAC of the combined networks simultaneously. The objective function also determines the optimal network configuration and utility consumptions for CHAMENs. Equation 3.53 represents the economic objective function.

$$\min \left\{ \sum_{p\in P} \left\{ \left\{ \begin{array}{l} \left[\frac{DOP_p}{\sum_{p=1}^{NOP} DOP_p} \cdot \sum_{r\in R}\sum_{l\in S}\sum_{k\in K} LSC_l \cdot L_{l,p} \right] \\ + \frac{DOP_p}{\sum_{p=1}^{NOP} DOP_p} \cdot \sum_{l\in S}\sum_{v\in V}\sum_{kr\in Kr} RSC_v \cdot QR_{v,p} \end{array} \right\} \right.\right.$$
$$\left.\left. + \left\{ \begin{array}{l} \frac{DOP_p}{\sum_{p=1}^{NOP} DOP_p} \cdot \sum_{ih\in HU}\sum_{jc\in CP}\sum_{kh\in Kh} HUC_{ih} \cdot q_{ih,jc,kh,p} \\ + \frac{DOP_p}{\sum_{p=1}^{NOP} DOP_p} \cdot \sum_{ih\in HP}\sum_{jc\in CU}\sum_{kh\in Kh} CUC_{jc} \cdot q_{ih,jc,kh,p} \end{array} \right\} \right\}$$
$$+AF_{MEN} \left\{ \begin{array}{l} \sum_{r\in R}\sum_{l\in S}\sum_{k\in K} CF_{l,s} \cdot zmn_{r,l,k} \\ + \sum_{r\in R}\sum_{l\in S}\sum_{k\in K} ACH_{r,l} \left[\frac{mass_{r,l,k,p}}{K_w} \cdot LMCD_{r,l,k,p} \right]^{D_{r,l}} \end{array} \right\}$$
$$+ AF_{REN} \left\{ \begin{array}{l} \sum_{l\in S}\sum_{v\in V}\sum_{kr\in Kr} CF_{l,v} \cdot zrn_{l,v,kr} \\ + \sum_{l\in S}\sum_{v\in V}\sum_{kr\in Kr} ACH_{l,v} \left[\frac{rmass_{l,v,kr,p}}{K_w} \cdot LMCD_{l,v,kr,p} \right]^{D_{l,v}} \end{array} \right\}$$
$$+ AF_{HEN} \left\{ \begin{array}{l} \sum_{ih\in HP}\sum_{jc\in CP}\sum_{kh\in Kh} CF_{ih,jc} \cdot zhn_{ih,jc,kh} \\ + \sum_{ih\in HP}\sum_{jc\in CP}\sum_{kh\in KH} AC_{ih,jc} \cdot \left[\frac{q_{ih,jc,kh,p}}{U_{ih,jc}\left(LMTD_{ih,jc,kh,p}\right)} \right]^{ACE} \end{array} \right\}$$
$$+ AF_{SP}\left(ACSC_{ih,jc} \cdot ASC_{ih,jc,kh}\right) + AF_{ST}\left(ACTC_{ih,jc} \cdot VTS_{ih,jc,kh}\right)$$
$$+ w \sum_{r\in R}\sum_{l\in S}\sum_{k\in K} \left(pzmn_{r,l,kr} + szmn_{r,l,kr}\right)$$
$$\left. + \; w \sum_{l\in S}\sum_{v\in V}\sum_{kr\in Kr} \left(pzrn_{l,v,kr} + szrn_{l,v,kr}\right) \right\} \tag{3.53}$$

The combined economic objective function consists of the operating costs of the annualised external MSAs, regenerants and heating/cooling utilities. The first four terms of the objective function are the operating costs of the three networks. The next are the annualised capital costs of MEN, REN, and HEN as well as the annualised capital cost of solar panels and thermal storage vessels. In MEN and REN, the equipment cost is defined in terms of shell mass

(Hallale, 1998). In HEN capital cost, Chen's *LMTD* approximation (1987) presented in Equation 3.13 is used as presented in the work of Yee and Grossmann (1990). Numerical stability terms for MEN and REN are the last two terms in Equation 3.53 where the *w* weighting factor is a large arbitrary number.

DOP_p is the duration of each period within a day where solar irradiation is available or not available, while NOP is the number of periods considered for each day. AF_{MEN}, AF_{REN}, AF_{HEN}, AF_{SP} and AF_{ST} are the annualization factors for the exchangers in MEN, REN, HEN, solar panels and heat storage tank respectively. $CF_{r,l}$, $CF_{l,v}$ and $CF_{ih,jc}$ are fixed costs for mass absorbers, regenerating columns and heat exchangers. $zmn_{r,l,k}$, $zrn_{l,v,kr}$ and $zhn_{ih,jc,kh}$ are the binary variables which indicate the presence of exchangers in a mass, regeneration and heat exchange network respectively. $ACH_{r,l}$ and $ACH_{l,v}$ are the cost per unit of shell mass of columns. $mass_{r,l,k,p}$ and $rmass_{l,v,kr,p}$ are mass of shells in MEN and REN respectively, while $q_{ih,jc,kh,p}$ is the amount of heat exchanged between the hot and cold streams. $U_{ih,jc}$ is the overall heat transfer coefficient, and K_w is the lumped mass transfer coefficient (Halalle, 1998). $D_{r,l,}$ $D_{l,v}$and ACE are cost exponents for units in MEN, REN and HEN respectively. $AC_{ih,jc}$, $ACSC_{ih,jc,}$ $ACTC_{ih,jc}$ are the costs per unit area for heat exchangers, costs per unit area for solar panels and costs per unit volume for the heat storage tank. LSC_l is the cost per unit of external lean streams while RSC_v is the cost per unit of regenerating streams. HUC_{ih} and CUC_{jc} are the costs per unit of hot and cold utilities respectively. $L_{l,p}$ and $QR_{v,p}$ are the flowrates of external mass separating agents and regenerants in period *p* respectively.

3.4.5 Environmental impact objective function

Environmental impact of HEN (EI_{HEN}) can be obtained through the Equation 3.54.

$$min\, EI_{HEN} = H_Y \sum_{p \in P} \left\{ \left[\frac{DOP_p}{\sum_{p=1}^{NOP} DOP_p} \cdot \sum_{ih \in HU} \sum_{jc \in CP} \sum_{kh \in Kh} q_{ih,jc,kh,p} \cdot EIHU_{ih} \right] + \left[\frac{DOP_p}{\sum_{p=1}^{NOP} DOP_p} \cdot \sum_{ih \in HP} \sum_{jc \in CU} \sum_{kh \in Kh} q_{ih,jc,kh,p} \cdot EICU_{jc} \right] \right\} \quad (3.54)$$

Equation 3.54 is presented in the work of Isafiade et al. (2017) for HENS, where H_Y is the operating time in a year. The term involving DOP_p is used to allow the model to consider the exact quantities of utilities in each period. The environmental impact is calculated by multiplying the heat exchanged between the hot utility (HU) and cold process streams (CP) in temperature location kh with the environmental impact of the hot utility ($EIHU_{ih}$) concerned. The same calculation is applied to the match involving the cold utility (CU) and hot process streams (HP) in which environmental impact of cold utility ($EICU_{jc}$) is used. The same logic is adapted and applied to MENS to calculate the environmental impact of such network (EI_{MEN})

$$min\, EI_{MEN} = H_Y \sum_{p \in P} \left\{ \left[\frac{DOP_p}{\sum_{p=1}^{NOP} DOP_p} \cdot \sum_{r \in R} \sum_{l \in S} \sum_{k \in K} L_{l,p} \cdot EIMN_l \right] + \left[\frac{DOP_p}{\sum_{p=1}^{NOP} DOP_p} \cdot \sum_{l \in S} \sum_{v \in V} \sum_{kr \in Kr} QR_{v,p} \cdot EIRN_v \right] \right\} \quad (3.55)$$

Where the environmental impact of lean streams ($EIMN_l$) and the environmental impact of regenerating streams ($\mathrm{EIRN_v}$) is multiplied with the flow rate of lean and regenerating streams respectively. The ReCipe method in SimaPro, 2016 (Huijbregts et al., 2016) for LICA was used to quantify the environmental impacts of the utilities generated from both

renewable and fossil-based energy sources for HEN. The same method was applied to obtain EI of MSAs and regenerating streams in MEN and REN.

3.4.6 Multi-objective function

In this thesis, the modified goal method presented in Gxavu and Smaill, (2012) is used to simultaneously optimise combined network in terms of both economic and environmental objective functions as follows.

$$\min Z = R_g \times \frac{TAC}{TAC_{\min}} + \left(1 - R_g\right) \times \frac{EI}{EI_{\min}} \tag{3.56}$$

where R_g is the weighting parameter which determines the weighting of TAC in the objective function. Notice that $TAC_{\min}$ and $EI_{\min}$ are the minimum objective values for TAC and environmental impact respectively. The Equation 3.56 can minimise both objectives by calculating the ratio between the minimum objective values and the actual objectives which becomes dimensionless.

The last step of the mathematical programming approach is to optimise the formulated mathematical problem. The presented model is solved as a MINLP problem, and it is optimised using General Algebraic Modelling Systems (GAMS) with DICOPT solver which uses CPLEX for the MILP and CONOPT for the NLP sub-problems (Rosenthal, 2007). The machine platform is an Intel® Core™ i5-7200U 2.70 GHz CPU with 4.00 GB of RAM.

3.4.7 Initialisations and Convergence

Attempting to obtain a feasible solution with the combined set of model equations for HENs, MENs and RENs can be challenging as there are many unknown variables related through highly nonlinear constraints. Finding an initial value for such variables and the associated boundaries is therefore essential. It is suggested to do an exploratory run of the separate

MINLP models of the HEN, MEN, and REN in order to obtain initial values for the following variables/parameters:

- *EMAC*, *REMAC* and *EMAT*
- $\Omega_{p,\mathrm{MEN}}$, and $\Omega_{p,\mathrm{REN}}$
- the upper and the lower initialisation values of lean and regenerating stream flow rates
- the thermal flow rates of recyclable MSAs
- the number of temperature/composition locations in the superstructure

These initial values are inputted into the CHAMENs model and solved simultaneously. The values may require additional exploratory runs with slightly changed values of the variables/parameters listed above until the solver has produced the optimal solutions. Small changes in the values can have a significant influence on the direction of the search for the solvers. The initialisation step is therefore likely to guide the solver to find the region which contains the feasible solutions.

In many complex problems, apart from the best network, several good alternatives may exist (Kemp, 2005). Therefore, in the next section, the developed CHAMENs synthesis approach is implemented to show its applicability in obtaining good solutions.

CHAPTER 4

CASE STUDIES

Chapter 4 Case Study

This chapter presents two case studies to demonstrate the applicability of the developed methodology in the previous chapter. In each case study, the stream data and associated costing data for HEN, MEN and REN are presented. Since there is no other benchmark literature to compare the results of this thesis, it is aimed to study the solutions obtained in depth by investigating the interactions among the networks.

It is emphasised again that solving combined networks is not a trivial task due to the multi-dimensional nature of the problem as well as the presence of multiple utility streams in MEN and REN. Therefore, the initialisation strategy presented in Chapter 3 is implemented to obtain feasible solutions. Each network is initialized with the values obtained from the exploratory runs, after which it is then combined with the initialized versions of other networks to form the CHAMENs model. Solving the CHAMEN model in this form results in feasible solutions. The model's ability to handle additional regeneration network involving multiple MSAs and multiple regeneration streams are presented in the case studies. Also, multi-period representation of solar thermal energy and MOO of the economic and the environmental impact of CHAMENs are presented through the case studies of this chapter.

4.1 Ammonia removal (Case study 1)

This case study is obtained from Hallale (1998) where the author applied pinch technology to synthesise the MEN involving ammonia removal process. The case study was chosen as the complete set of stream data allows economic optimization. The original case study involves the removal of ammonia, in continuous contact columns, from five gaseous process streams which are mainly composed of air. In order to remove the ammonia, three water-based lean streams are used in the original data where S_1 and S_2 are process MSAs while S_3 is an external MSA. Many other authors have solved this case study in its original form. Some of the authors include Szitkai et al. (2006), Isafiade and Fraser (2008) and Emhamed et al. (2005). Recently, Isafiade, (2017) solved this case study as a CHAMEN problem considering

the regeneration of the only external MSA involved by including heating/cooling stream data. Some modifications in stream flowrates and compositions were done.

In order to extend this existing MENs case study to the context of this thesis which involves MEN and REN with multiple recyclable external MSAs, the existing data is modified. The modification entails having multiple recyclable MSAs by regarding S_2 as an external MSA. So, in the modified case study, S_1 is a process MSA, while S_2 and S_3 are external MSAs which can be regenerated. The stream data for S_2, including its equilibrium constant, were obtained from El-Halwagi (1997). Two regenerants are considered for the recovery of the spent external MSAs S_2 and S_3. The regenerants are low-pressure steam and air stripping. For the process MSA, S_1, no operating cost is associated with it since it is readily available onsite. Its flowrate is bounded by its availability in the plant and may not exceed a value of the maximum, L_c. On the other hand, the external MSAs can be purchased from the market and corresponding flowrates are determined based on economic considerations. Table 4.1 shows the stream composition data (in mass fractions) with equilibrium constants (m) of the streams involved in MENs.

Table 4.1: The MENs stream data for case study 1 (concentrations given in mas fractions; Data from Hallale, 1998)

Rich Streams	Flow (Kg/s)	y^s	y^t	Lean Streams	Flow (Kg/s)	m	x^s	x^t
R_1	2.0	0.005	0.0010	**S_1**	1.8	1.2	0.0017	0.0071
R_2	4.0	0.005	0.0025	***S_2**	∞	0.1	0.0040	0.1090
R_3	3.5	0.011	0.0025	**S_3**	∞	0.5	0.00008	0.0170
R_4	1.5	0.010	0.0050					
R_5	0.5	0.008	0.0025					

* S_2 data was obtained from El-Halwagi (1997). S_3 data was obtained from Hallale (1998) with inlet compositions was modified.

The modified MEN stream data is presented in Table 4.1. The exhausted external MSAs are transported to the REN and can be regenerated through two options of regenerants involving

steam stripping and air stripping. In the case of air stripping, the process is advantageous compared to another similar processes since principles involving air stripping is relatively simple and is a mechanical process which does not require solvent regeneration. Also, the presence of other toxic compounds does not affect air stripping performances (EPA, 2000). However, air stripping tends to simply transfer the pollution from the liquid phase to the gas phase and therefore, may require additional treatment steps. On the other hand, the stripping steam cost, in general, is much higher than the air stripping cost, but the top product of the steam stripping column is usually a pure volatile organic compound that can be used in another process. The study of Toth and Mizsey, (2015) showed that the overall cost of steam stripping could be cheaper than its air counterpart as exhausted stripping air in general, requires extra purification steps which can be expensive. The stream data of the multiple regenerating streams are presented in Table 4.2.

Table 4.2: The RENs stream data for case study 1 (compositions given in mass fractions)

Regenerating Streams	***m***	$\mathbf{z^s}$	$\mathbf{z^t}$
QR1 (steam stripping)	0.12650	4.682×10^{-5}	1.587×10^{-4}
QR2 (air stripping)	0.00972	0.0000	0.0440

One of the challenges faced in the expansion of regeneration network was the scarcity, in the literature, of stream and equilibrium data associated with the regenerating streams. The target composition of the stripping process was aimed to be equal to or less than 50% of the lower explosive limit (LEL) of ammonia as suggested in El-Halwagi (2017). The LEL of ammonia is 15% in air (Pfahl et al., 2000). This value was converted to mass fraction, and the target composition value of 0.0440 was obtained for the stripping air stream. The related calculations on compositions are found in Appendix A1.

In the case of steam stripping, the supply and the target compositions were varied until a feasible solution was obtained. At the compositions presented in Table 4.2, It was possible to obtain a feasible solution involving the two regenerating streams. Note that the target

composition of the stripping steam is below 50 percent of LEL of ammonia. Note also that within the allowed range, the compositions can vary to obtain different sets of feasible solutions. It is worth mentioning that this case study is theoretical and more realistic results can be obtained when more accurate composition data is available for the regenerating streams. The equilibrium constants of the regenerating streams were obtained by using Equation 2.37 presented in Chapter 2. The details of the calculations are presented in Appendix A2.

The ReCipe method indicator values associated with the water-based lean streams and regenerating streams are presented in Table 4.3. These values are used in Equation 3.55 to compare the results of the MEN (i.e. the first step in the synthesis procedure) and the MEN-REN (i.e. the second step of the synthesis procedure).

Table 4.3: The environmental impact of lean and regenerating streams

			ReCiPe method indicator values (1/kg)
MEN:	S_1	Process MSA (water)	6.86×10^{-6}
	*S_2	External MSA (Acetic acid)	0.503
	*S_3	External MSA (Phosphoric acid)	0.666
REN:	QR_1	Stripping Steam	0.0720
	QR_2	Stripping Air	0.00522

* The indicator values (1/kg) of S_2 and S_3 are associated with concentrated acetic acid and phosphoric acid respectively. Getting values for the aqueous solutions are beyond the scope of this work.

In the work of Hallale (1998), the lean streams were grouped as aqueous solvents. So, the current author assumed that S_1 is pure water stream while S_2 and S_3 are aqueous acetic acid and phosphoric acid to quantify the environmental impacts associated with each stream. It is worth mentioning that the environmental indicator values used in this study are for preliminary optimisation. In order to get more realistic values, more detailed LCIA should be performed.

4.1.1 Simultaneous synthesis of MEN (The first step)

Constructing CHAMENs model involving multiple external MSAs and multiple regenerating streams to obtain a feasible solution is not a simple task, and therefore, a separate MEN was first synthesised to obtain initial values for *EMAC*, upper and lower bound values for lean stream flowrates and the upper bound values for exchangeable mass ($\Omega_{p,\mathrm{MEN}}$). The operating cost data associated with the streams, and the capital cost data, are presented in Appendix A3. Figure 4.1 presents the synthesised MEN configuration.

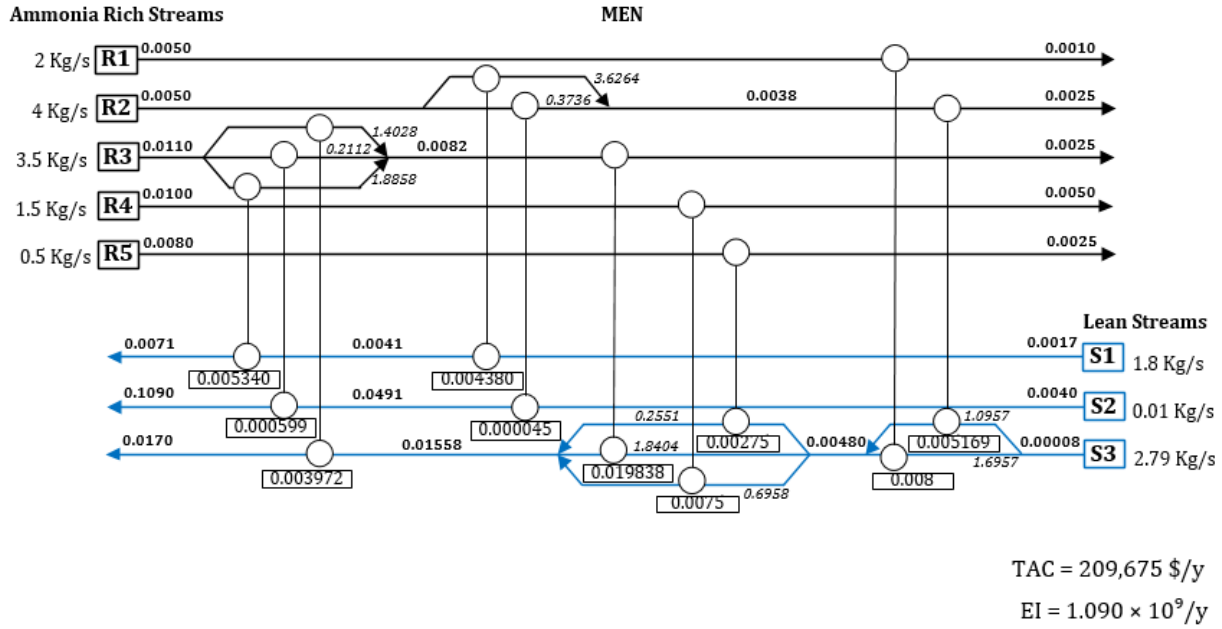

Figure 4.1: The MEN configuration of case study 1 (values above streams are composition in mass fractions; while values in boxes indicate mass load transferred in mass exchangers [kg/s])

The resulting TAC of the MEN is 209,675 $/y . The *EMAC* value of 0.00001 (wt fraction) was used, and the $\Omega_{p,\mathrm{MEN}}$ value of 0.0089 was applied in the model. Four composition stages were used to initialize the network. Lower bounds of 0.12 kg/s, 0.01 kg/s and 0.05 kg/s were used for the flowrates of S_1, S_2 and S_3 respectively. Upper bounds of 1.8 kg/s, 1 kg/s and 5 kg/s were used for S_1, S_2 and S_3 flowrates respectively. Based on these values, the optimal solution was found to have lean stream flowrates of 1.8 kg/s, 0.01 kg/s and 2.79 kg/s for S_1, S_2 and S_3 respectively. The MEN has 10 mass exchangers with a 2-way split of R_2, a 3-way split of R_3, and 3- and 2-way splits of S_3 in different composition locations.

4.1.2 Synthesis of combined MEN and REN (The second step)

The MEN model presented in the previous section was then used to initialise an extended model involving a combination of MEN and REN. The regeneration network model equations presented in Equations 3.36 to 3.52 are implemented in the MENS formulation to synthesise the networks of MEN and REN simultaneously. The lean stream flowrates are treated as variables to be optimised in which regenerable external MSAs are allowed to flow through the MEN and REN to complete the recycle circuit. Note that the costs per unit of external MSAs are set to zero now that regeneration is involved since it is assumed that they to be regenerated completely without any solvent loss. The synthesised mass and regeneration network solution is presented in Figure 4.2.

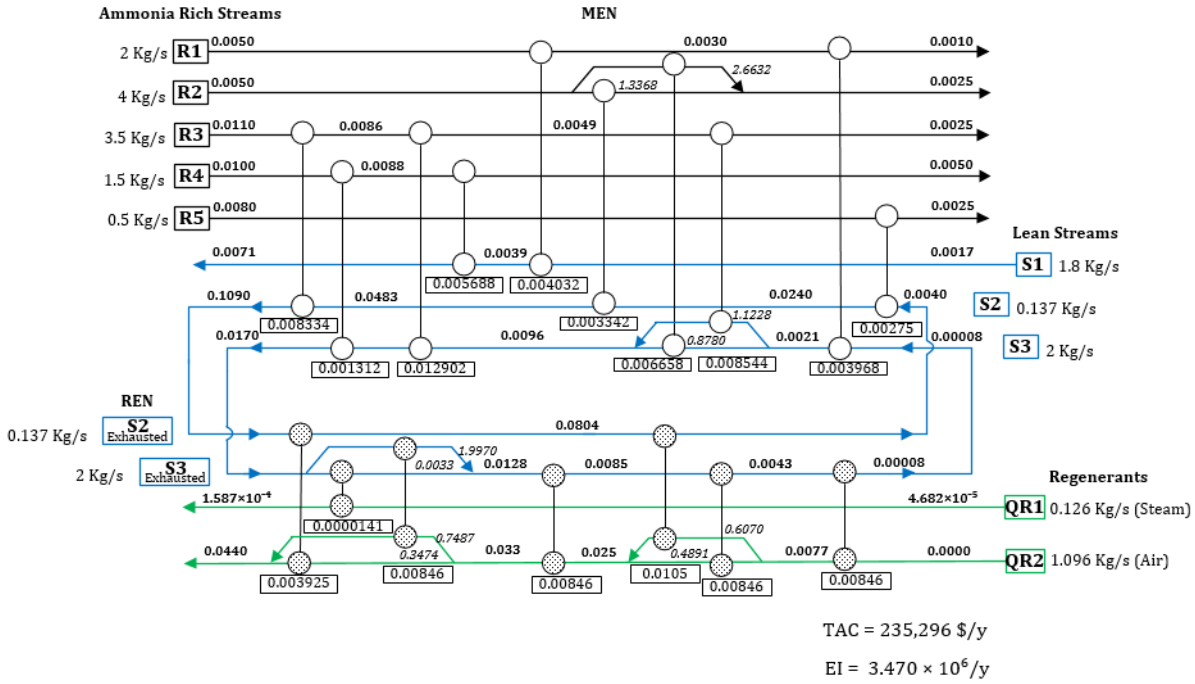

Figure 4.2: The MEN with REN configuration of case study 1 (values above streams are composition in mass fractions; while values in boxes indicate mass load transferred in mass exchangers [kg/s])

The resulting TAC of the combined MEN and REN is 235,296 $/y. The MEN consists of 10 mass exchangers as it was obtained in the individual MEN solution presented in Figure 4.1, while the REN involves 7 regeneration columns. In this solution, only 2-way splits are observed throughout the networks. The fresh lean streams enter the MEN superstructure from right to left. Note that exhausted external MSAs at the end of the MEN superstructure

is transported into the REN superstructure. The exhausted streams enter the REN from left to right to complete the recycle circuit.

The feasible solution was obtained at the *EMAC* value of 0.00001 and a *REMAC* value of 7.812×10^{-13}. As stated previously, some exploratory runs were necessary to get a feasible solution. A slightly changed $\Omega_{p,\mathrm{MEN}}$ value of 0.00722 was used in this second step together with a $\Omega_{p,\mathrm{REN}}$ value of 0.001 for the REN superstructure. Four composition stages were used to initialise both MEN and REN superstructures. The initialization values of the lean streams were as follows; lower bound values of 1.2 kg/s, 0.01 kg/s and 0.05 kg/s were used for S_1, S_2 and S_3 respectively, while the upper bound for S_1 was given its corresponding process MSA maximum capacity of 1.8 kg/s. For S_2 and S_3, a large upper bound value of 10 kg/s was used for both streams to allow the solver to find feasible solutions from a wide range of flowrate boundaries. The S_1, S_2 and S_3 flowrates are optimised to be 1.8 kg/s, 0.137 kg/s and 2 kg/s respectively. Note that the results used the full capacity of the process MSA and then implemented the external MSAs based on economical consideration. A sample code for this step of the case study is presented in Appendix B.

The REN, which involves two exhausted external MSAs, S_2 and S_3 and two regenerating streams QR_1 (steam) and QR_2 (air), is presented in the lower section of Figure 4.2. Stream flowrate lower bounds of 0.13 kg/s and 9.72×10^{-6} kg/s were used for QR_1 and QR_2 respectively, while their upper bound flow rates were 126.5 kg/s and 11.66 kg/s respectively. Even though the regeneration network is included in the developed model, the obtained TAC was in the same order of magnitude compared to the individual MEN solution of the first step presented in Figure 4.1. The solution of the combined MEN and REN is 10.8 % more expensive than that of the MEN only scenario.

The MEN only and the combined MEN-REN solution networks were then further investigated to determine environmental impacts. Equation 3.55 is used to calculate the environmental impact of streams disposed of into the environment where the ReCiPe indicator values presented in Table 4.3 are multiplied by the corresponding flow rates and then summed up

to provide the total environmental impact of a network per year. The MEN-only network has an environmental impact of 1.090×10^9/y which comprises ReCiPe indicator values of lean streams S_1, S_2 and S_3 while the combined MEN-REN network has 3.470×10^6/y which is based on the indicator values of S_1, QR_1 and QR_2. In the combined MEN-REN network, ReCiPe indicator values of the lean streams S_2 and S_3 are not included in the calculation as these streams are regenerated in the REN. From this result, the combined MEN-REN exerts less impacts on the environment. This result seems obvious as many industrial processes have implemented regeneration units to control wastes and pollutions. However, not so many case studies involving regeneration are presented in the process synthesis literature. As Szitkai (2004) mentioned that it is necessary to incorporate pollution prevention in the process synthesis step to adequately control the impact of pollutions, studying regeneration in the process synthesis step can assist in adequate consideration of all design parameters.

4.1.3 Simultaneous synthesis of CHAMENs with REN (The third step)

In order to synthesise CHAMENs, hot/cold stream data is needed as heating and cooling can enhance the mass transfer. The regenerable external MSAs exiting the MEN can heated up before entering the REN to promote the stripping process. After the MSAs are regenerated in the REN, they are then cooled down before being transported back to the MEN to enhance the absorption process. The HENs data used in this study was obtained from Isafiade (2017) which also investigated CHAMENS problems. Table 4.4 shows HENs stream data where H_1 and H_2 represent heating utility generated from solar thermal and fossil fuel respectively. The hot streams H_3 and H_4 are the external MSAs (S_2 and S_3) to be cooled to enhance absorption. The cold streams C_1 and C_2 are the external MSAs (S_2 and S_3) to be heated up to enhance stripping while C_3 is cold utility (cooling water).

Table 4.4: The HENs stream data and costs for case study 1

Streams	T^s (℃)	T^t (℃)	F (kW℃$^{-1}$)	h	Cp (Kj/kg·K)	Costs $/(kW·yr)	ReCiPe values (1/kJ)
H_1	120	60	-	0.2	-	0	2.02×10^{-6}
H_2	135	134	-	0.2	-	60	1.36×10^{-4}
H_3	100	30	*	0.2	4.2	-	-
H_4	80	30	*	0.2	4.2	-	-
C_1	30	100	*	0.2	4.2	-	-
C_2	30	80	*	0.2	4.2	-	-
C_3	5	10	-	0.2	-	30	4.67×10^{-5}

* The mass flowrate of H_3, H_4, C_1 and C_2 are converted to the corresponding thermal flowrates using the Cp values presented above.

Hot streams H_2 an H_3 are cooled down to 30 ℃ (shown as target temperature T^t in Table 4.4. On the other hand, since low pressure steam is operated at 100 ℃, C_1 is heated up to this temperature (shown as T^t in Table 4.4), while C_2 is heated up to 80 ℃ for air stripping (shown as T^t in Table 4.4). According to Saracco and Genon, (1994), an operating temperature of 80 ℃ for air stripping will lead to a reduction in the capital costs of columns by more than 50 per cent when compared to operating at a temperature as low as 40 ℃. Therefore, operating air strippers at high temperatures can be beneficial if cost-efficient and environment-friendly heating sources are integrated with the overall process. The cost of fossil-based utility (H_2) used in this study is 60 $/(kWy) while for utility obtained solar thermal (H_1), the cost was assumed to be zero. The thermal flowrate of the utilities are variables to be optimised. In contrast, the thermal flowrates of the external MSAs inputted to the superstructure as initial values of this third step are those obtained from the solution of the second step for S_2 and S_3. Thus, the thermal flowrates of H_3 and C_1 correspond to that of S_2 while those of H_4 and C_2 correspond to that of S_3. The CHAMEN model of this step was then ran until a feasible solution. The environmental impact study was also done for this CHAMENS step so as to evaluate the impact associated with the heating/cooling utilities. The ReCiPe method indicator values (1/kJ) associated with the utilities are presented in Table 4.4.

These values are used in Equation 3.54 to obtain the environmental impact of the HEN component of the combined network. Given these data, the CHAMEN is synthesised and presented in Figure 4.3

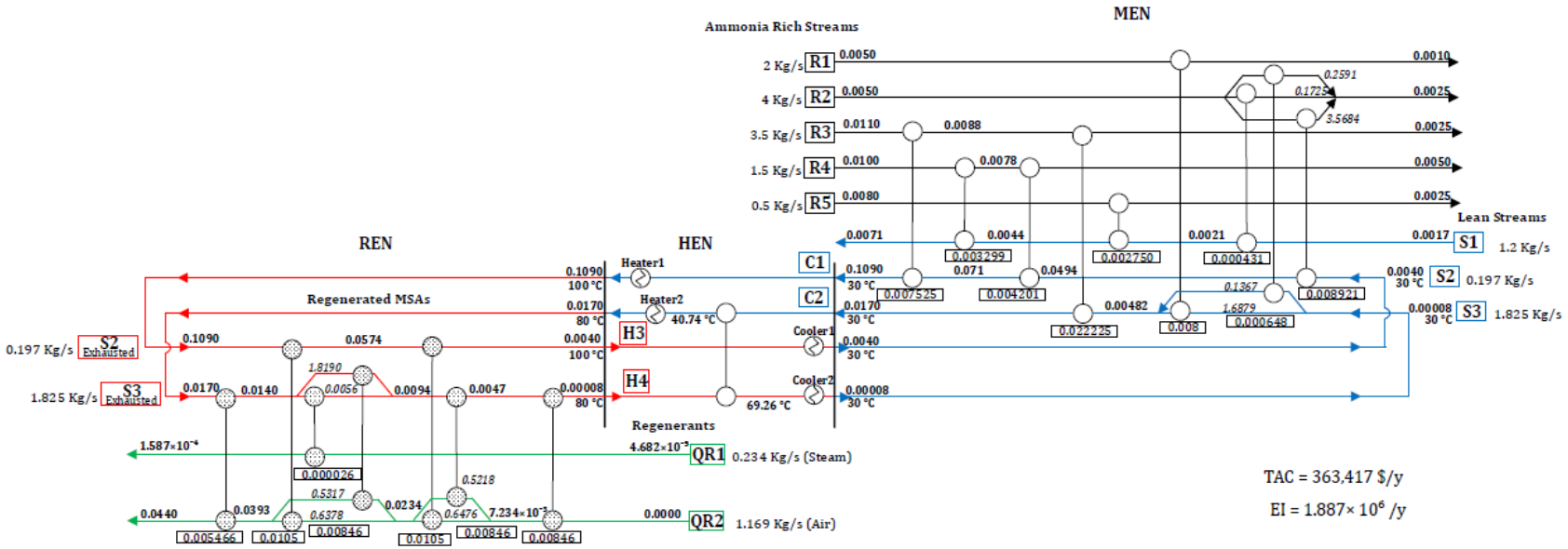

Figure 4.3: The multi-period CHAMENs configuration for case study 1 (values above streams are composition in mass fractions; while values in boxes indicate mass load transferred in mass exchangers [kg/s])

The resulting TAC of the CHAMEN in Figure 4.3 is 363,417 $/yr. The HEN superstructure involves 4 temperature stages while the MEN and REN superstructures used 6 and 4 composition stages respectively. Since the HEN is introduced into the combined MEN-REN model, the *EMAT* value of 9.8 was used to initialise the model. The combined CHAMEN model has 2,495 single equations, 1,741 single variables and 166 discrete variables. The model was solved in 21.60 s of CPU time.

The MEN is the right-hand side of the figure, while the REN is placed on left-hand side of the figure. The HEN is positioned between the MEN and the REN. The optimal flowrates for S_2 and S_3 are 0.197 kg/s and 1.825 kg/s respectively. The process lean stream S_1 flowrate obtained is 1.2 kg/s, which is below the full capacity of the process lean streams available on site. For the regenerants QR_1 and QR_2, the optimal flowrates of 0.234 kg/s and 1.169 kg/s were obtained respectively. The CHAMEN configuration of Figure 4.3 has 9, 7 and 5 exchangers in the MEN, REN and HEN respectively. Of the two hot utility sources available (solar thermal and fossil fuel), the solver selected based on economics. The two heaters shown in Figure 4.3 transfer heat generated from fossil-based fuel at a price of 60 $/(kW·y). This implies that solar thermal as a hot utility source is not competitive when fossil fuel price is relatively low. Also, the employment of such renewable-based utility source requires equipment such as solar panels and heat storage vessels, which both have capital costs. This may have prevented solar thermal from being selected in the CHAMEN solution.

Sensitivity analysis was then carried out so as to identify the unit cost of utility generated from fossil that will make solar thermal competitive. The fossil fuel price was gradually increased starting from 60 $/(kW·y). Feasible solutions were obtained at prices 82, 112, 120, 162, 175, 990 and 1250 $/(kW·y). At these prices, except the last one, networks employing the utility generated from fossil fuel were obtained. At the fossil fuel price of 1250 $/(kW·y), it became economically unviable to use fossil-based utility and therefore, the solver selected utility generated from solar thermal which requires minimal operating cost compared to that of fossil fuel. The 1250 $/(kW·y) price falls within the cost range (438 $/kW·y to 1489.2 $/kW·y) for fossil-based fuel reported by IRENA (2017) for the G20 countries. Isafiade, (2017) stated that such investigations can assist governments and stakeholders in making decisions associated with the prices of utilities generated from fossil fuels and renewable sources so as to make solar thermal and other renewables competitive. A network involving solar panels and heat storage vessels is presented in Figure 4.4. In this figure, there are two heaters supplying heat to the cold streams C_1 and C_2. Both heaters transfer heat generated from solar thermal rather than from fossil fuel. The TAC of the network in Figure 4.4 is 569,160 $/y.

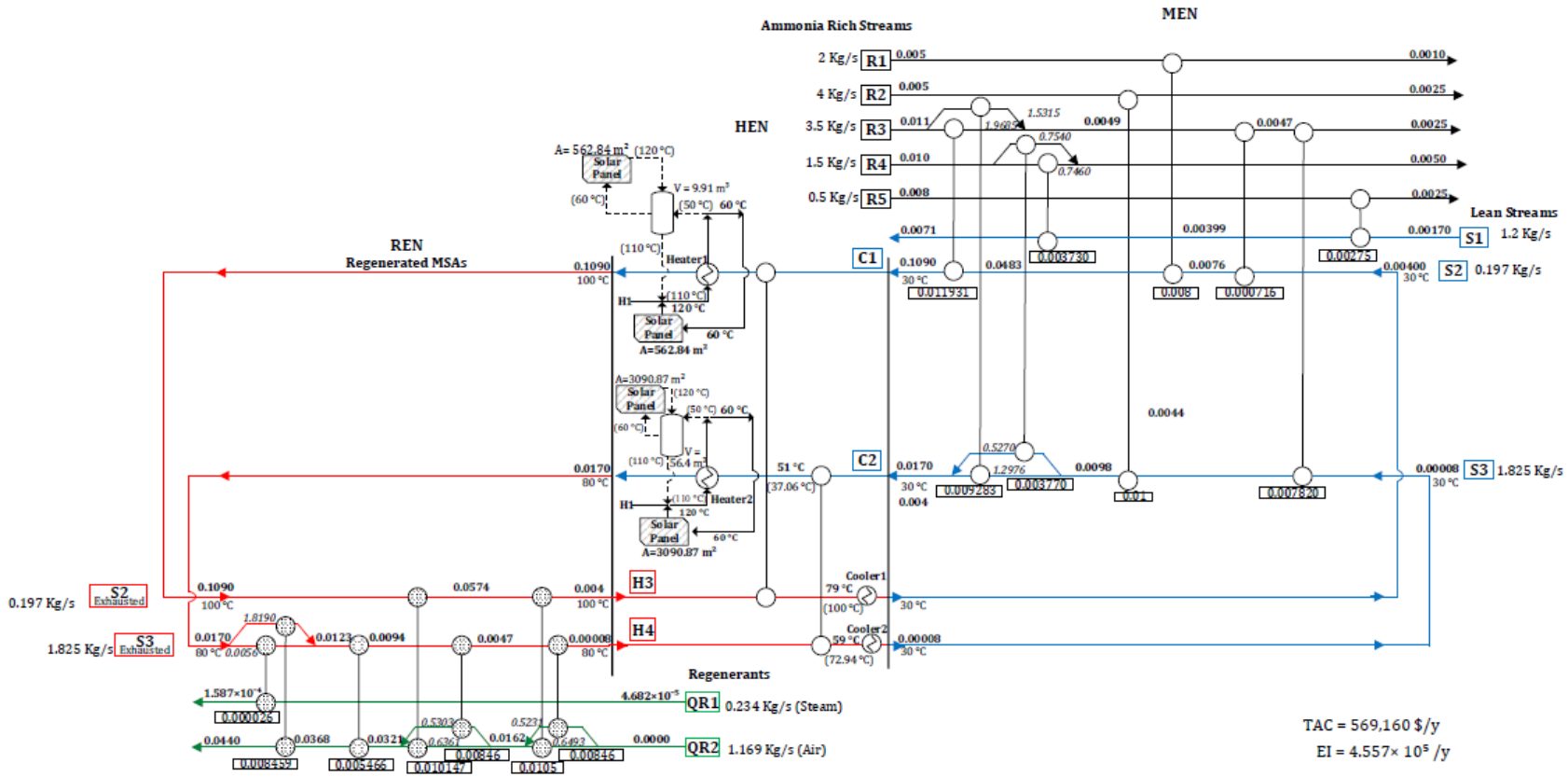

Figure 4.4: The multi-period CHAMENs configuration with solar panels and heat storage vessels.

In Figure 4.4, two solar panels are included in the HEN for cold stream C_1 and another two in the HEN for cold stream C_2. All the panels collect heat during the day (P =1). The panels connected to the solid lines in the figure supply thermal energy during the day directly to the cold streams, while the other panels connected to the dotted lines also collect solar thermal energy during the day but supply send the heat to the heat vessels for storage and subsequent usage at night time (P=2).

It can be observed in Figure 4.5, which is an expanded version of the solar network of Figure 4.4 for periods 1 and 2, that one of the heat exchangers is inactive during P=2, which is why the intermediate temperatures for C_1 differs in the two periods.

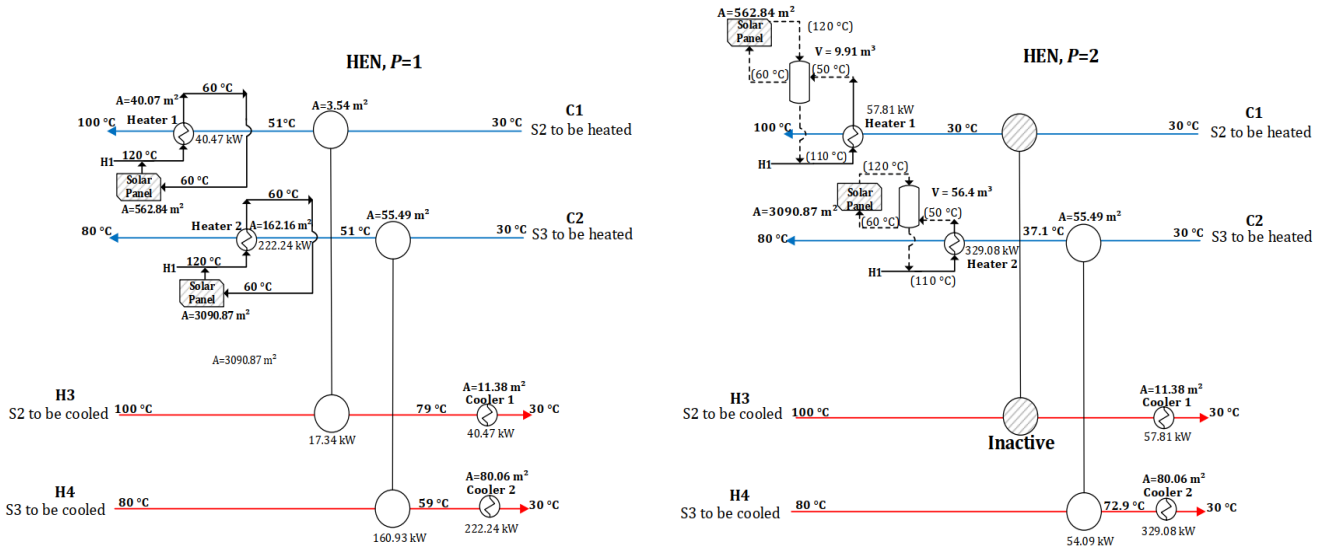

Figure 4.5: The HEN and solar network configurations of the CHAMEN for periods 1 and 2

Note that the total energy requirement in each period is conserved and summarised in Table 4.5.

Table 4.5: The total heat balance of HEN over the periods

	Streams	Period 1			Period 2		
		Q (kW)	Unit	Total (kW)	Q (kW)	Unit	Total (kW)
Q gain	C1	40.469	Heater1	**57.813**	57.813	Heater 1	**57.813**
		17.344	C_1-H_3		Inactive	C_1-H_3	
	C2	222.239	Heater 2	**383.170**	329.078	Heater 2	**383.170**
		160.931	C_2-H_4		54.092	C_2-H_4	
Q loss	H3	40.469	Cooler 1	**57.813**	57.813	Cooler 1	**57.813**
		27.735	C_1-H_3		Inactive	C_1-H_3	
	H4	222.239	Cooler 2	**383.170**	329.078	Cooler 2	**383.170**
		160.931	C_2-H_4		54.092	C_2-H_4	

As expected, the amount of heat gained by the cold streams equals the amount of heat given off by the hot streams. Also, the total amount of energy should be conserved in each period. The energy breakdown shown in Table 4.6 illustrates that the total energy is conserved and therefore, having an inactive exchanger in period 2 as shown in Figure 4.5 is justified. It is worth stating that the TAC of the CHAMEN without solar, i.e. Figure 4.4, is more economical compared to that of Figure 4.5, which includes solar panels. The breakdown of the annual capital cost (ACC) and the annual operating cost (AOC) of the two networks are shown in Figures 4.6 and 4.7.

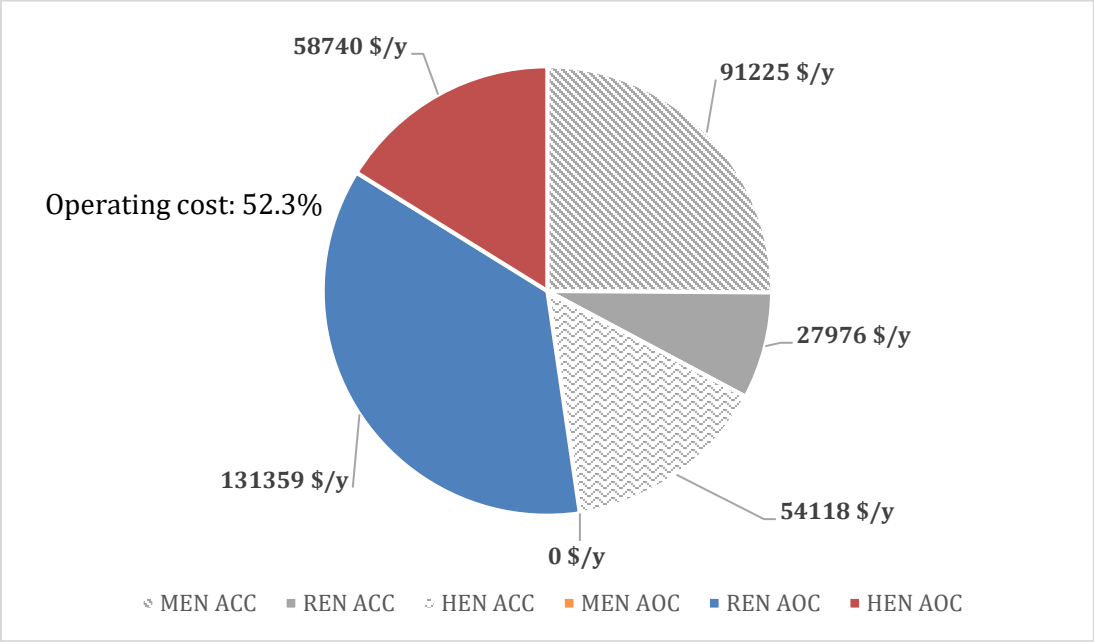

Figure 4.6:Detailed TAC for CHAMEN without solar panels for case study 1

In Figure 4.6, MEN AOC is zero since it was assumed that all the external MSAs are regenerated without any solvent loss. The combined AOC of HEN and REN constitutes 52.3 % of the TAC of the overall network.

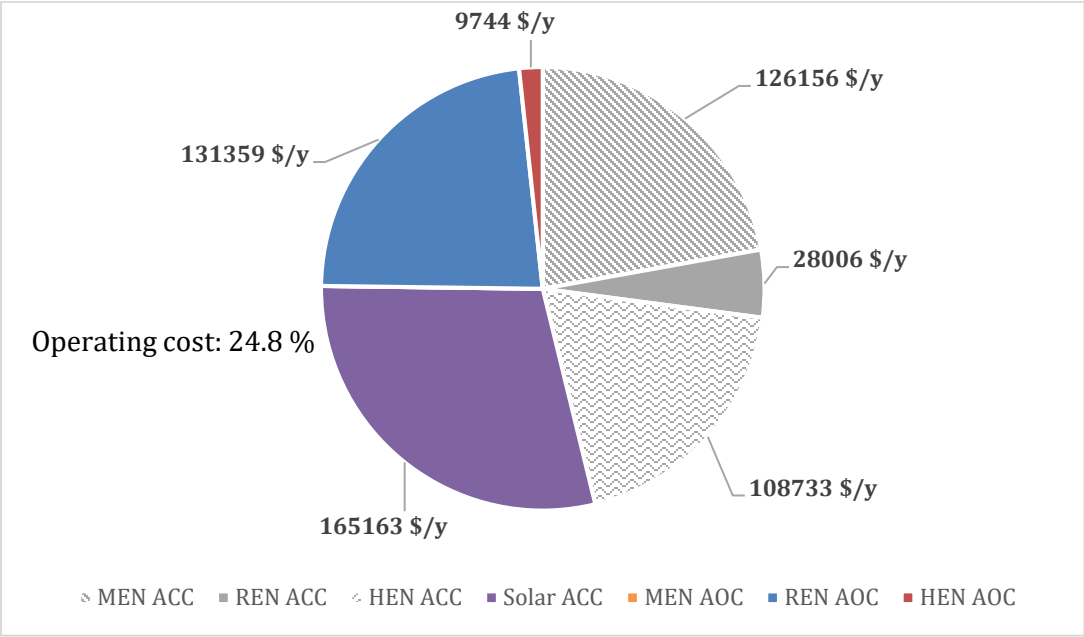

Figure 4.7: Detailed TAC for CHAMEN with solar panels for case study 1

The TAC of the CHAMEN involving solar panels and thermal storages are examined, and the details are presented in Figure 4.7. In this network, the ACC of the panels and thermal storage tank constitutes 24.8 % of the TAC of the overall network. Also, one of the significant differences between Figures 4.6 and 4.7 is the HEN AOC. The AOC of the utility generated from solar thermal is assumed to be zero. Therefore, it can be observed that this result in 83.4 % reduction in the HEN's AOC. However, the installation of solar panels resulted in bigger heat exchanger areas. The supply and the target temperature of H_1 (utility generated from solar thermal energy) was assumed to be fixed at 120 ℃ and 60 ℃ respectively while the supply and target temperature of H_2 (Steam generated from fossil-based source) is 135 ℃ and 134 ℃. The different supply and target temperatures will result in different *LMTD* values. Since the heat exchanger area is inversely proportional to *LMTD,* implementing H_1 in the HEN will result in a decrease in *LMTD* values, and this in turn, increases the heat exchanger areas. The cost implication of this is the increase in the HEN ACC from 54,118 $/y in Figure 4.6 to 108,733 $/y in Figure 4.7. The capital cost of 165,163 $/y was obtained for the solar panels and heat storage vessels which is 29 per cent of the total TAC presented in Figure 4.7. Although the inclusion of solar panels and heat storage vessel in the overall

network resulted in higher TAC compared to the network without solar thermal infrastructures, however, the implementation of such renewable energy is perceived to exert less environmental impacts.

The environmental indicator values shown in Table 4.4 were used to evaluate the impact of heating and cooling utilities in the overall network. In generating H_1, the option 'heat, solar' was selected in SimaPro. In the case of H_2, the steam was assumed to be generated from heat obtained from coal. Therefore, the option 'heat, coal' was selected. In the case of C_3, it was assumed that electricity is first generated from coal and then the cooling water was obtained. The cooling utility C_3 involved the option 'Electricity by fuel, coal'. These indicator values are obtained for preliminary design, but to get more realistic indicator values, more detailed LCIA studies are suggested. The indicator values obtained in SimaPro were used to calculate the environmental impact of the networks using Equation 3.54 in which the indicator values are multiplied by the corresponding heat duty of the heat exchanger. The CHAMEN without solar panel infrastructures resulted in the environmental impact value of 1.887×10^6/y while the network integrated with solar thermal has an impact value of 4.557×10^5/y. Therefore, it is observed that the network integrated with solar thermal can reduce the environmental impact by 76 percent. Table 4.6 shows the mass exchanger sizes of Figure 4.4 for the MEN and REN.

Table 4.6: Mass exchanger sizes of solar thermal integrated CHAMEN

MEN			REN		
Match	**Diameter (m)**	**Height (m)**	**Match**	**Diameter (m)**	**Height (m)**
R_3-S_2	1.45	0.48	S_3-QR_1	0.08	0.19
R_3-S_3	1.28	0.48	S_3-QR_2	1.40	0.20
R_4-S_1	0.90	0.41	S_3-QR_2	1.40	0.16
R_4-S_3	0.90	0.41	S_2-QR_2	0.46	0.40
R_2-S_3	2.07	0.41	S_3-QR_2	1.60	0.31
R_1-S_2	1.50	1.00	S_2-QR_2	0.52	1.22
R_3-S_2	0.46	0.38	S_3-QR_2	1.59	1.87
R_3-S_2	1.94	0.38			
R_5-S_1	0.73	0.70			

Note that due to the small split flow rate of '0.0056 kg/s' going through match S_2-QR_1 in the REN, an unrealistic column diameter of 0.08 m was obtained.

It is worth stating that for the various optimization scenarios, including the MOO, investigated for this case study, it was challenging to obtain feasible solutions due to the large number of streams and variables to be considered simultaneously. This case study is about the largest, in terms of stream number, presented in the literature. Thus, the environmental impact was only calculated after obtaining feasible network configurations, whereas a simultaneous optimization would have been a more correct approach to adopt. Nevertheless, this case study has demonstrated a systematic procedure for obtaining feasible network configurations for solar thermal integrated CHAMENs involving environmental impact analysis. Case study 2 involves fewer streams, hence a simultaneous MOO was done. Also, the equilibrium constants in the case study are expressed in terms of function of temperature, therefore, the lean streams were divided into sub-streams to find optimal operating temperatures in the MEN and REN respectively.

4.2 H2S removal (Case Study 2)

The coke-oven gas (COG) sweetening process (El-Halwagi and Manousiouthakis, 1989) involving H_2S removal was adapted in this study. The original example, involving two rich streams and two lean streams, was solved by various authors including Fraser and Hallale, (2000), Szitkai et al. (2006), Isafiade and Fraser (2008), and Azeez et al. (2012). The rich streams consist of a coke-oven gas (R_1) and tail-gas from a Claus unit (R_2). The two lean streams used in the original example were aqueous ammonia (S_1), which is a process MSA, and chilled methanol (S_2). A schematic representation of the problem is presented in Figure 4.8.

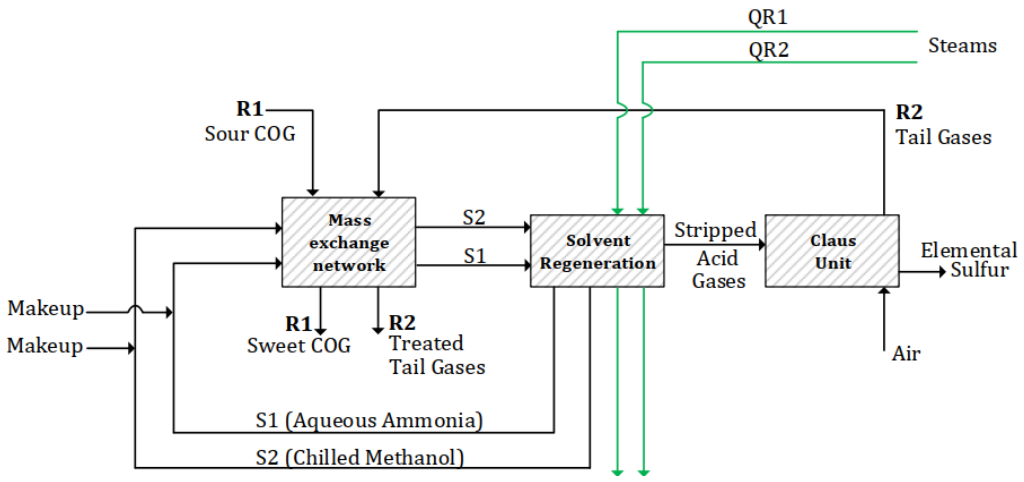

Figure 4.8: A schematic representation of Case study 2

Apart from the original lean streams used in the problem, an extra external MSA (S_3) which is 15 wt% MDEA (methyl diethanolamine) is introduced in the problem. Stream data of S_3 was obtained from Srinivas and El-Halwagi, (1994) where a similar problem involving H_2S was presented. The stream data of rich and lean streams are summarised in Table 4.7.

Table 4.7: The MEN stream data (compositions given in mass fractions; El-Halwagi and Manousiouthakis, 1989)

Rich streams	Flow Kg/s	y^s	y^t	Lean streams	Flow Kg/s	m	x^s	x^t
R_1	0.9	0.070	0.0003	**S_1**	2.3	1.45	0.0006	0.031
R_2	0.1	0.051	0.0001	**S_2**	∞	0.26	0.0002	0.0035
				S_3	∞	*	0.001	0.01

* S_3 equilibrium data is a function of temperature.

The equilibrium data for S_3 was obtained from Srinivas and El-Halwagi (1994) where the equilibrium data is a function of temperature, given as in Equation 4.1.

$$m = (9.386 \times 10^{-10}) \cdot 10^{(0.0215 \times T)} \quad (4.1)$$

As mentioned before, MENs and HENs interacts with each other through equilibrium relations where the relations are influenced by temperature. At lower temperature,

absorption is promoted while stripping is enhanced at a higher temperature (Seader et al., 1998). Data for the regeneration streams are presented in Table 4.8.

Table 4.8: The REN stream data (compositions given in mass fractions)

Regenerating Streams	***M***	$\mathbf{z^s}$	$\mathbf{z^t}$
QR_1 (Stripping steam 1)	0.0131	4.504×10^{-4}	1.522×10^{-3}
QR_2 (Stripping steam 2)	0.008	1.25×10^{-4}	0.011

The external MSAs are regenerated using two kinds of regenerating streams which are low-pressure steam (QR_1) and medium-pressure steam (QR_2). For the purpose of this thesis, the two regenerants are assumed to be generated and transported from a remote process nearby and used in the REN. The equilibrium constants of the regenerating streams are estimated by using Equation 2.37. The regeneration of S_3 can be achieved through a conventional steam stripping method while the regeneration of S_2 requires a lower-temperature of 100 °C or below. In the patent of Agata, (1998) stated that instead of using warm water which is generally employed approach used as a low-temperature heating source, implementing low-temperature steam can be more advantageous since the low-temperature steam has a large heat capacity per unit rate of flow rate and it is convenient to maintain the constant temperature unlike the warm water. At low pressure, low-temperature pressure can be obtained since the relationship between pressure and temperature of the steam is fixed and such data is widely available in many steam tables. In the case of amine strippers, heat and steam are utilised to reverse the chemical reactions between absorption medium and the pollutants such as CO_2 and H_2S. The steam's role in amine stripper is to remove volatile compounds from the liquid solution and to transport these pollutants to the overhead. In order to provide a proper mixing within the stripper, a tray column or packed columns are used (Arnold and Stewart, 1999).

The ReCiPe method indicator values associated with the lean streams and regenerating streams are presented in Table 4.9. These values are used to obtain the environmental

impact of a network. In the same way it has been done in case study 1, the ReCiPe method indicator values are used in Equation 3.55 to compare the results of the MEN and the MEN-REN.

Table 4.9: The environmental impact of lean and regenerating streams for Case Study 2

			ReCiPe method indicator values (1/kg)
MEN:	S_1	Aqueous ammonia	0.479
	S_2	Chilled methanol	0.204
	S_3	15 wt % MDEA	0.292
REN:	QR_1	Stripping steam 1	0.0741
	QR_2	Stripping steam 2	0.0723

4.2.1 Synthesis of MEN (The first step)

As it was done in the previous case study, the MEN was first synthesised independently in the first step. The data presented in Table 4.7 with the costing data presented in Appendix A3 were used to generate separate MEN. The capital cost of mass exchangers in MEN involves the sieve tray absorption columns. The costing data was presented by Papalexandri et al. (1994) and the annualised capital cost of 4552 $/year per equilibrium stage was used in Equation 2.13 presented in Chapter 2 to determine the number of equilibrium stages.

The MEN configuration presented in Figure 4.9 was obtained at the *EMAC* value of 4.22×10^{-8}(wt fraction), $\Omega_{p,\mathrm{MEN}}$ value of 0.01813. Lower bounds of 1.45 kg/s, 0.26 kg/s and 0.003 kg/s were used for S_1, S_2 and S_3 flowrates respectively. Upper bounds of 2.3 kg/s, 2.6 kg/s and 3.3 kg/s were used for S_1, S_2 and S_3 flowrates respectively.

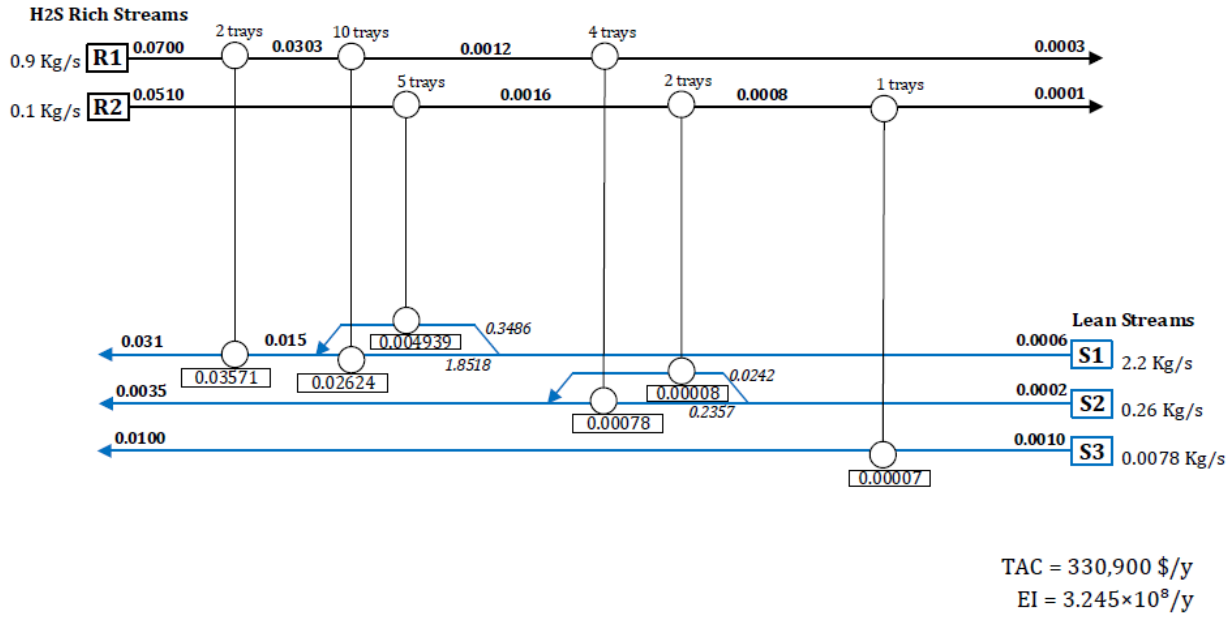

Figure 4.9: The MEN configuration of H_2S removal process (values above streams are composition in mass fractions; while values in boxes indicate mass load transferred in mass exchangers [kg/s])

In the MENS model, 5 superstructure stages were used to initialise the network. The optimised network consists of 6 mass exchangers. This MEN solution was then extended to include the REN model.

4.2.2 Simultaneous synthesis of MEN and REN (The second step)

The regeneration streams were initialised at lower bound flowrates of 0.013 kg/s and 8×10^{-5} kg/s for QR_1 and QR_2, while upper bound flowrates are set to 10.72 kg/s and 7.2 kg/s respectively. Note that the flow rates of lean streams through the MEN and REN, as well as the flow rates of regenerating streams, are variables in the optimisation problem. The combined model was solved as an MINLP, and the configuration presented in Figure 4.10 was obtained. As mentioned before, an exploratory run of the model was necessary to solve the problem. Note that two of the matches (R1-S1 and R2-S2) obtained in the MEN only case (Figure 4.9) do not appear in the combined MEN-REN solution. This is possible because the combined MEN-REN mode is solved as MINLP.

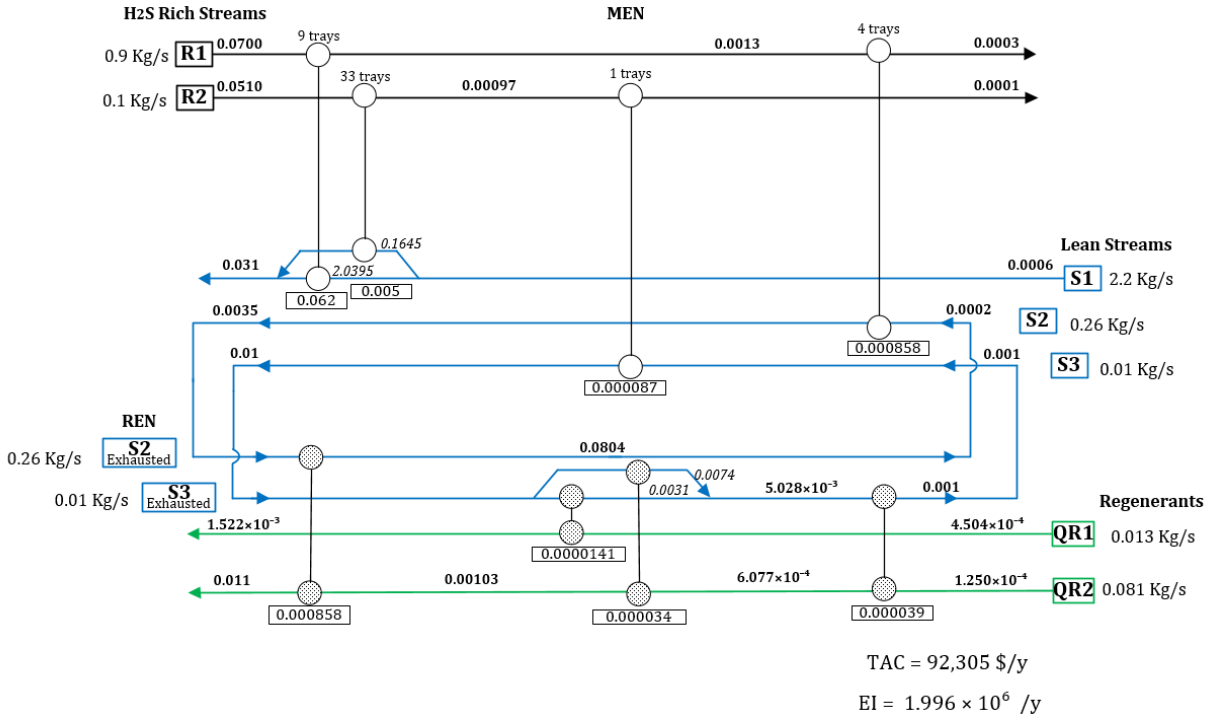

Figure 4.10 The MEN and REN configuration (values above streams are composition in mass fractions; while values in boxes indicate mass load transferred in mass exchangers [kg/s])

The network in Figure 4.10 has 4 mass exchangers in the MEN and 4 regeneration columns in the REN. Two-way stream splits were observed for S_1 in the MEN and S_3 in the REN. The environmental impact values presented in Figures 4.9 and Figure 4.10 were obtained by implementing the ReCiPe method indicator presented in Table 4.9 in Equation 3.55. As expected, the network with regeneration (Figure 4.10) exerts less impact on the environment (1.996×10^6/y) compared to that in Figure 4.9 (3.245×10^8/y) which does not include regeneration. This would be the case if the lean streams presented in the solution of Figure 4.9 are disposed off into the environment. To have a more accurate environmental impact, more detailed LCIA is required. The next step involves expanding the combined MEN-REN model to include HEN. Note that relevant data associated with the HEN is used to synthesise a separate HEN prior to step three. This individual network synthesis ensures that HEN data is rational and able to generate feasible solutions before being used in the combined network synthesis.

4.2.3 Simultaneous synthesis of MEN, REN and HEN (The third step)

The regeneration temperature of 100 °C was used for S_3 in the REN, and an absorption temperature of 30 °C was used as initial value to find preliminary feasible solutions. In the case of chilled methanol (S_2), the temperature of 68 °C was used to boil the methanol solvent for regeneration (Elvers, 2015) while –20 °C was used for absorption (ProSim, 2015). The equilibrium constant for regenerating streams were obtained using Equation 2.37 as presented in Appendix A2. Thermal data for the HEN is presented in Table 4.10.

Table 4.10: The HEN stream data for case study 2

Streams	T^s (°C)	T^t (°C)	F (kW°C^{-1})	h	Cp (Kj/kg K)	Costs $/(kWy)	ReCiPe values (1/kJ)
H_1	120	60	-	0.2	-	0	2.02×10^{-6}
H_2	135	134	-	0.2	-	60	1.36×10^{-4}
H_3	68	-20	*	0.2	2.6	-	
H_4	100	30	*	0.2	3.7	-	
C_1	-20	68	*	0.2	2.6	-	
C_2	30	100	*	0.2	3.7	-	
C_3	5	10	-	0.2	-	30	4.67×10^{-5}
C_4	-173	-173	-	0.2	-	121.05	0.0003

* The mass flowrate of H_3, H_4, C_1 and C_2 are converted to the corresponding thermal flowrates using the Cp values presented above

H_1 and H_2 are hot utilities generated from solar thermal and fossil, respectively. H_3 and H_4 are chilled methanol (S_2) and MDEA (S_3) respectively, which need to be cooled down to meet the suitable absorption temperature in MENs, while C_1 and C_2 are the same lean streams which need to be heated up to optimal regeneration temperature. There are two cold utilities used in this study, i.e. C_3 is cooling water, and C_4 is liquid nitrogen. The use of C_4 was necessary to cool S_2 streams to the desired temperature of -20 °C. The liquid nitrogen cost calculation can be found in Appendix A4. The combined model has 1497 single equations, 1295 single variables and 122 discrete variables. Since the number of streams is less than the streams involved in case study 1, it was less challenging to obtain a feasible solution.

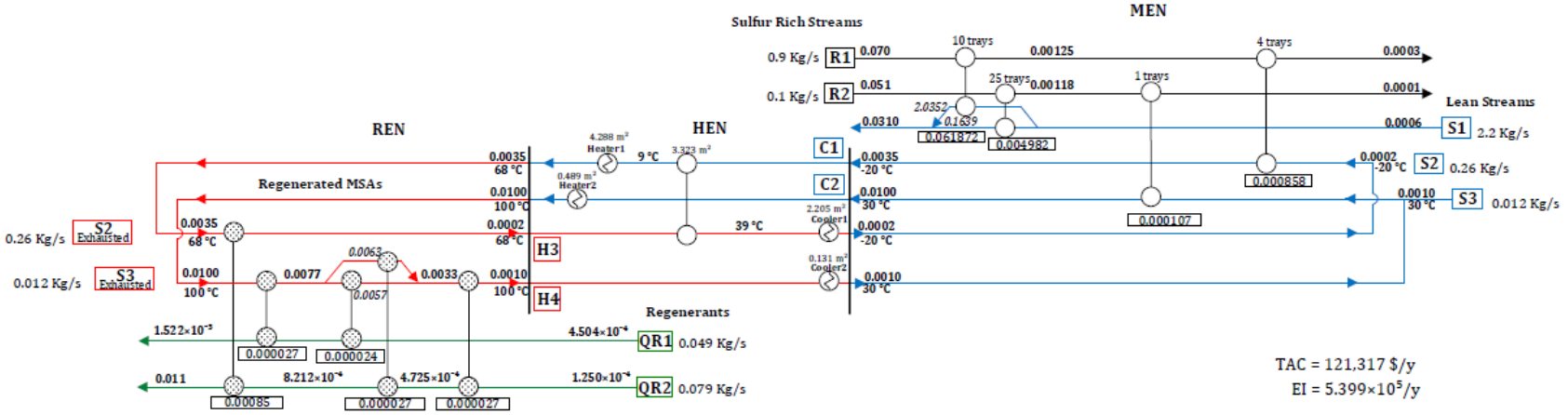

Figure 4.11: The CHAMENs configuration without solar panels for case study 2 (values above streams are composition in mass fractions; while values in boxes indicate mass load transferred in mass exchangers [kg/s])

Superstructure having 5, 3 and 4 stages were used to initialise MEN, REN and HEN respectively. The *EMAC* value of 4.424×10^{-8}, *REMAC* value of 7.7×10^{-8}, *EMAT* value of 10 °C, $\Omega_{p,\mathrm{MEN}}$ value of 0.01811 and $\Omega_{p,\mathrm{REN}}$ value of 8.144×10^{-4} were used to initialise the CHAMENs model.

The network configuration in Figure 4.11 involves 4, 5 and 5 exchangers in the MEN, HEN and REN. In the MEN, presented on the right side of the figure, the external lean streams (blue lines), S_2 and S_3 are fed into the MEN to remove H_2S in rich streams. The exhausted process lean stream, S_1 is sent to storage while the spent external lean streams are sent to the REN which is presented on the left side of the figure.

Before S_2 and S_3 enter the REN, they are heated up in the HEN which is situated in the center of the network configuration, to the desired stripping temperatures as specified in Table 4.10. The heated streams are represented as red lines in Figure 4.11. At a fossil hot utility price of 60 \$/(kW·y), all hot utility selected in the solution are fossil-based (i.e. H_2). The heated streams are then fed into the REN for regeneration. It was assumed that all exchangers operate isothermally and therefore, the stream temperatures remain constant through the networks unless the stream goes through a heat exchanger.

In the HEN, hot process streams H_3 and H_4, which are regenerated lean streams from the REN, are allowed to exchange heat with cold process streams C_1 and C_2 which are exhausted lean streams from MEN. In this case, through heat exchange between C_1-H_3, those stream temperatures were optimised and then the lean streams are further cooled down in the heaters/coolers to reach the operating temperature of REN and MEN respectively. The cooled S_2 and S_3 lean streams are then allowed to enter the MEN to complete the recycle procedure. As can be seen in the figure, the MEN and REN are connected through the lean streams S_2 and S_3, and the flowrates of these streams optimised in the model. The optimal flow rates for these two MSAs are found to be 0.26 kg/s and 0.012 kg/s, i.e. for S_2 and S_3 respectively. The process lean stream S_1 flowrate of 2.2 kg/s was obtained. For the regenerants QR_1 and QR_2, the optimal flowrates of 0.049 kg/s and 0.079 kg/s respectively were obtained. The resulting TAC of the combined network is 118,864 \$/yr.

The CHAMENs model was then extended to handle multi-period operation by introducing index '*p*' in the model equations to allow fluctuations in solar irradiations. The model was then tested at different fossil-fuel prices to find the maximum price at which the usage of fossil-fuel based utility becomes infeasible. At the fossil fuel price of 1,075 \$/(kW·y), the solver switched from using the fossil-based utility, H_2 to H_1, which is the solar thermal energy-based utility in both heaters in the HEN. The resulting combined network with solar panels showed a TAC of 145,021 \$/y. This network is further optimised by implementing optimised operating temperatures of MEN and REN. The optimisation procedure is discussed next.

4.2.4 Sub-stream temperature optimisation

To further optimise such combined networks, absorption and regeneration temperatures were varied to enhance mass transfer in MEN and REN further. The lean streams are divided into sub-streams with different temperatures. In this case study, the absorption temperature of S_3 was varied first. Once the optimal absorption temperature was identified in terms of the minimum TAC, then the S_3 stripping temperature was varied. Figures 4.12 – 4.15 show these variations and the associated TAC of the obtained networks at different temperatures.

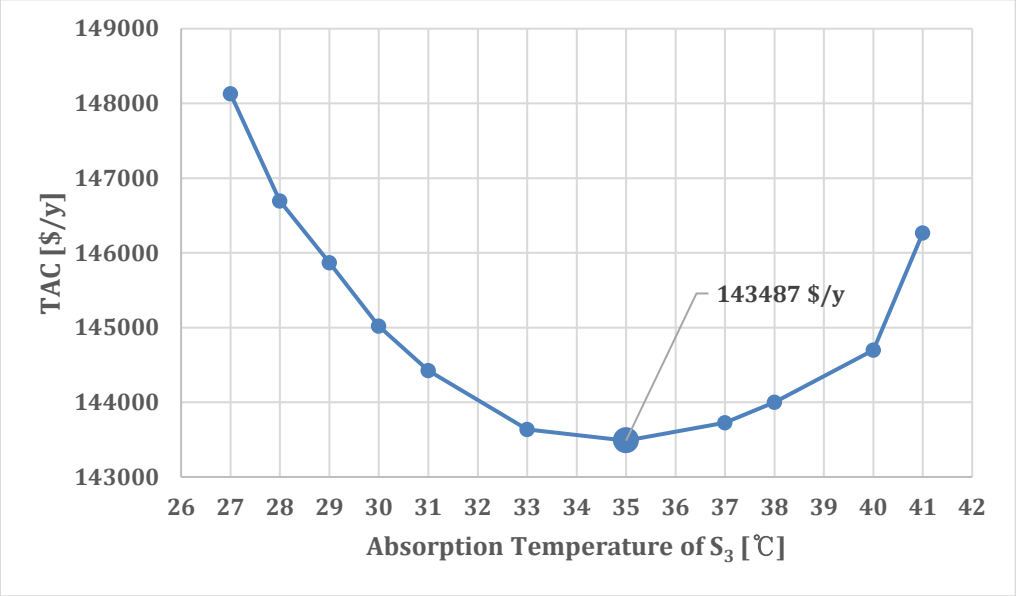

Figure 4.12: Variation of S_3 absorption temperature and the resulting TAC

As shown in Figure 4.12, the TAC of the networks decreases as the S_3 absorption temperature increases from 27 ℃ to 34 ℃. The TAC curve then goes through a minimum value of 143,487 $/y at the absorption temperature of 35 ℃. Further increase in the absorption temperature from 35 ℃ to 41 ℃ showed an increasing trend in the TAC. These results were obtained through investigating 11 sub-stream temperatures. Note that the mass transfer equilibrium is a function of temperature as presented in Equation 4.1. In each sub-stream temperature, a new equilibrium constant was calculated at each corresponding sub-stream temperature. These different equilibrium constants change the driving forces, and therefore, it affects the optimisation outcomes.

The next step of the investigation involved different stripping temperatures of S_3. In this study, 8 feasible solutions were obtained from 8 sub-streams. As compared to the previous investigation, the sets of feasible solutions are different in each investigation as it depends on the number of feasible solutions obtained over the tested temperature range which give local optima. The 8 sub-stream temperatures are plotted against the corresponding TACs in Figure 4.13.

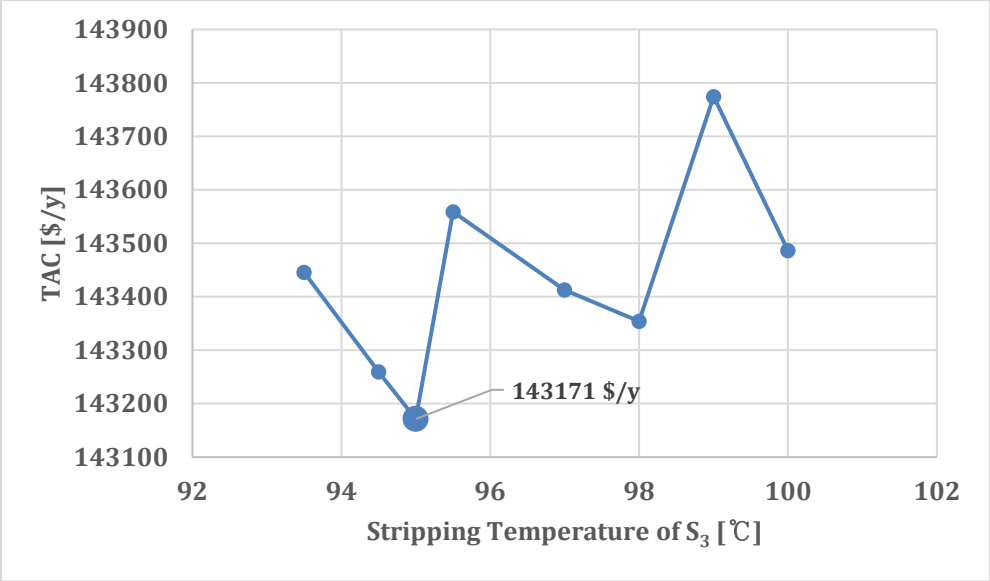

Figure 4.13: Variation of S_3 stripping temperature and the resulting TAC

The reduction in stripping temperature from 100 ℃ to 95 ℃ resulted in a slight decrease in TAC values from 143,487 $/y to 143,171 $/y. Further temperature reduction, however, increased the values of TACs. Note that S_3 flowrate is low compared to the other lean stream flowrates and therefore, change in S_3 stripping temperatures does not significantly affect the resulting TAC values. In general practice of steam stripping, the operating temperature is kept slightly below 100 ℃ to prevent corrosion (Addington and Ness, 2010). The same authors studied the effects of compositions on stripping temperature, and it showed that the increase in composition results in favouring higher stripping temperature. It was noted that the composition of effluents containing H_2S is low in this study and therefore, the benefit of

increasing the stripping temperature is not favourable. The study of Addington and Ness (2010) thus validates the result.

The optimal operating temperature of S_3 was found to be 35 °C for the absorption process and 95 °C for the regeneration process. These values were fixed in the following temperature investigation of S_2. The absorption temperature of S_2 was varied first while keeping the stripping temperature of S_2 and the S_3's operating temperatures as constants. Due to the sequential nature of this investigation, the current authors are aware that depending on the order of investigations, the results may differ. The S_2 absorption temperature variations are presented in Figure 4.14.

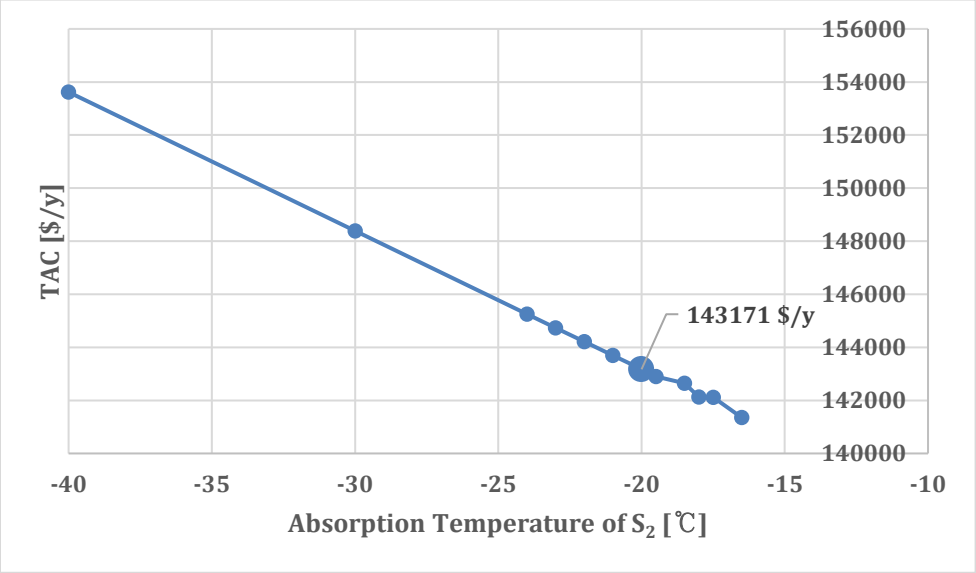

Figure 4.14: Variation of S2 absorption temperature and the resulting TAC

The overall trend depicted through 12 sets of sub-streams in Figure 4.14 shows an increasing trend of TAC as absorption temperatures decreases. This is due to more cooling requirements to achieve a low absorption temperature. Note that S_2 is the chilled methanol which is cooled below 0 °C for absorption. TAC values obtained in Figure 4.14 shows a decreasing trend as absorption temperature increases and the minimum point was not depicted within the tested temperature values. Therefore, literature absorption temperature

of -20 ℃ was selected for further investigation. The variations of the stripping temperature of S_2 is presented in Figure 4.15.

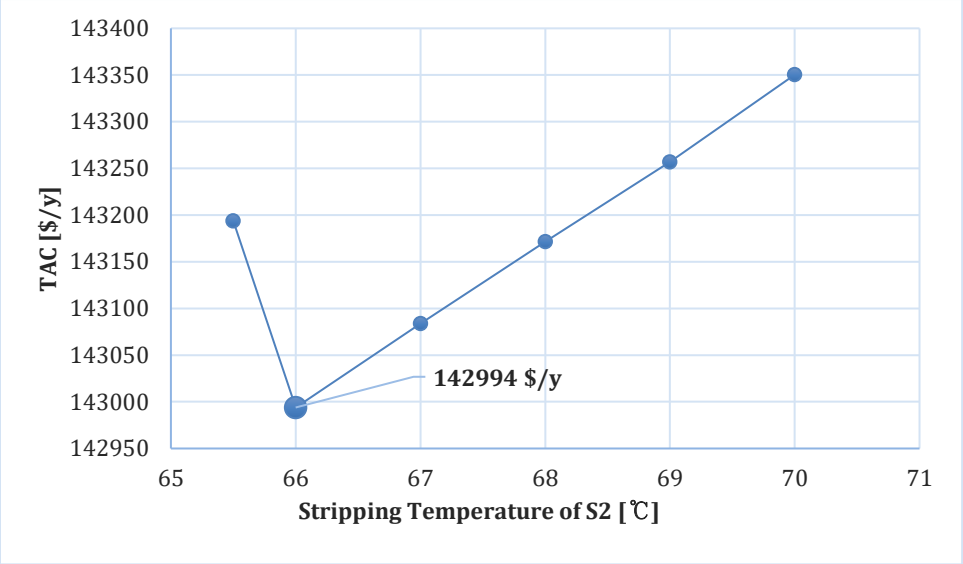

Figure 4.15: Variation of S_2 stripping temperature and the resulting TAC

The investigation showed that there is a rapid decrease in TAC values over the temperature ranges of 70 ℃ and 67 ℃. The minimum TAC of 142,994 $/y was obtained at the stripping temperature of 66 ℃. Thereafter, the further reduction in temperature causes the TAC curve to slightly increase in the TAC values. The stripping temperature of 66 ℃ is within the good operating temperature as the boiling point of the methanol is 64.7 ℃. With these optimised operating temperatures, the optimised CHAMENs configuration was obtained. Figure 4.16 presents an economically optimised CHAMENs.

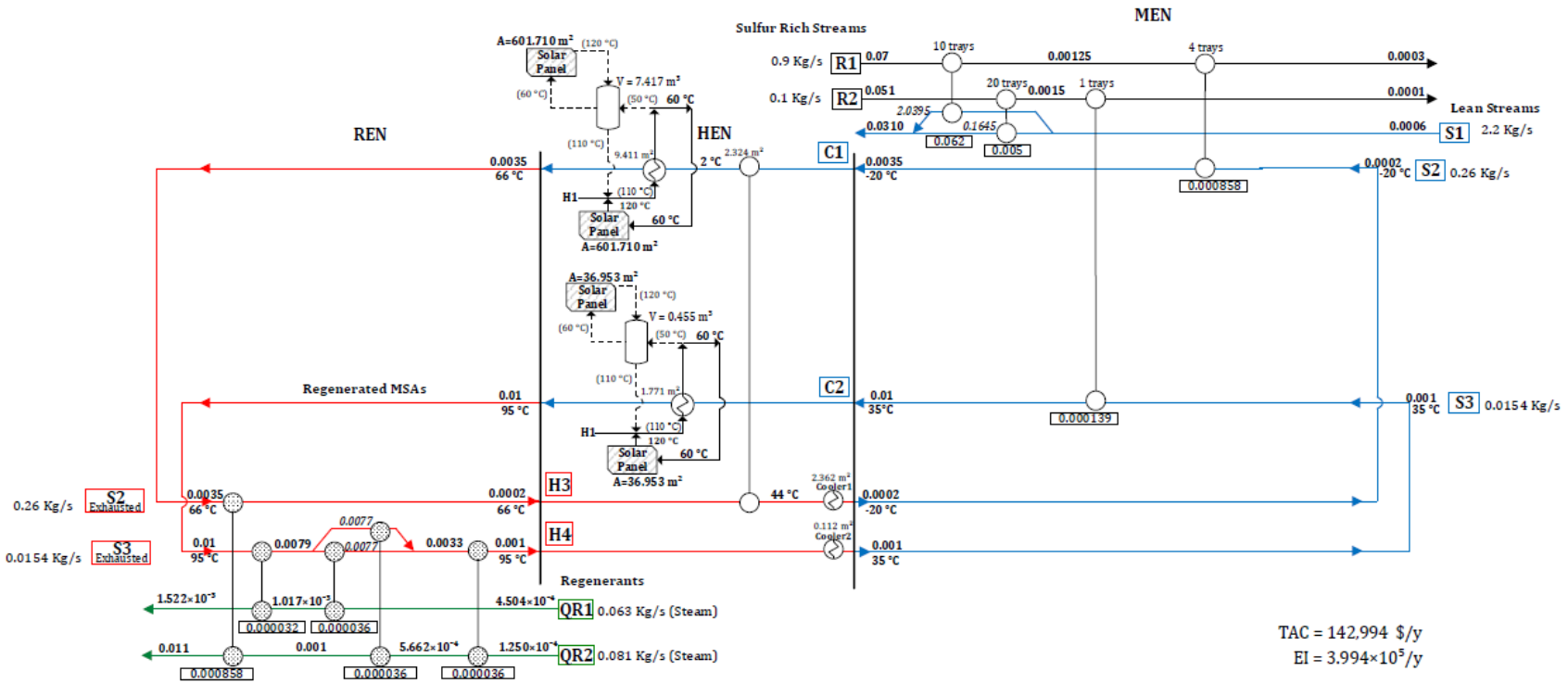

Figure 4.16: The economically optimised CHAMENs configuration (values above streams are composition in mass fractions; while values in boxes indicate mass load transferred in mass exchangers [kg/s])

The optimised network consists of 4, 5, and 5 exchangers in MEN, HEN and REN respectively. There is a two-way stream split involving S_1 in MEN with the split flow rates of 2.0395 kg/s and 0.1645 kg/s which sums up to the total flow rate of S_1. The exhausted S_3 in REN also involves a two-way stream split. As previously stated, the implementation of solar panels and heat storage vessels require the inclusion of the index '*p*' which discretises time into two different periods of daytime and nighttime.

The stream temperature during nighttime is presented with the bracket as shown in the HEN section of the combined networks. The optimised CHAMENs resulted in the TAC of 142,994 $/y. The details of the TAC of the combined networks is presented in Figure 4.17.

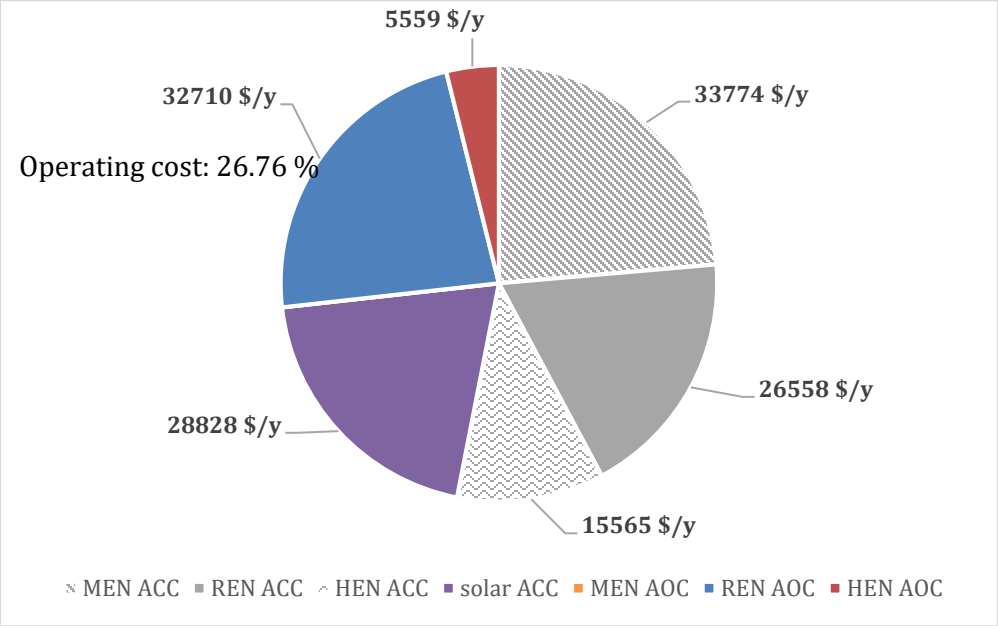

Figure 4.17: The CHAMENs with solar panels detailed TAC

As presented in the pie chart in Figure 4.17, the REN and HEN operating costs are presented in the blue and red sector of the chart respectively. The operating costs contribute 26.8 per cent of the total. The purple sector represents the capital cost involved in the solar panels and heat storages which accounts for 20.2 percent of the TAC. The combined networks without solar panels shown in Figure 4.11 is studied further, and the details of the TAC is presented in Figure 4.18.

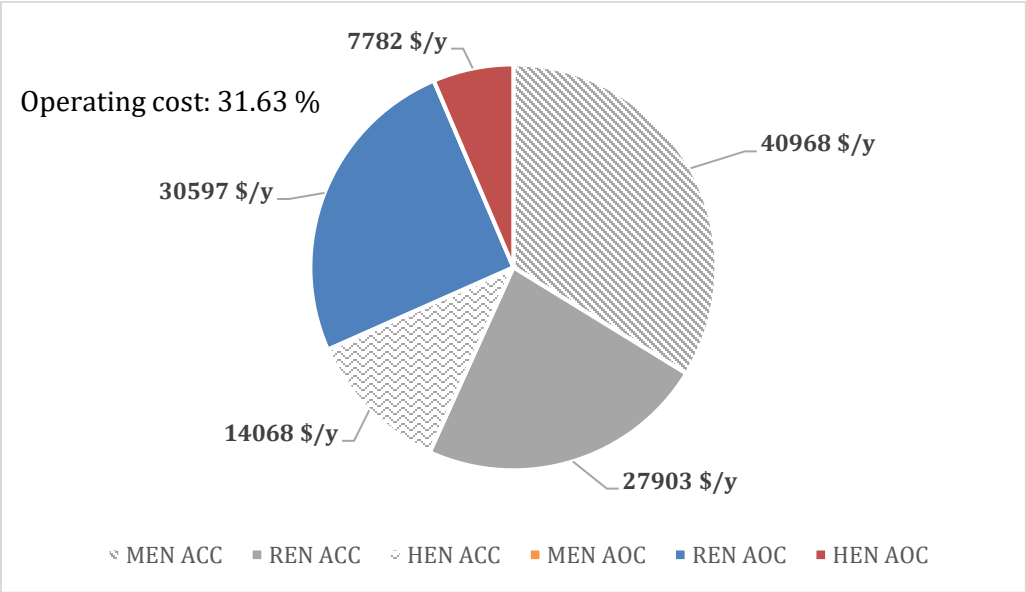

Figure 4.18: The CHAMENs without solar panels detailed TAC

In this case, the operating costs of the REN and HEN are 31.63 percent of the TAC. It can be observed that the resulting TAC of the network without solar panel (Figure 4.11) is 15 percent lower than the network with solar panels (Figure 4.16). However, implementation of solar panels and thermal storages can reduce the environmental impact by 26 percent. Further, temperature optimisation performed on the network (Figure 4.16) can result in HEN capital costs as well. However, the MEN capital cost is higher in the combined network with solar panels. This may have resulted from the trade-offs between the competing variables and the temperature effects on the equilibrium relation which affects the sizing of the mass exchangers.

Note that during the temperature variation presented in Figures 4.12-4.15, the combined networks were optimised in terms of the TAC only. To optimise a network simultaneously in terms of both the TAC and the environmental impact, the environmental objective function presented in Equation 3. 56 is used with the economic objective function in the model formulation.

4.2.5 The synthesis of the combined model with MOO

Due to the challenges in obtaining a feasible solution in a synthesis model involving MOO with the previously used data in this study, the stream data of S_3 is replaced with the N-methyl-2-pyrrolidone (NMP) data obtained from Srinivas and El-Halwagi (1994). Table 4.11 presents the stream data. The concentrations are given in mass fractions.

Table 4.11: NMP lean stream data (compositions given in mass fractions; Srinivas and El-Halwagi, 1994)

New lean stream data	m	z^s	z^t
S_3 (NMP)	*	1×10^{-5}	1×10^{-4}

Srinivas and El-Halwagi (1994) also presented the equilibrium relation of the NMP solvent as follows:

$$m(T) = 1.1907 \cdot T - 332.0 \tag{4.2}$$

The absorption temperature of NMP was assumed to be 10 °C. The regeneration of the NMP solvent can involve either steam stripping or inert gas (N_2). The REN data is presented in Table 4.12. The equilibrium constants of QR_v was obtained by using Equation 2.37. The other costing data follows the same as the case study 2 costing data.

Table 4.12: The regenerating stream data (compositions given in mass fractions)

New lean stream data	m	z^s	z^t
QR_1	0.0294	0.00201	0.00068
QR_2	0.0022	0.00045	0.0420

The model was initialised at the *EMAC* value of 4.15×10^{-13} (wt fraction), the *REMAC* value of 7.7×10^{-8} (wt fraction), the *EMAT* value of 5.1 °C. As mentioned before, some exploratory runs were necessary to get a feasible solution. The $\Omega_{p,\mathrm{MEN}}$ value of 0.01811 was used this time and the $\Omega_{p,\mathrm{REN}}$ value of 0.008144. To obtain different network configurations with

different TAC and environmental impact, the multi-objective function presented in Equation 3.56 is used (Gxavu and Smaill, 2012).

The TAC_{min} in Equation 3.56 is obtained by optimising the combined networks in terms of the *TAC* only. This was achieved by setting R_g, the weighting parameter to 1. In this way, the second term in the multi-objective function becomes zero. In the same way, the EI_{min} in Equation 41 was obtained by using the weighting parameter value of 0. The network obtained at these extremes is presented in Figure 4.19.

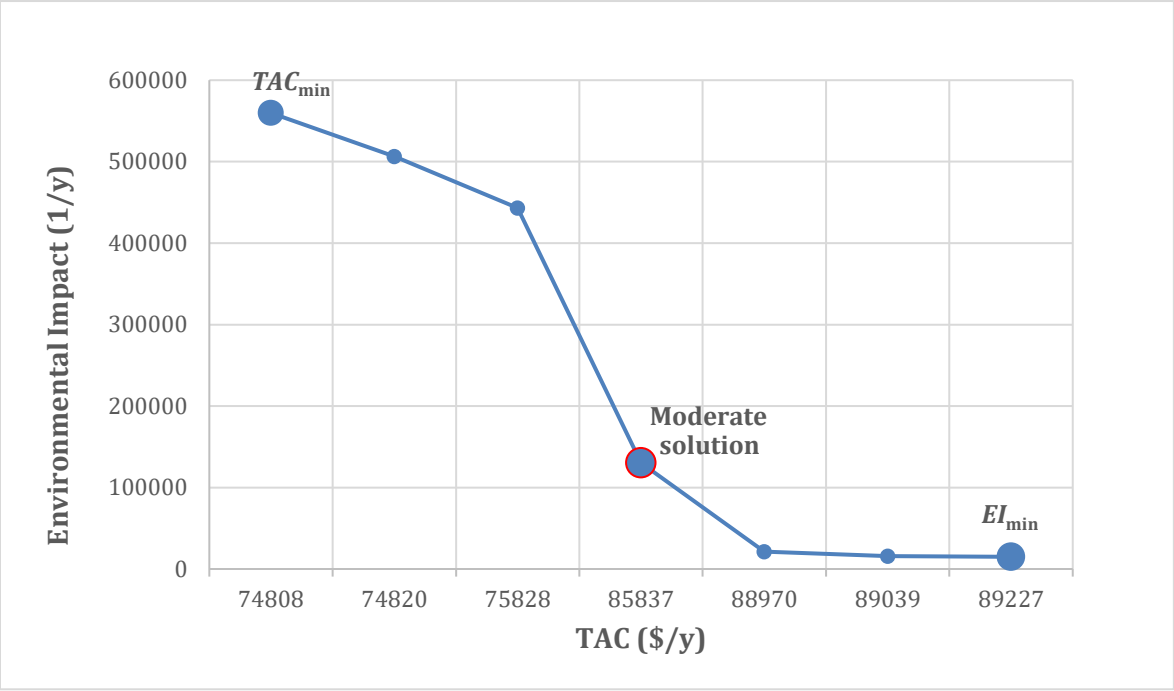

Figure 4.19: The Pareto optimal of the combined networks with NMP as S_3 solvent

Each data point in Figure 4.19 represents the different network configurations. The network representing TAC_{min} is shown at the left top corner of the pareto optimal curve while the network of EI_{min} is presented with the right bottom corner of the curve. It can be observed that the network with the minimum TAC use utilities generated from the fossil-based energy source at 60 \$/(kW·y). The implementation of solar panels is, in general, more expensive. However, the trade-off is that the implementation of such renewable infrastructures can reduce the environmental impact significantly, which results with network of EI_{min}.

The network with the minimum environmental impact resulted in the highest TAC value as this combined network involves solar panels and heat storages in each heater which raises the TAC. This agrees with the trend observed previously. In a practical process design context, it is desirable to synthesise a network with a moderate level of environmental impact which results in a reasonable level of TAC. The data points presented between the extremes are obtained by varying the weighting term in Equation 3.56.

In general, obtaining a feasible solution was not a trivial task, and therefore, few points are presented in Figure 4.19. The solution highlighted with the bigger point head was selected as the optimal combined networks of HEN, MEN and REN which resulted in moderate levels of both TAC and EI. The optimised network configuration is presented in Figure 4.20.

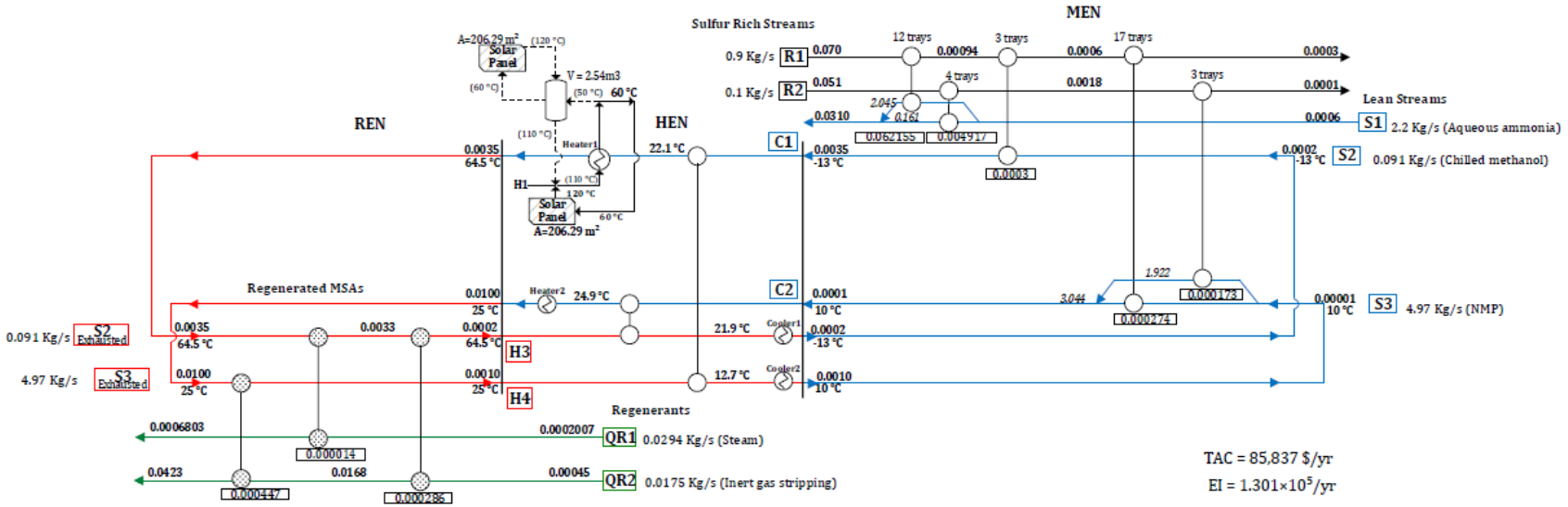

Figure 4.20: The combined networks with a moderate level of both TAC and EI (values above streams are composition in mass fractions; while values in boxes indicate mass load transferred in mass exchangers [kg/s])

Note that to obtain a moderate level of environmental impact, one of the heaters was matched with the utility generated from the solar thermal energy. The resulting configuration consists of 5, 6, and 3 exchangers in MEN, HEN and REN respectively. Note that heater 1 consists of the solar panels and heat storage vessels to heat the cold stream C_1 while the heater 2 uses the steam generated from fossil-based energy. More accurate equilibrium relations of regenerating streams could also be used to make the REN more realistic. The resulted TAC of 85,837 \$/y with the environmental impact of 1.301×10^5/y was obtained. A sample code for this MOO example is presented in Appendix B. The breakdown of the obtained TAC is presented in Figure 4.21.

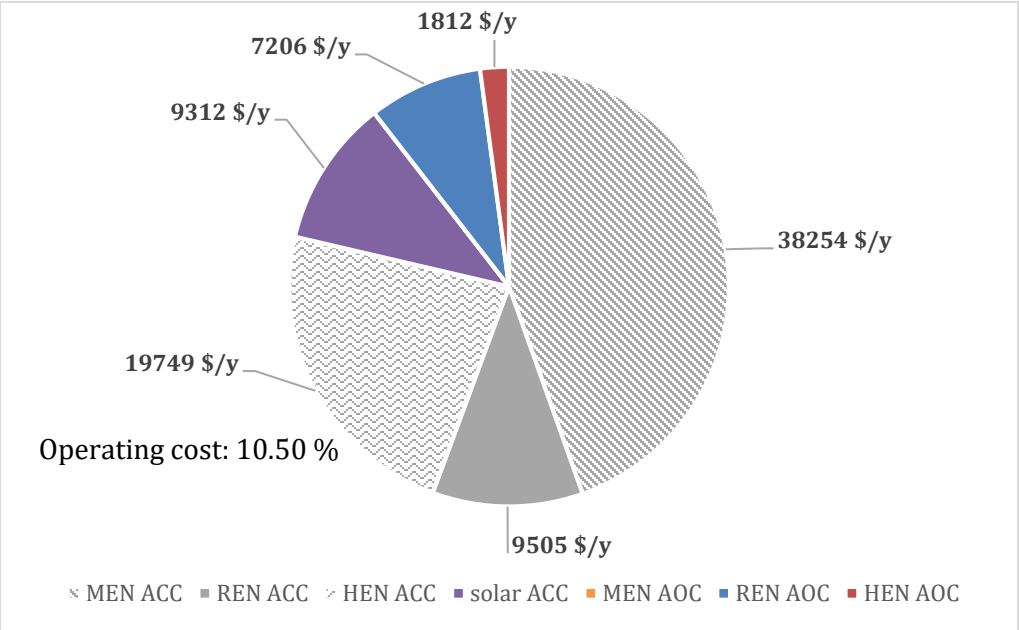

Figure 4.21: The CHAMENs with NMP detailed TAC

Compared to the previous problem data, NMP has a smaller operating cost than MDEA solvent. Also, the inert gas operating cost is much lower than the stripping steam used in the previous section. The biggest contribution to the significant difference in TACs of the configuration presented in Figure 4.16 and Figure 4.20 is the cost of solar panels and heat storage vessel capital costs. In the previous section, the resulting network configuration in Figure 4.16 involves solar panels and heat storage vessels in both heaters while only the heater 1 presented in Figure 4.20 involves solar panel infrastructures. It was also noticed that the match between H_1 and C_2 in Figure 4.16 has a small value of *LMTD*. This resulted in a big heat exchange area and caused high HEN and solar capital costs in the previous case. Since different S_3 data is used in MOO model, the results in this section cannot be compared directly to the previous results. However, the resulting configuration in Figure 4.20 demonstrated that it was possible to extend the combined CHAMENs model to include MOO.

CHAPTER 5

CONCLUSION AND FUTURE WORK

Chapter 5 Conclusions and Future works

This thesis has presented a synthesis method for CHAMENs. The traditional MEN and HEN synthesis methods were extended with a newly developed REN method to handle a CHAMENs problem involving multiple regenerable MSAs and multiple regenerating streams. Furthermore, solar thermal energy is integrated with the combined model to offset the environmental impact associated with the use of fossil-based energy sources. The "breadth first, depth later" approach is a key aspect of the overall design philosophy in this research field (El-Halwagi, 2017) and therefore, the model can be used to gain preliminary insights into the benefit of combining the synthesis of heat exchange networks with primary mass exchange and regeneration networks. The combined model was further extended to perform MOO of both economic and the environmental impact and the case study demonstrated its ability to minimise both factors simultaneously. However, it was noted that obtaining a feasible solution in the model was challenging especially when solving a problem involving many streams.

The proposed combined model uses the sub-stream approach of Srinivas and El-Halwagi (1994) which examines each sub-stream in a sequential manner. The same authors mentioned that a synthesis method of combining HEN and MEN should aim to search over all possible mass exchange temperatures and optimise network designs without preselecting the temperatures to study the economic trade-off between the networks. Therefore, in future work, the optimisation of the operating temperature of MEN and REN should be achieved without any preselecting the temperature in a sequential way. Furthermore, the regeneration stream data is very scarce, and it was challenging to find reasonable data. In order to obtain more practical REN configuration, it is suggested that more realistic regeneration data be implemented in a REN synthesis procedure.

It should be mentioned that the method presented in this thesis covered relatively simple cases which involve linear equilibrium relations, a single component problem and simple LCIA. The developed model can be extended to handle non-linear equilibrium relations and multi-components cases as well as handle different types of renewable energy sources such

as biomass, wind, geothermal etc. Recently, Short et al., (2018, 2016) published several papers to update the exchanger configurations obtained from GAMS to include individual exchanger design heuristics which makes the individual exchanger in the network more realistic and practical. This will also be considered in future studies.

REFERENCES

Aaltola, J., 2002. Simultaneous synthesis of flexible heat exchanger network. Appl. Therm. Eng. 22, 907–918.

Addington, L., Ness, C., 2010. An Evaluation of General "Rules of Thumb" in Amine Sweetening Unit Design and Operation. Bryan Res. Eng.

Agata, A., 1998. Low-temperature steam generator. Google Patents.

Ahmad, M.I., Zhang, N., Jobson, M., Chen, L., 2012. Multi-period design of heat exchanger networks. Chem. Eng. Res. Des. 90, 1883–1895.

Amararene, F., Bouallou, C., 2016. Study of Hydrogen Sulfide Absorption with Diethanolamine in Methanolic Aqueous Solutions. Chem. Eng. Trans. 52, 259–264.

Arnold, K., Stewart, M., 1999. Surface Production Operations, Volume 2:: Design of Gas-Handling Systems and Facilities. Elsevier.

Azeez, O., Isafiade, A.J., Fraser, D., 2013. Supply-based superstructure synthesis of heat and mass exchange networks. Comput. Chem. Eng. 56, 184–201.

Azeez, O.S., Isafiade, A., Fraser, D., 2012. Supply and target based superstructure synthesis of heat and mass exchanger networks. Chem. Eng. Res. Des. 90, 266–287.

Backhurst, J., Harker, J., 1973. Process Plant Design. Hieneman Educ. of Books, london.

Björk, K.-M., Westerlund, T., 2002. Global optimization of heat exchanger network synthesis problems with and without the isothermal mixing assumption. Comput. Chem. Eng. 26, 1581–1593.

Bogataj, M., Kravanja, Z., 2012. An alternative strategy for global optimization of heat exchanger networks. Appl. Therm. Eng. 43, 75–90.

Cerda, J., Westerburg, A.W., 1983. Synthesizing heat exchanger networks having restricted stream/stream matches using transportation problem formulations. Chem. Eng. Sci. 38, 1723–1740.

Charnes, A., Cooper, W.W., 1957. Management models and industrial applications of linear programming. Manag. Sci. 4, 38–91.

Chen, C.-L., Hung, P.-S., 2007. Synthesis of flexible heat exchange networks and mass exchange networks. Comput. Chem. Eng. 31, 1619–1632.

Chen, C.-L., Hung, P.-S., 2005. Simultaneous synthesis of mass exchange networks for waste minimization. Comput. Chem. Eng. 29, 1561–1576.

Chen, J., 1987. Comments on improvements on a replacement for the logarithmic mean. Chem. Eng. Sci. 42, 2488–2489.

Comeaux, R., 2000. Synthesis of MENs with minimum total cost. Manch. UMIST MPhil.

Coulson, J.M., Richardson, J.F., Sinnott, R.K., 1993. Chemical Engineering: Chemical Engineering Design. Pergamon.

Cragoe, C.S., Meyers, C.H., Taylor, C.S., 1920. THE VAPOR PRESSURE OF AMMONIA. J. Am. Chem. Soc. 42, 206–229.

Douglas, J.M., 1988. Conceptual design of chemical processes. McGraw-Hill New York.

Dyer, A., 2000. Ion exchange. Academic Press: New York.

Edgar, T., Huang, Y., 1993. Simultaneous Recovery of Waste Chemicals and Energy in an Oil Refinery, ACS Special Symposium on Emerging Technologies for Hazardous Waste Management, Book of Extended Abstracts, Ed. DW Tedder. Atlanta Sept 27–29.

El-Halwagi, M., El-Halwagi, A., Manousiouthakis, V., 1992. Optimal design of dephenolization networks for petroleum-refinery wastes. Process Saf. Environ. Prot. 70, 131–139.
El-Halwagi, M., Hamad, A., Garrison, G., 1996. Synthesis of waste interception and allocation networks. AIChE J. 42, 3087–3101.
El-Halwagi, M.M., 2017. Sustainable design through process integration: fundamentals and applications to industrial pollution prevention, resource conservation, and profitability enhancement. Butterworth-Heinemann.
El-Halwagi, M.M., 1998. Pollution prevention through process integration. Clean Prod. Process. 1, 5–19.
El-Halwagi, M.M., Foo, D.C., 2014. Process synthesis and integration. Kirk-Othmer Encycl. Chem. Technol.
El-Halwagi, M.M., Manousiouthakis, V., 1990. Simultaneous synthesis of mass-exchange and regeneration networks. AIChE J. 36, 1209–1219.
El-Halwagi, M.M., Manousiouthakis, V., 1989. Synthesis of mass exchange networks. AIChE J. 35, 1233–1244.
Elvers, B., 2015. Ullmann's Energy, 3 Volume Set: Resources, Processes, Products. John Wiley & Sons.
Emhamed, A.M., Lelkes, Z., Farkas, T., Fonyo, Z., Fraser, D.M., 2005. New hybrid method for mass exchange network optimisation, in: Computer Aided Chemical Engineering. Elsevier, pp. 877–882.
EPA, 2000. Waste water technology fact sheet: ammonia stripping. EPA.
EPA, U., 2006. Life cycle assessment: Principles and practice. Natl. Risk Manag. Res. Lab. Cincinnati OH USA.
Farkas, T., 2006. Chemical process synthesis using mixed integer nonlinear programming.
Fedkin, M., 2018. Life Cycle Assessment (LCA) methodology. College of Earth and Mineral Sciences, The Pennsylvan, Department of Mechanical and Nuclear Engineering.
Floudas, C., Ciric, A., 1989. Strategies for overcoming uncertainties in heat exchanger network synthesis. Comput. Chem. Eng. 13, 1133–1152.
Floudas, C.A., 1995. Nonlinear and mixed-integer optimization: fundamentals and applications. Oxford University Press.
Floudas, C.A., Grossmann, I.E., 1986. Synthesis of flexible heat exchanger networks for multiperiod operation. Comput. Chem. Eng. 10, 153–168.
Fraser, D.M., Hallale, N., 2000. Retrofit of mass exchange networks using pinch technology. AIChE J. 46, 2112–2117.
Furman, K.C., Sahinidis, N.V., 2002. A critical review and annotated bibliography for heat exchanger network synthesis in the 20th century. Ind. Eng. Chem. Res. 41, 2335–2370.
Garrard, A., Fraga, E.S., 1998. Mass exchange network synthesis using genetic algorithms. Comput. Chem. Eng. 22, 1837–1850.
Ghasemzadeh, N., Ghadiri, M., Behroozsarand, A., 2017. Optimization of chemical regeneration procedures of spent activated carbon. Adv. Environ. Technol. 3, 45–51.
Goedkoop, M., De Schryver, A., Oele, M., Durksz, S., de Roest, D., 2008. Introduction to LCA with SimaPro 7. PRé Consult. Neth.
Grossmann, I.E., 1996. Mixed-integer optimization techniques for algorithmic process synthesis, in: Advances in Chemical Engineering. Elsevier, pp. 171–246.

Guinée, J.B., 2002. Handbook on life cycle assessment operational guide to the ISO standards. Int. J. Life Cycle Assess. 7, 311–313.
Gupta, A., Manousiouthakis, V., 1994. Waste reduction through multicomponent mass exchange network synthesis. Comput. Chem. Eng. 18, S585–S590.
Gxavu, S., Smaill, P.A., 2012. Design of Heat Exchanger Networks to Minimise Cost and Environmentla Impact. (Thesis). University of Cape Town.
Haimes, Y., 1971. On a bicriterion formulation of the problems of integrated system identification and system optimization. IEEE Trans. Syst. Man Cybern. 1, 296–297.
Hallale, N., 1998. Capital cost targets for the optimum synthesis of mass exchange networks. University of Cape Town.
Hallale, N., Fraser, D., 2000a. Supertargeting for mass exchange networks: Part I: Targeting and design techniques. Chem. Eng. Res. Des. 78, 202–207.
Hallale, N., Fraser, D., 2000b. Supertargeting for Mass Exchange Networks: Part II: Applications. Chem. Eng. Res. Des. 78, 208–216.
Hallale, N., Fraser, D., 2000c. Capital and total cost targets for mass exchange networks: Part 1: Simple capital cost models. Comput. Chem. Eng. 23, 1661–1679.
Hallale, N., Fraser, D., 2000d. Capital and total cost targets for mass exchange networks: Part 2: Detailed capital cost models. Comput. Chem. Eng. 23, 1681–1699.
Hohmann, E.C., 1971. Optimum Networks for Heat Exchangers. University of Southern California, USA.
Howe, G., Mullins, M., Rogers, T., 1986. Evaluation and prediction of Henry's law constants and aqueous solubilities for solvents and hydrocarbon fuel components. Exp. Henry's Law Data Tech Rep NTIS 1.
Howe, K.J., Hand, D.W., Crittenden, J.C., Trussell, R.R., Tchobanoglous, G., 2012. Principles of water treatment. John Wiley & Sons.
Huijbregts, M., Steinmann, Z., Elshout, P., Stam, G., Verones, F., Vieira, M., Hollander, A., Zijp, M., Van Zelm, R., 2016. ReCiPe 2016: A harmonized life cycle impact assessment method at midpoint and endpoint level Report I: Characterization.
Institute for Environment and Sustainability, I.H., 2010. Framework and requirements for LCIA models and indicators. JRC Eur. Comm.
International Organization for Standardization, 2006a. Environmental Management: Life Cycle Assessment; Principles and Framework. ISO.
International Organization for Standardization, 2006b. Environmental Management: Life Cycle Assessments: Requirements and Guidelines. ISO.
IRENA, 2017. Renewable Power Generation Costs in 2017. International Renewable Energy Agency, Abu Dhabi.
Isafiade, A., Bogataj, M., Fraser, D., Kravanja, Z., 2015. Optimal synthesis of heat exchanger networks for multi-period operations involving single and multiple utilities. Chem. Eng. Sci. 127, 175–188.
Isafiade, A., Fraser, D., 2009. Interval based MINLP superstructure synthesis of combined heat and mass exchanger networks. Chem. Eng. Res. Des. 87, 1536–1542.
Isafiade, A., Fraser, D., 2008a. Interval-based MINLP superstructure synthesis of heat exchange networks. Chem. Eng. Res. Des. 86, 245–257.

Isafiade, A., Fraser, D., 2008b. Interval based MINLP superstructure synthesis of mass exchange networks. Chem. Eng. Res. Des. 86, 909–924.
Isafiade, A., Fraser, D., 2007. Optimization of combined heat and mass exchanger networks using pinch technology. Asia-Pac. J. Chem. Eng. 2, 554–565.
Isafiade, A.J., 2017a. Integration of Renewable Energy into Mass, Heat and Regeneration Network Synthesis. Chem. Eng. Trans. 61, 67–72.
Isafiade, A.J., 2017b. Integration of Renewable Energy into Mass, Heat and Regeneration Network Synthesis. Chem. Eng. Trans. 61, 67–72.
Isafiade, A.J., Fraser, D.M., 2010. Interval based MINLP superstructure synthesis of heat exchanger networks for multi-period operations. Chem. Eng. Res. Des. 88, 1329–1341.
Isafiade, A.J., Fraser, D.M., 2009. Interval Based MINLP Superstructure Synthesis of Multi-Period Mass Exchanger Networks. Chem. Prod. Process Model. 4.
Isafiade, A.J., Short, M., 2016. Synthesis of mass exchange networks for single and multiple periods of operations considering detailed cost functions and column performance. Process Saf. Environ. Prot. 103, 391–404.
Isafiade, A.J., Short, M., Bogataj, M., Kravanja, Z., 2017. Integrating renewables into multi-period heat exchanger network synthesis considering economics and environmental impact. Comput. Chem. Eng. 99, 51–65.
Jensen, A., Elkington, J., Christiansen, K., Hoffmann, L., Moller, B., Schmidt, A., van Dijk, F., 1997. Life cycle assessment: a guide to approaches, experiences and information sources. European Environment Agency, Copenhagen.
Kemp, I.C., 2011. Pinch analysis and process integration: a user guide on process integration for the efficient use of energy. Elsevier.
Kidnay, A.J., Parrish, W.R., McCartney, D.G., 2011. Fundamentals of natural gas processing. CRC press.
Kravanja, Z., Grossmann, I.E., 1997. Multilevel-hierarchical MINLP synthesis of process flowsheets. Comput. Chem. Eng. 21, S421–S426.
Linnhoff, B., Hindmarsh, E., 1983. The pinch design method for heat exchanger networks. Chem. Eng. Sci. 38, 745–763.
Liu, L., Du, J., Yang, F., 2015. Combined mass and heat exchange network synthesis based on stage-wise superstructure model. Chin. J. Chem. Eng. 23, 1502–1508.
Liu, L., El-Halwagi, M.M., Du, J., Ponce-Ortega, J.M., Yao, P., 2013. Systematic synthesis of mass exchange networks for multicomponent systems. Ind. Eng. Chem. Res. 52, 14219–14230.
López-Maldonado, L.A., Ponce-Ortega, J.M., Segovia-Hernández, J.G., 2011. Multiobjective synthesis of heat exchanger networks minimizing the total annual cost and the environmental impact. Appl. Therm. Eng. 31, 1099–1113.
Miettinen, K., Mäkelä, M., 1999. Comparative evaluation of some interactive reference point-based methods for multi-objective optimisation. J. Oper. Res. Soc. 50, 949–959.
Msiza, A.K., Fraser, D.M., 2003. Hybrid synthesis method for mass exchange networks, in: Computer Aided Chemical Engineering. Elsevier, pp. 227–232.
Müller, E., Berger, R., Blass, E., Sluyts, D., Pfennig, A., 2000. Liquid–liquid extraction. Ullmanns Encycl. Ind. Chem.

Na, J., Jung, J., Park, C., Han, C., 2015. Simultaneous synthesis of a heat exchanger network with multiple utilities using utility substages. Comput. Chem. Eng. 79, 70–79.
Nemet, A., Klemeš, J.J., Varbanov, P.S., Kravanja, Z., 2012. Methodology for maximising the use of renewables with variable availability. Energy 44, 29–37.
Obaid-ur-Rehman, S., Beg, S., 1990. Ammonia removal by air stripping—from origin to present state of technology. J. Environ. Sci. Health Part A 25, 343–365.
Papalexandri, K., Pistikopoulos, E., Floudas, A., 1994. Mass-exchange networks for waste minimization-a simultaneous approach. Chem. Eng. Res. Des. 72, 279–294.
Papoulias, S.A., Grossmann, I.E., 1983. A structural optimization approach in process synthesis—II: Heat recovery networks. Comput. Chem. Eng. 7, 707–721.
Perry, R.H., Green, D.W., Maloney, J.O., others, 1997. Perry's chemical engineers' handbook. McGraw-Hill, New York.
Pfahl, U., Ross, M., Shepherd, J., Pasamehmetoglu, K., Unal, C., 2000. Flammability limits, ignition energy, and flame speeds in H2–CH4–NH3–N2O–O2–N2 mixtures. Combust. Flame 123, 140–158.
Ponce-Ortega, J.M., Serna-González, M., Jiménez-Gutiérrez, A., 2010. Synthesis of heat exchanger networks with optimal placement of multiple utilities. Ind. Eng. Chem. Res. 49, 2849–2856.
ProSim, 2015. Syngas deacidification with rectisol process. ProSim, Laberge, France.
Rosenthal, R., 2007. GAMS–A User's Guide, GAMS Development Corporation, Washington, DC. World Wide Web Httpwww Gams ComdocsgamsGAMSUsersGuide Pdf.
Rudd, D.F., 1968. The synthesis of system designs: I. Elementary decomposition theory. AIChE J. 14, 343–349.
Rudd, D.F., Powers, G.J., Siirola, J.J., 1973. Process synthesis. Prentice-Hall.
Sander, R., 2015. Compilation of Henry's law constants (version 4.0) for water as solvent. Atmospheric Chem. Phys. 15.
Saracco, G., Genon, G., 1994. High temperature ammonia stripping and recovery from process liquid wastes. J. Hazard. Mater. 37, 191–206.
Scargiali, F., 2007. Gas-liquid dispersions in mechanically agitated contactors (PhD Thesis). Doctoral dissertation, PhD thesis, Universitá degli Studi di Palermo.
Seader, J.D., Henley, E.J., Roper, D.K., 1998. Separation process principles.
Shah, I.K., Pre, P., Alappat, B.J., 2013. Steam regeneration of adsorbents: an experimental and technical review. Chem Sci Trans 2, 1078–1088.
Shen, S., Wolsky, A.M., 1980. Energy and materials flows in the production of liquid and gaseous oxygen. Argonne National Lab., IL (USA).
Shenoy, U., Sinha, A., Bandyopadhyay, S., 1998. Multiple utilities targeting for heat exchanger networks. Chem. Eng. Res. Des. 76, 259–272.
Shenoy, U.V., Fraser, D.M., 2003. A new formulation of the Kremser equation for sizing mass exchangers.
Short, M., Isafiade, A.J., Biegler, L.T., Kravanja, Z., 2018. Synthesis of mass exchanger networks in a two-step hybrid optimization strategy. Chem. Eng. Sci. 178, 118–135.
Short, M., Isafiade, A.J., Fraser, D.M., Kravanja, Z., 2016. Two-step hybrid approach for the synthesis of multi-period heat exchanger networks with detailed exchanger design. Appl. Therm. Eng. 105, 807–827.

Sinnott, R., 1999. Coulson & Richardson's Chemical Enginering: Volume 6/Chemical Engineering Design. Elsevier Butterworth Heinemann.
Smith, R., 2005. Chemical process: design and integration. John Wiley & Sons.
Soršak, A., Kravanja, Z., 2002. Simultaneous MINLP synthesis of heat exchanger networks comprising different exchanger types. Comput. Chem. Eng. 26, 599–615.
Srinivas, B., El-Halwagi, M., 1994. Synthesis of combined heat and reactive mass-exchange networks. Chem. Eng. Sci. 49, 2059–2074.
Standards, N.I. of, Technology (NIST), 2018. Chemistry WebBook, SRD 69.
Szitkai, Z., 2004. Synthesis of mass exchange networks using mathematical programming.
Szitkai, Z., Farkas, T., Lelkes, Z., Fonyo, Z., Kravanja, Z., 2006. Fairly linear mixed integer nonlinear programming model for the synthesis of mass exchange networks. Ind. Eng. Chem. Res. 45, 236–244.
Toth, A., Mizsey, P., 2015. Comparison of air and steam stripping: removal of organic halogen compounds from process wastewaters. Int. J. Environ. Sci. Technol. 12, 1321–1330.
Townsend, D., Linnhoff, B., 1984. Surface area targets for heat exchanger networks, in: IChemE Annual Research Meeting. Bath UK.
Treybal, R.E., 1980. Mass transfer operations. N. Y. 466.
Ullmann, F., Gerhartz, W., Yamamoto, Y.S., Campbell, F.T., Pfefferkorn, R., Rounsaville, J.F., others, 1985. Ullmann's encyclopedia of industrial chemistry. VCH publishers.
Underwood, A., 1970. Simple formula to calculate mean temperature difference. CHEMICAL WEEK ASSOC 110 WILLIAM ST, 11TH FL, NEW YORK, NY 10038 USA.
Vaskan, P., Guillén-Gosálbez, G., Jiménez, L., 2012. Multi-objective design of heat-exchanger networks considering several life cycle impacts using a rigorous MILP-based dimensionality reduction technique. Appl. Energy 98, 149–161.
Velázquez-Guevara, M.Á., Uribe-Ramírez, A.R., Gómez-Castro, F.I., Ponce-Ortega, J.M., Hernández, S., Segovia-Hernández, J.G., Alfaro-Ayala, J.A., de Jesús Ramírez-Minguela, J., 2018. Synthesis of mass exchange networks: A novel mathematical programming approach. Comput. Chem. Eng. 115, 226–232.
Verheyen, W., Zhang, N., 2006. Design of flexible heat exchanger network for multi-period operation. Chem. Eng. Sci. 61, 7730–7753.
Warren, L., Warren, L., McCabe, W., Smith, J.C., 1976. Unit operations of chemical engineering. Mc Graw Hill Company.
Westerberg, A., 1987. Process synthesis: A morphological view, in: Recent Developments in Chemical Process and Plant Design. Wiley New York, pp. 127–145.
Yee, T.F., Grossmann, I.E., 1990. Simultaneous optimization models for heat integration—II. Heat exchanger network synthesis. Comput. Chem. Eng. 14, 1165–1184.
Zare Aliabad, H., Mirzaei, S., 2009. Removal of CO2 and H2S using aqueous alkanolamine solutions. World Acad. Sci. Eng. Technol. 49, 194–203.
Zhu, X., Oneill, B.K., Roach, J., Wood, R., 1995. A method for automated heat-exchanger network synthesis using block decomposition and nonlinear optimization. Chem. Eng. Res. Des. 73, 919–930.

Appendix A

A1: LEL to target composition conversion

The LEL of ammonia is 15%. When this is converted to ppm, the value of 150000 ppm is obtained. The ppm is further converted to mole fraction of 0.15. This mole fraction is converted to mass fraction:

$$0.15 \times \left(\frac{17.031 \frac{\text{g}}{\text{mol}}}{29 \frac{\text{g}}{\text{mol}}} \right) = 0.0881 \text{ (weight fraction)}$$

It was found that the outlet composition of air can be 50 percent of LEL. Therefore, the outlet composition of air stripper can be:

$$\text{Outlet stripping air composition} = \ 0.0881 \times 50\% = 0.044$$

A2: Henry's constants for case studies

Case Study 1

The air stripping of ammonia dissolved in the aqueous solvent is operated at 80°C. The relevant data used in Equation 2.37 is summarised in Table A2.1.

Table A2. 1: The data used in Henry's constant estimation (case study 1)

$\boldsymbol{P_{total}}$	202.6 kPa
$\boldsymbol{y_i^{\text{solubility}}}(\mathbf{80}°\text{C})$	0.1333 (wt %)
$\boldsymbol{P^0_{solute}}(\mathbf{80}°\text{C})$	4140.98 kPa (Cragoe et al., 1920)

The wt % solublity data of ammonia is converted to mole fraction of 0.123. Therefore, the Henry's constant for air stripping at 80°C is calculated as follows:

$$H(80\ ^{\circ}\text{C}) = \frac{(202.6\ \text{kPa}) \cdot (0.123)}{4140.98\ \text{kPa}} = 6.034 \times 10^{-3} \frac{\text{mol fraction of } NH_3 \text{ in water}}{\text{mol fraction of } NH_3 \text{ in air}} \times \left(\frac{29}{18}\right)$$

$$= 0.00972\ \frac{\text{weight fraction of } NH_3 \text{ in water}}{\text{weight fraction of } NH_3 \text{ in air}}$$

In the case of steam stripping, the steam is assumed to operate at the pressure of 202.6 kPa and the operating temperature of 100°C is used. Henry's constant of ammonia in water was obtained from Sander (2015). The unit of the Henry's constant is in $\frac{\text{mol}}{\text{kPa} \cdot \text{m}^3 \text{ water}}$. El-Halwagi (2017) presented a sample calculation to define the Henry's constant in terms of weight fraction:

$$H(100\ ^{\circ}\text{C}) = 34.682\ \frac{\text{mol}}{\text{kPa} \cdot \text{m}^3 \text{ water}} \times (202.6\ \text{kPa}) \times \left(\frac{\text{m}^3 \text{ water}}{10^6}\right) \times \left(\frac{18\ \text{g water}}{\text{mol of water}}\right)$$

$$= 0.1265 \frac{\text{weight fraction of } NH_3 \text{ in water}}{\text{weight fraction of } NH_3 \text{ in air}}$$

Case study 2

The case study 2 involves stripping of H_2S in methanol. The operating temperature of 68 °C was assumed as the methanol is stripped at the temperature close to its boiling point. In the work of Howe et al. (2012), the authors presented a set of equations to convert units of the Henry's constants as follows:

$$H_{Dimensionless} = \frac{H_{pressure}}{R \cdot T \cdot C}$$

$$H = \frac{1}{H_{Dimensionless} \cdot R \cdot T}$$

Where H is the Henry's constant defined as $\left(\frac{\text{mol}}{\text{kPa} \cdot \text{m}^3 \text{ solvent}}\right)$, $H_{Dimensionless}$ is the dimensionless Henry's constant and $H_{pressure}$ is defined as (kPa). The R is the universal gas constant and the T is the operating temperature of the stripping column. C is the concentration of solvent in $\left(\frac{\text{mol}}{\text{L}}\right)$. The C can be calculated as follows:

$$C = \frac{\text{Density of methanol}}{\text{Molecular weight of methanol}} = \frac{792\ \frac{\text{g}}{\text{L}}}{32.04\ \frac{\text{g}}{\text{mol}}} = 24.7191\frac{\text{mol}}{\text{L}} = 24719.1\ \frac{\text{mol}}{\text{m}^3}$$

Combining these two equations gives:

$$H = \frac{1}{\left(\frac{H_{pressure}}{R \cdot T \cdot C}\right) \cdot R \cdot T} = \frac{1}{\left(\frac{H_{pressure}}{C}\right)}$$

In order to calculate the Henry's constant for steam stripping of H_2S dissolved in methanol solvent, the Henry's constant obtained from Amararene and Bouallou, (2016) is used. The Henry's constant of H_2S in methanol at 68 ℃ was found to be 8660.8 kPa from the literature. Using the above equation, the Henry's constant defined in the unit of pressure is converted into the unit of $\left(\frac{\text{mol}}{\text{kPa}\cdot\text{m}^3\ \text{solvent}}\right)$.

$$H = \frac{1}{\left(\frac{8660.8\ \text{kPa}}{24719.1\ \frac{\text{mol}}{\text{m}^3}}\right)} = 2.854\ \frac{\text{mol}}{\text{kPa} \cdot \text{m}^3\ \text{methanol}}$$

Applying the same procedure as presented in El-halwagi (2017),

$$H(68\ ℃) = 2.854\ \frac{\text{mol}}{\text{kPa} \cdot \text{m}^3\ \text{methanol}} \times (202.6\ \text{kPa}) \times \left(\frac{\text{m}^3\ \text{methanol}}{792000}\right) \times \left(\frac{32.04\ \text{g}}{\text{mol of methanol}}\right) \times \left(\frac{18}{32.04}\right)$$

$$= 0.01314\frac{\text{weight fraction of } H_2S \text{ in methanol}}{\text{weight fraction of } H_2S \text{ in steam}}$$

In the case of steam stripping at 100 ℃ involving H_2S and 15 wt% MDEA, the relevant data is summarized in Table A2.2.

Table A2. 2: The data used in Henry's constant estimation (case study 2)

$\boldsymbol{P_{total}}$	202.6 kPa
$\boldsymbol{y_i^{solubility}}(\mathbf{100}\ ℃, \mathbf{202.6\ kPa})$	0.695 (mol fraction), (Standards and Technology (NIST), 2018)
$\boldsymbol{P^0_{solute}}(\mathbf{100}\ ℃)$	9000 kPa

The molecular weight of 15 wt% MDEA is calculated as follows:

$$15\% \times \left(119.163\ \frac{\text{g}}{\text{mol}}\right) + 85\% \times \left(18\ \frac{\text{g}}{\text{mol}}\right) = 33.17\ \frac{\text{g}}{\text{mol}}$$

With these data, the Henry's constant of H_2S in 15 wt % MDEA at 100 ℃ is calculated as follows:

$$H(100\ ℃) = \frac{(202.6\ \text{kPa}) \cdot (0.695)}{9000\ \text{kPa}} = 0.0156 \frac{\text{mol fraction of } H_2S \text{ in methanol}}{\text{mol fraction of } H_2S \text{ in steam}} \times \left(\frac{18}{33.17}\right)$$
$$= 0.008\ \frac{\text{weight fraction of } H_2S \text{ in methanol}}{\text{weight fraction of } H_2S \text{ in steam}}$$

A3: Capital and costing data

Table A3. 1: Capital and costing data for case study 1

Capital costs and sizing data	
MEN, Shell cost (installed):	$\$618 \cdot M^{0.66}$ (M in kg), (Hallale, 1998)
REN, Shell cost (installed):	$\$618 \cdot M^{0.66}$ (M in kg), (Hallale, 1998)
Packing:	2.54 mm Raschig rings
K_ya	2 kg ammonia/m^3/s
ρ_m	7833 kg/m^3 (Carbon Steel: Perry et al., 1997)
Pi	345 kPa
J	0.8
f	135 N/mm^2

HEN, counter current heat exchanger:	$1200 \cdot A^{0.6} + 10000$ (A in m^2), (Isafiade and Fraser, 2009)
Solar panel:	\$100/(y · m^2), (Isafiade, 2017)
Heat storage:	\$50/(y · m^3), (Isafiade, 2017)
Annualisation factor:	0.225
Annual operating time:	8150 h/y

Table A3. 2: The operating cost data for case study 1

Operating cost			
MEN:	S_1	Process MSA	0 \$/kg
	S_2	External MSA (Aqueous solvent)	0.160 \$/kg (El-Halwagi, 1997)
	S_3	External MSA (Aqueous solvent)	0.001 \$/kg (Isafiade and Fraser, 2009)
REN:	QR_1	Stripping Steam	0.0041 \$/kg
	QR_2	Stripping Air	0.003 \$/kg (El-Halwagi, 1997)
HEN:	HU_1	Steam generated from Solar thermal energy	0 \$/(kW · y)
	HU_2	Steam generated from fossil-based source	60 \$/(kW · y)
	CU_1	Cooling water	30 \$/(kW · y)

Table A3. 3: Capital and costing data for case study 2

Capital costs and sizing data	
MEN, Tray column cost (installed):	\$4552 N_{stages}/(stage · y), (Papalexandri et al., 1994)

REN, Shell cost (installed):	$\$1000 \cdot M^{0.66}$ (M in kg), (Isafiade and Fraser, 2009)
Packing:	2.54 mm Raschig rings
$K_y a$	1.70 Kmol $H_2S/m^3/s$ (Hallale, 1998)
ρ_m	7833 kg/m^3
Pi	7329 kPa (Zare Aliabad and Mirzaei, 2009)
J	0.8
f	135 N/mm^2 (Sinnott, 1999)
HEN, counter current heat exchanger:	$1200 \cdot A^{0.6} + 10000$ (A in m^2), (Isafiade and Fraser, 2009)
Solar panel:	$\$100/(y \cdot m^2)$, (Isafiade, 2017)
Heat storage:	$\$50/(y \cdot m^3)$, (Isafiade, 2017)
Annualisation factor:	0.225
Annual operating time:	8200 h/y

Table A3. 4: The operating cost data for case study 2

Operating cost			
MEN:	S_1	Process MSA (Aqueous ammonia)	117360 $\left(\frac{\$}{y}\right)\left(\frac{kg}{s}\right)$, (Szitkai et al., (2006)
	S_2	External MSA (Chilled Methanol)	176040 $\left(\frac{\$}{y}\right)\left(\frac{kg}{s}\right)$, (El-Halwagi and Manousiouthakis, 1989)
	S_3	External MSA (15 wt% MDEA)	295200 $\left(\frac{\$}{y}\right)\left(\frac{kg}{s}\right)$, (Srinivas and El-Halwagi, 1994)
	$*S_3$	External MSA (NMP)	206640 $\left(\frac{\$}{y}\right)\left(\frac{kg}{s}\right)$, (Srinivas and El-Halwagi, 1994)
REN:	QR_1	Stripping Steam	118080 $\left(\frac{\$}{y}\right)\left(\frac{kg}{s}\right)$

	QR_2	Stripping Steam	312811.63 $\left(\frac{\$}{y}\right)\left(\frac{kg}{s}\right)$
	*QR_2	Inert gas stripping (N_2)	212544 $\left(\frac{\$}{y}\right)\left(\frac{kg}{s}\right)$, (El-Halwagi, 2017)
HEN:	HU_1	Steam generated from Solar thermal energy	0 $\$/(kW \cdot y)$
	HU_2	Steam generated from fossil-based source	60 $\$/(kW \cdot y)$
	CU_1	Cooling water	30 $\$/(kW \cdot y)$
	CU_2	Liquid nitrogen	121.05 $\$/(kW \cdot y)$

A4: costs calculations

Steam costs

Equation 2.36 is used to calculate steam cost (Shah et al., 2013). Operating hour of 8200 h/ y, 1 kg/s of volatile compounds was loaded, and then current price of steam was 84.10 $/1000 Kg. after the calculation, cost of steam for regeneration came down to 30412.242 $/y and it's applied in H2S case study.

Liquid nitrogen cost

El-Halwagi (1997) presented cost of liquid nitrogen as 3.10×10^{-3} $/kg. Shen and Wolsky, (1980) provided amount of energy required to liquefy nitrogen gas which is 0.21 kWh/kg. The cost is divided by the energy requirement to obtain following utility cost:

$$\left(3.10 \times 10^{-3}\,\frac{\$}{kg}\right) \times \left(\frac{kg}{0.21\ kWh}\right) \times \left(\frac{8200\ h}{y}\right) = 121.05\ \frac{\$}{kWh}$$

A5: K_w Calculation

Lumped *Kw* Calculation equation was obtained from Hallale (1998).

For H_2S case study, the lumped overall mass transfer coefficient was calculated using Equation 2.28. The internal design pressure (P_i) of 7329.12 kPa was used (Zare Aliabad and Mirzaei, 2009). The single-welded joints are selected and the value of 0.8 was used. The design stress (f) of 135 $\frac{N}{mm^2}$ was obtained at design temperature of 50 °C (Sinnott, 1999). Carbon steel was selected and its density 7833 $\frac{\text{kg}}{\text{m}^3}$ was used (Perry et al., 1997). The fractional allowance for inactive height, extra components and corrosion were 15 per cent , 20 per cent and 50 per cent respectively. The overall mass transfer coefficient ($K_y a$) of 1.70 $\frac{\text{Kmol}}{\text{m}^3 s^{-1}}$was obtained from Hallale (1998) where it was back-calculated from the results obtained from Papalexandri et al. (1994). After substituting all the parameters into Equation 2.28, the lumped overall mass transfer coefficient of 0.0254 $\frac{\text{kg of } H_2S}{s \cdot \text{kg of Exchanger mass}}$ was obtained.

Appendix B

Sample code for the case study 1 (MEN with REG)

SCALARS

*MENS

NLUT number of lean utilities /3/

NRPS number of rich streams /5/

*REG

NRLUT number of Regeneratable enriched MSAs /2/

NREG number of Regenerating streams /2/

SETS

*=====

*MENS

I rich streams /1*5/

J lean streams and lean utilities /1*3/

K composition locations /1*5/

*REG

RJ rich Regeneratable lean MSAs streams /1*2/

R lean Regenerating streams /1*2/

KR composition locations /1*5/

*Multi-period

P Number of periods /1*2/

DATA data /CIN, COUT, tin, tout, F, H, COST, costhens, m, EIM/;

ALIAS

(J, JJ);

ALIAS

(RJ, RJJ);

*===

*Parameters for MEN

PARAMETERS

RPS(I,P) rich process streams

LPS(J,P) lean process streams

ST(P,K) stages

FIRST(P,K) first composition location

LAST(P,K) last composition location

first_tlrich(P,k)

SECLAST(P,K) second last composition location

```
ms_st(P,k)    mass transfer stages

lut_st(P,k)   lean utility stages

HEIGHT(I,J,K)

AOC(JJ);

RPS(I,P)          =YES$(ORD(I) <= NRPS);

LPS(J,P)          =YES$(ORD(J) <= NLUT);

ST(P,K)           =YES$(ORD(K) < CARD(K));

LAST(P,K)         =YES$(ORD(K) = CARD(K));

SECLAST(P,K)      =YES$(ORD(K) = card(k)-1);

first(P,k)        =yes$(ord(k) eq 1);

first_tlrich(P,k)   = yes$(ord(k)>=1 and ord(k) <card(k));

ms_st(P,k)        =yes$(ord(k)>=1 and ord(k)<card(k));

*=====================================================================

*Parameters for REG

PARAMETERS

RLUT(J,P)    Regeneratable enriched MSAs

REG(R,P)     Regenerating streams

RST(P,KR)    Regeneration stages

RFIRST(P,KR)    first composition location in Regeneration network

RLAST(P,KR)     last composition location in Regeneration network

Rfirst_tlrich(P,KR)

RSECLAST(P,KR)  second last composition location in Regeneration network

Rms_st(P,KR)    mass transfer stages in Regeneration network

RHEIGHT(J,R,KR)

RAOC(RJJ);
```

RLUT(J,P) =YES$(ORD(J) <= NRLUT);

REG(R,P) =YES$(ORD(R) <= NREG);

RST(P,KR) =YES$(ORD(KR) < CARD(KR));

RLAST(P,KR) =YES$(ORD(KR) = CARD(KR));

RSECLAST(P,KR) =YES$(ORD(KR) = card(KR)-1);

Rfirst(P,KR) =yes$(ord(KR) eq 1);

Rfirst_tlrich(P,KR) = yes$(ord(KR)>=1 and ord(KR) <card(KR));

Rms_st(P,KR) =yes$(ord(KR)>=1 and ord(KR)<card(KR));

*===

TABLE RICH(I,P,DATA) Rich streams data

	CIN	COUT	F
1.1	0.00500	0.00100	2.00
1.2	0.00500	0.00100	2.00
2.1	0.00500	0.00250	4.00
2.2	0.00500	0.00250	4.00
3.1	0.01100	0.00250	3.50
3.2	0.01100	0.00250	3.50
4.1	0.01000	0.00500	1.50
4.2	0.01000	0.00500	1.50
5.1	0.00800	0.00250	0.50
5.2	0.00800	0.00250	0.50;

*Note that S2 and S2 are external MSA where S2 is MDEA and S3 is water.

TABLE LEAN(J,P,DATA) Lean streams data

	CIN	COUT	m	EIM

1.1 0.00204 0.00852 1.2 0.00000686

1.2 0.00204 0.00852 1.2 0.00000686

2.1 0.0004 0.0109 0.1 0.503

2.2 0.0004 0.0109 0.1 0.503

3.1 0.00004 0.00850 0.5 0.666

3.2 0.00004 0.00850 0.5 0.666;

TABLE RICHMSA(J,P,DATA) Enriched regeneratable Mass Separating agents streams data

	CIN	COUT	F
1.1	0.0109	0.0004	0.00
1.2	0.0109	0.0004	0.00
2.1	0.00850	0.00004	0.00
2.2	0.00850	0.00004	0.00
3.1	0.00000	0.00000	0.00
3.2	0.00000	0.00000	0.00;

TABLE ZEAN(R,P,DATA) Regenerating streams data

	CIN	COUT	m	EIM
1.1	0.0000059	0.00002	0.1265	0.00000686
1.2	0.0000059	0.00002	0.1265	0.00000686
2.1	0.000000	0.000428	.00972	0.0731
2.2	0.000000	0.000428	.00972	0.0731;

*Regeneration network data

AZ(R,P) Annual operating cost per unit of regenerating stream

REMAC Regeneration network Exchanger minimum approach composition

RINT(KR) Interval in superstructure in Regeneration network

RE(J,KR) Rich stream existance coefficient

ROMEGA(J,R,P)

airStrippingCost

NOP

DOP(P) Duration of period P

W

H Height of exchanger between streams I and J in interval K

RH Height of regeneration exchanger between enriched MSA RJ and regeneration stream R in interval K;

ACH=618; D=0.66; AC('1',P)=0; AC('2',P)=4694400*0.1; AC('3',P)=14670; KW=0.02; AF=0.225; W=.000000000001;

EMAC=0.00001;

AZ('1',P)=121460*0.1265; AZ('2',P)=88020*0.00972;

airStrippingCost = 5425.57;

REMAC=.0000000000007812;

*NOP = number of periods.

NOP=24;

**Duration of periods

DOP('1')=12; DOP('2')=12;

*===

PARAMETER

*Used in Logical constraint for mass exchange in match (I,J,K)

OMEGA(I,J,P);

*This is the upper Omega boundary

```
OMEGA(I,J,P)=  0.00722;
*MAX(0,LEAN(J,'CIN')-RICH(I,'CIN'),LEAN(J,'CIN')-RICH(I,'COUT'),
*LEAN(J,'COUT')-RICH(I,'CIN'),LEAN(J,'COUT')-RICH(I,'COUT'));
*=====================================================================
INT(K)$(ORD(K)LT CARD(K))=1;
*Interval in superstructure is = 1 only if ORD(K) less than last K.
*=====================================================================
PARAMETER
*Used in Logical constraint for mass exchange in match (I,J,K)
ROMEGA(J,R,P);
*This is the upper Omega boundary
ROMEGA(J,R,P)= 0.001;
*MAX(0,LEAN(J,'CIN')-RICH(I,'CIN'),LEAN(J,'CIN')-RICH(I,'COUT'),
*LEAN(J,'COUT')-RICH(I,'CIN'),LEAN(J,'COUT')-RICH(I,'COUT'));
*=====================================================================
RINT(KR)$(ORD(KR)LT CARD(KR))=1;
*Interval in superstructure is = 1 only if ORD(K) less than last K.
*=====================================================================
*Flag for MENS
PARAMETER
A_CKR_LAST(I,P,K)
*Last interval for lean stream
A_CKL_LAST(J,P,K)
*I think this is for the last interval for lean stream exsistence check.
A_CKL_LASTEXT(J,P,K)
```

```
*=====================================================================

A_I(I,P,K)          DEFINE INTERVALS IN WHICH RICH STREAMS EXIST(I)

A_RPS(I,P,K)        DEFINE INTERVALS IN WHICH RICH PROCESS STREAM RPS(I) EXIST

A_LPS(J,P,K)        DEFINE INTERVALS IN WHICH LEAN PROCESS STREAM LPS(J)EXIST

*A_LUT(I,J,K)       INTERVAS IN WHICH LEAN UTILITY LUT(J) IS PRESENT

*=====================================================================

MATCH(I,J,P,K)      DEFINE POSSIBLE MATCHES BETWEEN STREAMS I-J IN INTERVAL
K

COMP_IN_RICH(I,P,K)

COMP_IN_LEAN(J,P,K)

COMP_OUT_RICH(I,P,K)

COMP_OUT_LEAN(J,P,K)

COMP_OUTEXT_LEAN(J,P,K);


*INITIALIZE FLAGS

A_I(I,P,K)=0;

A_RPS(I,P,K)=0;

A_LPS(J,P,K)=0;

MATCH(I,J,P,K)=0;

COMP_IN_RICH(I,P,K)=0;

COMP_IN_LEAN(J,P,K)=0;

COMP_OUT_RICH(I,P,K)=0;

COMP_OUT_LEAN(J,P,K)=0;

COMP_OUTEXT_LEAN(J,P,K)=0;

*=====================================================================

*First set of existence conditionals
```

A_RPS(I,P,K)$(ST(P,K) AND RPS(I,P) AND FIRST_tlrich(P,K)) =1;

*a_hps(i,k)$(hps(i) and first_tlhot(k))= 1;

A_LPS(J,P,K)$(LPS(J,P) AND FIRST_tlrich(P,K))=1;

MATCH(I,J,P,K)$((A_RPS(I,P,K) AND A_LPS(J,P,K)))=1;

COMP_IN_RICH(I,P,K)$RPS(I,P)= FIRST(P,K);

COMP_IN_LEAN(J,P,K)$LPS(J,P)=LAST(P,K);

COMP_OUT_RICH(I,P,K)= LAST(P,K);

COMP_OUT_LEAN(J,P,K)= FIRST(P,K);

DISPLAY RPS, LPS, K, first, last, ms_st, ST,A_RPS, A_LPS, MATCH, COMP_IN_LEAN, COMP_IN_RICH, SECLAST;

*===

*Flag for Regeneration network

PARAMETER

RA_CKRLUT_LAST(J,P,KR)

*Last interval for lean stream

RA_CKREG_LAST(R,P,KR)

*I think this is for the last interval for lean stream existence check.

RA_CKREG_LASTEXT(R,P,KR)

*===

RA_RLUT(J,P,KR) DEFINE INTERVALS IN WHICH ENRICHED REGENERATABLE MSAs RLUT(RJ) EXIST

RA_REG(R,P,KR) DEFINE INTERVALS IN WHICH REGENERATION STREAM REG(R)EXIST

*===

RMATCH(J,R,P,KR) DEFINE POSSIBLE MATCHES BETWEEN STREAMS RJ-R IN INTERVAL KR in Regeneration network

```
RCOMP_IN_RLUT(J,P,KR)

RCOMP_IN_REG(R,P,KR)

RCOMP_OUT_RLUT(J,P,KR)

RCOMP_OUT_REG(R,P,KR)

RCOMP_OUTEXT_REG(R,P,KR);

*INITIALIZE FLAGS

RA_RLUT(J,P,KR)=0;

RA_REG(R,P,KR)=0;

RMATCH(J,R,P,KR)=0;

RCOMP_IN_RLUT(J,P,KR)=0;

RCOMP_IN_REG(R,P,KR)=0;

RCOMP_OUT_RLUT(J,P,KR)=0;

RCOMP_OUT_REG(R,P,KR)=0;

RCOMP_OUTEXT_REG(R,P,KR)=0;

*=====================================================================

*First set of existence conditionals

RA_RLUT(J,P,KR)$(RST(P,KR) AND RLUT(J,P) AND RFIRST_tlrich(P,KR)) =1;

*a_hps(i,k)$(hps(i) and first_tlhot(k))= 1;

RA_REG(R,P,KR)$(REG(R,P)  AND RFIRST_tlrich(P,KR))=1;

RMATCH(J,R,P,KR)$((RA_RLUT(J,P,KR) AND RA_REG(R,P,KR)))=1;

RCOMP_IN_RLUT(J,P,KR)$RLUT(J,P)= RFIRST(P,KR);

RCOMP_IN_REG(R,P,KR)$REG(R,P)=RLAST(P,KR);

RCOMP_OUT_RLUT(J,P,KR)= RLAST(P,KR);

RCOMP_OUT_REG(R,P,KR)= RFIRST(P,KR);
```

DISPLAY RLUT, P, REG, KR, Rfirst, Rlast, Rms_st, RST,RA_RLUT, RA_REG, RMATCH, RCOMP_IN_REG, RCOMP_IN_RLUT, RSECLAST;

VARIABLES

TAC TOTAL ANNUAL COST;

*===

BINARY VARIABLE

Y1(I,J,K) MENs binary variable

RY1(J,R,KR) Regeneration network binary variable;

*===

*Positive variables for MEN

POSITIVE VARIABLES

CR(I,P,K) RICH STREAM COMPOSITION AT LOCATION K

CL(J,P,K) LEAN STREAM COMPOSITION AT LOCATION K

AVLEAN(J,P)

M(I,J,P,K) MASS EXCHANGED

L(J,P) FLOWRATE OF LEAN USED(J)ALL INCLUDED

DC(I,J,P,K) COMPOSITION DIFERENCE BETWEEN PAIR OF STREAM (I.J) IN STAGE K

PNHC(I,J,K) POSITIVE TOLERANCE

SNHC(I,J,K) NEGATIVE TOLERANCE

NHC(I,J,K) RELAXED BINARY VARIABLE

Y(I,J,K)

MX(I,J,K) Mass exchanged for exchangers in MEN;

*Variables for Regeneration Network

POSITIVE VARIABLES

CRLUT(J,P,KR) Regeneration network enriched MSAs STREAM COMPOSITION AT LOCATION KR

CREG(R,P,KR) Regenerating stream COMPOSITION AT LOCATION KR

AVREG(R,P) Available mass carriable by Regeneration streams.

RM(J,R,P,KR) MASS EXCHANGED IN REGENERATION NETWORK

FlowRLUT(J,P) FlOWRATE OF enriched MSAs streams that need to be recycled

FlowREG(R,P) FLOWRATE OF Regeneration streams USED(R) ALL INCLUDED

DR(J,R,P,KR) COMPOSITION DIFERENCE BETWEEN PAIR OF STREAM (RJ.R) IN STAGE KR in Regeneration network

RPNHC(J,R,KR) POSITIVE TOLERANCE FOR REGENERATION NETWORK

RSNHC(J,R,KR) NEGATIVE TOLERANCE FOR REGENERATION NETWORK

RNHC(J,R,KR) RELAXED BINARY VARIABLE FOR REGNERATION NETWORK

RY(J,R,KR)

MXR(J,R,KR) Mass exchanged for exchangers in Regeneration network;

*===

EQUATIONS

*Equations for MEN

CRICH_OUT(I,P,K)

CLEAN_OUT(J,P,K)

AVLEAN1(J,P)

CRICH_IN(I,P,K) ASIGNMENT OF RICH PROCESS STREAM INLET COMPOSITION

CLEAN_IN(J,P,K) ASIGNMENT OF LEAN PROCESS STREAM INLET COMPOSITION

TOTAL_MASS_RICH(I,P) TOTAL MASSS BALANCE OF RICH PROCESS STREAM RPS(I)

TOTAL_MASS_LEAN(J,P) TOTAL MASS BALANCE OF LEAN PROCESS STREAM LPS(I)

STAGE_MASS_RICH(I,P,K) STAGE MASS BALANCE OF RICH PROCESS STREAM RPS(I)

STAGE_MASS_LEAN(J,P,K) STAGE MASS BALANCE OF LEAN PROCESS STREAM LPS(I)

MONOT_RICH(I,P,K) MONOTONICITY ON CONCENTRATIONS - CONSTRAINT

MONOT_LEAN(J,P,K) MONOTONICITY ON CONCENTRATIONS - CONSTRAINT

Pconv(I,J,P,K)

S(I,J,P,K)

N1(I,J,P,K)

LOG_M_RPS_LPS(I,J,P,K) LOGICAL CONSTRAINT ON MASS EXCHANGED BETWEEN RPS(I) AND LPS(J)

LOG_DC_RPS_LPS_RS(I,J,P,K) LOGICAL CONSTRAINT ON RICH SIDE COMPOSITION DIFFERENCE BETWEEN RPS(I) AND LPS(J)

LOG_DC_RPS_LPS_RS1(I,J,P,K)

LOG_DC_RPS_LPS_LS(I,J,P,K) LOGICAL CONSTRAINT ON LEAN SIDE COMPOSITION DIFFERENCE BETWEEN RPS(I) AND LPS(J)

LOG_DC_RPS_LPS_LS1(I,J,P,K)

*Equations for Regeneration network

CRLUT_OUT(J,P,KR)

CREG_OUT(R,P,KR)

AVREG1(R,P)

CRLUT_IN(J,P,KR) ASIGNMENT OF enriched MSA STREAM INLET COMPOSITION

CREG_IN(R,P,KR) ASIGNMENT OF regenerating stream STREAM INLET COMPOSITION

TOTAL_MASS_RLUT(J,P) TOTAL MASSS BALANCE OF enriched MSA STREAM RLUT(RJ)

TOTAL_MASS_REG(R,P) TOTAL MASS BALANCE OF Regeneration STREAM REG(R)

STAGE_MASS_RLUT(J,P,KR) STAGE MASS BALANCE OF encircled MSAs STREAM RLUT(RJ)

STAGE_MASS_REG(R,P,KR) STAGE MASS BALANCE OF Regeneration STREAM REG(R)

MONOT_RLUT(J,P,KR) MONOTONICITY ON CONCENTRATIONS - CONSTRAINT FOR enriched MSA streams

MONOT_REG(R,P,KR) MONOTONICITY ON CONCENTRATIONS - CONSTRAINT FOR regenerating streams

RP(J,R,P,KR)

RS(J,R,P,KR)

RN1(J,R,P,KR)

LOG_M_RLUT_REG(J,R,P,KR) LOGICAL CONSTRAINT ON MASS EXCHANGED BETWEEN RLUT(RJ) AND REG(R)

LOG_DC_RLUT_REG_RS(J,R,P,KR) LOGICAL CONSTRAINT ON RICH SIDE COMPOSITION DIFFERENCE BETWEEN RLUT(RJ) AND REG(R)

LOG_DC_RLUT_REG_RS1(J,R,P,KR)

LOG_DC_RLUT_REG_LS(J,R,P,KR) LOGICAL CONSTRAINT ON LEAN SIDE COMPOSITION DIFFERENCE BETWEEN RLUT(RJ) AND REG(R)

LOG_DC_RLUT_REG_LS1(J,R,P,KR)

MX1(I,J,P,K)

MXR1(J,R,P,KR)

OBJECTIVE OBJECTIVE FUNCTION ;

*===

*assignment of stream inlet compositions

CRICH_IN(I,P,K)$(RPS(I,P) AND COMP_IN_RICH(I,P,K)).. CR(I,P,K) =E= RICH(I,P,'CIN');

CLEAN_IN(J,P,K)$(LPS(J,P) AND COMP_IN_LEAN(J,P,K)).. CL(J,P,K) =E= LEAN(J,P,'CIN');

CRICH_OUT(I,P,K)$(RPS(I,P) AND COMP_OUT_RICH(I,P,K)).. CR(I,P,K) =E= RICH(I,P,'COUT');

CLEAN_OUT(J,P,K)$(LPS(J,P) AND COMP_OUT_LEAN(J,P,K)).. CL(J,P,K) =E= LEAN(J,P,'COUT');

*===

Pconv(I,J,P,K)$(ST(P,K) AND A_RPS(I,P,K)) .. PNHC(I,J,K) =E=.00001;

S(I,J,P,K)$(ST(P,K) AND A_RPS(I,P,K)) .. SNHC(I,J,K) =E=.00001;

N1(I,J,P,K)$(INT(K) AND A_RPS(I,P,K))..Y(I,J,K) =E= Y1(I,J,K)+(PNHC(I,J,K)-SNHC(I,J,K));

*===

*Available mass in lean stream J

AVLEAN1(J,P)..AVLEAN(J,P) =E= L(J,P)*(LEAN(J,P,'COUT')-LEAN(J,P,'CIN'));

*===

*stream overall mass balance

TOTAL_MASS_RICH(I,P)$RPS(I,P) .. RICH(I,P,'F')*(RICH(I,P,'CIN')-RICH(I,P,'COUT')) =E=

SUM((J,K)$(MATCH(I,J,P,K)), M(I,J,P,K));

TOTAL_MASS_LEAN(J,P)$LPS(J,P).. L(J,P)*(LEAN(J,P,'COUT')-LEAN(J,P,'CIN'))
=E=SUM((I,K)$(MATCH(I,J,P,K)),M(I,J,P,K));

*===

*stream stage mass exchange

STAGE_MASS_RICH(I,P,K)$(RPS(I,P) AND SUM(J,MATCH(I,J,P,K)))..

RICH(I,P,'F')*(CR(I,P,K)-CR(I,P,K+1)) =E= SUM(J$MATCH(I,J,P,K), M(I,J,P,K));

STAGE_MASS_LEAN(J,P,K)$(LPS(J,P) AND SUM(I,MATCH(I,J,P,K)))..

L(J,P)*(CL(J,P,K)-CL(J,P,K+1)) =E= SUM(I$MATCH(I,J,P,K), M(I,J,P,K));

*===

*monotonic decrease of composition

MONOT_RICH(I,P,K)$(RPS(I,P) AND ST(P,K) AND A_RPS(I,P,K)).. CR(I,P,K) =G=
CR(I,P,K+1);

MONOT_LEAN(J,P,K)$(LPS(J,P) AND ST(P,K) AND A_LPS(J,P,K)).. CL(J,P,K) =G=
CL(J,P,K+1);

*===

*Logical constraint - Restrict amount of mass exchanged in a match to lesser of the mass loads of R and L in the match.

LOG_M_RPS_LPS(I,J,P,K)$(RPS(I,P) AND LPS(J,P) AND MATCH(I,J,P,K))..M(I,J,P,K) =L=
MIN(RICH(I,P,'F')*(RICH(I,P,'CIN')-RICH(I,P,'COUT')),L(J,P)*(LEAN(J,P,'COUT')-
LEAN(J,P,'CIN')))*Y(I,J,K);

*===

*Calculation of exchanger driving forces

LOG_DC_RPS_LPS_RS(I,J,P,K)$(RPS(I,P) AND LPS(J,P) AND MATCH(I,J,P,K))..DC(I,J,P,K) =L= CR(I,P,K) - CL(J,P,K) + OMEGA(I,J,P)*(1-Y(I,J,K));

LOG_DC_RPS_LPS_RS1(I,J,P,K)$(RPS(I,P) AND LPS(J,P) AND MATCH(I,J,P,K))..DC(I,J,P,K) =G= CR(I,P,K) - CL(J,P,K) - OMEGA(I,J,P)*(1-Y(I,J,K));

LOG_DC_RPS_LPS_LS(I,J,P,K)$(RPS(I,P) AND LPS(J,P) AND MATCH(I,J,P,K))..DC(I,J,P,K+1) =L= CR(I,P,K+1) - CL(J,P,K+1) + OMEGA(I,J,P)*(1-Y(I,J,K));

LOG_DC_RPS_LPS_LS1(I,J,P,K)$(RPS(I,P) AND LPS(J,P) AND MATCH(I,J,P,K))..DC(I,J,P,K+1) =G= CR(I,P,K+1) - CL(J,P,K+1) - OMEGA(I,J,P)*(1-Y(I,J,K));

*Equations for Regeneration network

*===

*assignment of stream inlet compositions

CRLUT_IN(J,P,KR)$(RLUT(J,P) AND RCOMP_IN_RLUT(J,P,KR)).. CRLUT(J,P,KR) =E= RICHMSA(J,P,'CIN');

CREG_IN(R,P,KR)$(REG(R,P) AND RCOMP_IN_REG(R,P,KR)).. CREG(R,P,KR) =E= ZEAN(R,P,'CIN');

CRLUT_OUT(J,P,KR)$(RLUT(J,P) AND RCOMP_OUT_RLUT(J,P,KR)).. CRLUT(J,P,KR) =E= RICHMSA(J,P,'COUT');

CREG_OUT(R,P,KR)$(REG(R,P) AND RCOMP_OUT_REG(R,P,KR)).. CREG(R,P,KR) =E= ZEAN(R,P,'COUT');

*===

RP(J,R,P,KR)$(RST(P,KR) AND RA_RLUT(J,P,KR)) .. RPNHC(J,R,KR) =E=.000001;

RS(J,R,P,KR)$(RST(P,KR) AND RA_RLUT(J,P,KR)) .. RSNHC(J,R,KR) =E=.000001;

RN1(J,R,P,KR)$(RINT(KR) AND RA_RLUT(J,P,KR))..RY(J,R,KR) =E= RY1(J,R,KR)+(RPNHC(J,R,KR)-RSNHC(J,R,KR));

*===

AVREG1(R,P)..AVREG(R,P) =E= FlowREG(R,P)*(ZEAN(R,P,'COUT')-ZEAN(R,P,'CIN'));

*===

*stream overall mass balance

```
TOTAL_MASS_RLUT(J,P)$RLUT(J,P).. L(J+1,P)*(RICHMSA(J,P,'CIN')-
RICHMSA(J,P,'COUT')) =E=

                SUM((R,KR)$(RMATCH(J,R,P,KR)), RM(J,R,P,KR));

TOTAL_MASS_REG(R,P)$REG(R,P).. FlowREG(R,P)*(ZEAN(R,P,'COUT')-ZEAN(R,P,'CIN'))
=E=SUM((J,KR)$(RMATCH(J,R,P,KR) and RLUT(J,P)),RM(J,R,P,KR));

*=====================================================================

*stream stage mass exchange

STAGE_MASS_RLUT(J,P,KR)$(RLUT(J,P) AND SUM(R,RMATCH(J,R,P,KR)))..

L(J+1,P)*(CRLUT(J,P,KR)-CRLUT(J,P,KR+1)) =E= SUM(R$RMATCH(J,R,P,KR),
RM(J,R,P,KR));

STAGE_MASS_REG(R,P,KR)$(REG(R,P) AND SUM(J$RLUT(J,P),RMATCH(J,R,P,KR)))..

FlowREG(R,P)*(CREG(R,P,KR)-CREG(R,P,KR+1)) =E= SUM(J$(RMATCH(J,R,P,KR) and
RLUT(J,P)), RM(J,R,P,KR));

*=====================================================================

*monotonic decrease of composition

MONOT_RLUT(J,P,KR)$(RLUT(J,P) AND RST(P,KR) AND RA_RLUT(J,P,KR))..
CRLUT(J,P,KR) =G= CRLUT(J,P,KR+1);

MONOT_REG(R,P,KR)$(REG(R,P) AND RST(P,KR) AND RA_REG(R,P,KR)).. CREG(R,P,KR)
=G= CREG(R,P,KR+1);

*=====================================================================

*Logical constraint - Restrict amount of mass exchanged in a match to lesser of the mass
loads of R and L in the match.

LOG_M_RLUT_REG(J,R,P,KR)$(RLUT(J,P) AND REG(R,P) AND
RMATCH(J,R,P,KR))..RM(J,R,P,KR) =L= MIN(L(J+1,P)*(RICHMSA(J,P,'CIN')-
RICHMSA(J,P,'COUT')),FlowREG(R,P)*(ZEAN(R,P,'COUT')-ZEAN(R,P,'CIN')))*RY(J,R,KR);

*=====================================================================

*Calculation of exchanger driving forces

LOG_DC_RLUT_REG_RS(J,R,P,KR)$(RLUT(J,P) AND REG(R,P) AND
RMATCH(J,R,P,KR))..DR(J,R,P,KR ) =L= CRLUT(J,P,KR) - CREG(R,P,KR) +
ROMEGA(J,R,P)*(1-RY(J,R,KR));
```

```
LOG_DC_RLUT_REG_RS1(J,R,P,KR)$(RLUT(J,P) AND REG(R,P) AND
RMATCH(J,R,P,KR))..DR(J,R,P,KR ) =G= CRLUT(J,P,KR) - CREG(R,P,KR) -
ROMEGA(J,R,P)*(1-RY(J,R,KR));

LOG_DC_RLUT_REG_LS(J,R,P,KR)$(RLUT(J,P) AND REG(R,P) AND
RMATCH(J,R,P,KR))..DR(J,R,P,KR+1) =L= CRLUT(J,P,KR+1) - CREG(R,P,KR+1) +
ROMEGA(J,R,P)*(1-RY(J,R,KR));

LOG_DC_RLUT_REG_LS1(J,R,P,KR)$(RLUT(J,P) AND REG(R,P) AND
RMATCH(J,R,P,KR))..DR(J,R,P,KR+1) =G= CRLUT(J,P,KR+1) - CREG(R,P,KR+1) -
ROMEGA(J,R,P)*(1-RY(J,R,KR));

*=====================================================================

MX1(I,J,P,K)$(MATCH(I,J,P,K))..

MX(I,J,K)=g=(M(I,J,P,K)*(1/KW)/((((1e-6)**3+

(DC(I,J,P,K)*DC(I,J,P,K+1))*((DC(I,J,P,K)+

DC(I,J,P,K+1))*0.5))**0.3333)+1E-6)+1E-6);

MXR1(J,R,P,KR)$(RMATCH(J,R,P,KR) AND RLUT(J,P))..

MXR(J,R,KR)=g=(RM(J,R,P,KR)*(1/KW)/((((1e-6)**3+

(DR(J,R,P,KR)*DR(J,R,P,KR+1))*((DR(J,R,P,KR)+

DR(J,R,P,KR+1))*0.5))**0.3333)+1E-6)+1E-6);


*OBJECTIVE

 OBJECTIVE..

*MENS capital cost equations

TAC =E=((AF*(SUM((I,J,K),Y(I,J,K))

+ACH*SUM((I,J,K),MX(I,J,K)**D)))


*REG capital cost equations

+(AF*(SUM((J,R,KR),RY(J,R,KR))

+ACH*SUM((J,R,KR),MXR(J,R,KR)**D)))
```

```
*tolerances to ensure that model converges
+W*(SUM((I,J,K),PNHC(I,J,K)+SNHC(I,J,K)))

*tolerances to ensure that model converges for regeneration network.
+W*(SUM((J,R,KR),RPNHC(J,R,KR)+RSNHC(J,R,KR))))

*Flowrate of regenerating stream multiplied by cost per unit of regenerating stream
+SUM((P),(DOP(P)/NOP)*SUM((R),FlowREG(R,P)*AZ(R,P)))

*Flowrate of MSAs stream multiplied by cost per unit of MSA stream
+SUM((P),(DOP(P)/NOP)*SUM((J),L(J,P)*AC(J,P)))
*=====================================================================
MODEL EXAMPLE1 /ALL/;
*=====================================================================
*INITIALISATIONS
*Initialisation for exchanger approach composition between RPS(I) AND LPS(J)
DC.L(I,J,P,K)$(RPS(I,P) AND LPS(J,P) AND MATCH(I,J,P,K))=RICH(I,P,'CIN')-
LEAN(J,P,'CIN') ;
DC.L(I,J,P,K+1)$(RPS(I,P) AND LPS(J,P) AND MATCH(I,J,P,K))=RICH(I,P,'CIN')-
LEAN(J,P,'CIN');
DC.LO(I,J,P,K)$(RPS(I,P) AND LPS(J,P) AND MATCH(I,J,P,K))=EMAC;
DC.LO(I,J,P,K+1)$(RPS(I,P) AND LPS(J,P) AND MATCH(I,J,P,K))=EMAC;
DC.UP(I,J,P,K)$(RPS(I,P) AND LPS(J,P) AND MATCH(I,J,P,K))=10;
DC.UP(I,J,P,K+1)$(RPS(I,P) AND LPS(J,P) AND MATCH(I,J,P,K))=10;
```

*Initialisation for exchanger approach composition between RPS(I) AND LPS(J)

DR.L(J,R,P,KR)$(RLUT(J,P) AND REG(R,P) AND RMATCH(J,R,P,KR))=RICHMSA(J,P,'CIN')-ZEAN(R,P,'CIN') ;

DR.L(J,R,P,KR+1)$(RLUT(J,P) AND REG(R,P) AND RMATCH(J,R,P,KR))=RICHMSA(J,P,'CIN')-ZEAN(R,P,'CIN');

DR.LO(J,R,P,KR)$(RLUT(J,P) AND REG(R,P) AND RMATCH(J,R,P,KR))=REMAC;

DR.LO(J,R,P,KR+1)$(RLUT(J,P) AND REG(R,P) AND RMATCH(J,R,P,KR))=REMAC;

DR.UP(J,R,P,KR)$(RLUT(J,P) AND REG(R,P) AND RMATCH(J,R,P,KR))=10;

DR.UP(J,R,P,KR+1)$(RLUT(J,P) AND REG(R,P) AND RMATCH(J,R,P,KR))=10;

L.L('1',P)=1; L.LO('1',P)=1; L.UP('1',P)=1.5;

L.L('2',P)=1; L.LO('2',P)=.1; L.UP('2',P)=100;

L.L('3',P)=1; L.LO('3',P)=.1; L.UP('3',P)=100;

FlowREG.L('1',P)=1; FlowREG.LO('1',P)=1; FlowREG.UP('1',P)=1000;

FlowREG.L('2',P)=.01; FlowREG.LO('2',P)=.001; FlowREG.UP('2',P)=1200;

*Initialisations for M(I,J,K) between RPS(I) and LPS(J)

M.L(I,J,P,K)$(RPS(I,P) AND MATCH(I,J,P,K))=(RICH(I,P,'F')*(RICH(I,P,'CIN')-RICH(I,P,'COUT')));

M.L(I,J,P,K)$(RPS(I,P) AND MATCH(I,J,P,K))=MIN(RICH(I,P,'F')*(RICH(I,P,'CIN')-RICH(I,P,'COUT')),L.L(J,P)*(LEAN(J,P,'COUT')-LEAN(J,P,'CIN')));

M.UP(I,J,P,K)$(RPS(I,P) AND LPS(J,P) AND MATCH(I,J,P,K))=MIN(RICH(I,P,'F')*(RICH(I,P,'CIN')-RICH(I,P,'COUT')),L.L(J,P)*(LEAN(J,P,'COUT')-LEAN(J,P,'CIN')));

M.UP(I,J,P,K)$(RPS(I,P) AND MATCH(I,J,P,K)) = RICH(I,P,'F')*(RICH(I,P,'CIN')-RICH(I,P,'COUT'));

*Initialisations for M(I,J,K) between RPS(I) and LPS(J)

RM.L(J,R,P,KR)$(RLUT(J,P) AND RMATCH(J,R,P,KR))=(L.L(J+1,P)*(RICHMSA(J,P,'CIN')-RICHMSA(J,P,'COUT')));

RM.L(J,R,P,KR)$(RLUT(J,P) AND RMATCH(J,R,P,KR))=MIN(L.L(J+1,P)*(RICHMSA(J,P,'CIN')-RICHMSA(J,P,'COUT')),FlowREG.L(R,P)*(ZEAN(R,P,'COUT')-ZEAN(R,P,'CIN')));

RM.UP(J,R,P,KR)$(RLUT(J,P) AND REG(R,P) AND RMATCH(J,R,P,KR))=MIN(L.L(J+1,P)*(RICHMSA(J,P,'CIN')-RICHMSA(J,P,'COUT')),FlowREG.L(R,P)*(ZEAN(R,P,'COUT')-ZEAN(R,P,'CIN')));

RM.UP(J,R,P,KR)$(RLUT(J,P) AND RMATCH(J,R,P,KR)) = L.L(J+1,P)*(RICHMSA(J,P,'CIN')-RICHMSA(J,P,'COUT'));

*Intialisations and bounds for intermediate compositions

CR.L(I,P,K)$(A_RPS(I,P,K))=RICH(I,P,'COUT');

CL.L(J,P,K)$(A_LPS(J,P,K) AND COMP_IN_LEAN(J,P,K))=LEAN(J,P,'CIN');

CR.LO(I,P,K)$(A_RPS(I,P,K) AND LAST(P,K))=RICH(I,P,'COUT');

CR.UP(I,P,K)$(A_RPS(I,P,K) AND COMP_IN_RICH(I,P,K))=RICH(I,P,'CIN');

CL.LO(J,P,K)$(A_LPS(J,P,K) AND COMP_IN_LEAN(J,P,K))=LEAN(J,P,'CIN');

CL.UP(J,P,K)$(A_LPS(J,P,K) AND COMP_OUT_LEAN(J,P,K))=LEAN(J,P,'COUT');

*Initialization of inlet and outlet composition of Regeneration network

CRLUT.L(J,P,KR)$(RA_RLUT(J,P,KR))=RICHMSA(J,P,'COUT');

CREG.L(R,P,KR)$(RA_REG(R,P,KR) AND RCOMP_IN_REG(R,P,KR))=ZEAN(R,P,'CIN');

CRLUT.LO(J,P,KR)$(RA_RLUT(J,P,KR) AND RLAST(P,KR))=RICHMSA(J,P,'COUT');

CRLUT.UP(J,P,KR)$(RA_RLUT(J,P,KR) AND RCOMP_IN_RLUT(J,P,KR))=RICHMSA(J,P,'CIN');

CREG.LO(R,P,KR)$(RA_REG(R,P,KR) AND RCOMP_IN_REG(R,P,KR))=ZEAN(R,P,'CIN');

```
CREG.UP(R,P,KR)$(RA_REG(R,P,KR) AND
RCOMP_OUT_REG(R,P,KR))=ZEAN(R,P,'COUT');

*=====================================================================

EXAMPLE1.optfile=1;

OPTION DOMLIM =10000;

OPTION ITERLIM =200000;

SOLVE EXAMPLE1 USING MINLP MINIMIZING TAC;
```

Sample code for the case study 2 with MOO

```
SCALARS

*MENS

NLUT number of lean utilities /3/

NRPS number of rich streams  /2/

*REG

NRLUT number of Regeneratable enriched MSAs /2/

NREG number of Regenerating streams  /2/

*HEN

nhut number of hot utilities /2/

ncut number of cold utilities /2/;


SETS

*MENS

I rich streams  /1*2/

J lean streams and lean utilities /1*3/

K composition locations /1*6/

*REG
```

RJ rich Regeneratable lean MSAs streams /2*3/

R lean Regenerating streams /1*2/

KR composition locations /1*4/

*HEN

ih hot streams /1*4/

jc cold streams /1*4/

kh temperature locations nok + 1 /1*5/

*Multi-period

P Number of periods /1*2/

DATA data /CIN, COUT, tin, tout, F, H, COST, costhens, m, EI/;

ALIAS

(J, JJ);

ALIAS

(RJ, RJJ);

*===

*Parameters for MEN

PARAMETERS

RPS(I,P) rich process streams

LPS(J,P) lean process streams

LUT(J,P) lean utilities

ST(P,K) stages

FIRST(P,K) first composition location

LAST(P,K) last composition location

first_tlrich(P,k)

SECLAST(P,K) second last composition location

ms_st(P,k) mass transfer stages

lut_st(P,k) lean utility stages

HEIGHT(I,J,K)

AOC(JJ);

RPS(I,P) =YES$(ORD(I) <= NRPS);

LPS(J,P) =YES$(ORD(J) <= NLUT);

LUT(J,P) =YES$(ORD(J) >= NLUT-1);

ST(P,K) =YES$(ORD(K) < CARD(K));

LAST(P,K) =YES$(ORD(K) = CARD(K));

SECLAST(P,K) =YES$(ORD(K) = card(k)-1);

first(P,k) =yes$(ord(k) eq 1);

first_tlrich(P,k) = yes$(ord(k)>=1 and ord(k) <card(k));

ms_st(P,k) =yes$(ord(k)>=1 and ord(k)<card(k));

*===

*Parameters for REG

PARAMETERS

RLUT(J,P) Regeneratable enriched MSAs

REG(R,P) Regenerating streams

RST(P,KR) Regeneration stages

RFIRST(P,KR) first composition location in Regeneration network

RLAST(P,KR) last composition location in Regeneration network

Rfirst_tlrich(P,KR)

RSECLAST(P,KR) second last composition location in Regeneration network

Rms_st(P,KR) mass transfer stages in Regeneration network

RHEIGHT(J,R,KR)

```
RAOC(RJJ)
FirstRStream(R,P);
FirstRStream(R,P) = YES $(ORD(R) = 1);
RLUT(J,P)          =YES$(ORD(J) <= NRLUT);
REG(R,P)          =YES$(ORD(R) <= NREG);
RST(P,KR)          =YES$(ORD(KR) < CARD(KR));
RLAST(P,KR)         =YES$(ORD(KR) = CARD(KR));
RSECLAST(P,KR)       =YES$(ORD(KR) = card(KR)-1);
Rfirst(P,KR)        =yes$(ord(KR) eq 1);
Rfirst_tlrich(P,KR)   = yes$(ord(KR)>=1 and ord(KR) <card(KR));
Rms_st(P,KR)        =yes$(ord(KR)>=1 and ord(KR)<card(KR));
*=====================================================================
PARAMETERS
*HEN
hut(ih,P)          hot utilities
hps(ih,P)          hot process streams
cps(jc,P)          cold process streams
cut(jc,P)          cold utilities
sth(P,kh)           stages
firsth(P,kh)        first temperature location
lasth(P,kh)         last temperature location
hx_st(P,kh)         heat recovery stages
hut_st(P,kh)        hot utility stages
cut_st(P,kh)        cold utility stages
```

*first temperature location for Hot Process Stream

fhps(P,kh) first temperature location of hps(ih)

*second temperature location for Cold Process Stream

fcps(P,kh) first temperature location of cps(jc)

first_tlhot(P,Kh) intervals where hps(ih) exist

last_tlhot(P,Kh) last temperature location of hps(ih)

first_tlcold(P,Kh) intervals where cps(jc) exist

last_tlcold(P,Kh) last temperature location of cps(jc);

*Temperature location stages for HEN.

*This consist of each element of 'kh' except the very last 'kh'

sth(P,kh) = yes$(ord(kh) < card(kh)) ;

*first temperature location which is 1

firsth(P,kh) = yes$(ord(kh) eq 1);

*Last temperature location

lasth(P,kh) = yes$(ord(kh) eq card(kh)) ;

hut(ih,P) = yes$(ord(ih) <=nhut);

*Cold utilities consist of each element of 'jc' = cold streams which should be more than (1+(number of cold utilities which is set to 0))

cut(jc,P) = yes$(ord(jc) > 1+ncut);

*Hot process stream consists of each element of 'ih' = hot streams which should be greater than the number of hot utilities which is set to 2

hps(ih,P) = yes$(ord(ih) >nhut);

*Cold process streams should be less than the number of cold utilities + 1

cps(jc,P) = yes$(ord(jc) <=1+ncut);

*Hot utility stages consist of each element of 'kh' temperature location when 'kh' = 1

```
hut_st(P,kh)        = yes$(ord(kh)=1);

*Cold utility stages are the last element of the 'kh' = temperature location

cut_st(P,kh)        = yes$(ord(kh)=card(kh)-1);

*Heat exchange stages (or heat recovery stages) are between 1st stagea and the last kh
stage - 2 stages

hx_st(P,kh)         = yes$(ord(kh)>1 and ord(kh)<=card(kh)-2);

*first temperature location for hot process stream is always 2nd temperature location

fhps(P,kh)          = yes$(ord(kh)=2);

**first temperature location of cold process stream is always last kh stage - 1

fcps(P,kh)          = yes$(ord(kh)=card(kh)-1);

**interval where hot process stream exsit consisit of (2 ~ less than the last kh stage)

first_tlhot(P,kh)    = yes$(ord(kh)>=2 and ord(kh) <card(kh));

**Last temperature location of hot process stream

last_tlhot(P,kh)     = yes$(ord(kh)=card(kh));

**Intervals where cold process streams exist consist of each element of 'kh' =
temperature location and less or equal to the last element of 'kh' - 2

first_tlcold(P,kh)   = yes$(ord(kh)<=card(kh)-2);

**Last temperature location of cold process stream is always 1.

last_tlcold(P,kh)    = yes$(ord(kh)=1);

*=====================================================================
TABLE RICH(I,P,DATA) Rich streams data

     CIN         COUT         F

1.1  0.07        0.0003       0.9

1.2  0.07        0.0003       0.9

2.1  0.051       0.0001       0.1

2.2  0.051       0.0001       0.1;
```

TABLE LEAN(J,P,DATA) Lean streams data

	CIN	COUT
1.1	0.00087	0.04495
1.2	0.00087	0.04495
2.1	0.000052	0.00091
2.2	0.000052	0.00091
3.1	0.000049681	0.00049681
3.2	0.000049681	0.00049681;

TABLE RICHMSA(J,P,DATA) enriched regeneratable Mass Separating agent streams data

CIN	COUT	F
1.1	0.00091	0.000052 0.00
1.2	0.00091	0.000052 0.00
2.1	0.00049681	0.000049681 0.00
2.2	0.00049681	0.000049681 0.00
3.1	0.00000	0.00000 0.00
3.2	0.00000	0.00000 0.00;

TABLE ZEAN(R,P,DATA) Regenerating streams data

	CIN	COUT
1.1	0.0000059	0.00002
1.2	0.0000059	0.00002
2.1	0.000001	0.00009307
2.2	0.000001	0.00009307;

*Ih = 1 is the solar based utility

*Ih = 2 is the fosil based utility

*Ih = 3... are the process MSA to be cooled.

TABLE HOTS(Ih,P,DATA) Hot streams data

	TIN	TOUT	F	H	COST	EI
1.1	393	333	0.00	0.2	0	0.00000202
1.2	383	323	0.00	0.2	0	0.00000202
2.1	408	407	0.00	0.2	60	0.000136
2.2	408	407	0.00	0.2	60	0.000136
3.1	337.5	260	0.35	0.2	0	0
3.2	337.5	260	0.35	0.2	0	0
4.1	298	283	1.00	0.2	0	0
4.2	298	283	1.00	0.2	0	0;

TABLE COLDS(Jc,P,DATA) Cold streams data

	TIN	TOUT	F	H	COST	EI
1.1	260	337.5	0.35	0.2	0	0
1.2	260	337.5	0.35	0.2	0	0
2.1	283	298	1.00	0.2	0	0
2.2	283	298	1.00	0.2	0	0
3.1	278	283	0.00	0.2	30	0.00111
3.2	278	283	0.00	0.2	30	0.00111
4.1	100	100	0.00	0.2	121.05	0.00105
4.2	100	100	0.00	0.2	121.05	0.00105;

*==========

PARAMETER

*Capital cost parameters

AF Annualisation factor

AF2 Annualisation factor for solar panel

ACH Annula cost per height of continuous contact column

D Area cost exponent for mass exchangers

Kw Lumped mass transfer coefficient

AC(J,P) Annual operating cost per unit of lean stream

EMAC Exchanger minimum approach composition

INT(K) Interval in superstructure

Rexi(I,K) Rich stream existance coefficient

OMEGA(I,J,P)

CLUTIN Inlet concentration of external MSA

CLUTOUT Outlet concentration of external MSA

*Regeneration network data

AZ(R,P) Annual operating cost per unit of regenerating stream

REMAC Regeneration network Exchanger minimum approach composition

RINT(KR) Interval in superstructure in Regeneration network

RE(J,KR) Rich stream existance coefficient

ROMEGA(J,R,P)

INTH(Kh) Interval in superstructure in Heat Exchange network

AChens Area cost

AE Area cost index

*Gamma sets boundary in boolean expressions.

gamma(ih,jc,P)

*Miniumum temperature approach for HEN

EMAT Exchanger minimum approach temperature

CF Investment cos

*Multi-period

*Number of Periods

NOP

DOP(P) Duration of period P

*W is used to stabilise the GAMS to solve

W

H Height of exchanger between streams I and J in interval K

RH Height of regeneration exchanger between enriched MSA RJ and regeneration stream R in interval K

*Solar panel parameters

*ambient Temperature

TAMB(P)

*Global Horizontal Irradiation for period of P

GHI(P)

*Thermal storage fluid density

RHO(IH,P)

*specific heat capacity of thermal storage fluid

CP(IH,P)

INSFACTOR(P)

EFFMAX

SCONST1

SCONST2

solarareacost

STORAGETANKCOST

airStrippingCost

*EI

ENVALUE

BEST Best values for objectives

WORST Worst values for objectives

DRatio Weighting for TAC in dual objective function /0/

CRatio Scaling of EI constraint /0/;

*===

ACH=1000; D=0.66; AC('1',P)=0; AC('2',P)=0; AC('3',P)=0; KW=0.0254; AF=0.225;

AF2 = 0.225;

W=.0001;

EMAC=0.0000000414787;

BEST('TAC') = 83905.092;

BEST('EII') = 0.01696697;

*Price of regenerating stream

AZ('1',P)=(118080*0.0294);

REMAC= 0.000000077;

*NOP = number of periods.

NOP=24;

*Duration of periods

DOP('1')=12; DOP('2')=12;

gamma(ih,jc,P) =1;

```
EMAT =5.1;

CF=10000;

AChens = 1200;

AE = 0.6;

INTH(Kh)$(ORD(Kh)LT CARD(Kh))=1;

*Ambient temperature for each period p

TAMB('1')= 32;

TAMB('2')= 32;

*Global horizontal irradiation for each period p

GHI('1')= .800;

GHI('2')= .800;

*Operating hours

INSFACTOR('1')=8100;

INSFACTOR('2')=8100;

*Density of thermal storage fluid

RHO('1','2') =1000;

*Heat capacity of thermal storage fluid

CP('1','2') = 4.200;

*Efficiency of solar panel

EFFmax = .764;

*Experimental constants for solar panel

SCONST1= .00153;

SCONST2= .0000003;

*Cost of solar panel per area

solarareacost= 100;
```

```
*Cost of storage tank per volume
STORAGETANKCOST = 50;
*=====================================================================
PARAMETER
*Used in Logical constraint for mass exchange in match (I,J,K)
OMEGA(I,J,P);
*This is the upper Omega boundary
OMEGA(I,J,P)=  0.01811;
*MAX(0,LEAN(J,'CIN')-RICH(I,'CIN'),LEAN(J,'CIN')-RICH(I,'COUT'),
*LEAN(J,'COUT')-RICH(I,'CIN'),LEAN(J,'COUT')-RICH(I,'COUT'));
*=====================================================================
INT(K)$(ORD(K)LT CARD(K))=1;
*Interval in superstructure is = 1 only if ORD(K) less than last K.
*=====================================================================
PARAMETER
*Used in Logical constraint for mass exchange in match (I,J,K)
ROMEGA(J,R,P);
*This is the upper Omega boundary
ROMEGA(J,R,P)= 0.0008144;
*MAX(0,LEAN(J,'CIN')-RICH(I,'CIN'),LEAN(J,'CIN')-RICH(I,'COUT'),
*LEAN(J,'COUT')-RICH(I,'CIN'),LEAN(J,'COUT')-RICH(I,'COUT'));
*=====================================================================
RINT(KR)$(ORD(KR)LT CARD(KR))=1;
*Interval in superstructure is = 1 only if ORD(K) less than last K.
```

```
*=====================================================================
*Flag for MENS
PARAMETER
*Last interval for rich stream
A_CKR_LAST(I,P,K)
*Last interval for lean stream
A_CKL_LAST(J,P,K)
*I think this is for the last interval for lean stream exsistence check.
A_CKL_LASTEXT(J,P,K)
*=====================================================================
A_I(I,P,K)          DEFINE INTERVALS IN WHICH RICH STREAMS EXIST(I)
A_RPS(I,P,K)        DEFINE INTERVALS IN WHICH RICH PROCESS STREAM RPS(I) EXIST
A_LPS(J,P,K)        DEFINE INTERVALS IN WHICH LEAN PROCESS STREAM LPS(J)EXIST
*=====================================================================
MATCH(I,J,P,K)      DEFINE POSSIBLE MATCHES BETWEEN STREAMS I-J IN INTERVAL
K
COMP_IN_RICH(I,P,K)
COMP_IN_LEAN(J,P,K)
COMP_OUT_RICH(I,P,K)
COMP_OUT_LEAN(J,P,K)
COMP_OUTEXT_LEAN(J,P,K);

*INITIALIZE FLAGS
A_I(I,P,K)=0;
A_RPS(I,P,K)=0;
A_LPS(J,P,K)=0;
```

```
MATCH(I,J,P,K)=0;

COMP_IN_RICH(I,P,K)=0;

COMP_IN_LEAN(J,P,K)=0;

COMP_OUT_RICH(I,P,K)=0;

COMP_OUT_LEAN(J,P,K)=0;

COMP_OUTEXT_LEAN(J,P,K)=0;


*First set of existance conditionals

A_RPS(I,P,K)$(ST(P,K) AND RPS(I,P) AND FIRST_tlrich(P,K)) =1;

A_LPS(J,P,K)$(LPS(J,P)  AND FIRST_tlrich(P,K))=1;

MATCH(I,J,P,K)$((A_RPS(I,P,K) AND A_LPS(J,P,K)))=1;

COMP_IN_RICH(I,P,K)$RPS(I,P)= FIRST(P,K);

COMP_IN_LEAN(J,P,K)$LPS(J,P)=LAST(P,K);

COMP_OUT_RICH(I,P,K)= LAST(P,K);

COMP_OUT_LEAN(J,P,K)= FIRST(P,K);

DISPLAY RPS, LPS, K, first, last, ms_st, ST,A_RPS, A_LPS, MATCH, COMP_IN_LEAN,
COMP_IN_RICH, SECLAST;

*=====================================================================

*Flag for Regeneration network

PARAMETER

RA_CKRLUT_LAST(J,P,KR)

*Last interval for lean stream

RA_CKREG_LAST(R,P,KR)

RA_CKREG_LASTEXT(R,P,KR)

*=====================================================================
```

RA_RLUT(J,P,KR) DEFINE INTERVALS IN WHICH ENRICHED REGENERATABLE MSAs RLUT(RJ) EXIST

RA_REG(R,P,KR) DEFINE INTERVALS IN WHICH REGENERATION STREAM REG(R)EXIST

*===

RMATCH(J,R,P,KR) DEFINE POSSIBLE MATCHES BETWEEN STREAMS RJ-R IN INTERVAL KR in Regeneration network

RCOMP_IN_RLUT(J,P,KR)

RCOMP_IN_REG(R,P,KR)

RCOMP_OUT_RLUT(J,P,KR)

RCOMP_OUT_REG(R,P,KR)

RCOMP_OUTEXT_REG(R,P,KR);

*INITIALIZE FLAGS

RA_RLUT(J,P,KR)=0;

RA_REG(R,P,KR)=0;

RMATCH(J,R,P,KR)=0;

RCOMP_IN_RLUT(J,P,KR)=0;

RCOMP_IN_REG(R,P,KR)=0;

RCOMP_OUT_RLUT(J,P,KR)=0;

RCOMP_OUT_REG(R,P,KR)=0;

RCOMP_OUTEXT_REG(R,P,KR)=0;

*First set of existance conditionals

RA_RLUT(J,P,KR)$(RST(P,KR) AND RLUT(J,P) AND RFIRST_tlrich(P,KR)) =1;

RA_REG(R,P,KR)$(REG(R,P) AND RFIRST_tlrich(P,KR))=1;

RMATCH(J,R,P,KR)$((RA_RLUT(J,P,KR) AND RA_REG(R,P,KR)))=1;

```
RCOMP_IN_RLUT(J,P,KR)$RLUT(J,P)= RFIRST(P,KR);

RCOMP_IN_REG(R,P,KR)$REG(R,P)=RLAST(P,KR);

RCOMP_OUT_RLUT(J,P,KR)= RLAST(P,KR);

RCOMP_OUT_REG(R,P,KR)= RFIRST(P,KR);

DISPLAY RLUT, P, REG, KR, Rfirst, Rlast, Rms_st, RST,RA_RLUT, RA_REG, RMATCH,
RCOMP_IN_REG, RCOMP_IN_RLUT, RSECLAST;

*=====================================================================

*Flag for HEN

PARAMETER

*Flags

a_hps(ih,P,kh)       intervals in which hps(ih) are present

a_cps(jc,P,kh)       intervals in which cps(jc) are present

a_hut(ih,P,kh)       intervals in which hot utilities are present

a_cut(jc,P,kh)       intervals in whc cold utilities are present

matchh(ih,jc,P,kh)     define possible macthes between streams ih and jc in interval kh

temp_in_hot(ih,P,kh)

temp_in_cold(jc,P,kh);


*Initialise flags

a_hps(ih,P,kh)$(hps(ih,P) and first_tlhot(P,kh))= 1;

a_cps(jc,P,kh)$(cps(jc,P) and first_tlcold(P,kh))= 1;

a_hut(ih,P,kh)= 0;

a_cut(jc,P,kh)= 0;

matchh(ih,jc,P,kh)=0;

temp_in_hot(ih,P,kh)=0;

temp_in_cold(jc,P,kh)=0;
```

*Assign flag values

a_hut(ih,P,kh)$(hut(ih,P) and hut_st(P,kh))=1;

a_cut(jc,P,kh)$(cut(jc,P) and cut_st(P,kh))=1;

matchh(ih,jc,P,kh)$(sth(P,kh) and ((a_hps(ih,P,kh) and a_cps(jc,P,kh)$(hps(ih,P) and cps(jc,P))) or (a_cut(jc,P,kh)$((hps(ih,P) and cut(jc,P)))) or (a_hut(ih,P,kh)$((hut(ih,P) and cps(jc,P))))))=1;

*Forbid match

matchh('1','2',p,kh)=0;

temp_in_hot(ih,P,kh)$hps(ih,P)=fhps(P,kh);

temp_in_cold(jc,P,kh)$cps(jc,P)= fcps(P,kh);

Display P, hut, hps, cps, cut, kh, sth, firsth, lasth, hut_st, cut_st, hx_st, fhps, fcps, first_tlhot, last_tlhot, first_tlcold, last_tlcold, a_hps, a_cps, a_hut, a_cut, matchh,temp_in_hot, temp_in_cold;

*===

VARIABLES

TAC TOTAL ANNUAL COST

EII

Dual;

*===

BINARY VARIABLE

Y1(I,J,K) MENs bianry variable

RY1(J,R,KR) Regeneration network binary variable

*For HEN

yh(ih,jc,kh);

*===

*Positive variables for MEN

POSITIVE VARIABLES

CR(I,P,K) RICH STREAM COMPOSITION AT LOCATION K

CL(J,P,K) LEAN STREAM COMPOSITION AT LOCATION K

AVLEAN(J,P)

M(I,J,P,K) MASS EXCHANGED

L(J,P) FLOWRATE OF LEAN USED(J)ALL INCLUDED

DC(I,J,P,K) COMPOSITION DIFERENCE BETWEEN PAIR OF STREAM (I.J) IN STAGE K

*For tray calculation

DC2(I,J,P,K)

DC3(I,J,P,K)

PNHC(I,J,K) POSITIVE TOLERANCE

SNHC(I,J,K) NEGATIVE TOLERANCE

NHC(I,J,K) RELAXED BINARY VARIABLE

Y(I,J,K)

NoStages(I,J,K);

*Variables for Regeneration Network

POSITIVE VARIABLES

CRLUT(J,P,KR) Regeneration network enchriched MSAs STREAM COMPOSITION AT LOCATION KR

CREG(R,P,KR) Regenerating stream COMPOSITION AT LOCATION KR

AVREG(R,P) Available mass carriable by Regeneration streams.

RM(J,R,P,KR) MASS EXCHANGED IN REGENERATION NETWORK

FlowRLUT(J,P) FlOWRATE OF enriched MSAs streams that need to be recycled

FlowREG(R,P) FLOWRATE OF Regeneration streams USED(R) ALL INCLUDED

DR(J,R,P,KR) COMPOSITION DIFERENCE BETWEEN PAIR OF STREAM (RJ.R) IN STAGE KR in Regeneration network

RPNHC(J,R,KR) POSITIVE TOLERANCE FOR REGENERATION NETWORK

RSNHC(J,R,KR) NEGATIVE TOLERANCE FOR REGENERATION NETWORK

RNHC(J,R,KR) RELAXED BINARY VARIABLE FOR REGNERATION NETWORK

RY(J,R,KR)

MXR(J,R,KR) Mass exchanged for exchangers in Regeneration network;

*===

*Positive variables for HEN

POSITIVE VARIABLES

dt(ih,jc,P,kh) approach between ih and jc in period p at location kh

*For hen

th(ih,P,kh) temperature of hot stream ih as it enters stage kh

tc(jc,P,kh) temperature of cold stream jc as it leaves stage kh

q(ih,jc,P,kh) energy exchanged between ih and jc in stage kh

*Heat exchange area

AX(ih,Jc,kh)

*Solar panel equations

AREA_SOLAR_1(ih,Jc,Kh)

AREA_SOLAR_2(ih,Jc,Kh)

SIZE_TANK_2(IH,Jc,Kh);

*===

EQUATIONS

*Equations for MEN

CRICH_OUT(I,P,K)

CLEAN_OUT(J,P,K)

AVLEAN1(J,P)

CRICH_IN(I,P,K) ASIGNMENT OF RICH PROCESS STREAM INLET COMPOSITION

CLEAN_IN(J,P,K) ASIGNMENT OF LEAN PROCESS STREAM INLET COMPOSITION

TOTAL_MASS_RICH(I,P) TOTAL MASSS BALANCE OF RICH PROCESS STREAM RPS(I)

TOTAL_MASS_LEAN(J,P) TOTAL MASS BALANCE OF LEAN PROCESS STREAM LPS(I)

STAGE_MASS_RICH(I,P,K) STAGE MASS BALANCE OF RICH PROCESS STREAM RPS(I)

STAGE_MASS_LEAN(J,P,K) STAGE MASS BALANCE OF LEAN PROCESS STREAM LPS(I)

MONOT_RICH(I,P,K) MONOTONICITY ON CONCENTRATIONS - CONSTRAINT

MONOT_LEAN(J,P,K) MONOTONICITY ON CONCENTRATIONS - CONSTRAINT

Pconv(I,J,P,K)

S(I,J,P,K)

N1(I,J,P,K)

LOG_M_RPS_LPS(I,J,P,K) LOGICAL CONSTRAINT ON MASS EXCHANGED BETWEEN RPS(I) AND LPS(J)

LOG_DC_RPS_LPS_RS(I,J,P,K) LOGICAL CONSTRAINT ON RICH SIDE COMPOSITION DIFFERENCE BETWEEN RPS(I) AND LPS(J)

LOG_DC_RPS_LPS_RS1(I,J,P,K)

LOG_DC_RPS_LPS_LS(I,J,P,K) LOGICAL CONSTRAINT ON LEAN SIDE COMPOSITION DIFFERENCE BETWEEN RPS(I) AND LPS(J)

LOG_DC_RPS_LPS_LS1(I,J,P,K)

*For tray calculation.

LOG_DC_RPS_LPS_RS2(I,J,P,K) LOGICAL CONSTRAINT ON RICH SIDE COMPOSITION DIFFERENCE BETWEEN RPS(I) AND LPS(J)

LOG_DC_RPS_LPS_RS3(I,J,P,K)

LOG_DC_RPS_LPS_LS2(I,J,P,K) LOGICAL CONSTRAINT ON LEAN SIDE COMPOSITION DIFFERENCE BETWEEN RPS(I) AND LPS(J)

LOG_DC_RPS_LPS_LS3(I,J,P,K)

*Equations for Regeneration network

CRLUT_OUT(J,P,KR)

CREG_OUT(R,P,KR)

AVREG1(R,P)

CRLUT_IN(J,P,KR) ASIGNMENT OF enriched MSA STREAM INLET COMPOSITION

CREG_IN(R,P,KR) ASIGNMENT OF regenerating stream STREAM INLET COMPOSITION

TOTAL_MASS_RLUT(J,P) TOTAL MASSS BALANCE OF enriched MSA STREAM RLUT(RJ)

TOTAL_MASS_REG(R,P) TOTAL MASS BALANCE OF Regeneration STREAM REG(R)

STAGE_MASS_RLUT(J,P,KR) STAGE MASS BALANCE OF encirhced MSAs STREAM RLUT(RJ)

STAGE_MASS_REG(R,P,KR) STAGE MASS BALANCE OF Regeneration STREAM REG(R)

MONOT_RLUT(J,P,KR) MONOTONICITY ON CONCENTRATIONS - CONSTRAINT FOR enriched MSA streams

MONOT_REG(R,P,KR) MONOTONICITY ON CONCENTRATIONS - CONSTRAINT FOR regenerating streams

RP(J,R,P,KR)

RS(J,R,P,KR)

RN1(J,R,P,KR)

LOG_M_RLUT_REG(J,R,P,KR) LOGICAL CONSTRAINT ON MASS EXCHANGED BETWEEN RLUT(RJ) AND REG(R)

LOG_DC_RLUT_REG_RS(J,R,P,KR) LOGICAL CONSTRAINT ON RICH SIDE COMPOSITION DIFFERENCE BETWEEN RLUT(RJ) AND REG(R)

LOG_DC_RLUT_REG_RS1(J,R,P,KR)

LOG_DC_RLUT_REG_LS(J,R,P,KR) LOGICAL CONSTRAINT ON LEAN SIDE COMPOSITION DIFFERENCE BETWEEN RLUT(RJ) AND REG(R)

LOG_DC_RLUT_REG_LS1(J,R,P,KR)

*==========

*HEN

THOT_IN(Ih,P,Kh) ASIGNMENT OF HOT PROCESS STREAM INLET TEMPERATURES

TCOLD_IN(Jc,P,Kh) ASIGNMENT OF COLD PROCESS STREAM INLET TEMPERATURES

TOTAL_HEAT_HOT(Ih,P) TOTAL HEAT BALANCE OF HOT PROCESS STREAM HPS(I)

TOTAL_HEAT_COLD(Jc,P) TOTAL HEAT BALANCE OF COLD PROCESS STREAM CPS(I)

STAGE_HEAT_HOT(Ih,P,Kh) STAGE HEAT BALANCE OF HOT PROCESS STREAM HPS(I)

STAGE_HEAT_COLD(Jc,P,Kh) STAGE HEAT BALANCE OF COLD PROCESS STREAM CPS(I)

MONOT_HOT(Ih,P,Kh) MONOTONICITY ON TEMPERATURES - CONSTRAINT

MONOT_COLD(Jc,P,Kh) MONOTONICITY ON TEMPERATURES - CONSTRAINT

LOG_Q_HPS_CPS(Ih,Jc,P,Kh) LOGICAL CONSTRAINT ON HEAT EXCHANGED BETWEEN HPS(I) AND CPS(J)

LOG_Q_HPS_CUT(Ih,Jc,P,Kh) LOGICAL CONSTRAINT ON HEAT EXCHANGED BETWEEN HPS(I) AND CUT(J)

LOG_Q_HUT_CPS(Ih,Jc,P,Kh) LOGICAL CONSTRAINT ON HEAT EXCHANGED BETWEEN HUT(I) AND CPS(J)

LOG_DT_HPS_CPS_HS(Ih,Jc,P,Kh) LOGICAL CONSTRAINT ON HOT SIDE TMEPERATURE DIFFERENCE BETWEEN HPS(I) AND CPS(J)

LOG_DT_HPS_CPS_CS(Ih,Jc,P,Kh) LOGICAL CONSTRAINT ON COLD SIDE TMEPERATURE DIFFERENCE BETWEEN HPS(I) AND CPS(J)

LOG_DT_HPS_CUT_HS(Ih,Jc,P,Kh) LOGICAL CONSTRAINT ON HOT SIDE TMEPERATURE DIFFERENCE BETWEEN HPS(I) AND CUT(J)

LOG_DT_HPS_CUT_CS(Ih,Jc,P,Kh) LOGICAL CONSTRAINT ON COLD SIDE TMEPERATURE DIFFERENCE BETWEEN HPS(I) AND CUT(J)

LOG_DT_HUT_CPS_HS(Ih,Jc,P,Kh) LOGICAL CONSTRAINT ON HOT SIDE TMEPERATURE DIFFERENCE BETWEEN HUT(I) AND CPS(J)

LOG_DT_HUT_CPS_CS(Ih,Jc,P,Kh) LOGICAL CONSTRAINT ON COLD SIDE TMEPERATURE DIFFERENCE BETWEEN HUT(I) AND CPS(J)

AX1(ih,Jc,P,kh)

MXR1(J,R,P,KR)

*Solar Panel Equation

SOLAR_HEAT_1(Ih,Jc,P,Kh)

SOLAR_HEAT_2(Ih,Jc,P,Kh)

SIZE_STORAGETANK_2(Ih,Jc,p,Kh)

*Constrain equation to set variable MSA flowrate = values in table

MSAflowConstrain1(J,Ih,P)

MSAflowConstrain2(J,Ih,P)

ConcenSame (I,P,K)

*Environmental Impact

EI_OBJ

Dual_objective

OBJECTIVE OBJECTIVE FUNCTION ;

*===

*Constrain equation to set variable MSA flowrate = values in table

MSAflowConstrain1(J,Ih,P)..L('2',P) =E= HOTS('3', P, 'F');

MSAflowConstrain2(J,Ih,P)..L('3',P) =E= HOTS('4', P, 'F');

ConcenSame(I,P,K)..CR(I,'1',K) =E= CR(I,'2',K);

*assignment of stream inlet compositions

CRICH_IN(I,P,K)$(RPS(I,P) AND COMP_IN_RICH(I,P,K)).. CR(I,P,K) =E= RICH(I,P,'CIN');

CLEAN_IN(J,P,K)$(LPS(J,P) AND COMP_IN_LEAN(J,P,K)).. CL(J,P,K) =E= LEAN(J,P,'CIN');

```
CRICH_OUT(I,P,K)$(RPS(I,P) AND COMP_OUT_RICH(I,P,K)).. CR(I,P,K) =E=
RICH(I,P,'COUT');

CLEAN_OUT(J,P,K)$(LPS(J,P) AND COMP_OUT_LEAN(J,P,K)).. CL(J,P,K) =E=
LEAN(J,P,'COUT');

*=====================================================================

Pconv(I,J,P,K)$(ST(P,K) AND A_RPS(I,P,K)) .. PNHC(I,J,K) =E=.00001;

S(I,J,P,K)$(ST(P,K) AND A_RPS(I,P,K)) .. SNHC(I,J,K) =E=.00001;

N1(I,J,P,K)$(INT(K) AND A_RPS(I,P,K))..Y(I,J,K) =E= Y1(I,J,K)+(PNHC(I,J,K)-SNHC(I,J,K));

*=====================================================================

*Available mass in lean stream J

AVLEAN1(J,P)..AVLEAN(J,P) =E= L(J,P)*(LEAN(J,P,'COUT')-LEAN(J,P,'CIN'));

*=====================================================================

*stream overall mass balance

TOTAL_MASS_RICH(I,P)$RPS(I,P) ..  RICH(I,P,'F')*(RICH(I,P,'CIN')-RICH(I,P,'COUT')) =E=

                SUM((J,K)$(MATCH(I,J,P,K)), M(I,J,P,K));

TOTAL_MASS_LEAN(J,P)$LPS(J,P).. L(J,P)*(LEAN(J,P,'COUT')-LEAN(J,P,'CIN'))
=E=SUM((I,K)$(MATCH(I,J,P,K)),M(I,J,P,K));

*=====================================================================

*stream stage mass exchange

STAGE_MASS_RICH(I,P,K)$(RPS(I,P) AND SUM(J,MATCH(I,J,P,K)))..

RICH(I,P,'F')*(CR(I,P,K)-CR(I,P,K+1)) =E= SUM(J$MATCH(I,J,P,K), M(I,J,P,K));


STAGE_MASS_LEAN(J,P,K)$(LPS(J,P) AND SUM(I,MATCH(I,J,P,K)))..

L(J,P)*(CL(J,P,K)-CL(J,P,K+1)) =E= SUM(I$MATCH(I,J,P,K), M(I,J,P,K));

*=====================================================================

*monotonic decrease of composition from k=1 to k=5
```

MONOT_RICH(I,P,K)$(RPS(I,P) AND ST(P,K) AND A_RPS(I,P,K)).. CR(I,P,K) =G= CR(I,P,K+1);

MONOT_LEAN(J,P,K)$(LPS(J,P) AND ST(P,K) AND A_LPS(J,P,K)).. CL(J,P,K) =G= CL(J,P,K+1);

*===

*Logical constraint - Restrict amount of mass exchanged in a match to lesser of the mass loads of R and L in the match.

LOG_M_RPS_LPS(I,J,P,K)$(RPS(I,P) AND LPS(J,P) AND MATCH(I,J,P,K))..M(I,J,P,K) =L= MIN(RICH(I,P,'F')*(RICH(I,P,'CIN')-RICH(I,P,'COUT')),L(J,P)*(LEAN(J,P,'COUT')-LEAN(J,P,'CIN')))*Y(I,J,K);

*===

*Calculation of exchanger driving forces

LOG_DC_RPS_LPS_RS(I,J,P,K)$(RPS(I,P) AND LPS(J,P) AND MATCH(I,J,P,K))..DC(I,J,P,K) =L= CR(I,P,K) - CL(J,P,K) + OMEGA(I,J,P)*(1-Y(I,J,K));

LOG_DC_RPS_LPS_RS1(I,J,P,K)$(RPS(I,P) AND LPS(J,P) AND MATCH(I,J,P,K))..DC(I,J,P,K) =G= CR(I,P,K) - CL(J,P,K) - OMEGA(I,J,P)*(1-Y(I,J,K));

LOG_DC_RPS_LPS_LS(I,J,P,K)$(RPS(I,P) AND LPS(J,P) AND MATCH(I,J,P,K))..DC(I,J,P,K+1) =L= CR(I,P,K+1) - CL(J,P,K+1) + OMEGA(I,J,P)*(1-Y(I,J,K));

LOG_DC_RPS_LPS_LS1(I,J,P,K)$(RPS(I,P) AND LPS(J,P) AND MATCH(I,J,P,K))..DC(I,J,P,K+1) =G= CR(I,P,K+1) - CL(J,P,K+1) - OMEGA(I,J,P)*(1-Y(I,J,K));

LOG_DC_RPS_LPS_RS2(I,J,P,K)$(RPS(I,P) AND LPS(J,P) AND MATCH(I,J,P,K))..DC2(I,J,P,K) =L= CR(I,P,K) - CR(I,P,K+1) + OMEGA(I,J,P)*(1-Y(I,J,K));

LOG_DC_RPS_LPS_RS3(I,J,P,K)$(RPS(I,P) AND LPS(J,P) AND MATCH(I,J,P,K))..DC2(I,J,P,K) =G= CR(I,P,K) - CR(I,P,K+1) - OMEGA(I,J,P)*(1-Y(I,J,K));

LOG_DC_RPS_LPS_LS2(I,J,P,K)$(RPS(I,P) AND LPS(J,P) AND MATCH(I,J,P,K))..DC3(I,J,P,K) =L= CL(J,P,K) - CL(J,P,K+1) + OMEGA(I,J,P)*(1-Y(I,J,K));

LOG_DC_RPS_LPS_LS3(I,J,P,K)$(RPS(I,P) AND LPS(J,P) AND MATCH(I,J,P,K))..DC3(I,J,P,K) =G= CL(J,P,K) - CL(J,P,K+1) - OMEGA(I,J,P)*(1-Y(I,J,K));

*===

*Equations for Regeneration network

*assignment of stream inlet compositions

CRLUT_IN(J,P,KR)$(RLUT(J,P) AND RCOMP_IN_RLUT(J,P,KR)).. CRLUT(J,P,KR) =E= RICHMSA(J,P,'CIN');

CREG_IN(R,P,KR)$(REG(R,P) AND RCOMP_IN_REG(R,P,KR)).. CREG(R,P,KR) =E= ZEAN(R,P,'CIN');

CRLUT_OUT(J,P,KR)$(RLUT(J,P) AND RCOMP_OUT_RLUT(J,P,KR)).. CRLUT(J,P,KR) =E= RICHMSA(J,P,'COUT');

CREG_OUT(R,P,KR)$(REG(R,P) AND RCOMP_OUT_REG(R,P,KR)).. CREG(R,P,KR) =E= ZEAN(R,P,'COUT');

*===

RP(J,R,P,KR)$(RST(P,KR) AND RA_RLUT(J,P,KR)) .. RPNHC(J,R,KR) =E=.000001;

RS(J,R,P,KR)$(RST(P,KR) AND RA_RLUT(J,P,KR)) .. RSNHC(J,R,KR) =E=.000001;

RN1(J,R,P,KR)$(RINT(KR) AND RA_RLUT(J,P,KR))..RY(J,R,KR) =E= RY1(J,R,KR)+(RPNHC(J,R,KR)-RSNHC(J,R,KR));

*===

*Available mass in regenerating stream

AVREG1(R,P)..AVREG(R,P) =E= FlowREG(R,P)*(ZEAN(R,P,'COUT')-ZEAN(R,P,'CIN'));

*===

*stream overall mass balance

TOTAL_MASS_RLUT(J,P)$RLUT(J,P).. L(J+1,P)*(RICHMSA(J,P,'CIN')-RICHMSA(J,P,'COUT')) =E=

SUM((R,KR)$(RMATCH(J,R,P,KR)), RM(J,R,P,KR));

TOTAL_MASS_REG(R,P)$REG(R,P).. FlowREG(R,P)*(ZEAN(R,P,'COUT')-ZEAN(R,P,'CIN')) =E=SUM((J,KR)$(RMATCH(J,R,P,KR) and RLUT(J,P)),RM(J,R,P,KR));

*===

*stream stage mass exchange

STAGE_MASS_RLUT(J,P,KR)$(RLUT(J,P) AND SUM(R,RMATCH(J,R,P,KR)))..

L(J+1,P)*(CRLUT(J,P,KR)-CRLUT(J,P,KR+1)) =E= SUM(R$RMATCH(J,R,P,KR), RM(J,R,P,KR));

STAGE_MASS_REG(R,P,KR)$(REG(R,P) AND SUM(J$RLUT(J,P),RMATCH(J,R,P,KR)))..

FlowREG(R,P)*(CREG(R,P,KR)-CREG(R,P,KR+1)) =E= SUM(J$(RMATCH(J,R,P,KR) and RLUT(J,P)), RM(J,R,P,KR));

*===

*monotonic decrease of composition

MONOT_RLUT(J,P,KR)$(RLUT(J,P) AND RST(P,KR) AND RA_RLUT(J,P,KR))..
CRLUT(J,P,KR) =G= CRLUT(J,P,KR+1);

MONOT_REG(R,P,KR)$(REG(R,P) AND RST(P,KR) AND RA_REG(R,P,KR)).. CREG(R,P,KR) =G= CREG(R,P,KR+1);

*===

*Logical constraint - Restrict amount of mass exchanged in a match to lesser of the mass loads of R and L in the match.

LOG_M_RLUT_REG(J,R,P,KR)$(RLUT(J,P) AND REG(R,P) AND RMATCH(J,R,P,KR))..RM(J,R,P,KR) =L= MIN(L(J+1,P)*(RICHMSA(J,P,'CIN')-RICHMSA(J,P,'COUT')),FlowREG(R,P)*(ZEAN(R,P,'COUT')-ZEAN(R,P,'CIN')))*RY(J,R,KR);

*===

*Calculation of exchanger driving forces

LOG_DC_RLUT_REG_RS(J,R,P,KR)$(RLUT(J,P) AND REG(R,P) AND RMATCH(J,R,P,KR))..DR(J,R,P,KR) =L= CRLUT(J,P,KR) - CREG(R,P,KR) + ROMEGA(J,R,P)*(1-RY(J,R,KR));

LOG_DC_RLUT_REG_RS1(J,R,P,KR)$(RLUT(J,P) AND REG(R,P) AND RMATCH(J,R,P,KR))..DR(J,R,P,KR) =G= CRLUT(J,P,KR) - CREG(R,P,KR) - ROMEGA(J,R,P)*(1-RY(J,R,KR));

LOG_DC_RLUT_REG_LS(J,R,P,KR)$(RLUT(J,P) AND REG(R,P) AND RMATCH(J,R,P,KR))..DR(J,R,P,KR+1) =L= CRLUT(J,P,KR+1) - CREG(R,P,KR+1) + ROMEGA(J,R,P)*(1-RY(J,R,KR));

LOG_DC_RLUT_REG_LS1(J,R,P,KR)$(RLUT(J,P) AND REG(R,P) AND RMATCH(J,R,P,KR))..DR(J,R,P,KR+1) =G= CRLUT(J,P,KR+1) - CREG(R,P,KR+1) - ROMEGA(J,R,P)*(1-RY(J,R,KR));

```
*=====================================================================

*Equations for HEN

*assignment of stream inlet temperatures

thot_in(ih,P,kh)$(hps(ih,P) and temp_in_hot(ih,P,kh))..

  th(ih,P,kh) =e= hots(ih,P,'tin');

tcold_in(jc,P,kh)$(cps(jc,P) and temp_in_cold(jc,P,kh))..

  tc(jc,P,kh) =e= colds(jc,P,'tin');

TOTAL_HEAT_HOT(Ih,P)$(HPS(Ih,P))..  (HOTS(Ih,P,'F'))*(HOTS(Ih,P,'TIN')-
HOTS(Ih,P,'TOUT')) =e=

                SUM((Jc,Kh)$(matchh (ih,jc,P,kh)), Q(Ih,Jc,P,Kh));

TOTAL_HEAT_COLD(Jc,P)$(CPS(Jc,P)).. (COLDS(Jc,P,'F'))*(COLDS(Jc,P,'TOUT')-
COLDS(Jc,P,'TIN')) =e=

                SUM((Ih,Kh)$(matchh (ih,jc,P,kh)), Q(Ih,Jc,P,Kh));

*stream stage heat exchange

STAGE_HEAT_HOT(Ih,P,Kh)$(HPS(Ih,P) AND SUM(Jc,matchh (ih,jc,P,kh)))..

(HOTS(Ih,P,'F'))*(TH(Ih,P,Kh)-TH(Ih,P,Kh+1)) =e= SUM(Jc$matchh (ih,jc,P,kh),
Q(Ih,Jc,P,Kh));

STAGE_HEAT_COLD(Jc,P,Kh)$(CPS(Jc,P) AND SUM(Ih,matchh (ih,jc,P,kh)))..

(COLDS(Jc,P,'F'))*(TC(Jc,P,Kh)-TC(Jc,P,Kh+1)) =e= SUM(Ih$matchh (ih,jc,P,kh),
Q(Ih,Jc,P,Kh));

*monotocity of temperature

MONOT_HOT(Ih,P,Kh)$(HPS(Ih,P) AND STh(P,kh) AND A_HPS(Ih,P,Kh)).. TH(Ih,P,Kh)
=G= TH(Ih,P,Kh+1);

MONOT_COLD(Jc,P,Kh)$(CPS(Jc,P) AND STh(P,kh) AND A_CPS(Jc,P,Kh)).. TC(Jc,P,Kh)
=G= TC(Jc,P,Kh+1);

LOG_Q_HPS_CPS(Ih,Jc,P,Kh)$(HPS(Ih,P) AND CPS(Jc,P) AND matchh (ih,jc,P,kh))..
```

```
Q(Ih,Jc,P,Kh) =L= MIN((HOTS(Ih,P,'F'))*(HOTS(Ih,P,'TIN')-
HOTS(Ih,P,'TOUT')),((COLDS(Jc,P,'F'))*(COLDS(Jc,P,'TOUT')-
COLDS(Jc,P,'TIN'))))*Yh(Ih,Jc,Kh);

LOG_Q_HPS_CUT(Ih,Jc,P,Kh)$(HPS(Ih,P) AND CUT(Jc,P) AND matchh (ih,jc,P,kh))..

Q(Ih,Jc,P,Kh) =L= ((HOTS(Ih,P,'F'))*(HOTS(Ih,P,'TIN')-HOTS(Ih,P,'TOUT')))*Yh(Ih,Jc,Kh);

LOG_Q_HUT_CPS(Ih,Jc,P,Kh)$(HUT(Ih,P) AND CPS(Jc,P) AND matchh (ih,jc,P,kh))..

Q(Ih,Jc,P,Kh) =L= ((COLDS(Jc,P,'F'))*(COLDS(Jc,P,'TOUT')-
COLDS(Jc,P,'TIN')))*Yh(Ih,Jc,Kh);

LOG_DT_HPS_CPS_HS(Ih,Jc,P,Kh)$(HPS(Ih,P) AND CPS(Jc,P) AND matchh
(ih,jc,P,kh))..DT(Ih,Jc,P,Kh) =L= TH(Ih,P,Kh) - TC(Jc,P,Kh) + GAMMA(Ih,Jc,P)*(1-
Yh(Ih,Jc,Kh));

LOG_DT_HPS_CPS_CS(Ih,Jc,P,Kh)$(HPS(Ih,P) AND CPS(Jc,P) AND matchh
(ih,jc,P,kh))..DT(Ih,Jc,P,Kh+1) =L= TH(Ih,P,Kh+1) - TC(Jc,P,Kh+1) + GAMMA(Ih,Jc,P)*(1-
Yh(Ih,Jc,Kh));

LOG_DT_HPS_CUT_HS(Ih,Jc,P,Kh)$(HPS(Ih,P) AND CUT(Jc,P) AND matchh
(ih,jc,P,kh))..DT(Ih,Jc,P,Kh)$(HPS(Ih,P) AND CUT(Jc,P) AND matchh (ih,jc,P,kh)) =L=
(TH(Ih,P,Kh) - COLDS(Jc,P,'TOUT')) + GAMMA(Ih,Jc,P)*(1-Yh(Ih,Jc,Kh));

LOG_DT_HPS_CUT_CS(Ih,Jc,P,Kh)$(HPS(Ih,P) AND CUT(Jc,P) AND matchh
(ih,jc,P,kh))..DT(Ih,Jc,P,Kh+1)$(HPS(Ih,P) AND CUT(Jc,P) AND matchh (ih,jc,P,kh)) =L=
(TH(Ih,P,Kh+1) - COLDS(Jc,P,'TIN')) + GAMMA(Ih,Jc,P)*(1-Yh(Ih,Jc,Kh));

LOG_DT_HUT_CPS_HS(Ih,Jc,P,Kh)$(HUT(Ih,P) AND CPS(Jc,P) AND matchh
(ih,jc,P,kh))..DT(Ih,Jc,P,Kh)$(HUT(Ih,P) AND CPS(Jc,P) AND matchh (ih,jc,P,kh)) =L=
(HOTS(Ih,P,'TIN') - TC(Jc,P,Kh)) + GAMMA(Ih,Jc,P)*(1-Yh(Ih,Jc,Kh));

LOG_DT_HUT_CPS_CS(Ih,Jc,P,Kh)$(HUT(Ih,P) AND CPS(Jc,P) AND matchh
(ih,jc,P,kh))..DT(Ih,Jc,P,Kh+1)$(HUT(Ih,P) AND CPS(Jc,P) AND matchh (ih,jc,P,kh))
=L=(HOTS(Ih,P,'TOUT') - TC(Jc,P,Kh+1)) + GAMMA(Ih,Jc,P)*(1-Yh(Ih,Jc,Kh));

AX1(ih,Jc,P,kh)$(matchh (ih,jc,P,kh))..

AX(ih,Jc,kh)=g=(Q(ih,Jc,P,kh)*(1/HOTS(ih,P,'H')+1/COLDS(Jc,P,'H'))/

(((1e-6)**3+((2/3)*(DT(Ih,Jc,P,Kh)*DT(Ih,Jc,P,Kh+1))**0.5)+(1/3*(DT(Ih,Jc,P,Kh)+

DT(Ih,Jc,P,Kh+1))*0.5))+1E-6)+1E-6);

*=====================================================================
```

```
MXR1(J,R,P,KR)$(RMATCH(J,R,P,KR) AND RLUT(J,P))..

MXR(J,R,KR)=g=(RM(J,R,P,KR)*(1/KW)/((((1e-6)**3+

(DR(J,R,P,KR)*DR(J,R,P,KR+1))*((DR(J,R,P,KR)+

DR(J,R,P,KR+1))*0.5))**0.3333)+1E-6)+1E-6);

*=====================================================================

*Solar Equations

SOLAR_HEAT_1(Ih,Jc,P,Kh)$(HPS(ih,P) and MATCHH('1',Jc,'1',Kh))..

AREA_SOLAR_1('1',Jc,Kh)=G=

(Q('1',Jc,'1',Kh)/((effmax*GHI('1'))-
((SCONST1)*(((HOTS('1','1','TIN')+HOTS('1','1','TOUT'))/2)-(TAMB('1'))))-
((SCONST2)*((((HOTS('1','1','TIN')+HOTS('1','1','TOUT'))/2)-(TAMB('1')))**2))));

SOLAR_HEAT_2(Ih,Jc,P,Kh)$(HPS(ih,P) and MATCHH('1',Jc,'1',Kh) )..

AREA_SOLAR_2('1',Jc,Kh)=G=

(Q('1',Jc,'1',Kh)/((effmax*GHI('1'))-
((SCONST1)*(((HOTS('1','1','TIN')+HOTS('1','1','TOUT'))/2)-(TAMB('1'))))-
((SCONST2)*((((HOTS('1','1','TIN')+HOTS('1','1','TOUT'))/2)-(TAMB('1')))**2))));

SIZE_STORAGETANK_2(Ih,Jc,p,Kh)$(HPS(IH,P) and MATCHH('1',Jc,'2',Kh))..

SIZE_TANK_2('1',Jc,Kh)=G=

(DOP('2')*3600*(Q('1',Jc,'2',Kh)/((CP('1','2')*RHO('1','2'))*(HOTS('1','2','TIN')-
HOTS('1','2','TOUT')))));

*=====================================================================

*Objective function

 OBJECTIVE..

*MENS capital cost equations

TAC =E= (AF*(SUM((I,J,K),Y(I,J,K))

+4552*(SUM((I,J,K)$(MATCH(I,J,'1',K)),((((((DC2(I,J,'1',K))**0.3333)

+((DC3(I,J,'1',K))**0.3333))/((DC(I,J,'1',K)**0.3333)
```

```
+(DC(I,J,'1',K+1)**0.3333)))**(1/(0.3333)))))))
+0*(SUM((I,J,K)$(MATCH(I,J,'2',K)),((((((DC2(I,J,'2',K))**0.3333)
+((DC3(I,J,'2',K))**0.3333))/((DC(I,J,'2',K)**0.3333)
+(DC(I,J,'2',K+1)**0.3333)))**(1/(0.3333)))))))

*REG capital cost equations
+(AF*(SUM((J,R,KR),RY(J,R,KR))
+ACH*SUM((J,R,KR),MXR(J,R,KR)**D)))

*tolerances to ensure that model converges
+W*(SUM((I,J,K),PNHC(I,J,K)+SNHC(I,J,K)))

*tolerances to ensure that model converges for regeneration network.
+W*(SUM((J,R,KR),RPNHC(J,R,KR)+RSNHC(J,R,KR)))

*Flowrate of regenerating stream multiplied by cost per unit of regenerating stream
+SUM((P),(DOP(P)/NOP)*FlowREG('1',P)*AZ('1',P))
+SUM((P),(DOP(P)/NOP)*FlowREG('2',P)*(212544*0.0022058))

*Flowrate of MSAs stream multiplied by cost per unit of MSA stream
+SUM((P),(DOP(P)/NOP)*SUM((J),L(J,P)*AC(J,P)))

*TAC of HEN
+AF*((CF*(SUM((Ih,Jc,Kh),Yh(Ih,Jc,Kh))))+
      (AChens*((SUM((Ih,Jc,kh),(AX(ih,Jc,kh)))))))
```

```
      +SUM((P),(DOP(P)/NOP)* SUM((Ih,Jc,Kh),COLDS(Jc,p,'COST')*Q(Ih,Jc,p,Kh)))

      +SUM((P),(DOP(P)/NOP)*SUM((Ih,Jc,Kh),HOTS(Ih,p,'COST')*Q(Ih,Jc,p,Kh)))


*Solar panel costing equations

+(AF2*((solarareacost*(SUM((IH,JC,kH),(AREA_SOLAR_1(IH,JC,KH)))))+

(solarareacost*(SUM((IH,JC,kH),(AREA_SOLAR_2(IH,JC,KH)))))

+(storagetankcost*(SUM((IH,JC,kH),(SIZE_TANK_2(IH,JC,KH)))))) ;


EI_OBJ..  EII*1000=E=8000*3.600*(SUM((P),(DOP(P)/NOP)*SUM((Ih,Jc,Kh)$(HUT(Ih,P)
AND CPS(Jc,P) AND MATCHh(Ih,Jc,P,Kh)),HOTS(Ih,P,'EI')*Q(Ih,Jc,P,Kh))))

       +SUM((P),(DOP(P)/NOP)*SUM((Ih,Jc,Kh)$(CUT(Jc,P) AND HPS(Ih,P) AND
MATCHh(Ih,Jc,P,Kh)),COLDS(Jc,P,'EI')*Q(Ih,Jc,P,Kh)));


*Dual objective function

Dual_objective..Dual=e= (0.5*(TAC/BEST('TAC')))+((0.5)*(EII/BEST('EII')));

*=====================================================================

MODEL EXAMPLE1 /ALL/;

*=====================================================================

*INITIALISATIONS

*Initialisation for exchanger approach composition between RPS(I) AND LPS(J)

DC.L(I,J,P,K)$(RPS(I,P) AND LPS(J,P) AND MATCH(I,J,P,K))=RICH(I,P,'CIN')-
LEAN(J,P,'CIN') ;

DC.L(I,J,P,K+1)$(RPS(I,P) AND LPS(J,P) AND MATCH(I,J,P,K))=RICH(I,P,'CIN')-
LEAN(J,P,'CIN');

DC.LO(I,J,P,K)$(RPS(I,P) AND LPS(J,P) AND MATCH(I,J,P,K))=EMAC;

DC.LO(I,J,P,K+1)$(RPS(I,P) AND LPS(J,P) AND MATCH(I,J,P,K))=EMAC;
```

DC.UP(I,J,P,K)$(RPS(I,P) AND LPS(J,P) AND MATCH(I,J,P,K))=10;

DC.UP(I,J,P,K+1)$(RPS(I,P) AND LPS(J,P) AND MATCH(I,J,P,K))=10;

*Initialisation for exchanger approach composition between RPS(I) AND LPS(J)

DR.L(J,R,P,KR)$(RLUT(J,P) AND REG(R,P) AND RMATCH(J,R,P,KR))=RICHMSA(J,P,'CIN')-ZEAN(R,P,'CIN') ;

DR.L(J,R,P,KR+1)$(RLUT(J,P) AND REG(R,P) AND RMATCH(J,R,P,KR))=RICHMSA(J,P,'CIN')-ZEAN(R,P,'CIN');

DR.LO(J,R,P,KR)$(RLUT(J,P) AND REG(R,P) AND RMATCH(J,R,P,KR))=REMAC;

DR.LO(J,R,P,KR+1)$(RLUT(J,P) AND REG(R,P) AND RMATCH(J,R,P,KR))=REMAC;

DR.UP(J,R,P,KR)$(RLUT(J,P) AND REG(R,P) AND RMATCH(J,R,P,KR))=10;

DR.UP(J,R,P,KR+1)$(RLUT(J,P) AND REG(R,P) AND RMATCH(J,R,P,KR))=10;

L.L('1',P)=1; L.LO('1',P)=.1; L.UP('1',P)=2.3;

L.L('2',P)=1; L.LO('2',P)=.1; L.UP('2',P)=100;

L.L('3',P)=1; L.LO('3',P)=1; L.UP('3',P)=100;

FlowREG.L('1',P)=1; FlowREG.LO('1',P)=1; FlowREG.UP('1',P)=2000;

FlowREG.L('2',P)=.1; FlowREG.LO('2',P)=.01; FlowREG.UP('2',P)=2000;

*Initialisations for M(I,J,K) between RPS(I) and LPS(J)

M.L(I,J,P,K)$(RPS(I,P) AND MATCH(I,J,P,K))=(RICH(I,P,'F')*(RICH(I,P,'CIN')-RICH(I,P,'COUT')));

M.L(I,J,P,K)$(RPS(I,P) AND MATCH(I,J,P,K))=MIN(RICH(I,P,'F')*(RICH(I,P,'CIN')-RICH(I,P,'COUT')),L.L(J,P)*(LEAN(J,P,'COUT')-LEAN(J,P,'CIN')));

M.UP(I,J,P,K)$(RPS(I,P) AND LPS(J,P) AND MATCH(I,J,P,K))=MIN(RICH(I,P,'F')*(RICH(I,P,'CIN')-RICH(I,P,'COUT')),L.L(J,P)*(LEAN(J,P,'COUT')-LEAN(J,P,'CIN')));

```
M.UP(I,J,P,K)$(RPS(I,P) AND MATCH(I,J,P,K)) = RICH(I,P,'F')*(RICH(I,P,'CIN')-
RICH(I,P,'COUT'));


*Initialisations for M(I,J,K) between RPS(I) and LPS(J)

RM.L(J,R,P,KR)$(RLUT(J,P) AND RMATCH(J,R,P,KR))=(L.L(J+1,P)*(RICHMSA(J,P,'CIN')-
RICHMSA(J,P,'COUT')));

RM.L(J,R,P,KR)$(RLUT(J,P) AND
RMATCH(J,R,P,KR))=MIN(L.L(J+1,P)*(RICHMSA(J,P,'CIN')-
RICHMSA(J,P,'COUT')),FlowREG.L(R,P)*(ZEAN(R,P,'COUT')-ZEAN(R,P,'CIN')));

RM.UP(J,R,P,KR)$(RLUT(J,P) AND REG(R,P) AND
RMATCH(J,R,P,KR))=MIN(L.L(J+1,P)*(RICHMSA(J,P,'CIN')-
RICHMSA(J,P,'COUT')),FlowREG.L(R,P)*(ZEAN(R,P,'COUT')-ZEAN(R,P,'CIN')));

RM.UP(J,R,P,KR)$(RLUT(J,P) AND RMATCH(J,R,P,KR)) = L.L(J+1,P)*(RICHMSA(J,P,'CIN')-
RICHMSA(J,P,'COUT'));


*Intialisations and bounds for intermediate compositions

CR.L(I,P,K)$(A_RPS(I,P,K))=RICH(I,P,'COUT');

CL.L(J,P,K)$(A_LPS(J,P,K) AND COMP_IN_LEAN(J,P,K))=LEAN(J,P,'CIN');

CR.LO(I,P,K)$(A_RPS(I,P,K) AND LAST(P,K))=RICH(I,P,'COUT');

CR.UP(I,P,K)$(A_RPS(I,P,K) AND COMP_IN_RICH(I,P,K))=RICH(I,P,'CIN');


CL.LO(J,P,K)$(A_LPS(J,P,K) AND COMP_IN_LEAN(J,P,K))=LEAN(J,P,'CIN');

CL.UP(J,P,K)$(A_LPS(J,P,K) AND COMP_OUT_LEAN(J,P,K))=LEAN(J,P,'COUT');


*Initialization of inlet anda outlet composition of Regeneration network

CRLUT.L(J,P,KR)$(RA_RLUT(J,P,KR))=RICHMSA(J,P,'COUT');

CREG.L(R,P,KR)$(RA_REG(R,P,KR) AND RCOMP_IN_REG(R,P,KR))=ZEAN(R,P,'CIN');

CRLUT.LO(J,P,KR)$(RA_RLUT(J,P,KR) AND RLAST(P,KR))=RICHMSA(J,P,'COUT');
```

CRLUT.UP(J,P,KR)$(RA_RLUT(J,P,KR) AND
RCOMP_IN_RLUT(J,P,KR))=RICHMSA(J,P,'CIN');

CREG.LO(R,P,KR)$(RA_REG(R,P,KR) AND RCOMP_IN_REG(R,P,KR))=ZEAN(R,P,'CIN');

CREG.UP(R,P,KR)$(RA_REG(R,P,KR) AND
RCOMP_OUT_REG(R,P,KR))=ZEAN(R,P,'COUT');

*initialization for HEN

DT.L(Ih,Jc,P,Kh)$(HPS(Ih,P) AND CPS(Jc,P) AND matchh (ih,jc,P,kh))=HOTS(Ih,P,'TIN')-
COLDS(Jc,P,'TIN') ;

DT.L(Ih,Jc,P,Kh+1)$(HPS(Ih,P) AND CPS(Jc,P) AND matchh
(ih,jc,P,kh))=HOTS(Ih,P,'TIN')-COLDS(Jc,P,'TIN');

DT.LO(Ih,Jc,P,Kh)$(HPS(Ih,P) AND CPS(Jc,P) AND matchh (ih,jc,P,kh))=EMAT;

DT.LO(Ih,Jc,P,Kh+1)$(HPS(Ih,P) AND CPS(Jc,P) AND matchh (ih,jc,P,kh))=EMAT;

DT.UP(Ih,Jc,P,Kh)$(HPS(Ih,P) AND CPS(Jc,P) AND matchh (ih,jc,P,kh))=500;

DT.UP(Ih,Jc,P,Kh+1)$(HPS(Ih,P) AND CPS(Jc,P) AND matchh (ih,jc,P,kh))=500;

*Initialisation for exchanger approach temperatures between HPS(I) AND CUT(J)

DT.L(Ih,Jc,P,Kh)$(HPS(Ih,P) AND CUT(Jc,P) AND matchh (ih,jc,P,kh))=HOTS(Ih,P,'TIN')-
COLDS(Jc,P,'TIN');

DT.L(Ih,Jc,P,Kh+1)$(HPS(Ih,P) AND CUT(Jc,P) AND matchh
(ih,jc,P,kh))=HOTS(Ih,P,'TIN')-COLDS(Jc,P,'TIN');

DT.LO(Ih,Jc,P,Kh)$(HPS(Ih,P) AND CUT(Jc,P) AND matchh (ih,jc,P,kh))=EMAT;

DT.LO(Ih,Jc,P,Kh+1)$(HPS(Ih,P) AND CUT(Jc,P) AND matchh (ih,jc,P,kh))=EMAT;

DT.UP(Ih,Jc,P,Kh)$(HPS(Ih,P) AND CUT(Jc,P) AND matchh (ih,jc,P,kh))=500;

DT.UP(Ih,Jc,P,Kh+1)$(HPS(Ih,P) AND CUT(Jc,P) AND matchh (ih,jc,P,kh))=500;

*Initialisation for exchanger approach temperatures between HUT(I) AND CPS(J)

```
DT.L(Ih,Jc,P,Kh)$(HUT(Ih,P) AND CPS(Jc,P) AND matchh (ih,jc,P,kh))=HOTS(Ih,P,'TIN')-
COLDS(Jc,P,'TIN');

DT.L(Ih,Jc,P,Kh+1)$(HUT(Ih,P) AND CPS(Jc,P) AND matchh
(ih,jc,P,kh))=HOTS(Ih,P,'TIN')-COLDS(Jc,P,'TIN');

DT.LO(Ih,Jc,P,Kh)$(HUT(Ih,P) AND CPS(Jc,P) AND matchh (ih,jc,P,kh))=EMAT;

DT.LO(Ih,Jc,P,Kh+1)$(HUT(Ih,P) AND CPS(Jc,P) AND matchh (ih,jc,P,kh))=EMAT;

DT.UP(Ih,Jc,P,Kh)$(HUT(Ih,P) AND CPS(Jc,P) AND matchh (ih,jc,P,kh))=500;

DT.UP(Ih,Jc,P,Kh+1)$(HUT(Ih,P) AND CPS(Jc,P) AND matchh (ih,jc,P,kh))=500;


*Initialisations for Q(I,J,K) between HPS(I) and CPS(J)

Q.L(Ih,Jc,P,Kh)$(HPS(Ih,P) AND CPS(Jc,P) AND matchh
(ih,jc,P,kh))=MIN((HOTS(Ih,P,'F')) *(HOTS(Ih,P,'TIN')-
HOTS(Ih,P,'TOUT')),((COLDS(Jc,P,'F')) *(COLDS(Jc,P,'TOUT')-COLDS(Jc,P,'TIN'))));

Q.L(Ih,Jc,P,Kh)$(HPS(Ih,P) AND CUT(Jc,P) AND matchh (ih,jc,P,kh)) =
((HOTS(Ih,P,'F'))*(HOTS(Ih,P,'TIN')-HOTS(Ih,P,'TOUT')));

Q.L(Ih,Jc,P,Kh)$(HUT(Ih,P) AND CPS(Jc,P) AND matchh (ih,jc,P,kh))=
((COLDS(Jc,P,'F'))*(COLDS(Jc,P,'TOUT')-COLDS(Jc,P,'TIN')));


Q.UP(Ih,Jc,P,Kh)$(HPS(Ih,P) AND CPS(Jc,P) AND matchh
(ih,jc,P,kh))=MIN((HOTS(Ih,P,'F'))*(HOTS(Ih,P,'TIN')-
HOTS(Ih,P,'TOUT')),((COLDS(Jc,P,'F')) *(COLDS(Jc,P,'TOUT')-COLDS(Jc,P,'TIN'))));

Q.UP(Ih,Jc,P,Kh)$(HPS(Ih,P) AND CUT(Jc,P) AND matchh (ih,jc,P,kh)) =
((HOTS(Ih,P,'F'))*(HOTS(Ih,P,'TIN')-HOTS(Ih,P,'TOUT')));

Q.UP(Ih,Jc,P,Kh)$(HUT(Ih,P) AND CPS(Jc,P) AND matchh (ih,jc,P,kh))=
((COLDS(Jc,P,'F'))*(COLDS(Jc,P,'TOUT')-COLDS(Jc,P,'TIN')));


*Intialisations and bounds for intermediate temperatures

TH.L(Ih,P,Kh)$(firsth(P,kh))=HOTS(Ih,P,'TIN');

TC.L(Jc,P,Kh)$(lasth(P,kh))=COLDS(Jc,P,'TIN');
```

```
TH.LO(Ih,P,Kh)$(lasth(P,kh))=HOTS(Ih,P,'TOUT');

TH.UP(Ih,P,Kh)$(firsth(P,kh))=HOTS(Ih,P,'TIN');


TC.LO(Jc,P,Kh)$(lasth(P,kh))=COLDS(Jc,P,'TIN');

TC.UP(Jc,P,Kh)$(firsth(P,kh))=COLDS(Jc,P,'TOUT');

*=====================================================================

EXAMPLE1.optfile=1;

OPTION DOMLIM =1000000;

OPTION ITERLIM =20000000;

SOLVE EXAMPLE1 USING MINLP MINIMIZING TAC;

SOLVE EXAMPLE1 USING MINLP MINIMIZING EII;

SOLVE EXAMPLE1 USING MINLP MINIMIZING DUAL;
```